

Investigating the impact of subcutaneous and visceral adiposity on metabolism using an adipose tissue transplantation model

Author:

Hocking, Samantha Louise

Publication Date:

2011

DOI:

<https://doi.org/10.26190/unsworks/15788>

License:

<https://creativecommons.org/licenses/by-nc-nd/3.0/au/>

Link to license to see what you are allowed to do with this resource.

Downloaded from <http://hdl.handle.net/1959.4/52228> in <https://unsworks.unsw.edu.au> on 2024-03-29

Investigating the impact of subcutaneous and visceral adiposity on metabolism using an adipose tissue transplantation model

Samantha Louise Hocking

A thesis submitted in fulfillment of the requirements for
the degree of Doctor of Philosophy, Faculty of Medicine,
University of New South Wales

Diabetes and Obesity Research Program
The Garvan Institute of Medical Research

August 2011

PLEASE TYPE**THE UNIVERSITY OF NEW SOUTH WALES
Thesis/Dissertation Sheet**Surname or Family name: **Hocking**First name: **Samantha**Other name/s: **Louise**Abbreviation for degree as given in the University calendar: **PhD**School: **St Vincents Clinical School**Faculty: **Medicine**

Title:

**Investigating the impact of subcutaneous
and visceral adiposity on metabolism
using an adipose tissue transplantation
model****Abstract 350 words maximum: (PLEASE TYPE)**

Intra-abdominal (AB) obesity is associated with a higher risk of diabetes than subcutaneous (SC) obesity. To determine whether this is due to differences in anatomical location or intrinsic differences in fat depots, the metabolic effects of transplantation of SC or AB fat into the SC or AB space of recipient mice were determined.

Donor inguinal (SC) and epididymal (AB) fat was transplanted into the SC (SC-SC and AB-SC) or AB (SC-AB and AB-AB) space in high fat-fed (45% calories from fat) male C57BL6/J mice. Sham-operated mice underwent surgery without fat transplantation (SHAM). 11-13 weeks after transplantation metabolic studies were performed and adipose tissue harvested for analysis including microarray.

Mice receiving SC-AB grafts displayed significantly reduced fat mass, in both transplanted and endogenous fat depots, and improved glucose tolerance compared with SHAM. These metabolic effects were not observed in mice receiving SC-SC, AB-SC or AB-AB grafts. Microarray analysis of transplanted and endogenous fat depots revealed increased expression of genes controlled by the transcription factor myocyte enhancer factor 2 (MEF2-genes) in SC-AB grafts and the endogenous inguinal adipose tissue (ENDOG-SC) from mice receiving a SC-AB graft. Increased uncoupling protein-1 (UCP-1) gene expression was observed uniquely in ENDOG-SC fat.

At 13 weeks post-transplantation SC-AB grafts had decreased in mass. Failure of SC grafts to expand in the AB compartment suggests that cross-talk between adipocyte and non-adipocyte components of adipose tissue is depot-specific. Lectin affinity chromatography combined with partial metabolic labelling and mass spectrometry determined quantitative differences in the secretomes of SC and AB whole adipose tissue, preadipocytes and microvascular endothelial cells, suggesting intrinsic depot-specific differences are present in all cell types within adipose tissue.

These findings suggest a unique beneficial metabolic effect of SC-AB transplantation that is mediated by a secreted factor acting uniquely on SC fat to increase expression of MEF2-genes and UCP-1. As chronic B3-adrenergic stimulation of white adipose tissue increases UCP-1 and MEF2 expression is increased by adrenergic stimulation in non-adipose adult tissues, increased adrenergic-stimulation of subcutaneous fat is a putative mechanism. The identity of the secreted factor is important as it may provide a novel treatment for obesity-induced metabolic disease.

Declaration relating to disposition of project thesis/dissertation

I hereby grant to the University of New South Wales or its agents the right to archive and to make available my thesis or dissertation in whole or in part in the University libraries in all forms of media, now or here after known, subject to the provisions of the Copyright Act 1968. I retain all property rights, such as patent rights. I also retain the right to use in future works (such as articles or books) all or part of this thesis or dissertation.

I also authorise University Microfilms to use the 350 word abstract of my thesis in Dissertation Abstracts International (this is applicable to doctoral theses only).



Signature

Witness

.....21st August 2011.....
Date

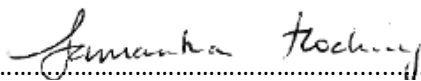
The University recognises that there may be exceptional circumstances requiring restrictions on copying or conditions on use. Requests for restriction for a period of up to 2 years must be made in writing. Requests for a longer period of restriction may be considered in exceptional circumstances and require the approval of the Dean of Graduate Research.

FOR OFFICE USE ONLY

Date of completion of requirements for Award:

ORIGINALITY STATEMENT

'I hereby declare that this submission is my own work and to the best of my knowledge it contains no materials previously published or written by another person, or substantial proportions of material which have been accepted for the award of any other degree or diploma at UNSW or any other educational institution, except where due acknowledgement is made in the thesis. Any contribution made to the research by others, with whom I have worked at UNSW or elsewhere, is explicitly acknowledged in the thesis. I also declare that the intellectual content of this thesis is the product of my own work, except to the extent that assistance from others in the project's design and conception or in style, presentation and linguistic expression is acknowledged.'

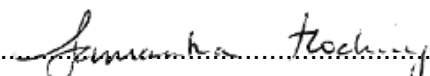
Signed.....

Date21st August 2011.....

COPYRIGHT STATEMENT

'I hereby grant the University of New South Wales or its agents the right to archive and to make available my thesis or dissertation in whole or part in the University libraries in all forms of media, now or here after known, subject to the provisions of the Copyright Act 1968. I retain all proprietary rights, such as patent rights. I also retain the right to use in future works (such as articles or books) all or part of this thesis or dissertation.

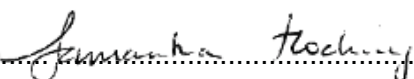
I also authorise University Microfilms to use the 350 word abstract of my thesis in Dissertation Abstract International (this is applicable to doctoral theses only). I have either used no substantial portions of copyright material in my thesis or I have obtained permission to use copyright material; where permission has not been granted I have applied/will apply for a partial restriction of the digital copy of my thesis or dissertation.'

Signed 

Date 21st August 2011

AUTHENTICITY STATEMENT

'I certify that the Library deposit digital copy is a direct equivalent of the final officially approved version of my thesis. No emendation of content has occurred and if there are any minor variations in formatting, they are the result of the conversion to digital format.'

Signed 

Date 21st August 2011

Abstract

Intra-abdominal (AB) obesity is associated with a higher risk of diabetes than subcutaneous (SC) obesity. To determine whether this is due to differences in anatomical location or intrinsic differences in fat depots, the metabolic effects of transplantation of SC or AB fat into the SC or AB space of recipient mice were determined.

Donor inguinal (SC) and epididymal (AB) fat was transplanted into the SC (SC-SC and AB-SC) or AB (SC-AB and AB-AB) space in high fat-fed (45% calories from fat) male C57BL6/J mice. Sham-operated mice underwent surgery without fat transplantation (SHAM). 11-13 weeks after transplantation metabolic studies were performed and adipose tissue harvested for analysis including microarray.

Mice receiving SC-AB grafts displayed significantly reduced fat mass, in both transplanted and endogenous fat depots, and improved glucose tolerance compared with SHAM. These metabolic effects were not observed in mice receiving SC-SC, AB-SC or AB-AB grafts. Microarray analysis of transplanted and endogenous fat depots revealed increased expression of genes controlled by the transcription factor myocyte enhancer factor 2 (MEF2-genes) in SC-AB grafts and the endogenous inguinal adipose tissue (ENDOG-SC) from mice receiving a SC-AB graft. Increased uncoupling protein-1 (UCP-1) gene expression was observed uniquely in ENDOG-SC fat.

At 13 weeks post-transplantation SC-AB grafts had decreased in mass. Failure of SC grafts to expand in the AB compartment suggests that cross-talk between adipocyte and non-adipocyte components of adipose tissue is depot-specific. Lectin affinity chromatography combined with partial metabolic labelling and mass spectrometry determined quantitative differences in the secretomes of SC and AB whole adipose tissue, preadipocytes and microvascular endothelial cells, suggesting intrinsic depot-specific differences are present in all cell types within adipose tissue.

These findings suggest a unique beneficial metabolic effect of SC-AB transplantation that is mediated by a secreted factor acting uniquely on SC fat to increase expression of MEF2-genes and UCP-1. As chronic β 3-adrenergic stimulation of white adipose tissue increases UCP-1 and MEF2 expression is increased by adrenergic stimulation in non-adipose adult tissues, increased adrenergic-stimulation of subcutaneous fat is a putative mechanism. The identity of the secreted factor is important as it may provide a novel treatment for obesity-induced metabolic disease.

Acknowledgements

The work presented in this thesis would not have been possible without the help of many people.

First and foremost my thanks go to my supervisors Professor David James and Professor Don Chisholm. I would like to thank David for his inspirational ideas, guidance, patience and support and Don for his calm advice, reassurance and constant offers of assistance. I am especially grateful for the opportunity to have worked under the supervision of two exceptional researchers in the field of diabetes.

I am also extremely grateful to everyone in the James Lab and the broader Diabetes and Obesity Research Program for their support, camaraderie and scientific input throughout my candidature. I would particularly like to thank Lindsay Wu for his collaboration on depot-specific adipose tissue protein secretion, Kyle Hoehn for his advice regarding animal experiments, Nigel Turner for his guidance in metabolic assays, Ronaldo Enriquez for his assistance with DEXA analysis, Katarina Mele for her assistance with HCA-Vision analysis and Mark Larence for patiently answering my constant questions about all things scientific.

I am also grateful for the collaboration established with Genentech and in particular the assistance provided by Dr Ganesh Kolumam with RNA extraction and microarray analysis. I am similarly grateful to Dr Warren Kaplan from the Peter Wills Bioinformatics Centre for his collaborative assistance with bioinformatic analysis of the microarray data.

The financial support provided by the Garvan Institute of Medical Research in addition to my NHMRC Medical Postgraduate Research Scholarship, has been greatly appreciated. I have also been fortunate to be awarded an Eli Lilly Endocrinology Research Grant and a GlaxoSmithKline Research Support Grant through the course of my candidature.

Beyond the laboratory, I have been immensely supported by my family, who have granted me the opportunity to undertake a postgraduate research degree. I would like to thank my parents for their support, understanding and many hours of child minding. I am especially thankful to my husband Philip who has demonstrated immense patience and encouragement during this journey. Over the course of my candidature he has supported me through the major milestones of my career and the challenges of new parenthood following the births of our two sons Toby and Alex. Finally, to my two little boys, thank you for the delight you have brought to my life. For me, the memories of your early years will always echo from the pages of this thesis

Table of Contents

List of Tables	vii
List of Figures	viii
List of Appendices	ix
List of Abbreviations	x
Publications arising from this thesis	xiii
Chapter 1. - General Introduction	1
<i>Obesity, insulin resistance and type 2 diabetes – the global pandemic.</i>	2
<i>Visceral adiposity increases the risk of type 2 diabetes.</i>	4
<i>Adipose tissue is now recognized as a metabolic and endocrine organ.</i>	6
<i>The physiology of adipose tissue.</i>	7
<i>The importance of adipose tissue - the metabolic consequences of lipodystrophy.</i>	10
<i>Paradoxical metabolic benefit from inhibition of angiogenesis.</i>	11
<i>Obesity and insulin resistance – the ectopic lipid hypothesis.</i>	12
<i>Visceral adiposity and insulin resistance – the portal hypothesis.</i>	13
<i>Visceral adiposity and insulin resistance – the endocrine hypothesis.</i>	14
<i>Visceral adiposity and insulin resistance – the chronic inflammation hypothesis.</i>	15
<i>Visceral adiposity and insulin resistance – cell-autonomous differences between subcutaneous and visceral adipocytes.</i>	16
<i>Summary of mechanisms responsible for the adverse metabolic consequences of visceral adiposity</i>	17
<i>Adipose tissue transplantation – an emerging tool to study adipose tissue physiology</i>	18
<i>Adipose tissue transplantation in cosmetic and reconstructive surgery.</i>	19
<i>Adipose tissue transplantation - a tool for studying adipose tissue biology.</i>	19
<i>Adipose tissue transplantation - a tool for studying the regulation of adipose tissue mass.</i>	21
<i>Adipose tissue transplantation - a tool for studying the metabolic effects of increased adipose tissue mass.</i>	23
<i>Proteomics and the identification of secretory proteins.</i>	27
<i>Protein secretion – classical and non-classical.</i>	31
<i>Proteomics and the identification of adipokines.</i>	33

<i>Enrichment of secreted proteins by lectin affinity chromatography.</i>	35
<i>Specific aims of this investigation.</i>	36
 Chapter 2. - Subcutaneous adipose tissue transplantation into the intra-abdominal compartment reveals a unique and beneficial effect on metabolism.	39
<i>Abstract</i>	40
<i>Introduction</i>	41
<i>Research design and methods</i>	43
Choice of animal model	43
Animals	45
Adipose tissue transplantation	45
Metabolic assays	48
Analysis of tissue weights and histology	48
Measurement of adipocyte area	48
Data analysis	49
<i>Results</i>	49
Graft Integrity	49
Adipocyte area	49
Body Weight	53
Adiposity	53
Energy balance	55
Glucose tolerance	58
Fasting insulin and HOMA-IR	58
<i>Discussion</i>	61
 Chapter 3. - Gene expression analysis of transplanted and endogenous adipose tissue.	65
<i>Abstract</i>	66
<i>Introduction</i>	68
<i>Research design and methods</i>	75
Animals	75
Adipose tissue transplantation	75
Adipose tissue harvesting and RNA extraction	76
RNA preparation for microarrays	78
Microarray analysis	79

<i>Results</i>	80
<i>Discussion</i>	99
 Chapter 4. - Intrinsic depot-specific differences in the secretome of adipose tissue, preadipocytes and adipose tissue derived microvascular endothelial cells	 107
<i>Abstract</i>	108
<i>Introduction</i>	110
<i>Research design and methods</i>	113
Materials and buffers	113
Animals	114
Preparation of Anti-CD31 (Anti-PECAM-1) antibody-coated magnetic beads to isolate endothelial cells	114
Adipose tissue explants	114
Preadipocyte and endothelial cell isolation and culture	115
Lectin affinity chromatography	116
Mass spectrometry	116
<i>Results</i>	119
<i>Discussion</i>	131
 Chapter 5. - General Discussion	 137
<i>Current knowledge of the relationship between subcutaneous and visceral adiposity and metabolic disease.</i>	138
<i>The technique of adipose tissue transplantation.</i>	142
<i>Intra-abdominal transplantation of subcutaneous adipose tissue reduces obesity and improves glucose tolerance in fat-fed mice</i>	143
<i>Future directions</i>	145
<i>Final conclusions.</i>	151
 References	 154

List of Tables

TABLE 2.1. Total body weight, endogenous adipose tissue weights and weights of harvested and implanted transplants.	50
TABLE 3.1. Genes upregulated more than two fold in SC-AB compared with SC-SC grafts.	81
TABLE 3.2. Genes upregulated more than two fold in SC-SC compared with SC-AB grafts.	82
TABLE 3.3. Genes upregulated more than ten fold in ENDOG-SC compared with SHAM-SC grafts.	84
TABLE 3.4. Genes upregulated more than ten fold in SHAM-SC compared with ENDOG-SC grafts.	85
TABLE 3.5. Genes upregulated more than ten fold in ENDOG-SC compared with ENDOG-VIS grafts.	86
TABLE 3.6. Genes upregulated more than ten fold in ENDOG-VIS compared with ENDOG-SC grafts.	87
TABLE 3.7. Gene sets identified by gene set enrichment analysis for transcription factor targets comparing SC-AB and SC-SC grafts. Gene sets showing statistically significant, concordant differences between SC-AB and SC-SC grafts with a normalised enrichment score greater than 2.0 are shown.	89
TABLE 4.1. Secreted proteins identified from visceral and subcutaneous adipose tissue explants.	120
TABLE 4.2. Secreted proteins identified from visceral and subcutaneous preadipocytes.	123
TABLE 4.3. Secreted proteins identified from visceral and subcutaneous microvascular endothelial cells.	126
TABLE 4.4. Summary of numbers of proteins detected, and relative abundance between visceral and subcutaneous adipose tissue samples.	133

List of Figures

Figure 1.1. Relationship between BMI and risk of type 2 diabetes in men and women.	3
Figure 1.2. Central obesity and insulin resistance.	5
Figure 1.3. Immature adipose tissue grafts develop into mature adipose tissue pads.	20
Figure 1.4. Adipose tissue transplanted from lean and obese donors assumes the characteristics of the host endogenous adipose tissue with respect to cell size (A) and lipid content (B).	22
Figure 1.5. Viability of adipose tissue grafts weighing up to 900 mg after transplantation	24
Figure 1.6. Generic mass spectrometry (MS)-based proteomics experiment.	28
Figure 2.1. Schematic of adipose tissue transplantation experiments.	47
Figure 2.2. Average cross-sectional adipocyte area of transplanted and endogenous adipose tissue.	51
Figure 2.3. Macroscopic appearance and histology of transplanted and endogenous adipose tissue.	52
Figure 2.4. Body weight after transplantation.	54
Figure 2.5. Body composition after transplantation.	56
Figure 2.6. Respiratory quotient and energy expenditure after transplantation	57
Figure 2.7. Glucose tolerance test after transplantation	59
Figure 2.8. Fasting glucose, insulin and calculated HOMA-IR after transplantation	60
Figure 3.1. Schematic of adipose tissue transplantation experiments.	77
Figure 3.2. Normalised gene expression of myogenin (A) and myogenic differentiation 1 (MyoD1) (B) across adipose tissue depots.	91
Figure 3.3. Heatmap of normalised gene expression across all adipose tissue depots of genes upregulated more than five fold in SC-AB compared with SC-SC grafts.	92
Figure 3.4. Heatmap of normalised gene expression across all adipose tissue depots of MEF2 isoforms.	93
Figure 3.5. Normalised gene expression of leptin (A), adiponectin (B), resistin (C) and RBP4 (D) across adipose tissue depots.	94
Figure 3.6. Normalised gene expression of UCP-1 across adipose tissue depots.	96
Figure 3.7. Normalised gene expression of β 3-adrenergic receptors across adipose tissue depots.	97
Figure 3.8. Normalised gene expression of glycogen phosphorylase (muscle) across adipose tissue depots.	98
Figure 4.1. LAC-CILAIR workflow for comparing protein synthesis and secretion from two different samples.	118
Figure 4.2. Adipose tissue explants secretory proteins are secreted in greater amounts from visceral adipose tissue.	121
Figure 4.3. Preadipocyte secretory proteins are secreted in greater amounts from visceral adipose tissue.	124
Figure 4.4. Endothelial cell secretory proteins are secreted in greater amounts from visceral adipose tissue.	127
Figure 4.5. Venn diagram showing protein secretion from white adipose tissue explants, preadipocytes and microvascular endothelial cells.	129
Figure 4.6. Venn diagram showing protein secretion from whole adipose tissue (WAT) explants, 3T3-L1 adipocytes and isolated rat adipocytes (from Chen et al 2005) (143)	130

List of Appendices

Appendix 1 Secreted proteins identified from visceral and subcutaneous whole

adipose tissue explants

Appendix 2 Secreted proteins identified from visceral and subcutaneous

microvascular endothelial cells

List of Abbreviations

¹⁸ F –FDG PET	¹⁸ F – fluorodeoxyglucose positron emission tomography
3T3-L1 adipocytes	A murine preadipocyte cell line that can be converted to lipid-laden adipocytes
α-MSH	α-melanocyte-stimulating hormone
AB	Intra-abdominal (epididymal)
AB-AB	Abdominal (epididymal) adipose tissue transplant into the abdominal compartment
AB-SC	Abdominal (epididymal) adipose tissue transplant into the subcutaneous compartment
Actb	b-actin promoter
AEBP1	adipocyte enhancer binding protein 1
AMP	Adenosine monophosphate
aP2/FABP4 gene	Adipocyte protein 2 / fatty acid binding protein 4
ATP	Adenosine triphosphate
AUC	Area under the curve
BMI	Body mass index
BSA	Bovine serum albumin
C/EBP	CCAAT-enhancer-binding proteins
cAMP	Cyclic adenosine monophosphate
CGRP	Calcitonin gene-related peptide
CID	Collision – induced dissociation
CILAIR	comparison of <i>isotope</i> -labelled <i>amino acid</i> <i>incorporation</i> rates
CT	Computerised tomography
DAVID	Database for Annotation, Visualisation and Integrated Discovery
<i>db/db</i>	Mice obese due to leptin receptor deficiency
DEXA	Dual-energy X-ray absorptiometry
DGAT1	Acyl CoA:diacylglycerol acyltransferase 1
DMEM	Dulbecco's modified eagle medium
DMEM/K-/R-	Low glucose Dulbecco's modified eagle medium without leucine, lysine and arginine supplemented with 0.105 g/L leucine, 100 units/mL penicillin, 0.1 mg/mL streptomycin, 0.0159 g/L phenol red and 100 nM insulin
ENDO-SC	Endogenous inguinal adipose tissue from mice receiving a subcutaneous (inguinal) adipose tissue transplant into the subcutaneous compartment
ENDO-VIS	Endogenous epididymal adipose tissue from mice receiving a subcutaneous (inguinal) adipose tissue transplant into the subcutaneous compartment
ER	Endoplasmic reticulum
ESI	Electrospray ionisation
FDR	False discovery rate
GAS6	Growth arrest specific 6

GEF	Glucose enhancer factor
GLUT4	glucose transporter 4
GSEA	Gene Set Enrichment Analysis
H/L	Heavy to light isotope ratio
HBSS-FCS	Hank's balanced salt solution containing 5% foetal calf serum
HDACs	Histone deacetylases
HOMA-IR	Homeostasis model assessment index - insulin resistance
HSL	Hormone sensitive lipase
ICAT	Isotope coded affinity tag
IL-6	Interleukin-6
IL-8	Interleukin-8
ip	intra-peritoneal
ipGTT	intra-peritoneal glucose tolerance test
iTRAQ	Isobaric tags for relative and absolute quantitation
JNK	c-Jun N-terminal kinases
KO	Knock out
LAC	Lectin affinity chromatography
LAC-CILAIR	Lectin affinity chromatography followed by comparison of isotope-labelled amino acid incorporation rates
LC-MS/MS	Liquid chromatography-tandem mass spectrometry
LXR	Liver x receptor
M/L	Medium to light isotope ratio
m/z	Mass to charge ratio
MAP	Mitogen activated protein
MCM1	Minichromosome maintenance 1
MCP-1	Monocyte chemotactic protein 1 (
MEF2	Myocyte enhancer factor 2
MS	Mass spectrometry
MTII	Melanotan II
MVECS	Microvascular endothelial cells
Myf5	Myocyte factor 5
MyoD1	Myogenic differentiation 1
NEFAs	Non-esterified fatty acids
NF-kb	Nuclear factor kappa-light-chain-enhancer of activated B cells
<i>ob/ob</i>	Mice obese due to leptin deficiency
PAI-1	Plasminogen activator inhibitor-1
PDGF	Platelet -derived growth factor
PECAM-1	Platelet endothelial cell adhesion molecule
PGC-1	PPAR γ coactivator 1
PPAR-g	Peroxisome proliferator-activated receptor
PTX3	Pentraxin-related protein 3
PXR	Pregnane X receptor
RBP4	Retinol-binding protein-4
RMA	Robust multichip average
RYGB	Roux-en Y gastric bypass
SC	Subcutaneous (inguinal)

SC-AB	Subcutaneous (inguinal) adipose tissue transplant into the abdominal compartment
SC-SC	Subcutaneous (inguinal) adipose tissue transplant into the subcutaneous compartment
SD	Standard deviation
SDS-PAGE	Sodium dodecyl sulfate polyacrylamide gel electrophoresis
SEM	Standard error of mean
SHAM	Mice that underwent surgery without fat transplantation
SHAM-SC	Endogenous inguinal adipose tissue from mice that underwent abdominal surgery without fat transplantation
SILAC	stable <i>isotope</i> labelling by <i>amino</i> acids in cell culture
SNS	Sympathetic nervous system
SP	Substance P
SPARC	Osteonectin
SRE	Serum-response element
SST	Signal sequence trap
TNF α	Tumour necrosis factor- α
Type 2 diabetes	Type 2 diabetes mellitus
UCP-1	Uncoupling protein-1
VEGF	Vascular endothelial growth factor
VO ₂	Oxygen consumption rate
WAT	Whole adipose tissue
WHO	World Health Organisation

Publications arising from this thesis

Hocking SL, Chisholm DJ, James DE. Studies of regional adipose transplantation reveal a unique and beneficial interaction between subcutaneous adipose tissue and the intra-abdominal compartment. *Diabetologia* 2008; 51(5): 900-2.

Hocking SL, Wu LE, Guilhaus M, Chisholm DJ, James DE. Intrinsic depot-specific differences in the secretome of adipose tissue, preadipocytes and adipose tissue derived microvascular endothelial cells. *Diabetes* 2010; 59(12): 3008 - 16.

Wu L, **Hocking S**, James D. Macrophage infiltration and cytokine release in adipose tissue: angiogenesis or inflammation? *Diabetology International* 2010; 1(1): 1-9.

Chapter 1

General Introduction

Obesity, insulin resistance and type 2 diabetes – the global pandemic.

Obesity is increasing in prevalence both worldwide and in Australia. The World Health Organisation (WHO) currently estimates the global prevalence of obesity at 300 million. As body fat content is difficult to measure, body mass index (BMI), a ratio of weight to height (kg/m^2) is a commonly used tool to estimate body fat. The assumption underlying this calculation is that in adults of the same height, most of the variation in weight is due to adiposity. WHO categorizes adults as healthy weight (BMI 18.5 – 24.9), overweight (BMI 25 – 29.9) and obese class I (BMI 30 – 34.9), obese class II (BMI 35 – 39.9) and obese class III (BMI ≥ 40) (1). In Australia in the years 1999 – 2000, 19% of males and 22% of females aged 25 years or over were obese and an additional 48% of males and 30% of females were overweight, according to BMI. The prevalence of obesity was more than double that observed in 1980 for both men and women (2).

Obesity is associated with a number of health problems including hypertension, gallstones, coronary artery disease, type 2 diabetes and certain malignancies, including breast, colon, kidney and endometrium (3). Being overweight or obese increases the risk for type 2 diabetes, in both men and women (Figure 1.1). In men with a BMI of 26, the risk of type 2 diabetes is about four times the risk in men with a BMI of less than 21 (4). For the same comparison in women, the risk of type 2 diabetes is eight times (5). Furthermore, weight gain in adulthood, irrespective of BMI, is associated with an increased risk of type 2 diabetes (4, 5). For example, women who gain between 5 and 7.9 kg in weight, increase their risk of type 2 diabetes by approximately two fold compared with women with stable weight (weight gain or loss of less than 5 kg). The increase in risk is even greater with larger weight gains (5). This illustrates a limitation of the current recommendations for healthy weight defined by BMI, as an individual at the lower end of the BMI range can gain a substantial amount of weight (up to 15 kg) and still remain within the healthy weight category. Therefore it may be better, from a population health perspective, to advocate maintaining adult body weight within 5 kg of body weight at age 20 years rather than promote healthy weight targets by BMI.

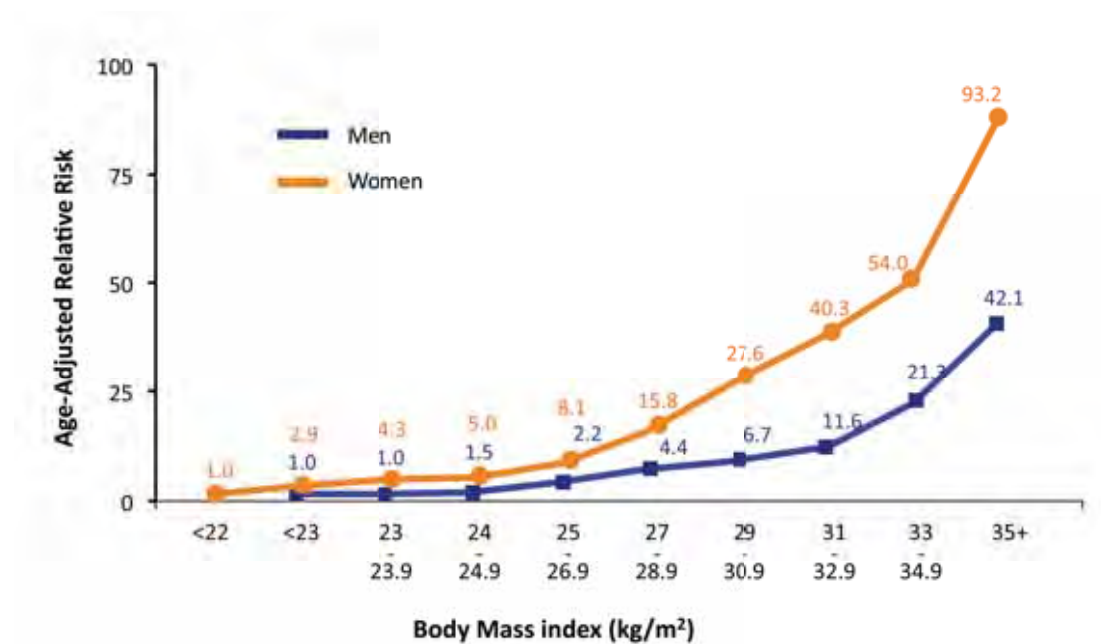


Figure 1.1. Relationship between BMI and risk of type 2 diabetes in men and women.

As BMI increases the risk of Type 2 diabetes increases exponentially in both men and women. Taken from Chan J et al. 1994 (4) and Colditz G et al. 1995 (5).

Visceral adiposity increases the risk of type 2 diabetes.

While it is clear from population studies that being overweight or obese increase the risk of developing type 2 diabetes, the distribution of body fat is more important than overall adiposity. The accumulation of central or visceral adiposity is associated with an increased risk of insulin resistance, dyslipidemia, hypertension and type 2 diabetes compared with the accumulation of gluteofemoral or subcutaneous adiposity (6-8). This relationship between increased abdominal fat and insulin resistance persists even in non-obese individuals (9) (Figure 1.2). In contrast, the accumulation of subcutaneous or peripheral adiposity (in the gluteofemoral regions) is associated with a decreased risk of developing type 2 diabetes (10). Body fat distribution displays ethnic differences with Asian-Indian men having higher amounts of total abdominal fat and visceral fat compared with Caucasian men of similar age and BMI. Asian-Indians are insulin resistant and at higher risk of developing diabetes and coronary heart disease, compared with Caucasians (11). Providing further evidence for the association between visceral fat and insulin resistance, the improvement in insulin sensitivity that occurs with exercise is predicted by reduction in visceral but not peripheral fat mass (12). Dietary interventions resulting in a 15% – 25% reduction in visceral adipose tissue are associated with a 25% - 50% increase in insulin sensitivity in skeletal muscle and liver (13-15). Conversely, thiazolidinedione therapy (a pharmacotherapy for type 2 diabetes), which increases total adiposity, improves insulin sensitivity as it selectively increases subcutaneous adipose tissue depots (16). Further evidence that visceral adiposity has a stronger detrimental metabolic impact than subcutaneous adiposity is provided by surgical studies in which liposuction (removal of subcutaneous fat alone) has not resulted in any improvement in insulin sensitivity (17) whereas the removal of omental (visceral fat) has improved insulin sensitivity (18). However, recent surgical studies in which visceral adipose tissue has been removed have providing conflicting results. In each of these studies, surgical removal of the greater omentum (a component of visceral adipose tissue), also termed omentectomy, has been performed in obese patients in conjunction with bariatric (obesity) surgery. In the first of these studies, subjects randomized to

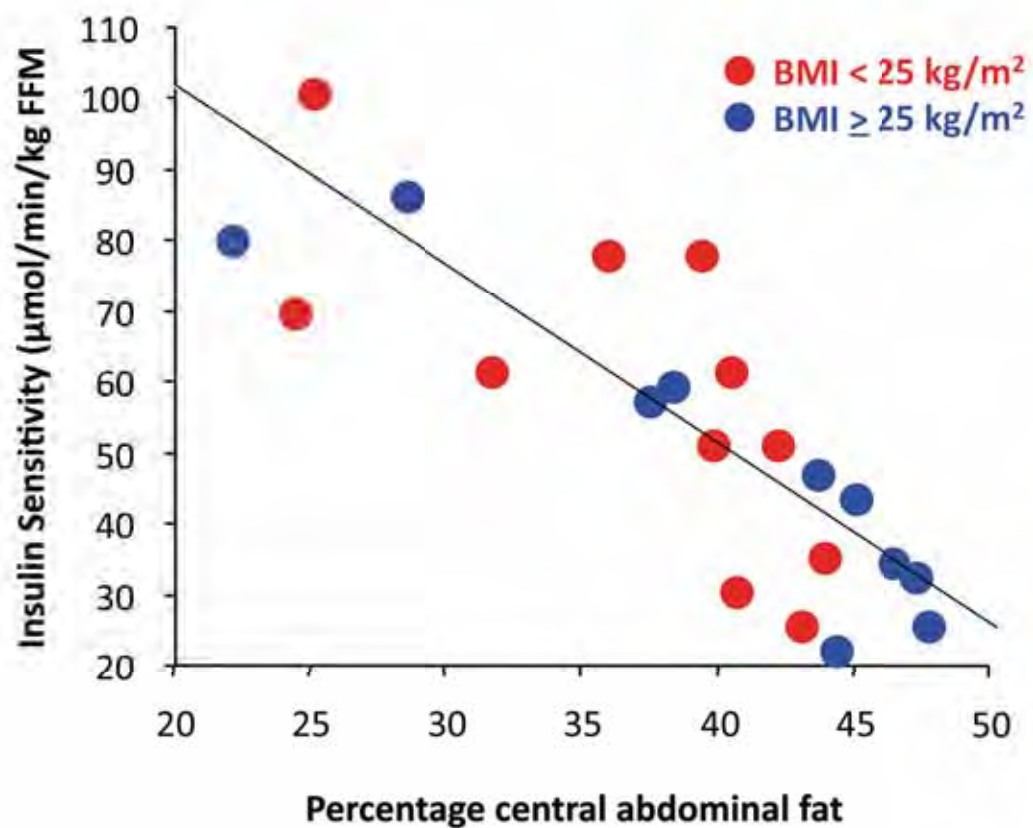


Figure 1.2. Central obesity and insulin resistance.

Increasing central or visceral fat is more strongly associated with decreasing insulin sensitivity or increasing insulin resistance than overall body fat in both obese and lean subjects. Taken from Carey D et al 1996 (9).

roux-en Y gastric bypass (RYGB) surgery plus omentectomy or RYGB alone showed no difference in hyperglycemia and hyperinsulinemia two years after surgery (19). In this study insulin sensitivity was not directly assessed. A subsequent study evaluating roux-en Y gastric bypass (RYGB) surgery plus omentectomy or RYGB alone, showed no additional benefit on metabolic parameters with the addition of omentectomy over RYGB alone (20). A possible explanation for these findings is the amount of weight loss in both treatment groups was so profound (up to 30% at one year), it masked the metabolic benefits of omentectomy, in which approximately 800 g of visceral adipose tissue is removed. A third study evaluating omentectomy, alone or in combination with RYGB surgery, showed no improvement in metabolic function in obese patients (21). In this study, hepatic and skeletal muscle insulin sensitivity was assessed using the hyperinsulinemic – euglycemic clamp technique. A limitation of this study was the high insulin infusion rate chosen during the clamp procedure, resulting in near-maximal stimulation of glucose disposal. It is possible that differences in insulin sensitivity may have manifested if studied at lower insulin infusion rates. Overall, these data provide evidence for an association between increased visceral adiposity and metabolic disease, however the precise mechanisms responsible for the adverse metabolic consequences of visceral adiposity remain elusive.

Adipose tissue is now recognized as a metabolic and endocrine organ.

Since the discovery of adiponectin, an adipocyte-derived serine protease that is secreted systemically and markedly down regulated in rodent obesity (22), adipose tissue has been increasingly recognised as a complex and highly active metabolic and endocrine organ. It is now established that in addition to acting as a storage reservoir for lipid, adipose tissue expresses and secretes a variety of bioactive peptides known as adipokines. Therefore, differences in anatomical location, as well as the metabolic and endocrine properties of subcutaneous and visceral adipose tissue must be considered as putative mechanisms accounting for the association between visceral but not subcutaneous adiposity and metabolic disease.

The physiology of adipose tissue.

Adipose tissue is composed principally of adipocytes, which specialise in storing energy as lipid, embedded in a connective tissue matrix of extracellular collagen. Small blood vessels and nerves, which supply adipose tissue, travel through the connective tissue matrix. These non-adipocyte components of adipose tissue are referred to as the stromovascular fraction, comprised of microvascular endothelial cells, neurons, immune cells and preadipocytes. There are two types of adipose tissue – white adipose tissue and brown adipose tissue. White adipose tissue is composed of unilocular adipocytes containing a single large lipid droplet surrounded by a thin layer of cytoplasm. Brown adipose tissue is composed of brown adipocytes containing numerous lipid droplets and abundant cytoplasm with numerous mitochondria. Brown adipose tissue differs from white adipose tissue by its high degree of vascularisation and sympathetic innervation. The most important distinction between brown and white adipose tissue is the presence of uncoupling protein-1 (UCP-1). UCP-1 is a mitochondrial protein found in brown adipocytes that uncouples oxidative phosphorylation, resulting in inefficient production of ATP and release of energy in the form of heat. It has long been established in animals that brown adipose tissue is crucial for the process of non-shivering thermogenesis (23). Until recently, brown adipose tissue was considered to be non-functioning in human adults. Recent studies utilising ^{18}F – fluorodeoxyglucose positron emission tomography (^{18}F –FDG PET) and computerised tomography (CT) scanning have identified substantial metabolic activity in brown adipose tissue located in the neck, supraclavicular, mediastinal and paraspinal areas of adult humans (24-29). ^{18}F –FDG PET combined with CT scanning is commonly used to detect highly metabolically active cancer cells based on their uptake of large amounts of ^{18}F – fluorodeoxyglucose and “accidentally” discovered these areas of putative brown adipose tissue; formal proof that the areas contain functioning brown adipose tissue has been provided by tissue biopsies, which reveal the morphological and molecular characteristics of brown adipose tissue, including expression of the brown adipose tissue-specific protein UCP1 (24, 26-28). These recent human brown adipose tissue studies suggest an inverse correlation between brown adipose tissue

activity and BMI (24, 26, 28), however, the impact of brown adipose tissue mediated thermogenesis on metabolism and the development of obesity remains unresolved.

White adipose tissue functions as a reservoir for energy storage – when energy intake is greater than energy expenditure, excess calories are stored within adipose tissue. Therefore, white adipose tissue, unlike most other adult tissues, can expand and regress throughout adulthood. Adipose tissue mass can expand by either increasing the number (hyperplasia) or size (hypertrophy) of adipocytes (30). Recent evidence suggests that although adipocyte number is an important determinant of adipose tissue mass in adulthood, the number of adipocytes stays constant in adulthood in both lean and obese individuals. However, the adipocyte pool is not static, with 10% of adipocytes renewed annually at all adult ages and levels of body mass index (31). This suggests that the number of adipocytes is set during childhood and adolescence and that changes in adipose tissue mass in adulthood can mainly be attributed to changes in adipocyte volume (31). In rodents, however, adipocyte hyperplasia (or adipogenesis) contributes to the increased adipose tissue mass in obesity (32). It has been proposed that adipocytes have a limited capacity for expansion and once a critical adipocyte cell volume is reached, enlarged adipocytes secrete growth factors that induce preadipocyte proliferation (33). Until recently, the identification *in vivo* of adipocyte precursors, capable of differentiating into mature adipocytes, has been limited. Two recent publications have identified a population of white adipose tissue precursor cells in murine adipose tissue vasculature, providing evidence that adipose tissue expansion by hyperplasia is possible *in vivo* (34, 35).

Irrespective of whether adipose tissue expansion occurs by adipocyte hypertrophy or hyperplasia, remodelling of vascular networks is necessary to supply newly differentiating or hypertrophic adipocytes with oxygen and nutrients (36). Indeed, circulating serum levels of angiogenic regulatory molecules such as VEGF correlate with obesity (37) and in particular with visceral obesity (38). Adipose tissue

development during embryogenesis is spatially and temporally associated with microvessel growth, with angiogenesis often preceding adipogenesis (39). Endothelial cell proliferation also occurs in expanding adult adipose tissue, possibly mediated by paracrine interactions between endothelial cells and preadipocytes (39). Adipocytes and endothelial cells may even share a common progenitor that can trans-differentiate into mature adipocytes or endothelial cells depending on the differentiation conditions it is exposed to (40). Preadipocytes can influence proliferation and reduce apoptosis in mature endothelial cells (41) and conversely, endothelial cell conditioned media promotes the proliferation and differentiation capacity of pre-adipocytes in vitro (42). The importance of neo-vascularisation for adipose tissue growth has been clearly demonstrated by studies in which systemic administration of angiogenesis inhibitors results in weight reduction and adipose tissue loss in various mouse models of obesity (43). The exact mechanisms governing the coordinated expansion of adipose tissue and its microvasculature remain unresolved.

As mentioned previously, in order for adipose tissue expansion to proceed by either adipocyte hypertrophy or hyperplasia, the extracellular matrix must be remodelled. In adipose tissue the extracellular matrix is composed of a number of collagen species with collagen VI being substantially enriched in adipose tissue (44). In *db/db* and *ob/ob* mice, genetic mouse models of obesity, there is a significant up-regulation of collagen VI, implying a state of 'adipose tissue fibrosis' that is thought to occur in response to hypertrophied adipocytes. It is proposed that this invokes rigidity in the extracellular matrix, limiting the further expansion of individual adipocytes (44). Surprisingly however, collagen VI KO mice exposed to a high fat diet display reduced weight gain due to reduced adipose tissue accumulation, despite having larger adipocytes, compared to their wild-type littermates. In the setting of a destabilized extracellular matrix as a consequence of collagen VI deletion, unlimited adipose tissue expansion should theoretically occur. In keeping with this, collagen VI KO mice did have larger adipocytes compared with their wild-type littermates with improved glucose tolerance. Unexpectedly however, collagen

VI KO mice had reduced food intake and reduced energy expenditure, suggesting that deletion of collagen VI mediates its whole body effects remotely from adipose tissue (44). The reason for this altered metabolism in collagen VI KO mice remains unclear.

Macrophages, immune cells found in the stromovascular fraction of adipose tissue, may also play a key role in adipose tissue angiogenesis. Macrophage infiltration into adipose tissue may be triggered by hypertrophic adipocytes as macrophage numbers in adipose tissue, in both rodents and humans, are positively correlated with adipocyte cell size (45). Macrophages secrete a variety of pro-angiogenic molecules including PDGF and VEGF (46-48). In fact, macrophage infiltration may be an essential process needed for angiogenesis in adipose tissue, due to the abundant secretion of PDGF from macrophages (49). The secretory protein for which macrophages are best known, TNF α , can also induce angiogenesis (50).

Macrophages secrete a variety of other proteins that demonstrate powerful pro-angiogenic effects including monocyte chemotactic protein 1 (MCP-1) (51), macrophage inhibitory factor (52), and interleukin-6 (IL-6) (53). If adipocytes do possess a limited capacity for hypertrophy, it is possible that once a critical threshold is reached, adipocytes secrete macrophage chemoattractant proteins and other paracrine growth factors to induce angiogenesis as a necessary prerequisite for preadipocyte hyperplasia.

The importance of adipose tissue - the metabolic consequences of lipodystrophy.

Human lipodystrophy syndromes provide an excellent example of the metabolic complications that arise when an individual has insufficient adipose tissue and is unable to partition lipid into adipose tissue stores. Human lipodystrophy syndromes are comprised of a heterogeneous group of congenital and acquired disorders characterised by a partial or near complete absence of adipose tissue. Clinically patients with lipodystrophy syndromes have insulin resistance, hepatic steatosis and dyslipidemia, with the severity of the metabolic disturbance being inversely related to the amount of adipose tissue (54). This leads to the question of what

governs adipose tissue expandability? Mature adipocytes are derived from preadipocytes, which in turn are derived from mesenchymal stem cells. Transcription factors such as ADD/SREB-1, C/EBP- α , - β , - δ and PPAR- γ are important in the control of adipogenesis. There are two isoforms of PPAR- γ , PPAR- γ 1 that is expressed ubiquitously and PPAR- γ 2 that is found almost exclusively in adipose tissue. A number of humans with heterozygous mutations in PPAR- γ have been identified. All have severe insulin resistance and many have a marked reduction in body fat (particularly affecting gluteal and peripheral limb deposits), hepatic steatosis and severe dyslipidemia (raised triglycerides, low high-density lipoprotein cholesterol) (55-57). These individuals are phenotypically similar to individuals with other congenital lipodystrophy syndromes, further supporting the concept that a limitation of adipose tissue expansion leads to insulin resistance and subsequent metabolic complications. In addition to an inability to store triglycerides in adipocytes, a marked reduction in adipokine production (particularly leptin and adiponectin) may also contribute substantially to the metabolic derangement in lipodystrophy, as evidenced by the effectiveness of leptin therapy in reducing hyperglycemia, hypertriglyceridemia and hepatic steatosis in individuals with lipodystrophy syndromes (58-61).

Paradoxical metabolic benefit from inhibition of angiogenesis.

Human lipodystrophy syndromes clearly demonstrate the adverse metabolic consequences of being unable to partition excess lipid within adipose tissue. Remarkably, in direct contrast to lipodystrophy models, inhibition of adipose tissue angiogenesis, which also results in reduction of adipose tissue mass, improves insulin sensitivity, even when the animal is challenged with high fat feeding (62, 63). Administration of anti-angiogenic agents to mice from different obesity models results in dose-dependent weight reduction and adipose tissue loss (43, 63). Targeting of a pro-apoptotic peptide specific to the white adipose tissue vasculature similarly causes a reduction in fat mass (62). Extraordinarily, the reason for the reduction in fat mass and paradoxical improvement in insulin sensitivity in animals treated with this pro-apoptotic peptide appears to be linked to reduced appetite -

these animals consume approximately 30% less energy during high fat feeding (64). Similarly, treatment of mice with the general angiogenesis inhibitor TNP-470 decreases food intake (43, 63). Likewise, administration of the anti-angiogenic cytokine angiostatin decreases food intake (43). The mechanism responsible for the reduction in food intake is independent of known anorectic hypothalamic neural circuits involving leptin, neuropeptide Y and Agouti-related protein (64). These data support the presence of direct neural communication between the centers in the brain, which control appetite and hunger, and the adipose tissue vasculature. This may represent another adipose tissue – brain – adipose tissue neural circuit that functions independently of leptin. Autonomic nerves and microvasculature in adipose tissue are intimately related (65, 66) and it is conceivable that regression of adipose tissue vasculature by endothelial apoptosis confers a paracrine interaction between microvasculature and nerve cells, functioning to limit food intake via the central nervous system. In the context of shrinking adipose tissue depots, a reduction in food intake protects the animal from ectopic storage of lipid in muscle and liver, with its resultant detrimental metabolic consequences, which would otherwise be the inevitable consequence of unbridled caloric intake. Further research is required to ascertain the mechanism by which inhibition of angiogenesis improves metabolism.

Obesity and insulin resistance – the ectopic lipid hypothesis.

In obesity, just as in lipodystrophy syndromes, there is excess lipid storage in the liver, skeletal muscle and pancreatic beta cell (67). This ectopic accumulation of lipid in non-adipose tissues leads to cell dysfunction (lipotoxicity) and lipid-induced programmed cell death (lipoapoptosis). This subsequently causes insulin resistance and type 2 diabetes. This has led to the hypothesis that obesity is another ectopic fat storage syndrome. However, in direct contrast to subjects with lipodystrophy, obese patients have adequate or markedly enlarged adipose tissue stores. There are two possible mechanisms whereby ectopic lipid storage may occur. The first is the failure of adipose cells to proliferate and act as a buffer against excessive exposure to circulating free fatty acids (the 'push' factor). The cornerstone of this

hypothesis is that individuals' possess a maximum capacity for adipose tissue expansion and that once this limit is reached, adipose tissue is unable to store excess energy efficiently as lipid and lipids begin to accumulate in other non-adipose tissues. The second is impairment in the capacity of non-adipose organs and tissues to increase fat oxidation to match dietary fat intake (the 'pull' factor). This may occur as a consequence of obesity, resulting from alterations in the secretion of adipokines, such as leptin, and adiponectin, which increase lipid oxidation (68, 69). Alterations in adipokine production in obesity will be discussed in more detail below.

A principal aspect of the ectopic lipid hypothesis is that ectopic storage of lipid in non-adipose tissue sites results in insulin resistance. In muscle, the major site of insulin-stimulated glucose disposal, accumulation of intra-myocellular lipid is strongly correlated with *in vivo* insulin resistance (70, 71). Similarly in liver, hepatic accumulation of lipid is strongly correlated with insulin resistance (72). A substantive problem with this hypothesis is that highly trained athletes, who are very insulin sensitive, have high intramyocellular lipid content (73). The reason for this paradox remains incompletely understood but may be due to differences in "quarantining" fatty acids as metabolically inactive triglycerides in trained versus untrained muscle or in muscle fatty acid oxidation capacity between trained and untrained subjects. Another major problem with the ectopic lipid hypothesis is that it fails to account for the strong association between visceral adiposity and metabolic disease.

Visceral adiposity and insulin resistance – the portal hypothesis.

There are a number of distinct physiological differences between visceral and subcutaneous adipose tissue depots that could account for the link between visceral fat and insulin resistance, the most obvious being anatomical location. The venous drainage of visceral adipose tissue is via the portal vein directly into the liver (74). Visceral adipose tissue is particularly sensitive to lipolytic stimuli, being more lipolytic in response to catecholamines and insensitive to the antilipolytic effects of

insulin (75). Therefore an enlarged visceral adipose tissue depot will result in an increased flux of free-fatty acids in the portal circulation. This in turn results in increased hepatic gluconeogenesis and hepatic insulin resistance (74, 76). Although important, the anatomical location of visceral adipose tissue cannot be the sole mechanism whereby visceral adiposity causes insulin resistance. Studies in obese mice have shown that removal of gonadal adipose tissue results in improved glucose tolerance and insulin sensitivity (77, 78). Unlike other visceral fat depots in mice and in humans, gonadal fat pads are not drained by the portal vein, and so these data argues against the portal hypothesis. Thus, the role of anatomical location in mediating the deleterious effects of visceral adipose tissue per se remains unresolved.

Visceral adiposity and insulin resistance – the endocrine hypothesis.

Adipose tissue is now recognised as an important endocrine organ secreting numerous proteins, collectively termed adipokines, with potent effects on the metabolism of distant tissues and also on the adipose tissue itself via a paracrine effect (79). Differences in adipokine secretion may contribute to the differing metabolic consequences of visceral and subcutaneous adiposity. The discovery of leptin, an adipocyte-derived hormone which has a profound effect on whole-body metabolism by stimulating energy expenditure and inhibiting food intake firmly established adipose tissue as an important endocrine organ (80). Leptin is differentially expressed between subcutaneous and visceral adipose tissue, with lower mRNA expression in omental adipose tissue (81). Unfortunately leptin as a treatment for typical obesity has been unsuccessful due to resistance to the satiety and weight-reducing effects of leptin in obese individuals, the reason for which has not been elucidated (82). Other adipocyte-derived factors were subsequently discovered including adiponectin, resistin and retinol-binding protein-4 (RBP4). Adiponectin is highly and specifically expressed in differentiated adipocytes and circulates at high levels in the bloodstream (83). Data on depot-specific differences in adiponectin expression and secretion are conflicting with one study finding higher adiponectin secretion and mRNA expression in subcutaneous adipose tissue

(84), another study reporting higher adiponectin secretion from visceral adipocytes (85), and a third reporting higher mRNA expression in subcutaneous adipose tissue but higher secretion from visceral adipose tissue (86). There is a strong and consistent inverse association between adiponectin and both insulin resistance, due to either obesity or lipodystrophy, and inflammatory states (83). Adiponectin is known to increase insulin sensitivity by increasing energy expenditure and fatty-acid oxidation (87). Resistin is expressed by adipocytes in mice but is expressed by macrophages in humans (88). Its role in human insulin resistance remains unclear. RBP4 causes insulin resistance when overexpressed or injected into mice (89). However, the relationship between RBP4 and insulin sensitivity in humans is less clear. RBP4 is more highly expressed in visceral than in subcutaneous adipose tissue (90).

Visceral adiposity and insulin resistance – the chronic inflammation hypothesis.

Concurrent with the discovery of leptin, adipose tissue was identified as a source of pro-inflammatory cytokines with the discovery of TNF- α expression in the adipose tissue of obese humans (91). This was the first adipose tissue derived factor thought to be the link between inflammation, obesity and type 2 diabetes. Originally, it was thought that TNF- α was derived from adipocytes but it is now recognised that adipose tissue macrophages from the stromovascular fraction are the primary source and that macrophage infiltration is increased in obesity (45). Furthermore, visceral adipose tissue exhibits increased macrophage infiltration compared with subcutaneous adipose tissue in both the lean and obese state, with central adiposity exaggerating this preferential accumulation of macrophages into visceral adipose tissue (92). Subsequently, it has been found that other pro-inflammatory macrophage-derived cytokines including MCP-1, IL-8 and IL-6 are expressed in higher amounts in visceral adipose tissue (93-95). Chronic inflammation in adipose tissue, and particularly visceral adipose tissue, has been proposed as the link between obesity and insulin resistance (96) as pro-inflammatory cytokines can directly impair insulin sensitivity, principally through the NF- κ B and JNK pathways (97). However, an obvious question is what causes macrophages to accumulate in

adipose tissue in obesity. It is known that larger, hypertrophied adipocytes secrete higher levels of adipokines and that as adipocytes become larger, there is a shift towards the production of pro-inflammatory and macrophage chemoattractant adipokines (98). It has been proposed that as adipocytes enlarge they become hypoxic. Hypoxia in adipocytes leads to the secretion of a number of inflammation-related adipokines, including angiopoietin-like protein 4, IL-6, leptin, macrophage migration inhibitory factor and vascular endothelial growth factor (99). In this context, it is suggested the hypertrophied adipocytes are signaling that they are soon to become necrotic and are therefore recruiting macrophages in anticipation of scavenging the cellular debris that will result. In support of this theory, when macrophages are observed in adipose tissue they often form crown-like structures around dead adipocytes, where they fuse to form syncytia that sequester and scavenge the residual “free” adipocyte lipid droplet (100). However, the majority of macrophages in obese adipose tissue are associated with fibrosis and are not organised in crown-like structures, arguing against this hypothesis. Furthermore, macrophages in crown-like structures are predominantly M1 (pro-inflammatory), but most other macrophages, particularly those in fibrotic areas, are M2 (anti-inflammatory) (101).

Visceral adiposity and insulin resistance – cell-autonomous differences between subcutaneous and visceral adipocytes.

The divergent metabolic effects associated with visceral and subcutaneous adipose tissue may be due to intrinsic cell-autonomous differences between visceral and subcutaneous adipose tissue. Visceral adipose tissue displays higher rates of fatty acid uptake and release (75); reduced antilipolytic response to insulin (75); increased lipolytic response to catecholamines (102); higher glucocorticoid receptor levels (103) and increased response to glucocorticoids with increased lipoprotein lipase activation (104). The increased rate of lipolysis in visceral adipose tissue may result in higher circulating free fatty acids concomitant with insulin desensitisation in tissues such as liver and skeletal muscle. In rodents, visceral and subcutaneous adipose tissue depots respond differently in response to a high fat diet. Visceral

adipocytes display a greater degree of hypertrophy, whilst subcutaneous adipocytes display a greater degree of hyperplasia (105). Visceral and subcutaneous adipose tissues vary in their susceptibility to the lipodystrophy that occurs during treatment with antiretroviral drugs, which appears to be selective for subcutaneous, but not visceral adipose tissue, an effect that can be recapitulated in adipocytes differentiated from preadipocytes derived from these different adipose tissue depots (106). Studies of gene expression have found major differences in expression of patterning and developmental genes in whole fat tissue as well as adipocytes and preadipocytes from visceral and subcutaneous adipose tissue depots supporting the hypothesis that cells from each location display intrinsic differences at a very early stage of cell differentiation (107). Taken as a whole, these data point to the existence of intrinsic differences between the cells that make up visceral and subcutaneous adipose tissue.

Summary of mechanisms responsible for the adverse metabolic consequences of visceral adiposity

Human lipodystrophy, in which there is limited adipose tissue expansion, mimics many of the metabolic problems seen in obesity including hepatic steatosis, insulin resistance, type 2 diabetes and hypertension. This has led to the hypothesis that limited adipose tissue expandability may account for the link between obesity and metabolic disease in normal individuals. However, inhibition of angiogenesis in adipose tissue, which results in decreased adipose tissue stores, results in paradoxically improved metabolism, in direct conflict with this hypothesis.

Modification of the extracellular matrix by deletion of collagen VI should permit limitless adipose tissue expansion, but collagen VI KO animals display reduced food intake despite having enlarged adipocytes. A critical element of the adipose tissue expandability hypothesis is the ectopic accumulation of triglyceride in non-adipose tissues, which results in a detrimental impact on metabolism. However, this is not universally true as illustrated by elite athletes. While many theories have been proposed to describe the mechanism behind the association between obesity and insulin resistance, the majority do not convincingly explain the epidemiological

association between increased visceral adiposity and insulin resistance. With the failure of the portal hypothesis, the association of visceral adiposity with insulin resistance is best accounted for by intrinsic differences between visceral and subcutaneous adipocytes - both metabolic and endocrine. To test this hypothesis, it is necessary to selectively increase subcutaneous or visceral adipose tissue in a whole animal model, and assess the impact of these selective increases on whole body metabolism.

Adipose tissue transplantation – an emerging tool to study adipose tissue physiology

To interrogate the metabolic impact of selectively increasing visceral or subcutaneous adipose tissue, an *in vivo* technique is required enabling selective manipulation of the visceral or subcutaneous adipose tissue beds. Such selectivity is not possible with increased caloric intake. Therefore, it has been necessary to develop new methods to overcome this problem. Adipose tissue transplantation is one method that has offered great promise. In 2000, Reitman's group pioneered a technique whereby large amounts of adipose tissue, up to 900mg, could be transplanted from a donor mouse into a recipient mouse with a lipodystrophy phenotype. They were able to demonstrate a profound impact on the recipient mouse's metabolism. This study is discussed in further detail below. The importance of the adipose tissue transplantation technique is that it provides a tool for interrogating the metabolic and endocrine communication between adipose tissue and the rest of the body. This is not possible using cell culture systems and was previously only possible after the development of adipose tissue specific animal knock outs or transgenic models. Furthermore the technique of adipose tissue transplantation permits depot-specificity for both the donor graft and for the recipient engraftment site. The challenge in using this technique to study the impact of adipose tissue transplantation on metabolism has been the optimization of the size of the transplanted graft and the site of engraftment, in order to maintain graft tissue integrity with absence of inflammation, until the termination of the experiment.

Adipose tissue transplantation in cosmetic and reconstructive surgery.

Adipose tissue transplantation has been the subject of research for over one hundred years, principally in the field of cosmetic and reconstructive surgery. The first use of adipose tissue autographs in humans was described by Neuber in 1893, who used multiple small adipose tissue grafts from the upper arm to fill a soft-tissue depression in the face caused by tuberculosis. Neuber noted that only small adipose tissue grafts could be utilised, stating “grafts larger than an almond would not give good results” (108). To the present time the use of adipose tissue transplants for aesthetic and reconstructive purposes is plagued by unpredictable rates of adipose tissue resorption, leading to loss of graft volume (109). Recipients of cosmetic adipose tissue transplants have not been studied regarding the metabolic impact of these transplants but given the low volumes of adipose tissue transplanted, the metabolic impact of the adipose tissue graft is unlikely to be meaningful.

Adipose tissue transplantation - a tool for studying adipose tissue biology.

Hausberger, when studying the development of adipose tissue in rodents, performed adipose tissue transplants using immature, perigonadal (epididymal) adipose tissue, which he transplanted subcutaneously into the anterior abdominal wall (Figure 1.3). The adipose tissue grafts consisted of the entire left epididymal fat pad, harvested from a 5 – 6 day old male Wistar rat. These grafts were devoid of lipid and indistinguishable from connective tissue. Hausberger demonstrated that these immature fat pads developed into typical mature adipose tissue and that the final amount of adipose tissue generated was dependent upon the size of the donor graft (110). Similar studies performed by Iyama and colleagues demonstrated that immature epididymal adipose tissue pads transplanted subcutaneously showed development of mature adipocytes, particularly in areas adjacent to growing capillaries, supporting the hypothesis that adipose tissue development and expansion is dependent upon vascularisation (111). Ashwell and colleagues performed numerous adipose tissue transplantation experiments to determine whether the enlarged adipocytes in obesity were due to intrinsic defects within the adipocytes themselves or due to an obesogenic environment. By transplanting

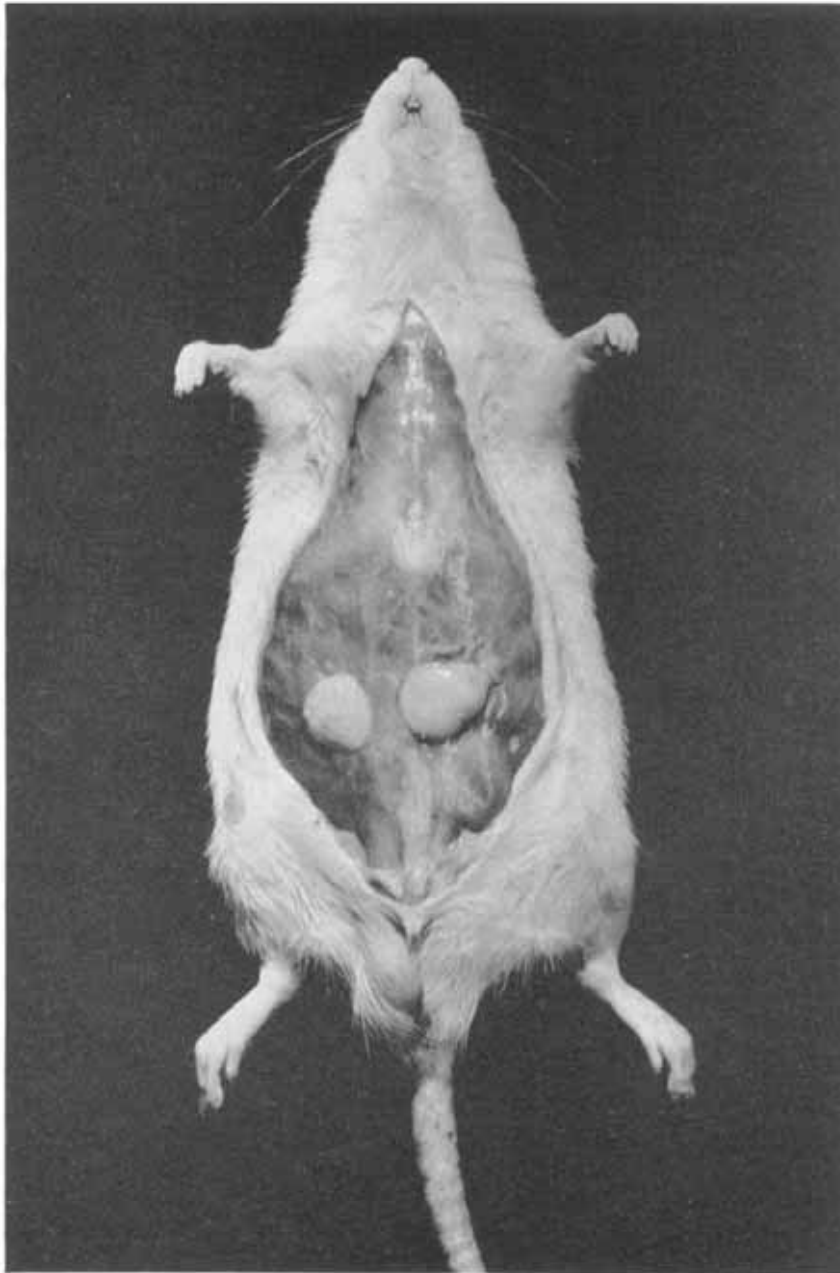


Figure 1.3. Immature adipose tissue grafts develop into mature adipose tissue pads.

The left immature testicular fat pad, divided into two approximately equal parts, transplanted into the right and left subcutaneous space on the abdominal wall. Weight of right transplant, 383 mg; of left transplant, 488 mg. Taken from Hausberger et al 1955 (110).

small amounts (5 – 10 mg) of adipose tissue beneath the renal capsule between lean and obese mice, they elegantly demonstrated that adipocytes within the grafts grow or shrink to match those of the host in both size and fatty acid composition (Figure 1.4) ((112, 113) and reviewed in (114)), indicating that environment was a more powerful determinant than origin in determining these physical characteristics of fat cells. These early studies demonstrated that both immature and mature adipose tissue could successfully survive transplantation, however the amounts of adipose tissue were small and the metabolic impact of the transplants was not determined.

Adipose tissue transplantation - a tool for studying the regulation of adipose tissue mass.

Lipectomy studies in rodents indicate that compensatory fat hypertrophy occurs in remaining endogenous adipose tissue depots in response to surgical depletion of adipose tissue stores (reviewed in (115)). Adipose tissue transplantation experiments were performed to determine whether surgical addition of adipose tissue would provoke a compensatory loss of endogenous adipose tissue. Rooks and colleagues transplanted perigonadal adipose tissue subcutaneously in mice to increase total body fat stores by approximately 10%. In the first experiment, surgical addition of adipose tissue resulted in a significant reduction in the mass of endogenous adipose tissue stores at 5 weeks after transplantation, but this result was unable to be replicated in a second experiment (116). A similar study performed in Siberian hamsters also showed no compensatory decrease in adipose tissue stores after the surgical addition of perigonadal fat to a subcutaneous location (117) and in some experiments an increase in endogenous adipose tissue stores (118). Interestingly, if adipose tissue is replaced after lipectomy as subcutaneous transplants, resulting in no net change in adipose tissue mass, the compensatory hypertrophy of endogenous adipose tissue depots is exaggerated but only if epididymal adipose tissue, and not inguinal adipose tissue is transplanted (117). Unfortunately whether inguinal and perigonadal adipose tissue grafts had a differential impact on metabolism was not investigated.

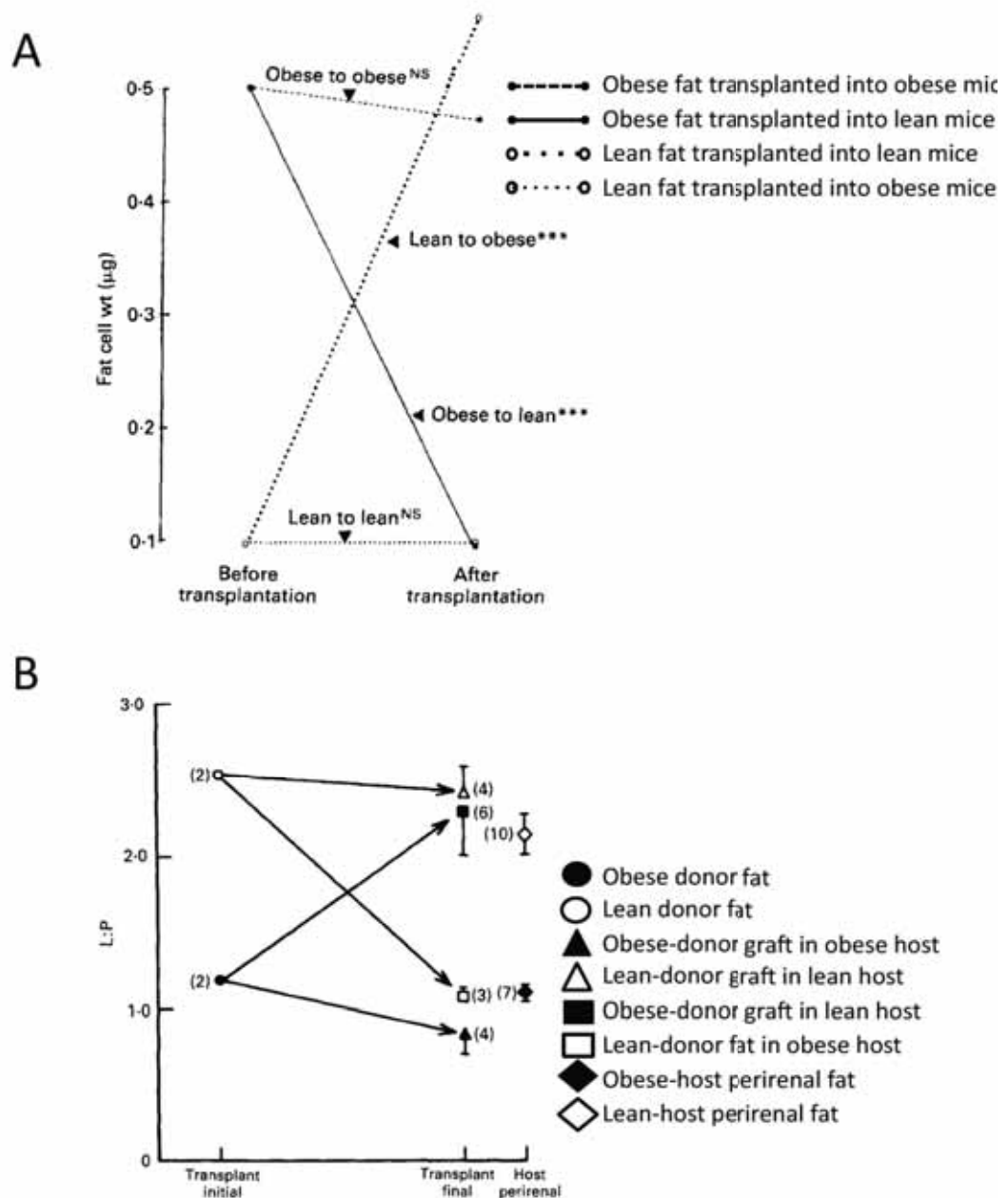


Figure 1.4. Adipose tissue transplanted from lean and obese donors assumes the characteristics of the host endogenous adipose tissue with respect to cell size (A) and lipid content (B).

Fat cell size in grafts between genetically obese mice (*ob/ob*) and their lean counterparts (A). *** $p < 0.001$. NS, not significant.

Changes in the ratio of linoleic acid:palmitoleic acid (L:P) in the neutral lipids of adipose tissue transplanted between lean and obese mice (B). The results are means with standard errors represented by vertical bars for the number of animals shown in parentheses. Taken from Ashwell et al 1992 (114))

Adipose tissue transplantation - a tool for studying the metabolic effects of increased adipose tissue mass.

Adipose tissue transplantation as a tool for studying the metabolic impact of surgically increasing adipose tissue mass has been historically limited by the small size of the adipose tissue grafts (<50 mg). In 2000, Reitman's group developed a technique of adipose tissue transplantation using metabolically meaningful amounts of adipose tissue (119). A mouse-model of lipodystrophy, A-ZIP/F-1, which has virtually no adipose tissue, was used as the recipient animal. The A-ZIP/F-1 mice express a dominant negative protein that heterodimerizes with and inactivates members of the C/EBP and JUN families of B-ZIP transcription factors selectively in adipose tissue, inhibiting adipose differentiation. These animals have a phenotype that resembles human lipodystrophy, with absence of adipose tissue, insulin resistance and hyperglycemia, hyperlipidemia, fatty liver and organomegaly. Reitman's group hypothesized that if the phenotype of these animals was due to lack of adipose tissue, transplantation of adipose tissue from normal donors should reverse the diabetic phenotype in these animals, proving that lack of adipose tissue was responsible for the adverse metabolic consequences of lipodystrophy.

The transplantation of up to 900mg of adipose tissue was successfully achieved using adipose tissue from wild-type littermates. Adipose tissue grafts were surgically implanted subcutaneously through small incisions in the skin of the back, inserting one graft weighing 100 – 150 mg per incision. At 13 weeks after transplantation, grafts remained viable with a healthy macro-and microscopic appearance (Figure 1.5). Transplantation of wild-type adipose tissue to the subcutaneous region had a profound impact on metabolism with decreased food intake, reversal of hyperglycemia and lowered serum insulin levels, reduced hepatic steatosis and increased insulin sensitivity and glucose uptake into muscle (119) (120). This confirmed that diabetes in A-ZIP/F1 mice is caused by a lack of adipose tissue. This was the first study to describe the successful transplantation of adipose tissue in amounts large enough to impact on metabolism. Interestingly, both inguinal (subcutaneous) and parametrial (intra-abdominal) fat grafts were equally

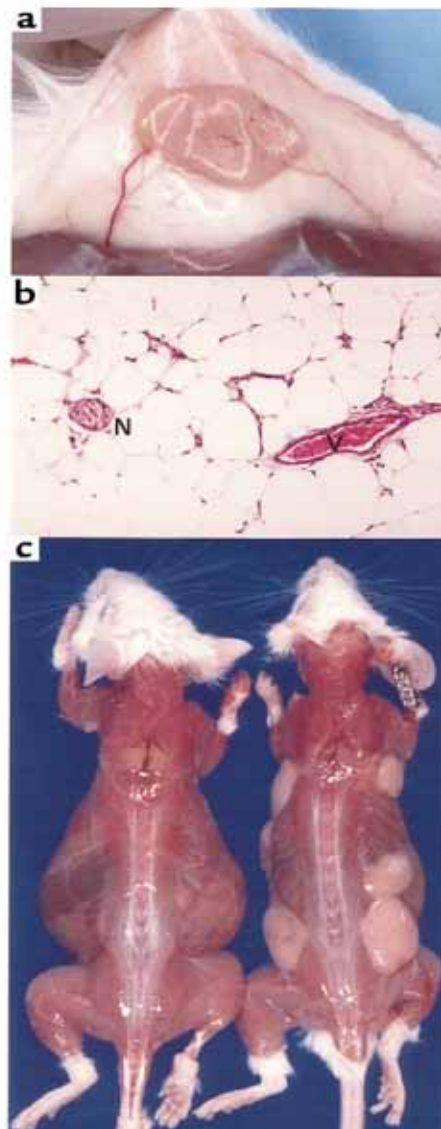


Figure 1.5. Viability of adipose tissue grafts weighing up to 900 mg after transplantation

(a) Adipose tissue graft 3 weeks after transplantation. The graft (yellow, at center, originally 100 mg), attached to the skin (white), was dissected from the muscle (brown at bottom). (b) Adipose tissue graft 13 weeks after transplantation. Hematoxylin and eosin stain. Original magnification x200. Note the blood vessel (V) and nerve (N). (c) A-ZIP/F-1 mice 13 weeks after transplantation. Skin was dissected from a sham-operated mouse (left) and from a mouse that received 900 mg of parametrial fat (right) in seven grafts (a ventral graft is not visible) From Gavrilova et al, 2000 (119).

efficacious in reversing the diabetic phenotype (119). The beneficial effects of transplantation were dose-dependent, suggesting a possible endocrine mechanism for the antidiabetic action of adipose tissue, in which hormone production is proportional to fat mass. The metabolic benefits of adipose tissue transplantation were observed in A-ZIP/F1 mice despite sub-physiological amounts of adipose tissue being achieved. At 900 mg, adipose tissue grafts represent less than 4% of body weight, less than the normal 5 – 23% body fat. Using the technique of adipose tissue transplantation, the causative role of lack of adipose tissue in lipoatrophic diabetes was clearly demonstrated, and the researchers postulated this was the result of a lack of leptin secretion and the failure of adipose tissue to take up glucose, triglyceride and free fatty acids. As a consequence, triglyceride is stored in liver and muscle, which has adverse effects on glucose metabolism.

To further investigate the mechanism whereby transplantation of adipose tissue reversed the diabetic phenotype in A-ZIP/F1 mice, adipose tissue transplantation was performed using leptin-deficient *ob/ob* fat (121). Adipose tissue transplantation using leptin-deficient *ob/ob* fat had no effect on the phenotype of A-ZIP/F1 mice, whereas leptin infusion improved metabolism. Furthermore, the presence of *ob/ob* adipose tissue did not result in additional metabolic improvement in conjunction with leptin infusion (121). These results suggest that leptin deficiency, rather than the inability to store lipid per se, plays a major role in causing the metabolic complications of lipoatrophy. These results illustrate that adipose tissue transplantation is a powerful technique for studying the endocrine communication between adipose tissue and the rest of the body.

Although the adipose tissue transplants performed by Reitman's group were small, the leptin produced from the adipose tissue grafts was sufficient to have a profound impact on metabolism. Therefore the technique of adipose tissue transplantation can be used as a tool to interrogate the metabolic effects of altered adipokine secretion from adipose tissue, and in particular to study the metabolic impact of genetic manipulations in adipose tissue that alter adipokine secretion. Mice that

lack acyl CoA:diacylglycerol acyltransferase 1 (DGAT1), a key enzyme in the synthesis of mammalian triglycerides, display a lean phenotype and have increased insulin sensitivity. These mice are protected against diet-induced obesity and insulin resistance. DGAT1 is expressed highly in white adipose tissue and was hypothesized to alter the secretion of adipocyte-derived factors that act to increase whole body energy expenditure and glucose metabolism (122). If this hypothesis were correct, transplantation of adipose tissue lacking DGAT1 into wild-type mice would result in secretion of these adipocyte-derived factors, protecting the recipient animals from obesity and insulin resistance.

Wild-type mice, *Agouti yellow* (obese mice that are insulin and leptin resistant due to antagonism of melanocortin receptors) and *ob/ob* (obese due to leptin deficiency) mice received perigonadal adipose tissue transplants (500mg) from donor *DGAT1*^{-/-} mice into a subcutaneous site, equivalent to a 30% increase in total adipose tissue stores for wild-type mice and less than 10% for *Agouti yellow* and *ob/ob* mice. High fat-fed wild-type mice receiving *DGAT1*^{-/-} adipose tissue grafts demonstrated improved metabolism with decreased body weight, decreased adipose tissue pads, decreased muscle triglyceride content, increased energy expenditure and increased insulin sensitivity. *Agouti yellow* mice receiving *DGAT1*^{-/-} adipose tissue grafts showed an identical metabolic improvement, whereas *ob/ob* mice transplanted with *DGAT1*^{-/-} adipose tissue grafts showed no metabolic improvement, possibly because the degree of obesity and insulin resistance in *ob/ob* mice is too severe. *DGAT1*^{-/-} adipose tissue has a two-fold increased expression of adiponectin, which enhances fatty acid oxidation and insulin sensitivity. Wild-type mice receiving *DGAT1*^{-/-} adipose tissue grafts had significantly higher serum levels of adiponectin than control animals (122). Remarkably, this study demonstrates that a small amount of transplanted adipose tissue is able to have an important endocrine effect on whole body metabolism. Adipose tissue transplantation is a valuable and effective tool to interrogate the endocrine and metabolic effects of genetically engineered adipose tissue. Therefore, adipose

tissue transplantation should be an effective tool to interrogate the differential endocrine and metabolic effects of visceral and subcutaneous adipose tissue.

Proteomics and the identification of secretory proteins.

Since the identification of leptin and TNF- α as adipose secretory factors, there has been considerable interest in the identification of novel adipokines, especially those that are differentially produced by visceral and subcutaneous adipose tissue. Given the candidates are unknown, mass spectrometry based proteomics is an ideal approach. A typical mass spectrometry experiment involves five stages. In stage 1 (Figure 1.6), a complex mixture of polypeptides, such as a cell lysate, is simplified using some form of fractionation or enrichment, such as affinity purification or SDS-PAGE. As intact proteins are less amenable to electrospray ionization, proteins are enzymatically cleaved to produce peptides in stage 2, usually by trypsin. Trypsin is chosen as it produces peptides with C-terminally protonated amino acids, which are typically 15 amino acids long. Peptides of this length are optimal for mass spectrometry as they ionize well and their amino acid sequences, in contrast to shorter peptides, can be identified as unique. Only two unique peptides are usually sufficient to recognize a protein (123). In stages 3 – 5, the peptides are typically subjected to liquid chromatography coupled tandem mass spectrometry. The liquid chromatography step in stage 3 further separates peptides, typically based on their hydrophobicity. Peptides are sprayed directly from the liquid chromatography column into an ion source during which they are nebulized into small, highly charged droplets. These droplets rapidly evaporate and impart their charge onto the peptides. In stage 4, multiply protonated peptides enter the first stage of the mass spectrometer and a mass spectrum of all peptides eluting at this time point is produced. In stage 5, one peptide species out of the mixture is selected in the ion trap and is then dissociated by collision with an inert gas, such as argon or nitrogen. The resultant collision – induced dissociation (CID) fragments are separated in the second stage of the mass spectrometer, producing the MS/MS spectrum. At the conclusion of the experiment, the stored peptide mass and the peak pattern in the MS/MS spectrum are matched against a protein sequence database to determine

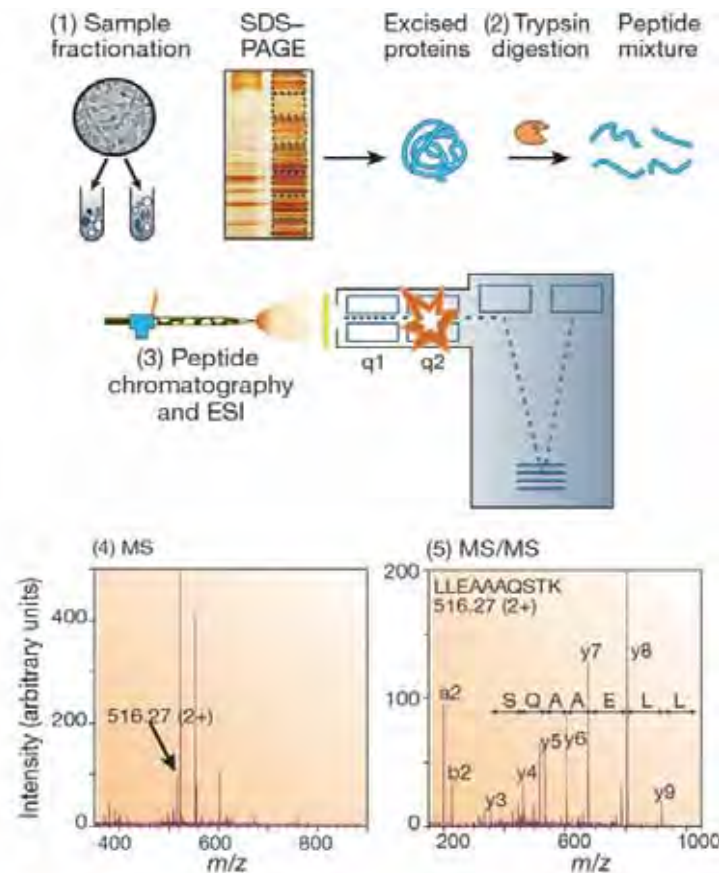


Figure 1.6. Generic mass spectrometry (MS)-based proteomics experiment.

The typical proteomics experiment consists of five stages. In stage 1, proteins are isolated from cell lysate or tissues by biochemical fractionation or affinity selection. This often includes a final step of one-dimensional gel electrophoresis, and defines the 'sub-proteome' to be analysed. MS of whole proteins is less sensitive than peptide MS and the mass of the intact protein by itself is insufficient for identification. Therefore, proteins are degraded enzymatically to peptides in stage 2, usually by trypsin, leading to peptides with C-terminally protonated amino acids, providing an advantage in subsequent peptide sequencing. In stage 3, the peptides are separated by one or more steps of high-pressure liquid chromatography in very fine capillaries and eluted into an electrospray ion source where they are nebulized in small, highly charged droplets. After evaporation, multiply protonated peptides enter the mass spectrometer and, in stage 4, a mass spectrum of the peptides eluting at this time point is taken (MS_1 spectrum, or 'normal mass spectrum'). The computer generates a prioritized list of these peptides for fragmentation and a series of tandem mass spectrometric or 'MS/MS' experiments ensues (stage 5). These consist of isolation of a given peptide ion, fragmentation by energetic collision with gas, and recording of the tandem or MS/MS spectrum. The MS and MS/MS spectra are typically acquired for about one second each and stored for matching against protein sequence databases. The outcome of the experiment is the identity of the peptides and therefore the proteins making up the purified protein population. Taken from Aebersold et al. 2003 (124).

the identity of the peptide and subsequently the protein of origin (124). This technique allows the rapid identification of thousands of polypeptides and, in turn, the corresponding proteins from which they are derived in a relatively short time. Due to the stochastic nature of peptide selection, and limitations in sequencing speed, only a selection of the peptides present is typically sequenced. To increase depth of coverage, it is essential to optimize the sample preparation and remove contaminating proteins that might dominate the MS. This issue is particularly relevant to the identification of low abundance proteins, which may be of the most bioactive relevance, in comparison to highly abundant proteins, for example structural and cytoskeletal proteins.

Mass spectrometry is very useful for identifying proteins in complex samples. To take this method to the next level it was necessary to develop quantitative methods, so that one could compare the level of different proteins between two or more experimental conditions. The advent of isotopic labelling techniques has allowed the relative quantification of a protein between two separate samples by mass spectrometry. Isotopic labelling exploits the existence of naturally occurring, stable isotopes of hydrogen, carbon, nitrogen and oxygen (^2H , ^{13}C , ^{15}N , and ^{18}O) (125). The rationale behind stable isotope labelling is to create a mass shift that distinguishes identical peptides from different samples within a single MS analysis. Therefore, if two samples, labelled with two different isotopes are mixed together in equal ratio and subjected to mass spectrometry each peptide identified will have two peaks of intensity (one peak for each labelled isotope). These peaks represent shifts in the mass to charge ratio of the peptide as a result of the incorporation of the isotope. The relative intensities of the peaks provide a quantitative guide to the abundance of the protein in each of the two samples. This technique is especially useful as it can allow the relative quantification of thousands of protein species in a single experiment.

There are a number of quantitative proteomic methods that have been developed. One method is proteolytic ^{18}O -labelling, in which isotope labelling occurs

concurrently with trypsin digestion of proteins (126). Using this method, only two sample groups can be compared. One sample incorporates ^{16}O by digestion with trypsin in H_2^{16}O solvent, and the other sample incorporates ^{18}O by digestion with trypsin in H_2^{18}O . Samples are then mixed together and subjected to mass spectrometry. The incorporation of either a ^{16}O or ^{18}O atom results in a molecular weight shift that allows for relative protein quantification. There are a number of limitations with this approach. First, variability may arise from different efficiencies in the proteolytic step, as the two samples cannot be mixed prior to trypsin digestion. Second, this approach relies heavily upon the scrupulous evaporation of pre-existing water molecules prior to the addition of either H_2^{16}O or H_2^{18}O . Third, given the existence of only two isotopes of oxygen only two samples can be compared.

Alternate approaches analogous to proteolytic ^{18}O -labelling involve using commercially available isotope coded chemical tags that can be covalently added to trypsin-digested proteins. These techniques include iTRAQ (isobaric tags for relative and absolute quantitation) (127) and ICAT (isotope coded affinity tag) (128). As with proteolytic ^{18}O -labelling, the isotope tag is added after the trypsin digest reaction. This is disadvantageous as performing manipulations of different samples independently of one another may introduce experimental error into several, but not all, samples, resulting in false reporting of protein changes between samples. An advantage of iTRAQ technology is that more than two samples can be analyzed at a time (129).

An alternate method, which circumvents the limitations of the former methodologies by incorporating isotope label prior to experimental manipulation, is SILAC (stable isotope labelling by amino acids in cell culture) (130). This method involves growing cells in culture media supplemented with non-radioactive, isotopically labelled amino acids; one contains “light” (normal) isotopes in the amino acid(s) and the other contains one or more “heavy” isotopes in the amino acid(s). The heavy amino acid(s) can contain ^2H instead of H , ^{13}C instead of ^{12}C or ^{15}N

instead of ^{14}N . Incorporation of the heavy amino acid into a peptide leads to a known mass shift compared with the peptide that contains the light version of the amino acid (for example, 6 Dalton in the case of L-arginine and ^{13}C -labelled L-arginine), but importantly does not cause any other chemical changes. As the objective of SILAC is to compare two or more proteomes by the molecular weight of the light or heavy amino acids incorporated during the growth of the cell populations, complete labelling is essential. Even for proteins with no significant turnover, complete labelling – that is the replacement of normal with SILAC amino acids in all proteins – is achieved after five cell doublings (131). SILAC labelling with arginine and lysine, followed by digestion with trypsin, ensures that every peptide contains either one labelled arginine or lysine, as trypsin cleaves peptide chains on the C-terminal side of lysine or arginine. Cell populations labelled with different isotopes may be treated with the intervention of interest, and proteins obtained through cell lysis or collection of conditioned media. At this early stage of the experiment, different samples are mixed together in equal proportions. The extracted proteins are digested with trypsin and the generated peptides are subsequently quantified by mass spectrometry. Shifts in peptide molecular weight, resulting from incorporation of a single labelled arginine or lysine, are used to identify changes in relative protein abundance between samples, as described above. Although this technique relies on extensive labelling of cells in culture with amino acid isotopes, thereby excluding the use of this technique for non-viable samples, it has the advantage of being able to mix samples at an early stage in the experiment, to avoid later experimental bias. Any protein/peptide losses in the remaining steps should occur equally for the light and heavy isotope-containing proteins/peptides.

Protein secretion – classical and non-classical.

Determining the subcellular localization of a protein is an important clue to its function. Proteins have intrinsic signals that govern their transport and localization in the cell (132, 133). Soluble secretory proteins typically contain signal peptides, which direct them to the translocation apparatus of the endoplasmic reticulum (ER)

(134, 135). The signal peptide is an N-terminal peptide, typically 15–30 amino acids long, which is cleaved off during translocation of the protein across the membrane. There is no simple consensus sequence for signal peptides, but they typically show three distinct compositional zones: an N-terminal region (n-region) which often contains positively charged residues, a hydrophobic region (h-region) of at least six residues and a C-terminal region (c-region) of polar uncharged residues with some conservation at the - 3 and - 1 positions relative to the cleavage site. Once secretory proteins have been translocated into the endoplasmic reticulum they are transported through the Golgi apparatus and released into the extracellular space by fusion of Golgi-derived secretory vesicles with the plasma membrane. This pathway of protein export from eukaryotic cells is known as the classical or ER/Golgi-dependent secretory pathway (136). However, not all proteins with a signal peptide are actually secreted to the outside of the cell – some proteins have specific retention signals that divert them to other intracellular compartments, such as lysosomes. Similarly, not all secretory proteins have signal peptides, with some proteins including fibroblast growth factors, interleukins and galectins, being secreted by the ‘non-classical’ pathway. Although non-classical protein secretion was recognized more than 15 years ago, the molecular mechanisms regulating this process remain poorly defined (136).

The presence of a signal peptide can be exploited by genetic approaches to facilitate the identification of secreted proteins. One method is the signal sequence trap (SST) developed by Tashiro and colleagues in 1993 (137). The method identifies signal-sequence containing cDNAs by their ability to direct a signal sequence–deficient CD25 to the cell surface where it can be detected by antibody staining. Using this methodology, cell or tissue specific cDNA libraries can be screened to identify novel secretory proteins. Since 1993, SST methodologies have been refined to improve sensitivity and efficiency, using different reporters to demonstrate the presence of a signal peptide. SST has been used to identify adipocyte specific genes encoding membrane and secreted proteins from rodent adipose tissue and 3T3-L1 adipocytes, a preadipocyte cell line that can be converted to lipid-laden adipocytes

in the presence of 1-methyl-3-isobutylxanthine, dexamethasone and insulin. Several novel adipokines have been identified including interferon-stimulated gene 12b (ISG12b), chemerin and five previously unidentified proteins (138-140).

Bioinformatic approaches have also been developed to computationally predict secretory proteins based on their amino acid sequence. SignalP identifies classically secreted proteins by the presence of signal peptidase I cleavage sites (141). As not all secreted proteins have a signal peptide, the SecretomeP program has been developed to predict non-classically secreted proteins (142). These internet-accessible tools can assist in predicting whether a protein identified using high-throughput mass-spectrometry experiments is likely to be a secretory protein.

Proteomics and the identification of adipokines.

In order to identify novel adipokines differentially produced by subcutaneous and visceral adipose tissue, a quantitative proteomic approach is required such as SILAC. While there have been a number of studies using quantitative proteomic approaches to interrogate the adipocyte secretome (143-146), none have quantified differences in the secretomes from subcutaneous and visceral adipose tissue. Chen and co-workers in 2005 utilised quantitative mass spectrometry to identify changes in protein secretion from primary rat adipocytes incubated in the presence or absence of insulin (143). Conditioned media was obtained, concentrated and subjected to extensive separation by liquid chromatography. Eight protein fractions were collected and subjected to Lys-C and trypsin digestion. Aliquots of the tryptic peptides from basal and insulin-treated samples were evaporated to dryness and redissolved in H_2^{16}O or H_2^{18}O , respectively. This results in the incorporation of ^{16}O or ^{18}O atoms into peptides from the basal and insulin-treated samples respectively, causing a small shift in peptide molecular weight that can be detected by mass spectrometry as a shift in the mass to charge ratio. This ratio reflects the relative abundance of proteins from different samples, and in this case was used to determine the effect of insulin on protein secretion from adipocytes. Using this approach 183 proteins were identified, however, there was a

possibility that many of these proteins were contaminating cytosolic proteins as a result of cell lysis. To circumvent this, each of the 183 candidates was scanned for the presence of a signal peptide using SignalP. Only 84 proteins contained a signal peptide. Therefore the majority of proteins detected by this technique were cellular contaminants. This is a significant limitation of this technique as the presence of a large number of contaminating proteins could block the detection of low abundance secreted proteins.

Alvarez-Llamas and co-workers in 2007 were the first to utilize metabolic labelling to interrogate the adipose tissue secretome (144). In these experiments minced visceral adipose tissue explants rather than isolated primary adipocytes were used so that cross-talk between adipocytes and non-adipocyte components of the stromovascular fraction, which contribute to the secretome and modulate adipokine secretion by adipocytes, was not disrupted. The use of minced adipose tissue explants introduced entrapped serum as another source of possible protein contaminants in addition to cytosolic protein contaminants from cell lysis. To minimise serum contaminants, numerous wash steps were undertaken. Only after this comprehensive washing protocol were explants incubated with SILAC medium. Subsequently, conditioned media was collected and proteins were subjected to mass spectrometry. The incorporation of an isotopic label in a protein indicated that the protein was newly synthesized ex-vivo in the visceral adipose tissue explant and was not derived from a serum contaminant. This allowed discrimination between adipose derived secretory proteins and serum proteins that may exist in the tissue explants. However, again contamination from cytosolic proteins was not accounted for by this technique. Furthermore, the multiple washing steps required to eliminate contaminating serum proteins resulted in explants being cultured for 48 - 114 hours, which likely induces metabolic stress, such as hypoxia, which may influence adipokine secretion.

In 2009, Roelofsen and co-workers adapted the SILAC labelling experimental protocol described above (146), which had been published earlier by the same

group (144). In their first study, ^{13}C -labelled lysine incorporation into secreted proteins was simply used to indicate the origin of the identified protein. In this study, the effect of insulin on the secretome was determined by comparing incorporation rates of ^{13}C -labelled lysine in the presence and absence of insulin. This approach was given the name CILAIR (comparison of *i*sotope-/*l*abelled *a*mino acid incorporation rates) (146). As in their earlier study, prolonged washing steps, long ex-vivo incubation times and contamination by cytosolic proteins persisted as disadvantages of this technique. A further limitation of this technique was the use of a single isotope label. As only one label was used, the basal and insulin-stimulated samples could not be mixed prior to concentration by ultrafiltration, fractionation by SDS-PAGE, in-gel digestion of excised bands and LC-MS/MS analyses, potentially introducing experimental bias. For example, it would have been far more efficient if different isotopes were used for each treatment, so that samples could be mixed together and subjected to mass spectrometry at the same time, avoiding bias from different mass spectrometry runs. I have used an adaptation of the CILAIR protocol to analyse the secretomes from subcutaneous and visceral adipose tissue, and this is described in more detail in Chapter 4.

Enrichment of secreted proteins by lectin affinity chromatography.

Previous attempts to interrogate the secretome of adipocytes or adipose tissue by mass spectrometry have been limited by the presence of cytoplasmic proteins from dead or dying cells, which dilute low-abundance true secretory proteins in the conditioned media, rendering them less detectable by mass spectrometry. Lectin affinity chromatography provides an ideal way to circumvent this limitation, by enriching the conditioned media sample for secretory proteins. Secretory proteins differ from cytosolic proteins in their synthesis. As discussed above, unlike cytosolic proteins, secretory proteins uniquely possess an N-terminal hydrophobic signal peptide, which targets them to ribosomes on the surface of the endoplasmic reticulum (132, 133, 147). As the growing polypeptide chain is fed into the lumen of the endoplasmic reticulum carbohydrate side chains are conjugated to asparagine residues that lie within the Asn – X – (Ser/Thr) motif (148). The addition of these

carbohydrates is termed N-glycosylation, and this post-translational modification is thought to add stability to secretory proteins in the extracellular space (148-150). N-glycosylation is a characteristic common to secretory proteins and largely absent from cytosolic proteins. Therefore, selectively enriching conditioned media for N-glycosylated proteins would largely exclude contaminating cytosolic proteins and enrich secretory proteins. Lectins are a class of proteins that have high affinity for glycosylated proteins (151) and lectin affinity chromatography has recently been used with some success to identify secreted proteins from serum (152). Lectin affinity chromatography using the lectin Concanavalin A, which preferentially binds to mannose residues of the type found in N-linked secretory glycoproteins, has been successfully used by our group to enrich for secreted proteins in conditioned media from 3T3-L1 adipocytes (153). In this study, the technique of lectin affinity chromatography using Concanavalin A has been adapted to enrich for secreted proteins in conditioned media from adipose tissue explants, primary pre-adipocytes and adipose tissue microvascular endothelial cells as described in Chapter 4.

Specific aims of this investigation.

I hypothesize that visceral and subcutaneous adipocytes are intrinsically discrete adipocyte lineages and that the metabolic differences that have been ascertained in these adipocytes are independent of their environment and are genetically programmed. In mammals, two different classes of adipocytes have been described – white adipocytes and brown adipocytes. I suggest that white adipocytes should be further subclassified into multiple subsets. As visceral adipocytes are intrinsically different to subcutaneous adipocytes, I hypothesize that the transplantation of additional visceral adipose tissue in a diet-induced obesity mouse model of type 2 diabetes will have a different effect on metabolic parameters compared with the transplantation of additional subcutaneous adipose tissue. I predict that the transplantation of visceral adipose tissue will increase the rapidity and severity of insulin resistance and hyperglycemia in this model and that the transplantation of subcutaneous adipose tissue will have a protective or null effect on metabolism. Using gene technology I plan to identify changes in gene expression in the

transplanted adipose tissue responsible for the metabolic effects observed after transplantation.

I further hypothesize that non-adipocyte components of adipose tissue, including pre-adipocytes and microvascular endothelial cells also display depot-specificity in a manner similar to mature adipocytes. This will be investigated by determining the secretomes of pre-adipocytes and microvascular endothelial cells from subcutaneous and visceral adipose tissue depots using a quantitative proteomics approach. A key component of this hypothesis is that depot-specific cross-talk exists between adipocyte and non-adipocyte components of adipose tissue.

The specific aims of this research are:

1. To develop a cross-depot adipose tissue transplantation technique in a mouse model of diet-induced type 2 diabetes. The development of this animal model is extremely important, as it will allow the investigation of the fundamental differences between discrete adipose tissue depots. The long-term maintenance of a depot-specific environment is not possible using any *in-vitro* techniques.
2. To test the hypothesis that the metabolic difference between discrete adipose tissue beds is an intrinsic property of the adipocytes rather than the environment in which the cells reside utilizing the cross-depot adipose tissue transplantation technique. I hypothesize that the addition of visceral adipose tissue will accelerate the onset of insulin resistance and hyperglycemia in a diet-induced obesity mouse model of type 2 diabetes whereas addition of subcutaneous adipose tissue will have a protective or null effect on metabolism.
3. To use gene technology to identify changes in gene expression in the transplanted adipose tissue potentially responsible for the metabolic effects observed after transplantation.
4. To determine the secretome of non-adipose components of visceral and subcutaneous adipose tissue using quantitative proteomics to determine

whether intrinsic, depot-specific differences are also present in the non-adipocyte components of adipose tissue.

Chapter 2

Subcutaneous adipose tissue transplantation into the intra-abdominal compartment reveals a unique and beneficial effect on metabolism.

Data from this chapter were published in “Studies of regional adipose transplantation reveal a unique and beneficial interaction between subcutaneous adipose tissue and the intra-abdominal compartment.” Hocking SL, Chisholm DJ, James DE. Diabetologia 51(5): 900-2, 2008.

Abstract

Obesity is a risk factor for insulin resistance and type 2 diabetes. Intra-abdominal adipose tissue confers a higher risk for these diseases than subcutaneous adipose tissue. To determine whether intra-abdominal adipose tissue has deleterious effects due to its location or the unique properties of intra-abdominal adipocytes I have used a regional adipose tissue cross-transplantation approach in which subcutaneous and intra-abdominal adipose tissue pads from donor C57BL/6J mice were transplanted into the subcutaneous or intra-abdominal compartment of recipient, genetically identical C57BL/6J mice placed on a high fat diet. Mice receiving subcutaneous transplants into the intra-abdominal compartment displayed significantly reduced fat mass, in both transplanted and endogenous adipose tissue beds, and improved glucose tolerance. These metabolic benefits were not observed in mice transplanted with subcutaneous adipose tissue into the subcutaneous space nor with intra-abdominal adipose tissue into either compartment. These findings suggest a unique beneficial metabolic effect of transplanting subcutaneous adipose tissue into the intra-abdominal compartment that is likely due to the secretion of one or more factors capable of acting systemically to confer this metabolic advantage.

Introduction

Obesity is associated with numerous adverse medical consequences including insulin resistance and Type 2 diabetes. The regional distribution of adipose tissue, as opposed to overall adiposity, is a more accurate determinant of risk. In particular, accumulation of adipose tissue in the abdominal or visceral space carries a more severe disease risk than accumulation of subcutaneous fat (6-8, 10).

The disparity in disease risk with accumulation of abdominal or subcutaneous adipose tissue has raised two major questions. First, how does accumulation of adipose tissue in the abdominal space preferentially cause metabolic impairments? The 'portal hypothesis' proposes that increased abdominal fat mass increases the delivery of non-esterified fatty acids (NEFAs) through the portal circulation to the liver leading to glucose intolerance, hyperinsulinemia, insulin resistance and dyslipidemia (154). Alternatively, recent knowledge that adipose tissue secretes pro-inflammatory factors has raised the possibility that cytokine secretion may contribute to metabolic disease. Consistent with the latter model several key differences have been noted between abdominal and subcutaneous adipose tissue. Abdominal adipose tissue displays higher rates of fatty acid uptake and release (75); reduced antilipolytic response to insulin (75); higher glucocorticoid receptor levels (103); increased response to glucocorticoids with increased lipoprotein lipase activation (104); increased lipolytic response to catecholamines (102); elevated expression and secretion of angiotensinogen, interleukin-6 and plasminogen-activator inhibitor-1 and reduced expression and secretion of leptin and adiponectin (102). In rodents, surgical removal of abdominal but not subcutaneous adipose tissue, improved insulin sensitivity and glucose tolerance (77, 78). However, in these studies the adipose tissue depots removed did not drain through the portal circulation, so the mechanism for insulin resistance with abdominal fat accumulation cannot be explained by the portal hypothesis alone.

In view of the physiological and molecular differences between abdominal and subcutaneous adipose tissue the second and perhaps more fundamental question is how do these unique characteristics arise? The two most likely possibilities, which are not mutually exclusive, are either that the local environment changes the properties of adipose tissue to induce changes such as those described above or that such differences are an intrinsic property of the adipocyte itself that is independent of environment. The former could include innervation, blood supply or the presence of discrete subsets of non-parenchymal cells such as macrophages, while the latter may be due to lineage specificity in the adipocyte differentiation program. DNA microarray analysis has revealed discrete differences between these two adipose tissue depots. The expression of a number of developmental genes, including Nr2f1, Gpc4, Thbd, HoxA5 and HoxC8 was found to be higher in abdominal versus subcutaneous adipose tissue, and these differences in expression persisted during *in vitro* culture and differentiation (107), supporting the hypothesis that cells from each location display intrinsic differences at a very early stage of cell differentiation. However, the complication of such studies is the difficulty excluding the possibility that the local environment programs the adipocyte rather than it being an intrinsic feature of the cell per se. Pre-adipocytes have been isolated from different locations and studied in culture. Adipocytes generated from abdominal pre-adipocytes retain some of the features of the native tissue such as reduced leptin secretion, increased TNF α production and a greater lipolytic response to catecholamines compared to adipocytes generated from subcutaneous pre-adipocytes (155). However, because pre-adipocytes isolated under such conditions display limited differentiation potential *in vitro* it is again difficult to exclude a role for the local environment that is retained when the cells are in culture.

To address the contribution of adipocyte origin versus local environment to whole body metabolism I have utilised a regional adipose tissue cross transplantation approach in which subcutaneous and intra-abdominal adipose tissue pads from donor mice were transplanted into the subcutaneous or intra-abdominal compartment of recipient high fat fed mice. Our studies reveal the surprising

finding that transplantation of abdominal fat into either the abdominal or subcutaneous space is without consequence on the metabolism of a recipient animal whereas transplantation of subcutaneous adipose tissue selectively into the abdominal space had a significant protective effect on adiposity and glucose tolerance.

Research design and methods

Choice of animal model

As previously mentioned, the technique of adipose tissue transplantation using metabolically meaningful amounts of adipose tissue was first described in 2000 by Reitman's group (119). This was the first study to describe the successful transplantation of adipose tissue into mice in amounts large enough to impact on metabolism. Mice were chosen as the rodent model for Reitman's study and in the experiments conducted for this thesis as in-bred mouse strains are genetically identical and transplantation of adipose tissue between littermates can occur without the need for immunosuppression to prevent rejection.

Numerous mouse models of obesity, insulin resistance and type 2 diabetes are available for experimental purposes. Several strains of mice have been identified and propagated because of spontaneous mutations that result in obese phenotypes. The *Lep^{ob}/Lep^{ob} (ob/ob)* mouse has a spontaneous single base substitution (C428T) in the leptin gene that results in premature termination of leptin synthesis, prohibiting the secretion of mature leptin. This results in hyperphagia, hypothermia, hyperglycemia, hyperinsulinemia, hypercorticotesteronemia, hypothyroidism, reduced energy expenditure, infertility and early-onset morbid obesity (80, 156, 157). *Lep^{db}/Lep^{db} (db/db)* mice have a similar phenotype to *ob/ob* mice with hyperphagia, hypothermia, hyperglycemia, hyperinsulinemia, hypercorticotesteronemia, hypothyroidism, reduced energy expenditure, infertility and early-onset morbid obesity. *db/db* mice are resistant to leptin because of a mutated leptin receptor (157, 158). *Agouti yellow* mice are obese and slightly larger

than their non-yellow siblings. The yellow mouse obesity syndrome is due to dominant mutations at the Agouti locus resulting in ectopic expression of the agouti gene product in multiple tissues. Ectopic expression of the agouti gene product in the hypothalamus functionally antagonises α -melanocyte-stimulating hormone (α -MSH) at melanocortin receptors 3 and 4 producing obesity and increased growth. The mouse agouti protein induces hair follicle melanocytes to switch from the synthesis of black pigment to yellow pigment, resulting in a mottled yellow-coloured mouse with hyperglycemia, hyperinsulinemia, hyperleptinemia and obesity (159). *Ob/ob*, *db/db* and *Agouti yellow* mice were not chosen as the rodent model in this study as these spontaneous monogenetic mouse models of diabetes are of little relevance to human diabetes, which is rarely the result of a defect in a single gene. Furthermore, as the degree of obesity in *ob/ob* mice is severe, previous adipose tissue transplantation experiments were unable to overcome the severe insulin resistance in *ob/ob* mice. Transplantation of *Dgat1*^{-/-} adipose tissue decreases adiposity and enhances glucose disposal in wild-type and *Agouti yellow* but not *ob/ob* mice (122).

The high fat diet-fed C57BL/6J mouse, first described in 1988, is a robust model for impaired glucose tolerance and early type 2 diabetes (160). In C57BL/6J mice impaired glucose tolerance is manifest after only 1 week on a high fat diet. Over time, maintenance on a high fat diet results in progressive body weight gain, stable hyperglycemia and progressively increased hyperinsulinemia (161). C57BL/6J mice are more susceptible to high fat diet induced impaired glucose tolerance compared with other mice strains (162, 163). Therefore, the high fat fed C57BL/6J mouse is a model of environmentally induced obesity and impaired glucose tolerance in a genetically susceptible population. This provides an excellent model for human obesity and type 2 diabetes, that is most likely a polygenetic condition unmasked by environmental factors, particularly decreased energy expenditure (physical activity) and increased caloric intake (abundant high-fat foods).

In summary, C57BL/6J mice were chosen as the rodent model in the experiments conducted for this thesis as they are an in-bred mouse strain so littermates can be used as tissue donors without rejection; they are inexpensive and easily accessible; they are sufficiently robust to recover rapidly from surgery and they are particularly susceptible (in comparison to other mouse strains) to high fat diet induced adiposity, insulin resistance and hyperglycemia, making them an excellent model for human obesity and type 2 diabetes.

Animals

Male C57BL/6J mice were purchased from the animal resources centre (Perth, Australia). Animals were kept in a temperature-controlled room ($22 \pm 1^\circ\text{C}$), 80% relative humidity on a 12-h light/dark cycle with free access to food and water. Mice were fed ad libitum with a high fat diet (45% calories from fat, 20% calories from protein, and 35% calories from carbohydrates, 4.7 kcal/g, based on rodent diet no. D12451; Research Diets, New Brunswick, NJ). Experiments were carried out with the approval of the Garvan Institute/St. Vincent's Hospital Animal Experimentation Ethics Committee, following guidelines issued by the National Health and Medical Research Council of Australia.

Adipose tissue transplantation

To avoid rejection, C57BL/6J mice, which are inbred and therefore genetically identical, were used as donor and recipient mice. Only male mice were used in this study. Transplantation surgery was performed at 7 wks of age. Mice were anesthetized with ketamine (100 mg/kg ip)/xylazine (20 mg/kg ip). Inguinal (subcutaneous) and epididymal (abdominal) fat pads were removed from a donor mouse, weighed and rinsed with sterile phosphate buffered saline. For each donor mouse there were two recipient mice - one transplant recipient received subcutaneous (inguinal) adipose tissue grafts and a second transplant recipient received abdominal (epididymal) adipose tissue grafts. Donor and recipient mice were age and weight matched to minimize rejection as described by Chen et al 2003 (122). Mice were divided into two groups. One group received transplants into the

subcutaneous compartment and the second group received transplants into the intra-abdominal compartment (Figure 2.1). For transplants into the subcutaneous compartment, adipose tissue grafts were divided into two equal sized pieces and implanted subcutaneously, through a small incision in the back, into a pocket created by blunt-dissection between the skin and muscle layers, following the technique described by Gavrilova et al 2000 (119). Adipose tissue transplantation into the intra-abdominal compartment had not been previously described and several techniques were attempted. In the first, adipose tissue grafts were inserted between folds of mesentery. This resulted in unpredictable rates of adipose tissue engraftment, in many cases leading to failure of engraftment and graft atrophy. Where adipose tissue engraftment was successful it was difficult to distinguish the adipose tissue graft from the surrounding endogenous adipose tissue. In order to improve graft identification using this technique, transplanted adipose tissue was 'marked' with a non-absorbable suture (4-0 Silk, Johnson and Johnson Medical). This resulted in the development of adhesions between adipose tissue grafts and adjacent loops of bowel. This technique was abandoned due to significant concerns that bowel adhesions could obstruct the mouse's digestive tract and unpredictably influence its caloric intake. In the second technique attempted, the adipose tissue graft was sutured onto the mesentery of the small intestine. This technique resulted in the immediate development of bowel ischemia, requiring the recipient mouse to be euthanized in all cases. In the third technique attempted, successful adipose tissue engraftment was consistently achieved by suturing the adipose tissue graft to the peritoneal surface of the anterior abdominal wall through a vertical midline incision in the rectus abdominus muscles. Adipose tissue grafts were sutured using absorbable suture material (5-0 vicryl, Johnson and Johnson Medical) to prevent the development of adhesions and minimize the inflammatory reaction to the suture material (164). . Sham operated mice received identical surgical treatment without transplant. Skin incisions were closed with wound clips (Autoclip, BD).

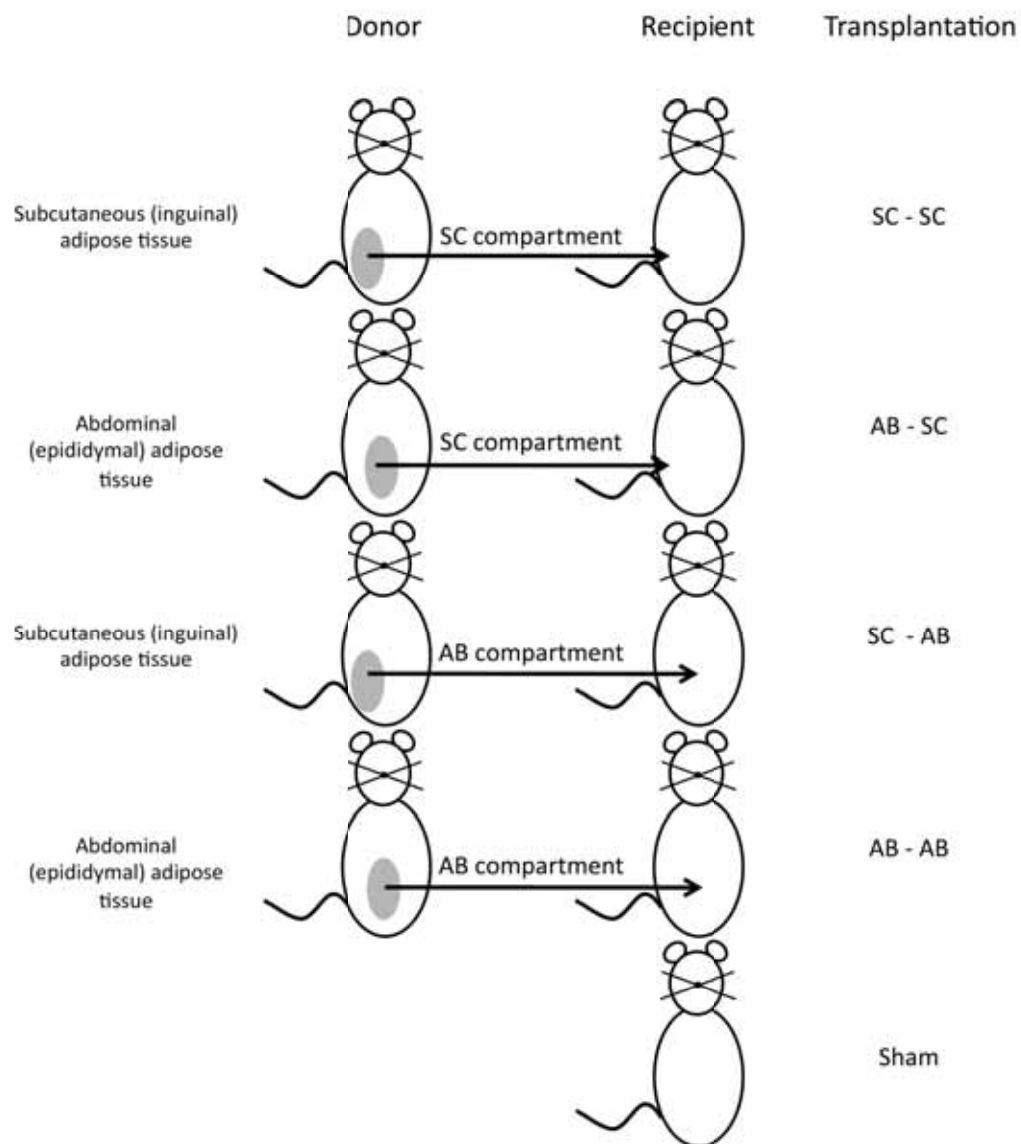


Figure 2.1. Schematic of adipose tissue transplantation experiments.

Subcutaneous (SC; inguinal) or intra-abdominal (AB; epididymal) adipose tissue from donor mice was transplanted into the intra-abdominal (AB) or subcutaneous (SC) compartment of wild-type C57BL/6 host mice. The sham group had surgery in the AB or SC compartment, but no fat was transplanted.

Metabolic assays

Glucose tolerance tests (ipGTT) were performed on overnight fasted animals 11-13 weeks after transplantation surgery. Glucose (2g/kg) was injected intraperitoneally and blood samples were obtained from the tail tip at 0, 15, 30, 45, 60 and 90 minutes after injection. Glucose levels were measured using a glucometer (AccuCheck II; Roche). Insulin levels were measured from whole blood by ELISA (Crystal Chem). Blood was obtained from the tail tip after an overnight fast. Insulin resistance was measured using the homeostasis model assessment index (HOMA) with the formula described by Matthews *et al.*, ($\text{HOMA-IR} = \text{fasting glucose (mmol/L)} \times \text{fasting insulin} / 22.5$) (165) which has been validated for use in C57BL/6J mice (166, 167). Oxygen consumption rate (VO_2) was measured using an eight-chamber indirect calorimeter (Oxymax series; Columbus Instruments) with airflow of 0.6 L/min. Studies were commenced after 2 h of acclimation to the metabolic chamber (20 x 10 x 12.5 cm). VO_2 was measured in individual mice over a 24-h period under a consistent environmental temperature (22°C). During the study, mice had ad libitum access to food and water. Fat and lean body mass were measured using dual-energy X-ray absorptiometry (Lunar PIXImus2 mouse densitometer; GE Healthcare) in accordance with the manufacturer's instructions.

Analysis of tissue weights and histology

Mice were killed by cervical dislocation, tissues dissected free and wet weights recorded. Histological sections were cut from fat pads embedded in paraffin wax after fixation in 10% phosphate-buffered formalin and subsequently stained with hematoxylin and eosin according to standard procedures.

Measurement of adipocyte area

Histology sections were viewed at 10x magnification. For each adipose tissue depot, total number and cross-sectional area of adipocytes was calculated using the neuron body detection module (HCA-vision, CSIRO www.hca-vision.com). The output from the neuron body detection module was compared with the original histology image to ensure accuracy (Figure 2.2A). Results were directly loaded into a

spreadsheet program (Excel, Microsoft Inc.) for analysis.

Data analysis

Data are presented as mean \pm SEM and statistical analysis was performed using an unpaired Student's t test or ANOVA as indicated. Differences at $p < 0.05$ were considered statistically significant.

Results

Graft Integrity

Weight matched recipient C57BL/6J mice received a subcutaneous (inguinal) graft, abdominal (epididymal) graft or sham operation into the subcutaneous (Group 1) or abdominal (Group 2) compartment. An equivalent amount of subcutaneous and abdominal adipose tissue was transplanted in both groups, ranging from 300 – 340mg (Table 2.1). At the time of sacrifice (12-13 weeks post-transplantation) adipose tissue grafts were clearly identified in both compartments. In the subcutaneous compartment, grafts were located in connective tissue immediately below the skin of the back. In the abdominal compartment, grafts were adherent to the peritoneum on the anterior abdominal wall. Visually the grafts appeared viable with evidence of angiogenesis. Histologically grafts retained the morphologic features of their respective endogenous beds comprising principally well-defined adipocytes interspersed with stromal vascular cells (Figure 2.3).

Adipocyte area

The average cross-sectional area of adipocytes in the transplanted and endogenous inguinal and epididymal adipose tissue for both transplanted and sham-operated mice was determined (Figure 2.2). There was no difference in the average cross-sectional area of adipocytes in transplanted or endogenous subcutaneous adipose

TABLE 2.1.

Total body weight, endogenous adipose tissue weights and weights of harvested and implanted transplants.

	Subcutaneous space			Intra-abdominal space		
	Sham (<i>n</i> =12)	SC graft recipients (<i>n</i> =17)	AB graft recipients (<i>n</i> =15)	Sham (<i>n</i> =14)	SC graft recipients (<i>n</i> =14)	AB graft recipients (<i>n</i> =15)
Initial weight (g)	21.6±0.4	21.3±0.3	21.0±0.3	21.4±0.4	21.8±0.4	21.7±0.4
Final weight (g)	30.8±1.1	29.8±0.5	29.7±0.7	29.9±0.9	29.3±0.7	29.6±0.7
Fat depots (mg)						
Inguinal	776±94	714±46	720±53	707±44	533±33 ^a	560±52 ^b
Epididymal	1245±128	1012±59	1104±95	1195±126	817±72 ^c	874±94
Retroperitoneal	406±43	370±24	339±28	373±31	263±27 ^d	284±32
Interscapular	248±24	235±9	242±13	241±12	198±12 ^e	207±11
Harvested transplant		305±19	480±40 ^f		185±13	364±27 ^g
Implanted transplant		315±16	327±10		313±18	315±14

Values are means ± SEM

^a *p* = 0.004 vs sham

^b *p* = 0.04 vs sham

^c *p* = 0.02 vs sham

^d *p* = 0.01 vs sham

^e *p* = 0.02 vs sham

^f *p* < 0.001 vs subcutaneous space SC graft recipients

^g < 0.001 vs Intra-abdominal space SC graft recipients (Student's *t* test)

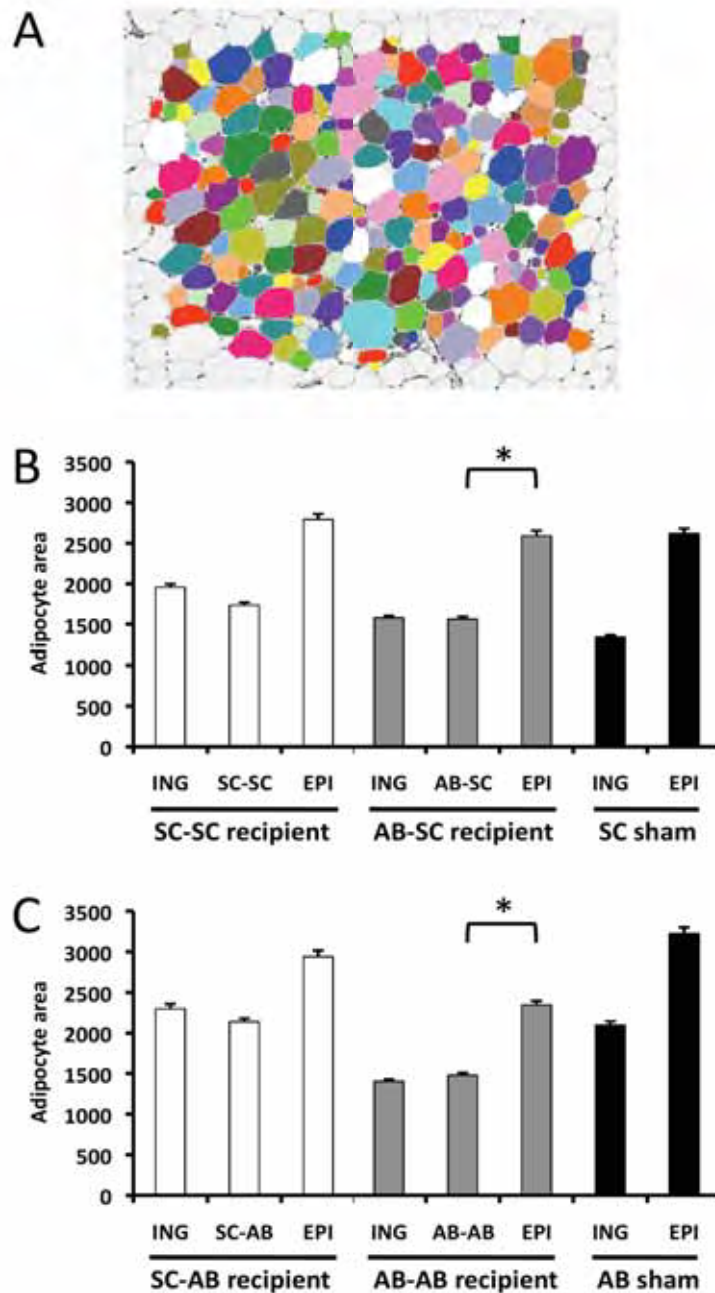


Figure 2.2. Average cross-sectional adipocyte area of transplanted and endogenous adipose tissue.

Overlay of computer-generated image and hematoxylin and eosin-stained histology section of endogenous epididymal adipose tissue (A). Adipocyte area was measured in transplanted and endogenous adipose tissue in mice receiving transplants into the SC compartment (B) and abdominal compartment (C). Results represent the mean \pm SEM ($n = 2-3$ per group). * denotes statistical significance at $p=0.06$.

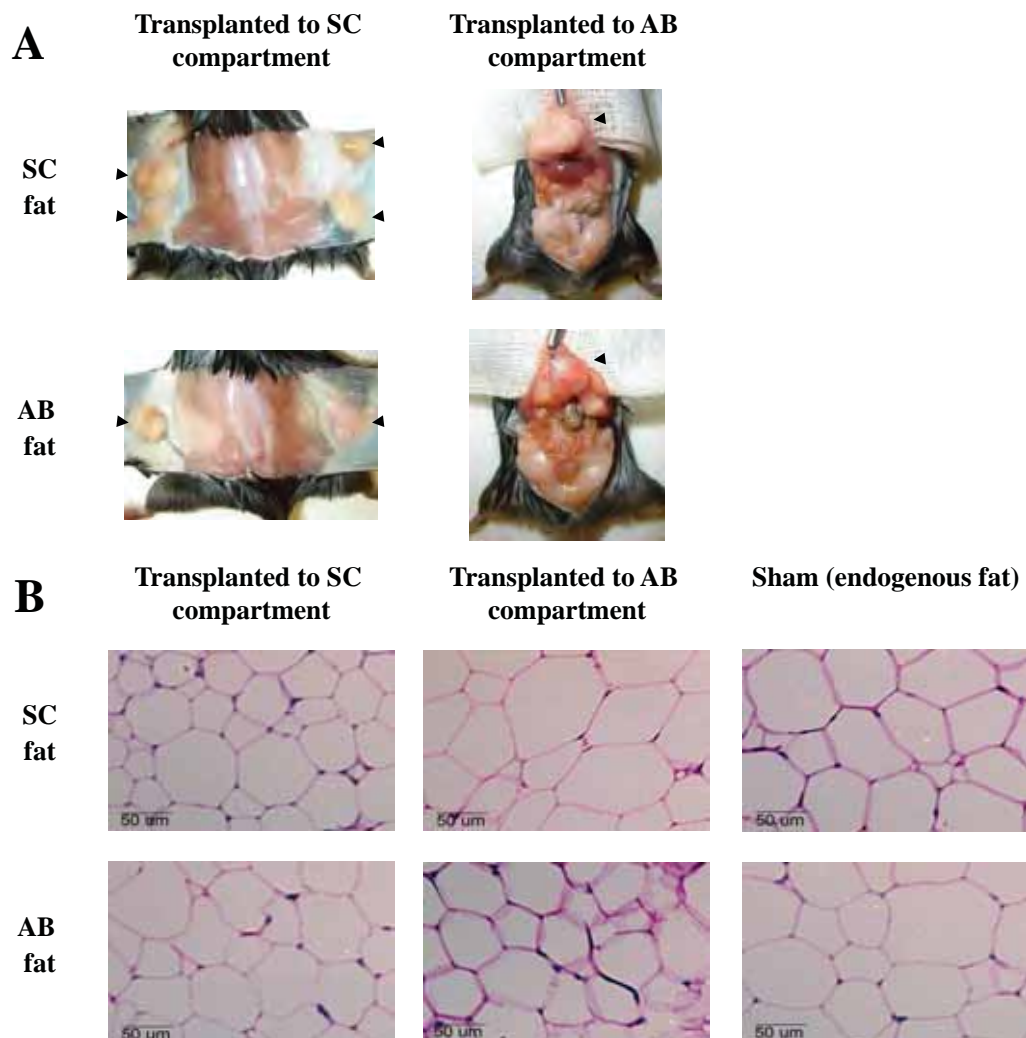


Figure 2.3. Macroscopic appearance and histology of transplanted and endogenous adipose tissue.

Adipose tissue grafts (arrow heads) are easily identified in the subcutaneous and abdominal compartments and appear viable with evidence of new vessel formation (A). Hematoxylin and eosin (H&E) staining of subcutaneous (SC) and abdominal (AB) adipose tissue grafts and endogenous adipose tissue (B). Transplanted subcutaneous and abdominal adipose tissue grafts had normal histology in comparison to endogenous subcutaneous and abdominal adipose tissue in the sham group.

tissue (Figure 2.2B). The average cross-sectional area of adipocytes in transplanted epididymal adipose tissue decreased compared with the average cross-sectional area of adipocytes in endogenous (non-transplanted) adipose tissue beds, although this was not statistically significant ($p=0.06$) (Figure 2.2C). After transplantation, the average cross-sectional area of adipocytes in transplanted epididymal adipose tissue was similar to the average cross-sectional area of adipocytes in subcutaneous adipose tissue, irrespective of whether the epididymal adipose tissue graft had been transplanted into the subcutaneous or intra-abdominal compartment.

Body Weight

To examine the consequences of adipose cross transplantation on insulin resistance and adiposity mice were fed a high fat diet, commencing one week prior to transplantation and continued for the duration of the study. Mice receiving transplants gained weight at a similar rate to sham-operated mice in both groups (Figure 2.4). Weight gain in mice receiving transplants into the subcutaneous compartment (Group 1) diverged somewhat at 7 weeks after transplantation with mice receiving both types of transplant gaining weight more slowly (Figure 2.4A). Mice receiving subcutaneous or abdominal fat transplants into the abdominal compartment (Group 2) showed no difference in weight gain compared with sham-operated controls (Figure 2.4B). There was no overall statistical difference in body weight at sacrifice for mice receiving adipose tissue transplants or sham surgery in either group (Table 1).

Adiposity

Strikingly, mice receiving subcutaneous fat into the abdominal compartment displayed a significant reduction in the mass of various endogenous adipose tissue beds compared with sham-operated controls (Table 1). Inguinal, epididymal, retroperitoneal and interscapular beds were reduced by 25, 32, 30 and 18%, respectively in these mice compared with sham-operated controls. This was not

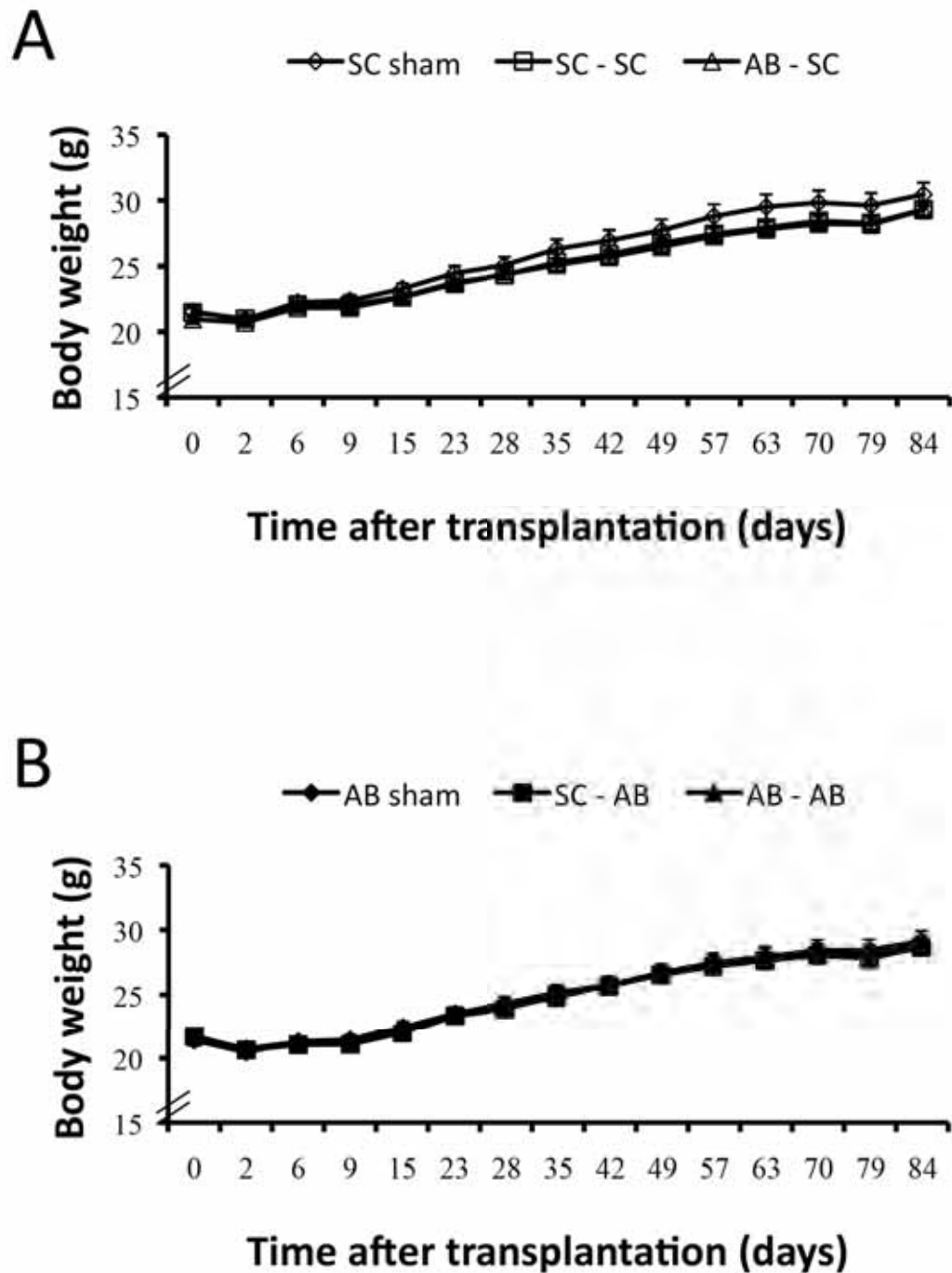


Figure 2.4. Body weight after transplantation.

Weight gain in animals receiving transplants or sham operations into the subcutaneous compartment (**A**) and abdominal compartment (**B**). Results represent the mean \pm SEM ($n = 12 - 17$ per group).

observed in mice transplanted with subcutaneous fat or abdominal fat into the subcutaneous compartment. Mice receiving abdominal fat into the abdominal compartment also displayed a reduction in the mass of endogenous adipose tissue beds, however with the exception of the inguinal depot, these reductions did not reach statistical significance. These reductions in endogenous fat mass were confirmed by dual-energy x-ray absorptiometry (DEXA) scan. Percent body fat (fat mass divided by total body weight) was similar among mice receiving transplants or sham surgery in the subcutaneous compartment (Group 1) (Figure 2.5A). However in mice receiving transplants into the abdominal compartment (Group 2) there was a significant 16% reduction in mice receiving subcutaneous fat into the abdominal compartment ($p=0.02$) (Figure 2.5B). Although donor tissue was weight matched at the commencement of study, the transplanted subcutaneous adipose tissue was reduced by 41% in abdominal compartment recipients and the transplanted abdominal fat increased by 47% in subcutaneous compartment recipients (Table1). Other transplants retained their original mass.

Energy balance

Assessment of energy expenditure was performed to determine what accounted for this observed difference in body fat. No differences were observed in respiratory quotient or energy expenditure in mice receiving transplants into the SC compartment (Group 1) (Figure 2.6A,C). There were also no significant differences in respiratory quotient or energy expenditure in mice receiving transplants into the abdominal compartment (Group 2) (Fig 2.6B,D), however there was a trend for mice receiving SC fat into the abdominal compartment to have higher energy expenditure in both the light and dark cycles. It may be that the differences in energy expenditure required to account for the differences in body composition observed were too small to detect using this technique.

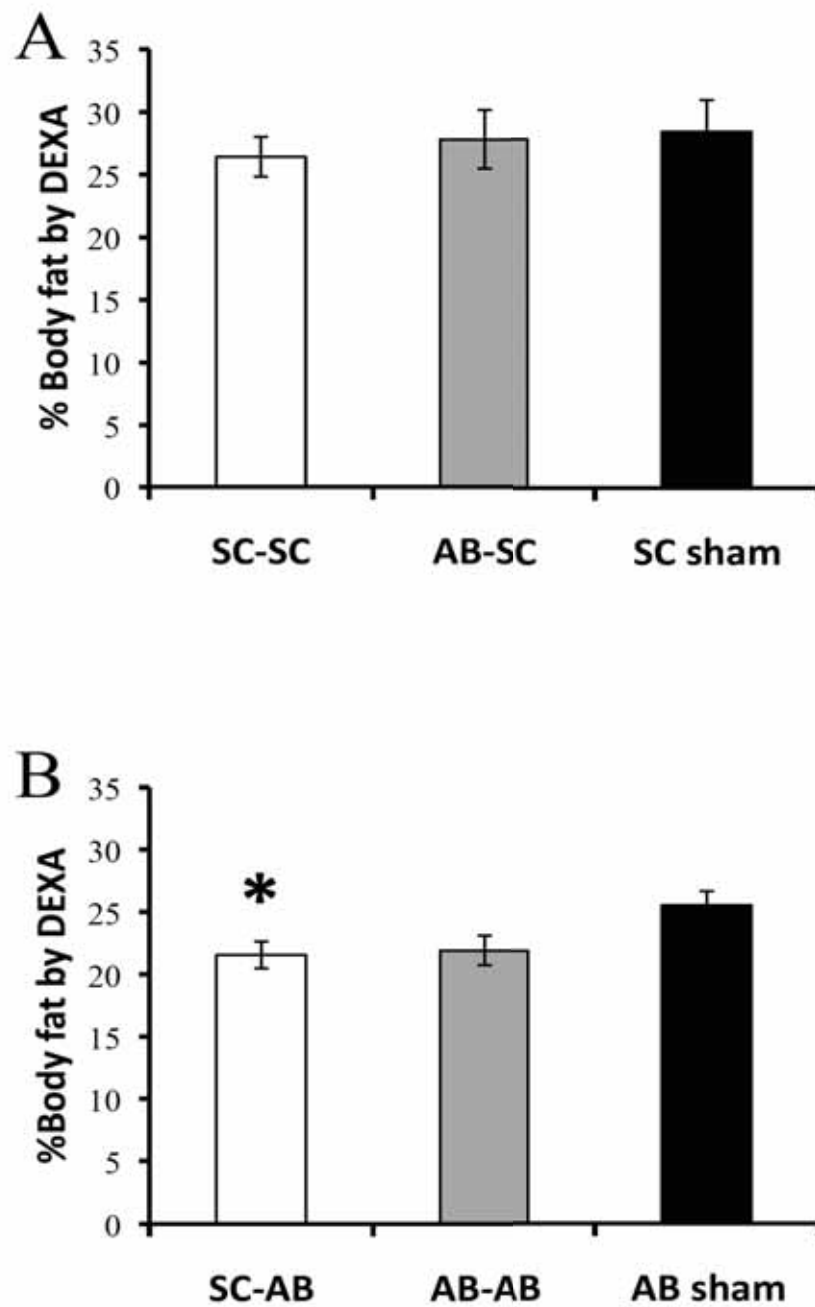


Figure 2.5. Body composition after transplantation.

Percent body fat was determined in mice receiving transplants into the subcutaneous compartment (**A**) and abdominal compartment (**B**). Results represent the mean \pm SEM ($n = 7 - 10$ per group). * denotes statistical significance at $p=0.02$.

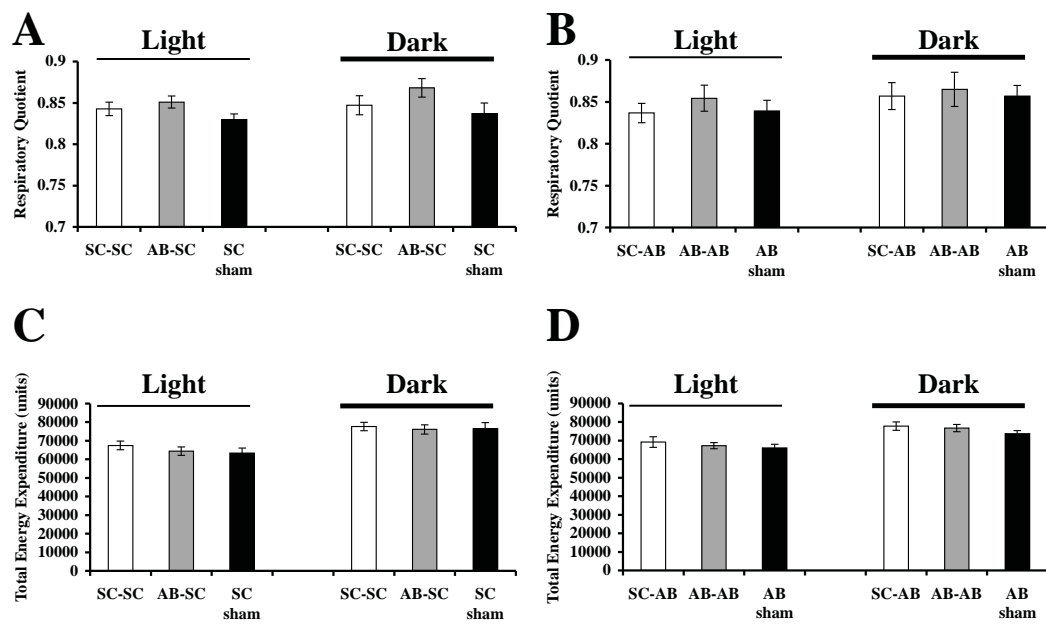


Figure 2.6. Respiratory quotient and energy expenditure after transplantation

Respiratory quotient and energy expenditure were determined in mice receiving transplants into the subcutaneous compartment (**A, C**) and abdominal compartment (**B, D**). Results represent the mean \pm SEM ($n = 8 - 10$ per group).

Glucose tolerance

To evaluate the effect of fat transplantation on glucose homeostasis ipGTTs were performed at 11-13 weeks post-transplantation in overnight fasted animals. Mice receiving SC fat transplants into the abdominal compartment exhibited improved glucose tolerance compared with sham-operated control animals with a 17% decrease in the AUC for glucose ($p=0.006$) (Figure 2.7). This beneficial metabolic effect was not observed when SC fat was transplanted into the SC compartment or when abdominal fat was transplanted into either compartment.

Fasting insulin and HOMA-IR

Fasting glucose and insulin levels were measured prior to the commencement of ipGTTs in overnight fasted animals. HOMA-IR was calculated. There were no significant differences in fasting glucose, insulin or calculated HOMA-IR in mice receiving transplants into the SC compartment (Group 1) (Figure 2.8A,C,E). There were also no significant differences in fasting glucose, insulin or calculated HOMA-IR in mice receiving transplants into the abdominal compartment (Group 2) (Figure 2.8B,D,F).

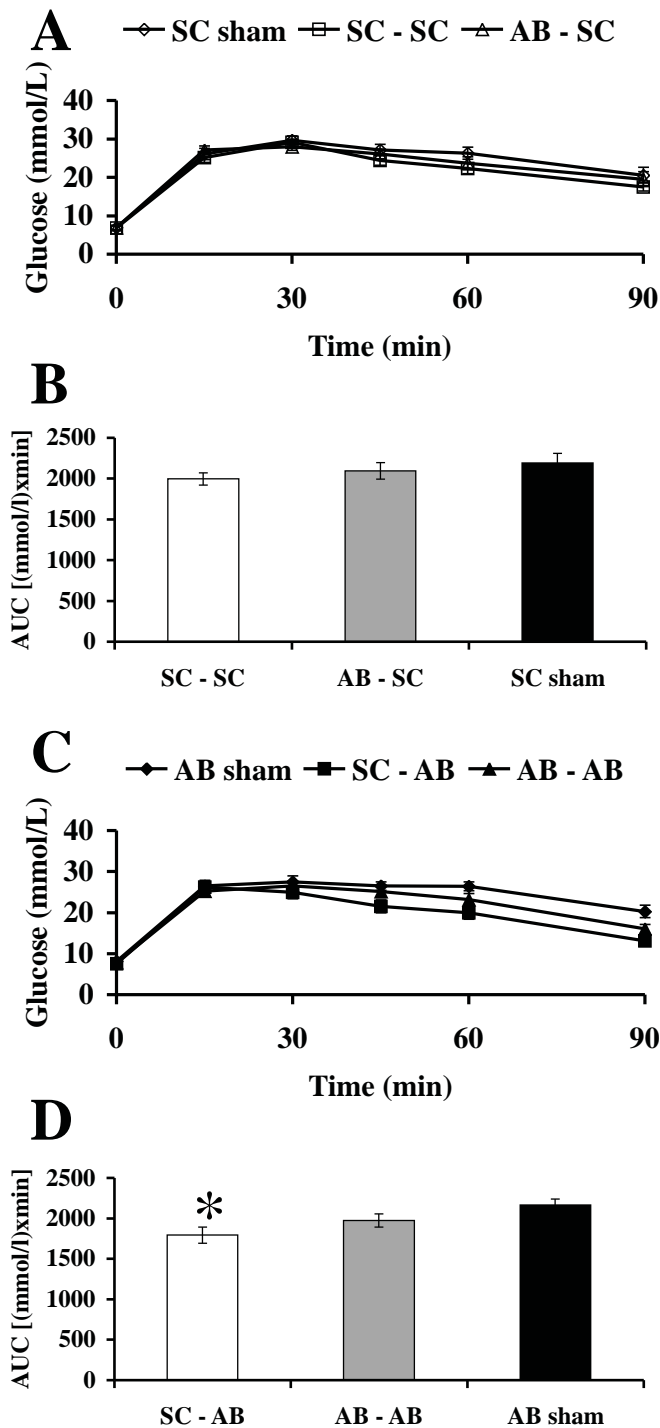


Figure 2.7. Glucose tolerance test after transplantation

Intraperitoneal GTT (2g glucose / kg body weight) were performed after an overnight fast and AUC determined in mice receiving transplants into the subcutaneous compartment (**A,B**) and abdominal compartment (**C,D**). Results represent the mean \pm SEM (n = 12 – 17 per group). * denotes statistical significance at $p < 0.01$.

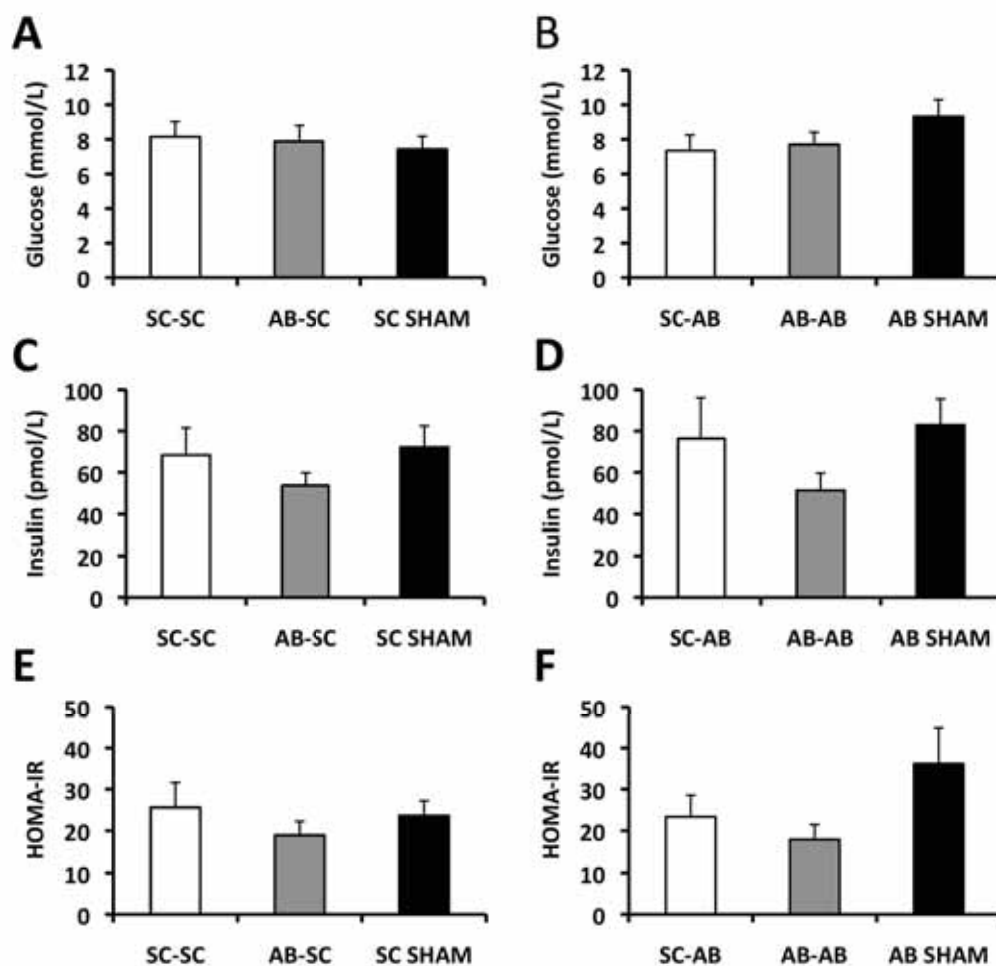


Figure 2.8. Fasting glucose, insulin and calculated HOMA-IR after transplantation

Fasting glucose and insulin were measured and HOMA-IR calculated in mice receiving transplants into the subcutaneous compartment (**A, C, E**) and abdominal compartment (**B, D, F**). Results represent the mean \pm SEM (n = 5 per group).

Discussion

I have employed a regional adipose tissue cross transplantation strategy in high fat fed mice to explore the basis for the proposed detrimental effects of increased abdominal fat mass. These studies have revealed two important findings. First, transplantation of epididymal fat into either the abdominal or subcutaneous space had no observed detrimental effects on metabolism as judged by body weight, adiposity or glucose tolerance. These findings are consistent with those of Konrad *et al.* (2007)(168) who found a beneficial rather than detrimental metabolic effect after increasing intra-abdominal fat mass by transplantation of epididymal fat from normal mice into lean recipients. In their study, transplantation of epididymal adipose tissue into the abdominal compartment improved fasting glucose tolerance and insulin sensitivity. In another adipose tissue cross transplantation study undertaken by Tran *et al.* (169), up to 1 gram of epididymal adipose tissue was transplanted into the dorsal subcutaneous compartment or the intra-abdominal compartment. In agreement with my study, there was no effect on body weight, fat mass, glucose tolerance or insulin sensitivity after transplantation of epididymal fat into either the abdominal or subcutaneous space. Taken together, these findings indicate that the adverse metabolic consequences of intra-abdominal obesity are not due simply to an increase in intra-abdominal fat mass but rather due to the alterations in intra-abdominal adipose tissue metabolism and physiology that result from obesity. In both our study and that of Konrad *et al.* (2007)(168), transplants into the abdominal compartment were sutured to the peritoneal surface of the anterior abdominal wall. It is likely that the venous drainage from this location is into the systemic rather than portal circulation. However it cannot be argued that the lack of portal venous drainage is the explanation for the absence of detrimental metabolic effects. In rodents, gonadal adipose tissue beds do not drain through the portal circulation, yet the selective removal of gonadal adipose tissue improves insulin sensitivity and glucose tolerance (77, 78). Furthermore, the technique utilized by Tran *et al.* (169), in which transplants into the intra-abdominal area were carefully lodged deep between folds within sliced portions of the endogenous

epididymal fat of the recipient animal and lodged next to the mesenteric fat just below the liver, resulted in multiple sites of intra-abdominal engraftment, many of which had the potential for portal venous drainage. As previously mentioned, this study also showed no impact on metabolism from transplantation of epididymal fat into either the abdominal or subcutaneous space. Therefore it is unlikely that the balance between systemic and portal drainage determines the detrimental effects of intra-abdominal adiposity on insulin sensitivity. Notably, the amount of adipose tissue transplanted in my study (~ 25% of total endogenous abdominal fat) was expected to make a significant contribution to the metabolic outcome of the animal since this is similar to the reduction in abdominal adiposity observed after caloric restriction in obese men which results in decreased insulin resistance (15). After transplantation, the average adipocyte area decreased in epididymal adipose tissue transplanted into either the subcutaneous or abdominal compartment. This observation may explain the non-detrimental impact of epididymal adipose tissue grafts on metabolism as smaller adipocytes are more insulin sensitive and secrete fewer pro-inflammatory adipokines than hypertrophied adipocytes (98).

Second and most interestingly, the selective transplantation of subcutaneous fat into the abdominal space resulted in a significant reduction in body fat mass as well as improved glucose tolerance. Importantly I did not observe this effect when subcutaneous fat was transplanted into the subcutaneous space of a recipient animal. This suggests that the beneficial metabolic effects are due to the specific combination of the subcutaneous origin of the fat depot and its abdominal transplant location. These findings were confirmed by the above mentioned study by Tran *et al.* (2008)(169) who observed a reduction in body weight, total fat mass, glucose and insulin levels in lean mice transplanted with subcutaneous fat into the abdominal compartment. In my study, there was no reduction in insulin resistance, as measured by HOMA-IR, in mice receiving a subcutaneous transplant into the abdominal compartment, however Tran *et al.* found improved insulin sensitivity during hyperinsulinemic-euglycemic clamp in these mice. The discrepancy in these findings can be explained by the weaker correlation between HOMA-IR and clamp

data in mice compared with humans (166). Furthermore, the observed improvements in glucose metabolism in my study may have been underestimated. The standard procedure of performing an overnight fast prior to the performance of intraperitoneal glucose tolerance tests was utilised in my study. Since the animal work for this thesis was undertaken, Andrikopoulos *et al.* have shown that 6 hours fasting reveals greater differences in glucose tolerance after intraperitoneal glucose tolerance testing compared with overnight fasting in high-fat fed compared with chow-fed animals (170). Fasting duration also had a profound impact on plasma glucose and insulin levels. For example, 24 hours of fasting reduced basal plasma insulin levels in both chow- and high-fat-fed mice by three- and fivefold, respectively, compared with their respective controls, which were fasted for 0 hours. As HOMA-IR is calculated using fasting values of glucose and insulin, HOMA-IR was significantly reduced after prolonged fasting in both high-fat fed and chow-fed animals, such that differences between the groups were no longer detected (170). In light of these findings, it is possible that the overnight fasting values for plasma glucose and insulin used to calculate HOMA-IR in my study were falsely low and if a shorter fasting period of 6 hours was utilized this may have resulted in significant differences in HOMA-IR being observed.

Collectively, these findings suggest that subcutaneous fat transplanted into the abdominal compartment produces a substance or substances that can act systemically to reduce adiposity and improve glucose metabolism. A possible mechanism behind the selective metabolic advantage of transplanting subcutaneous adipose tissue into the abdominal compartment is suggested by my finding that subcutaneous transplants underwent a significant reduction in size when transposed into the abdominal space and abdominal transplants significantly increased in size when transposed into the subcutaneous space. This suggests there may be a fortuitous mismatch between the origin and destination of the transplant. It is interesting to consider previously published data in lieu of these findings, particularly regarding the influence of angiogenic cells and innervation on adipose tissue metabolism. It is now recognised that there is a paracrine interaction

between microvascular endothelial cells (MVECs) and pre-adipocytes that regulates adipose tissue growth (42, 171). It is feasible that just as pre-adipocytes and adipocytes from different adipose tissue depots display differing molecular and physiological properties, MVECs from subcutaneous and abdominal adipose tissue may also display depot-specific characteristics. It is possible that there is a depot-specific cross-talk between adipocytes and MVECs, which is disrupted by transposing subcutaneous and abdominal fat into a different compartment. Another important influence on adipose tissue metabolism is autonomic innervation. Subcutaneous and abdominal adipose tissue pads are innervated by separate sympathetic and parasympathetic neurons. Sympathetic input is catabolic and vagal input anabolic (172). It is possible that re-innervation of adipose tissue after transposition disrupts the autonomic balance resulting in the metabolic changes I have observed. In the case of either an endothelial or neural influence it is postulated that alterations in the adipocytes or stromovascular cells within the transplant must generate, via alterations in the secretory products of adipose tissue (adipokines/inflammatory cytokines), a systemic effect to reduce endogenous adipose tissue depots.

In conclusion, using a regional adipose tissue cross-transplantation strategy I have demonstrated a unique beneficial effect of subcutaneous adipose tissue transplanted into the abdominal compartment on whole-body adiposity and glucose tolerance. This must be due to a secreted factor capable of a systemic effect causing this metabolic advantage. The identification of this factor is important as it may provide new possibilities for the management of obesity and its related metabolic complications.

Chapter 3

**Gene expression analysis of transplanted and
endogenous adipose tissue.**

Abstract

Accumulation of adipose tissue in the abdominal or visceral space is associated more strongly with the development of insulin resistance and type 2 diabetes than accumulation of subcutaneous fat. To explore the mechanisms underlying the association between increased visceral adiposity and metabolic disease I used an adipose tissue cross-transplantation model, in which subcutaneous and intra-abdominal adipose tissue pads from donor mice were transplanted into the subcutaneous or intra-abdominal compartment of recipient high fat fed mice. Mice receiving subcutaneous transplants into the intra-abdominal compartment displayed significantly reduced fat mass, in both transplanted and endogenous adipose tissue beds, and improved glucose tolerance. These metabolic benefits were not observed in mice transplanted with subcutaneous adipose tissue into the subcutaneous space nor with intra-abdominal adipose tissue into either compartment. These findings suggest a unique beneficial metabolic effect of transplanting subcutaneous adipose tissue into the intra-abdominal compartment that is likely due to the secretion of one or more factors from the intra-abdominal subcutaneous adipose tissue graft capable of acting systemically to confer this metabolic advantage. I utilised gene expression analysis to compare gene expression in subcutaneous adipose tissue grafts transplanted into the intra-abdominal compartment with subcutaneous adipose tissue grafts transplanted into the subcutaneous compartment. I identified a selective upregulation of genes controlled by the transcription factor MEF2 in subcutaneous adipose tissue grafts transplanted into the intra-abdominal compartment. Similarly, I identified a selective upregulation of genes controlled by the transcription factor MEF2 in the endogenous subcutaneous adipose tissue of mice that received a subcutaneous adipose tissue graft into the intra-abdominal compartment. Furthermore, in the endogenous subcutaneous adipose tissue of mice that received a subcutaneous adipose tissue graft into the intra-abdominal compartment, increased uncoupling protein-1 (UCP-1) gene expression, decreased β 3-adrenoceptor gene expression and increased glycogen phosphorylase gene expression were uniquely observed.

This pattern of changes in gene expression is consistent with increased adrenergic-stimulation of endogenous subcutaneous adipose tissue. This suggests that a humoral or neural signal that selectively upregulates adrenergic stimulation of subcutaneous adipose tissue mediates the metabolic benefit observed after transplantation of subcutaneous adipose tissue into the intra-abdominal compartment. The identity of this signal is important as it may provide a novel treatment for obesity-induced metabolic disease.

Introduction

Accumulation of excess intra-abdominal (visceral) adipose tissue is strongly linked to the development of insulin resistance and type 2 diabetes in humans, however the specific mechanisms linking intra-abdominal adiposity with metabolic disease are incompletely understood. To explore the mechanisms underlying the association between increased visceral adiposity and metabolic disease I used an adipose tissue cross-transplantation model, in which subcutaneous and intra-abdominal adipose tissue pads from donor mice were transplanted into the subcutaneous or intra-abdominal compartment of recipient high fat fed mice, as discussed in Chapter 2. My results indicate that transplantation of epididymal (intra-abdominal) fat into either the abdominal or subcutaneous space had no observed detrimental effects on metabolism as judged by body weight, adiposity or glucose tolerance. However, the selective transplantation of subcutaneous fat into the abdominal space resulted in a significant reduction in body fat mass as well as improved glucose tolerance. Importantly, I did not observe this effect when subcutaneous fat was transplanted into the subcutaneous space of a recipient animal.

These findings are supported by two contemporaneous studies using the technique of adipose tissue transplantation. In the first, Konrad et al. (168) transplanted epididymal fat pads from 6-wk old male C57BL6/J mice into littermates, suturing them to the visceral side of the peritoneum, an identical technique to that used in my study. Four weeks after transplantation, recipient mice displayed improved glucose tolerance and lower fasting glucose levels relative to sham-operated mice. When mice were sacrificed at 10 weeks, the total perigonadal fat mass (endogenous + transplanted) was increased by 50%, however this did not result in a significant difference in total body weight between the recipient and control groups. Histological examination of the transplanted adipose tissue at 10 weeks post-transplantation revealed that adipocyte cell size remained unchanged in the transplanted fat pads, whereas it increased significantly in endogenous fat pads. As

smaller adipocytes are more sensitive to insulin and secrete higher levels of adiponectin, this may have accounted for the observed insulin sensitizing effects of the transplants. However, circulating levels of adiponectin, leptin, resistin and non-esterified fatty acids (NEFA) did not differ at 10 weeks post-transplant in recipients compared with sham-operated controls. Taken together, my findings and those of Konrad et al. (168) indicate that the adverse metabolic consequences of intra-abdominal obesity are not due simply to an increase in intra-abdominal fat mass but rather due to alterations in adipose tissue function that result from obesity. This suggests that adipose tissue metabolism and physiology and inter-organ cross-talk between adipose tissue and other important metabolic organs such as muscle and liver, are more important determinants of obesity-related metabolic derangements than adipose tissue mass per se. Importantly this cross-talk is not mediated by the well-known adipokines leptin, adiponectin or resistin. This suggests that novel adipokines may be involved or alternatively that the metabolic changes are mediated, at least in part, via afferent and efferent limbs of the autonomic nervous system.

In the second contemporaneous study, Tran et al. (169) performed experiments in 12-wk old C57BL/6J chow-fed mice, utilising an adipose tissue cross-transplantation strategy in which up to 1 g of visceral (intra-abdominal) or subcutaneous adipose tissue was transplanted from donor mice into either the visceral or peripheral subcutaneous regions of recipient mice. Similar to my study, transplants into the subcutaneous area were placed below the skin on the back of the recipient mouse. Utilising a different technique to my study, transplants into the intra-abdominal area were placed within sliced portions of the endogenous epididymal adipose tissue or next to the mesenteric adipose tissue just below the liver. By using this technique, endogenous and transplanted adipose tissue beds could not be easily distinguished, so C57BL/6 mice carrying GFP as a transgene on the β -actin promoter (Actb) were used as donors. As this transgene was expressed in all tissues of the donor mice, it was possible to identify the transplanted adipose tissue in the recipient mice using ultraviolet illumination.

Tran et al found that transplanting subcutaneous adipose tissue into the intra-abdominal cavity decreased body weight and total adipose tissue mass, relative to sham-operated mice (169). There were no differences in either food intake or energy expenditure, to account for this difference in body and fat mass, however the Comprehensive Lab Animal Monitoring System (CLAMS) technique utilized to detect differences in these variables may have lacked the sensitivity to detect small changes. Relative to sham-operated mice, plasma insulin and glucose levels were lower in mice receiving subcutaneous transplants into the intra-abdominal compartment and these mice displayed improved glucose tolerance, increased whole-body insulin sensitivity and increased insulin-mediated suppression of hepatic glucose production. Interestingly, [^{14}C] deoxyglucose uptake into the endogenous subcutaneous adipose tissue was significantly increased by 2.8-fold in the mice receiving a subcutaneous adipose tissue transplant into the intra-abdominal compartment in comparison to the sham group, whereas, by contrast, [^{14}C] deoxyglucose uptake into endogenous visceral adipose tissue was not different. Plasma leptin and adiponectin levels were lower in the mice receiving subcutaneous grafts into the abdominal space, which suggests that these adipokines do not mediate the beneficial effects of subcutaneous adipose tissue in this model (169).

In contrast to my findings, Tran et al found that transplantation of subcutaneous adipose tissue to the subcutaneous compartment also decreased body weight, adipose tissue mass and plasma glucose relative to sham-operated mice, with increased glucose uptake into transplanted and endogenous subcutaneous adipose tissue and increased hepatic insulin sensitivity, but to a lesser extent than in mice receiving a transplant of subcutaneous adipose tissue into the intra-abdominal compartment (169).

In agreement with my findings, Tran et al concluded that transplanting subcutaneous adipose tissue into the intra-abdominal space leads to reduced fat mass (of both the endogenous adipose tissue depots and the transplanted adipose tissue), improved glucose tolerance and enhanced whole-body insulin sensitivity,

with greater glucose uptake into endogenous subcutaneous adipose tissue, and greater suppression of hepatic glucose production by insulin (169). Tran et al observed a similar, although less significant, effect when subcutaneous fat was transplanted into the subcutaneous compartment (169). The absence of metabolic benefit from transplanting subcutaneous fat into the subcutaneous compartment in my study may be accounted for by high fat feeding, with the resulting insulin resistance masking the more subtle metabolic benefit from transplanting subcutaneous fat into the subcutaneous compartment, together with a smaller adipose tissue graft (approximately 300 mg in my study compared with 1 g in Tran et al. (169)). Taken together, these data suggest that cross-talk occurs between transplanted subcutaneous adipose tissue and endogenous adipose tissue beds, in particular with endogenous subcutaneous adipose tissue. This cross-talk is enhanced when subcutaneous fat is transplanted into the intra-abdominal compartment. In agreement with Konrad et al, Tran et al found that the beneficial metabolic effects of transplanting subcutaneous adipose tissue into the intra-abdominal compartment were not mediated by adiponectin or leptin (168, 169).

The concept of cross-talk between adipose tissue and distant organs is not novel and several previous studies involving tissue-specific genetic manipulations of the glucose transporter GLUT4, which mediates insulin-stimulated glucose uptake in adipocytes and muscle, or the insulin receptor have demonstrated that cross-talk exists between adipose tissue and distant organs (reviewed in Minokoshi, Kahn, Kahn 2003 (173)). Mice engineered to express an adipose tissue selective reduction of the glucose transporter GLUT4 (adipose-G4KO) display markedly reduced insulin-stimulated glucose uptake into adipose tissue, as expected, however, surprisingly, these mice develop systemic hyperinsulinemia and insulin resistance in liver and in muscle, despite preservation of GLUT4 expression in these tissues (174). Importantly, basal and insulin-stimulated glucose uptake are normal in muscle from these mice *ex vivo*, demonstrating that this defect is secondary to the *in vivo* milieu. The adipokines traditionally responsible for regulating insulin action in muscle and liver - leptin, TNF- α , resistin, and adiponectin (175)- are not altered in adipose-

G4KO mice (174). It was postulated that insulin resistance in muscle and liver of adipose-G4KO mice is caused by altered secretion of an adipocyte-derived molecule that affects insulin action in other tissues. This adipokine was subsequently identified as retinol binding protein-4 (RBP4) (89). Expression of retinol binding protein-4 (RBP4) is elevated in adipose tissue of adipose-G4KO mice (and reduced in mice overexpressing adipose GLUT4) and transgenic overexpression of human RBP4 or injection of recombinant RBP4 in normal mice causes insulin resistance. Conversely, genetic deletion of RBP4 enhances insulin sensitivity (89). Serum RBP4 levels are elevated in several insulin-resistant states in mice (89) however evidence from human studies is conflicting with some studies demonstrating an association between elevated serum levels of RBP4 and insulin resistance (89, 176-178) but other studies not supporting this association (179-184). At this time the role of RBP4 in human insulin resistance remains uncertain.

In a converse experiment, mice engineered with a muscle specific GLUT4 reduction (muscle-G4KO) have decreased insulin-induced glucose uptake in muscle, as expected, resulting in hyperglycemia and hyperinsulinemia (185). These mice display decreased insulin-stimulated glucose transport in adipose tissue and decreased insulin-induced suppression of hepatic glucose production, implying that muscle is releasing a factor acting on both adipose tissue and liver. However, these effects in adipose tissue and liver appear to be at least partly due to glucose toxicity because phloridzin treatment, which normalizes blood glucose by increased glycosuria, normalizes insulin action in adipose tissue and liver in muscle-G4KO mice (186).

In another example of inter-organ cross-talk, mice with a muscle-specific inactivation of the insulin receptor display decreased muscle mass but unexpectedly, no change in plasma glucose or insulin levels or glucose tolerance (187). These mice exhibit increased glucose uptake into adipose tissue and features of the metabolic syndrome including increased adipose mass and increased serum triglycerides and free fatty acids. This suggests that impairment of insulin signaling in muscle results

in repartitioning of glucose from muscle to adipose tissue, resulting in altered adipose insulin sensitivity, increased adiposity, and abnormal plasma lipid profiles (187). Whether muscle releases a factor that directly acts on adipose tissue is unknown.

Cross-talk between adipose tissue and distant organs can also occur through non-adipokine mediated pathways. Brain-adipose tissue cross-talk has been demonstrated. Adipose tissue beds have both sympathetic nervous system (SNS) and sensory innervation, demonstrated using anterograde and retrograde tract tracers (66, 188). The primary function of SNS innervation is lipid mobilization, with SNS stimulation resulting in lipolysis. The SNS innervation of white adipose tissue also regulates fat cell number, as noradrenaline inhibits and sympathetic denervation stimulates fat cell proliferation (66). Characterization of adipose tissue sensory nerves indicates that they are capsaicin-sensitive and immunoreactive for calcitonin gene-related peptide (CGRP) and substance P (SP) (189-191). Surgical removal of adipose tissue pads triggers compensatory increases in lipid accumulation in non-excised endogenous adipose tissue beds (190). Similarly, capsaicin-induced sensory denervation triggers increases in lipid accumulation in non-capsaicin-injected adipose tissue depots (190). This suggests that sensory nerves convey information about body fat stores to the brain (192). Another function of the sensory innervation of adipose tissue is to interact with the SNS innervation of adipose tissue to maintain adiposity. The sensory circuits originating in inguinal (subcutaneous) and epididymal (intra-abdominal) adipose tissue have been recently mapped in rodents, using anterograde transneuronal viral tract tracing (193). This technique reveals virally-immunoreactive cells first in the ipsilateral dorsal root ganglion (spinal sensory afferents), followed by the thoracic sympathetic ganglia, then the ascending spinothalamic and spinocerebellar circuits (which are thought to relay pain and proprioceptive information) and finally in brainstem and hypothalamic nuclei involved in the regulation of feeding behaviour and energy homeostasis. These findings indicate the existence of a feedback loop composed of afferent sensory nerves from adipose tissue and efferent sympathetic

nerves to adipose tissue regulated centrally by descending inputs from brainstem and hypothalamic control centers (193). Notably, SNS drive to adipose tissue depots is not homogeneous. For example, central melanocortin receptor agonism caused by a single 3rd ventricular melanotan II (MTII) injection increases sympathetic outflow to subcutaneous but not intra-abdominal adipose tissue beds (194). Time-course measurements performed by Tran et al. indicate that the beneficial effects of transplanting subcutaneous adipose tissue into the intra-abdominal compartment took at least 8 weeks to become apparent (169). Previous adipose tissue transplantation studies in mice have shown that innervation of adipose tissue grafts takes place sometime between 4 and 13 weeks after transplantation (119, 195). It is reasonable, therefore, to hypothesise that a neural signal may be conveyed from the adipose tissue graft via new sensory nerves that innervate the adipose tissue graft. This may then result in reflex activation of the SNS output to endogenous adipose tissue beds, increasing lipolysis and decreasing adipose tissue mass. As the beneficial effect of intra-abdominal transplantation was only observed with subcutaneous adipose tissue and not visceral adipose tissue, the factor stimulating the afferent neural signal must be unique to subcutaneous adipose tissue. Whether this factor is an adipokine or lipid signal remains undetermined.

My data, supported by the findings of Tran et al, suggests that cross-talk occurs between transplanted subcutaneous adipose tissue and endogenous adipose tissue beds, in particular with endogenous subcutaneous adipose tissue. Adipokines known to be responsible for mediating metabolic effects, including adiponectin and leptin, do not appear to play a role in this model (169). It is likely, therefore, that a novel adipokine is playing a crucial role in mediating the beneficial metabolic effects in this model. To address this hypothesis, I utilised gene expression analysis to compare gene expression in subcutaneous adipose tissue grafts transplanted into the intra-abdominal compartment with subcutaneous adipose tissue grafts transplanted into the subcutaneous compartment. I identified a selective upregulation of genes controlled by the transcription factor MEF2 in subcutaneous adipose tissue grafts transplanted into the intra-abdominal compartment. Similarly,

I identified a selective upregulation of genes controlled by the transcription factor MEF2 in the endogenous subcutaneous adipose tissue of mice that received a subcutaneous adipose tissue graft into the intra-abdominal compartment relative to the endogenous subcutaneous adipose tissue of sham-operated animals. In adult tissues, expression of MEF2 is increased in response to stress, including adrenergic stimulation (196). A pattern of changes in gene expression consistent with chronic adrenergic stimulation of adipose tissue was observed selectively in the endogenous subcutaneous adipose tissue of mice that received a subcutaneous adipose tissue graft transplanted into the intra-abdominal compartment, including increased expression of uncoupling protein 1. This suggests that a humoral or neural signal that selectively upregulates adrenergic stimulation of subcutaneous adipose tissue mediates the metabolic benefit observed after transplantation of subcutaneous adipose tissue into the intra-abdominal compartment.

Research design and methods

Animals

Male C57BL/6J mice were purchased from the animal resources centre (Perth, Australia). Animals were kept in a temperature-controlled room ($22 \pm 1^\circ\text{C}$), 80% relative humidity on a 12-h light/dark cycle with free access to food and water. Mice were fed ad libitum with a high fat diet (45% calories from fat, 20% calories from protein, and 35% calories from carbohydrates, 4.7 kcal/g, based on rodent diet no. D12451; Research Diets). Experiments were carried out with the approval of the Garvan Institute/St. Vincent's Hospital Animal Experimentation Ethics Committee, following guidelines issued by the National Health and Medical Research Council of Australia.

Adipose tissue transplantation

Transplantation experiments were performed as described in Chapter 2. In brief, transplantation surgery was performed at 7 wks of age. Mice were anesthetized with ketamine (100 mg/kg ip)/xylazine (20 mg/kg ip). Inguinal (subcutaneous) and

epididymal (abdominal) fat pads were removed from a donor mouse, weighed and rinsed with sterile phosphate buffered saline. For each donor mouse there were two recipient mice - one transplant recipient received subcutaneous (inguinal) adipose tissue grafts and a second transplant recipient received abdominal (epididymal) adipose tissue grafts. Donor and recipient mice were age and weight matched to minimize rejection as described by Chen et al 2003 (122). Mice were divided into two groups. One group received transplants into the subcutaneous compartment (n = 5 receiving a subcutaneous transplant and n = 5 receiving an intra-abdominal transplant) and the second group received transplants into the intra-abdominal compartment (n = 5 receiving a subcutaneous transplant and n = 5 receiving an intra-abdominal transplant) (Figure 3.1). For transplants into the subcutaneous compartment, adipose tissue grafts were divided into two equal sized pieces and implanted subcutaneously, through a small incision in the back, into a pocket created by blunt-dissection between the skin and muscle layers, following the technique described by Gavrilova et al 2000 (119). Transplants into the intra-abdominal compartment were sutured to the peritoneal surface of the anterior abdominal wall through a vertical midline incision in the rectus abdominus muscles. Sham operated mice (n = 5) received identical surgical treatment without transplant. Skin incisions were closed with wound clips (Autoclip, BD).

Adipose tissue harvesting and RNA extraction

At 13 wks after transplantation, mice were killed by cervical dislocation and endogenous and transplanted adipose tissue depots removed, blotted on gauze to remove excess blood and snap frozen in liquid nitrogen. RNA extraction was kindly performed by Dr Ganesh Kolumam, Genentech Inc., South San Francisco, USA. RNA was extracted from adipose tissue using an RNeasy Lipid Tissue kit (Qiagen) according to the manufacturer's protocol. RNA was extracted from the following adipose tissue depots – subcutaneous adipose tissue transplanted into the intra-abdominal compartment (SC-AB), subcutaneous adipose tissue transplanted into the subcutaneous compartment (SC-SC), endogenous subcutaneous (inguinal) adipose tissue from a SC-AB transplant recipient (ENDOG-SC), endogenous visceral

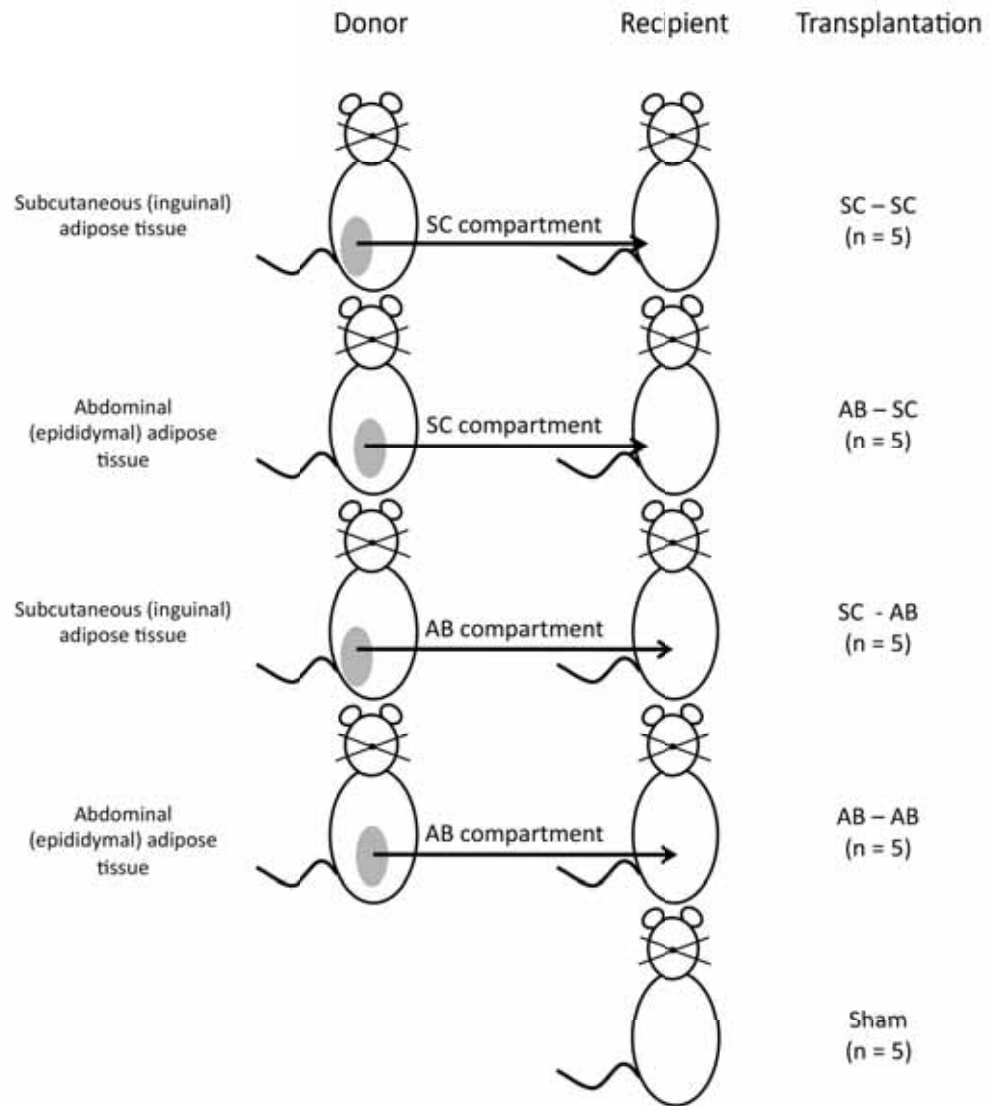


Figure 3.1. Schematic of adipose tissue transplantation experiments.

Subcutaneous (SC; inguinal) or visceral (VIS; epididymal) adipose tissue from donor mice was transplanted into the intra-abdominal (VIS) or subcutaneous (SC) compartment of wild-type C57BL/6 host mice. The sham group had surgery in the VIS or SC compartment, but no fat was transplanted.

(epididymal) adipose tissue from a SC-AB transplant recipient (ENDOG-VIS) and subcutaneous (inguinal) adipose tissue from a sham-operated animal (SHAM-SC). Adipose tissue was collected from 5 mice for each depot (SC-AB, SC-SC, ENDOG-SC, ENDOG-VIS, SHAM-SC). SC-AB, ENDOG-SC and ENDOG-VIS depots were harvested from the same mouse. From each of these depots, approximately 100mg of frozen adipose tissue was used for RNA extraction. Tissue disruption was performed using a TissueLyser II with stainless steel blades (Qiagen). A further homogenisation step was performed using a QIAshredder homogenizer (Qiagen) prior to the addition of 70% ethanol. Residual DNA was removed using a DNase digestion (Qiagen) after RNA purification.

RNA preparation for microarrays

Affymetrix Mouse Genome 430 2.0 array gene chips were used for this study. cRNA conversion, hybridization and scanning were performed at Genentech Inc., South San Francisco, USA. Quantity and quality of input total RNA was determined using an ND-1000 spectrophotometer (Thermo Scientific) and Bioanalyzer 2100 (Agilent Technologies), respectively. The methods for preparation of labelled cRNA and array hybridization were as provided by Affymetrix. Briefly, 3 µg of total RNA was converted into double-stranded cDNA using a cDNA synthesis kit SuperScript Choice (Invitrogen) and a T7-(dT)₂₄ oligomer primer (Integrated DNA Technologies). Double-stranded cDNA was purified using affinity resin Sample Cleanup Module Kit (Affymetrix). Labelled cRNA was generated using a T7 RNA polymerase and biotin-labelled nucleotides in an *in vitro* transcription reaction (Enzo Diagnostics). The labelled cRNA was purified using Sample Cleanup Module Kit (Affymetrix). The amount of labelled cRNA was determined by measuring absorbance at 260 nm and using the convention that 1 OD at 260 nm corresponds to 40 µg/ml of RNA. Labelled cRNA (15 µg) was fragmented by incubating at 94°C for 30 min in 40 mM Tris-acetate pH 8.1, 100 mM potassium acetate and 30 mM magnesium acetate. Fragmented cRNA (10 µg) was then hybridized to Mouse Genome 430 2.0 arrays at 45°C for 19 h in a rotisserie oven set at 60 rpm. Arrays were washed and stained in the Affymetrix Fluidics station and scanned on GeneChip scanner 3000. Data

analysis files were generated using manufacturer's GeneChip Command Console system (Affymetrix). For each depot (SC-AB, SC-SC, ENDOG-SC, ENDOG-VIS, SHAM-SC) 5 arrays, each representing RNA from one mouse, were analysed.

Microarray analysis

The 45,000 probe sets on Affymetrix MOE 430 2.0 microarrays representing over 39,000 transcripts and variants from over 34,000 well- characterized mouse genes were considered for analysis. Data analysis was performed using Genepattern (197). Normalisation and probeset summarisation was performed using the robust multichip average (RMA; (198)), implemented in the affy library (199) from R/Bioconductor (200, 201). Differential gene expression due to depots was assessed for each probeset using an empirical Bayes, moderated t-statistic, implemented in limma (202) from R/Bioconductor, using the limmaGP tool in GenePattern. P values were corrected for multiple hypothesis testing using the positive false discovery rate (FDR; (203)). Differences in gene expression of greater than two-fold were considered for analysis. Subsequently, Gene Set Enrichment Analysis (GSEA) (204) for transcription factor targets was performed against the c3_all collection of gene sets in the Molecular Signatures Database (MSigDB) (204). GSEA is a computational method that determines whether an a priori defined set of genes show statistically significant, concordant differences between two depots of interest. The gene sets are defined based on prior biological knowledge, such as published information about biochemical pathways or co-expression in previous experiments (204). GSEA was validated as a technique in a study analyzing data from muscle biopsies from subjects with diabetes compared with healthy controls (205). GSEA revealed that genes involved in oxidative phosphorylation showed reduced expression in diabetic subjects, although the average decrease per gene was only 20%. The results were independently validated by other microarray studies (206) and by *in vivo* functional studies (207).

Results

To address the hypothesis that novel adipokines are responsible for the metabolic benefits resulting from transplantation of subcutaneous adipose tissue into the intra-abdominal compartment, I performed gene expression analysis of whole adipose tissue depots taken from the following locations - subcutaneous adipose tissue transplanted into the intra-abdominal compartment (SC-AB), subcutaneous adipose tissue transplanted into the subcutaneous compartment (SC-SC), endogenous subcutaneous (inguinal) adipose tissue from a SC-AB transplant recipient (ENDOG-SC), endogenous visceral (epididymal) adipose tissue from a SC-AB transplant recipient (ENDOG-VIS) and subcutaneous (inguinal) adipose tissue from a sham-operated animal (SHAM-SC). Affymetrix MOE 430 2.0 microarrays were utilized, which have 45,000 probe sets to analyze the expression level of over 39,000 transcripts and variants from over 34,000 well- characterized mouse genes.

As the selective transplantation of subcutaneous adipose tissue into the intra-abdominal compartment resulted in a beneficial impact on metabolism, whereas transplantation of subcutaneous adipose tissue into the subcutaneous compartment had no impact on metabolism in my study, I determined which genes were differentially expressed between SC-AB and SC-SC grafts. By comparing gene expression between these two transplanted depots, genes that are differentially expressed as a result of the transplantation process itself should not be identified, whereas genes that are responsible for the selective metabolic benefit resulting from transplantation of subcutaneous adipose tissue into the intra-abdominal but not subcutaneous compartment should be differentially expressed. Comparing SC-AB and SC-SC grafts, 55 probe sets representing 44 genes were greater than two-fold differentially expressed ($q < 0.05$). Of these, 41 genes had greater than two-fold higher levels of expression in SC-AB grafts compared with SC-SC grafts (Table 3.1). Only 3 displayed greater than two-fold higher levels of expression in SC-SC compared with SC-AB grafts (Table 3.2).

TABLE 3.1.**Genes upregulated more than two fold in SC-AB compared with SC-SC grafts.**

Upregulated in	Description	q value	Fold change	Target of MEF2A
SC - AB	myosin, heavy polypeptide 4, skeletal muscle, Myh4	0.023	72.16	Yes
SC - AB	troponin T3, skeletal, fast, Tnnt3	0.016	67.63	No
SC - AB	myosin light chain, phosphorylatable, fast skeletal muscle, Mylpf	0.017	43.32	No
SC - AB	troponin C2, fast, Tnnc2	0.020	43.09	Yes
SC - AB	titin, Ttn	0.006	42.41	No
SC - AB	nebulin, Neb	0.021	39.83	No
SC - AB	myotilin, Myot	0.048	34.67	No
SC - AB	myosin binding protein C, fast-type, Mybpc2	0.023	29.60	Yes
SC - AB	creatine kinase, muscle, Ckm	0.025	25.51	Yes
SC - AB	small muscle protein, X-linked, Smpx	0.045	25.06	Yes
SC - AB	actinin alpha 3, Actn3	0.042	22.90	Yes
SC - AB	ATPase, Ca++ transporting, cardiac muscle, fast twitch 1, Atp2a1	0.016	22.39	No
SC - AB	parvalbumin, Pvalb	0.023	20.86	Yes
SC - AB	myomesin 2, Myom2	0.033	20.56	Yes
SC - AB	actin, alpha 1, skeletal muscle, Acta1	0.024	16.85	Yes
SC - AB	myoglobin, Mb	0.039	15.31	Yes
SC - AB	enolase 3, beta muscle, Eno3	0.045	11.26	Yes
SC - AB	troponin I, skeletal, fast 2, Tnni2	0.014	10.02	No
SC - AB	PDZ and LIM domain 3, Pdlim3	0.047	9.65	No
SC - AB	uroplakin 3B, Upk3b	0.000	8.00	No
SC - AB	R-spondin homolog (Xenopus laevis), Rspo1	0.000	7.76	No
SC - AB	fibromodulin, Fmod	0.000	7.51	No
SC - AB	myosin, light polypeptide 1, Myl1	0.039	6.77	Yes
SC - AB	C1q and tumor necrosis factor related protein 3, C1qtnf3	0.000	5.64	No
SC - AB	multimerin 1, Mmrn1	0.003	5.49	No
SC - AB	glycoprotein m6a, Gpm6a	0.030	4.56	No
SC - AB	sarcolipin, Sln	0.016	4.30	No
SC - AB	RIKEN cDNA B430119L13 gene, B430119L13Rik	0.037	4.22	No
SC - AB	Wilms tumor homolog, Wt1	0.007	4.04	No
SC - AB	RIKEN cDNA 1200016E24 gene, 1200016E24Rik	0.001	4.03	No
SC - AB	basonuclin 1, Bnc1	0.033	2.91	No
SC - AB	collagen, type VIII, alpha 2, Col8a2	0.001	2.84	No
SC - AB	carboxypeptidase X 2 (M14 family), Cpxm2	0.041	2.84	No
SC - AB	ATPase, Na+/K+ transporting, beta 1 polypeptide, Atp1b1	0.037	2.53	No
SC - AB	angiopoietin-like 1, Angptl1	0.024	2.50	No
SC - AB	steroidogenic acute regulatory protein, Star	0.021	2.49	No
SC - AB	microfibrillar-associated protein 4, Mfap4	0.008	2.43	No
SC - AB	FXD domain-containing ion transport regulator 6, Fxyd6	0.002	2.42	No
SC - AB	reelin, Reln	0.025	2.41	No
SC - AB	neural cell adhesion molecule 1, Ncam1	0.000	2.31	No
SC - AB	RIKEN cDNA 1500015O10 gene, 1500015O10Rik	0.039	2.06	No

TABLE 3.2.**Genes upregulated more than two fold in SC-SC compared with SC-AB grafts.**

Upregulated in	Description	<i>q</i> value	Fold change	Target of MEF2A
SC - SC	protein kinase, cGMP-dependent, type II, Prkg2	0.023	2.85	No
SC - SC	RIKEN cDNA D330017J20 gene, D330017J20Rik	0.023	2.52	No
SC - SC	cell division cycle 6 homolog (<i>S. cerevisiae</i>), Cdc6	0.047	2.19	No

In my study, mice receiving a subcutaneous adipose tissue transplant into the intra-abdominal compartment developed decreased fat mass, with reductions in size of both endogenous inguinal and epididymal adipose tissue beds. I determined which genes were differentially expressed between endogenous subcutaneous (inguinal) adipose tissue from a SC-AB transplant recipient (ENDOG-SC) and subcutaneous (inguinal) adipose tissue from a sham-operated animal (SHAM-SC), in order to explore the mechanisms underlying the decreased inguinal (subcutaneous) adipose tissue mass observed in mice receiving a subcutaneous adipose tissue transplant into the intra-abdominal compartment. Comparing ENDOG-SC and SHAM-SC grafts, 1578 probe sets were greater than two-fold differentially expressed ($q < 0.05$). Of these, 973 probe sets had greater than two-fold higher levels of expression in ENDOG-SC compared with SHAM-SC grafts, with 33 genes having greater than ten-fold higher levels of expression in ENDOG-SC grafts compared with SHAM-SC grafts (Table 3.3). Greater than two-fold lower levels of expression in ENDOG-SC compared with SHAM-SC grafts was observed for 605 probe sets, of which only 4 genes displayed greater than ten-fold higher levels of expression in SHAM-SC compared with ENDOG-SC grafts (Table 3.4). As the observed increase in glucose uptake in Tran's study was unique to endogenous subcutaneous adipose tissue despite both endogenous subcutaneous and visceral adipose tissue decreasing in size (169), I compared levels of gene expression between endogenous inguinal (ENDOG-SC) and epididymal (ENDOG-VIS) adipose tissue beds from mice receiving a subcutaneous transplant into the intra-abdominal compartment. Comparing ENDOG-SC and ENDOG-VIS grafts, 1463 probe sets were greater than two-fold differentially expressed ($q < 0.05$). Of these, 898 probe sets had greater than two-fold higher levels of expression in ENDOG-SC compared with ENDOG-VIS grafts with 27 genes having greater than ten-fold higher levels of expression in ENDOG-SC grafts compared with ENDOG-VIS grafts (Table 3.5). Greater than two-fold lower levels of expression in ENDOG-SC compared with ENDOG-VIS grafts was observed for 565 probe sets of which only 2 genes displayed greater than ten-fold higher levels of expression in ENDOG-VIS compared with ENDOG-SC grafts (Table 3.6).

TABLE 3.3.**Genes upregulated more than ten fold in ENDOG-SC compared with SHAM-SC grafts.**

Upregulated in	Description	q value	Fold change	Target of MEF2A
ENDOG-SC	myosin, heavy polypeptide 4, skeletal muscle, Myh4	0.001	63.36	Yes
ENDOG-SC	titin, Ttn	0.000	58.05	No
ENDOG-SC	major urinary protein 1 / major urinary protein 2 / RIKEN cDNA 2610016E04 gene	0.000	57.06	No
ENDOG-SC	troponin C2, fast, Tnnc2	0.001	43.64	Yes
ENDOG-SC	troponin T3, skeletal, fast, Tnnt3	0.002	35.92	No
ENDOG-SC	troponin I, skeletal, fast 2, Tnni2	0.001	34.33	No
ENDOG-SC	myosin light chain, phosphorylatable, fast skeletal muscle, Mylpf	0.002	26.53	No
ENDOG-SC	immunoglobulin heavy variable V14-2, Ighv14-2	0.012	22.95	No
ENDOG-SC	myosin, heavy polypeptide 1, skeletal muscle, adult, Myh1	0.004	21.01	No
ENDOG-SC	membrane-spanning 4-domains, subfamily A, member 1, Ms4a1	0.014	19.95	No
ENDOG-SC	membrane-spanning 4-domains, subfamily A, member 4B, Ms4a4b	0.001	19.68	No
ENDOG-SC	creatine kinase, muscle, Ckm	0.003	17.22	Yes
ENDOG-SC	myosin binding protein C, fast-type, Mybpc2	0.003	17.22	Yes
ENDOG-SC	nebulin, Neb	0.004	16.81	No
ENDOG-SC	CD79B antigen, Cd79b	0.007	16.69	No
ENDOG-SC	T-cell receptor beta, joining region / Tcrb-J	0.004	16.60	No
ENDOG-SC	Fas apoptotic inhibitory molecule 3, Faim3	0.011	15.98	No
ENDOG-SC	small muscle protein, X-linked, Smpx	0.004	15.71	Yes
ENDOG-SC	tropomyosin 2, beta, Tpm2	0.006	15.37	Yes
ENDOG-SC	histocompatibility 2, O region beta locus, H2-Ob	0.013	15.15	No
ENDOG-SC	lymphotoxin B, Ltb	0.005	13.58	No
ENDOG-SC	POU domain, class 2, associating factor 1, Pou2af1	0.016	13.14	No
ENDOG-SC	parvalbumin, Pvalb	0.003	12.57	Yes
ENDOG-SC	myotilin, Myot	0.012	12.50	No
ENDOG-SC	ATPase, Ca++ transporting, cardiac muscle, fast twitch 1, Atp2a1	0.003	11.80	No
ENDOG-SC	CD79A antigen (immunoglobulin-associated alpha) / Cd79a / LOC100047815	0.011	11.79	No
ENDOG-SC	purinergic receptor P2Y, G-protein coupled 10, P2ry10	0.007	11.76	No
ENDOG-SC	major urinary protein 1 / major urinary protein 2 / major urinary protein 3 / RIKEN cDNA 2610016E04 gene, 2610016E04Rik / Mup1 / Mup2 / Mup3	0.005	11.34	No
ENDOG-SC	CD3 antigen, gamma polypeptide, Cd3g	0.005	11.19	No
ENDOG-SC	RIKEN cDNA 2010309G21 gene / immunoglobulin lambda chain, constant region 2 / immunoglobulin lambda chain, constant region 3 / Igl-C2 / Igl-C3	0.026	11.15	No
ENDOG-SC	G protein-coupled receptor 174, Gpr174	0.006	11.04	No
ENDOG-SC	membrane-spanning 4-domains, subfamily A, member 4C, Ms4a4c	0.007	10.74	No
ENDOG-SC	B-cell CLL/lymphoma 11A (zinc finger protein), Bcl11a	0.007	10.42	No

TABLE 3.4.**Genes upregulated more than ten fold in SHAM-SC compared with ENDOG-SC grafts.**

Upregulated in	Description	<i>q</i> value	Fold change	Target of MEF2A
SHAM-SC	aristaless related homeobox gene (Drosophila) / similar to Arx homeoprotein, Arx / LOC100044440	0.000	26.52	No
SHAM-SC	uroplakin 3B, Upk3b	0.000	25.18	No
SHAM-SC	RIKEN cDNA B430119L13 gene, B430119L13Rik	0.000	13.34	No
SHAM-SC	R-spondin homolog (Xenopus laevis), Rspo1	0.000	10.46	No

TABLE 3.5.**Genes upregulated more than ten fold in ENDOG-SC compared with ENDOG-VIS grafts.**

Upregulated in	Description	q value	Fold change	Target of MEF2A
ENDOG-SC	myosin, heavy polypeptide 4, skeletal muscle, Myh4	0.002	61.46	Yes
ENDOG-SC	titin, Ttn	0.000	48.67	No
ENDOG-SC	troponin C2, fast, Tnnc2	0.001	35.73	Yes
ENDOG-SC	troponin I, skeletal, fast 2, Tnni2	0.001	33.92	No
ENDOG-SC	troponin T3, skeletal, fast, Tnnt3	0.003	32.71	No
ENDOG-SC	myosin light chain, phosphorylatable, fast skeletal muscle, Mylpf	0.002	26.21	No
ENDOG-SC	myosin, heavy polypeptide 1, skeletal muscle, adult, Myh1	0.004	22.40	No
ENDOG-SC	immunoglobulin heavy variable V14-2, Ighv14-2	0.015	20.16	No
ENDOG-SC	myosin binding protein C, fast-type, Mybpc2	0.003	17.16	Yes
ENDOG-SC	major urinary protein 1 / major urinary protein 2 / major urinary protein 3 / RIKEN cDNA 2610016E04 gene, 2610016E04Rik / Mup1 / Mup2 / Mup3	0.001	17.12	No
ENDOG-SC	nebulin, Neb	0.005	17.00	No
ENDOG-SC	creatine kinase, muscle, Ckm	0.003	16.49	Yes
ENDOG-SC	membrane-spanning 4-domains, subfamily A, member 1, Ms4a1	0.020	16.19	No
ENDOG-SC	membrane-spanning 4-domains, subfamily A, member 4B, Ms4a4b	0.003	15.43	No
ENDOG-SC	small muscle protein, X-linked, Smpx	0.005	14.86	Yes
ENDOG-SC	histocompatibility 2, O region beta locus, H2-Ob	0.015	14.47	No
ENDOG-SC	Fas apoptotic inhibitory molecule 3, Faim3	0.015	14.14	No
ENDOG-SC	tropomyosin 2, beta, Tpm2	0.007	14.06	No
ENDOG-SC	CD79B antigen, Cd79b	0.012	13.34	No
ENDOG-SC	T-cell receptor beta, joining region / Tcrb-J	0.007	13.09	No
ENDOG-SC	parvalbumin, Pvalb	0.003	12.95	No
ENDOG-SC	ATPase, Ca++ transporting, cardiac muscle, fast twitch 1, Atp2a1	0.003	12.06	No
ENDOG-SC	myotilin, Myot	0.014	11.83	No
ENDOG-SC	enolase 3, beta muscle, Eno3	0.002	11.17	Yes
ENDOG-SC	special AT-rich sequence binding protein 1, Satb1	0.001	10.47	No
ENDOG-SC	membrane-spanning 4-domains, subfamily A, member 4C, Ms4a4c	0.008	10.45	No
ENDOG-SC	CD79A antigen (immunoglobulin-associated alpha) / Cd79a / LOC100047815	0.015	10.10	No

TABLE 3.6.**Genes upregulated more than ten fold in ENDOG-VIS compared with ENDOG-SC grafts.**

Upregulated in	Description	<i>q</i> value	Fold change	Target of MEF2A
ENDOG-VIS	uroplakin 3B, Upk3b	0.000	20.87	No
ENDOG-VIS	aristaless related homeobox gene (Drosophila) / similar to Arx homeoprotein, Arx / LOC100044440	0.000	20.58	No

It was noted that many of the genes displaying increased expression in SC-AB grafts compared with SC-SC grafts encoded cytoskeletal components of skeletal muscle. To test the hypothesis that these genes may be under the control of a common transcription factor, gene set enrichment analysis (GSEA) for transcription factor targets was performed. This identified 21 gene sets with a normalized enrichment score of >2 and a positive false discovery rate of $q < 0.001$. Twelve of these 21 gene sets were pre-defined to contain genes with promoter regions matching the annotation for myocyte enhancer factor 2A (MEF2A) (Table 3.7). Consistent with this finding, of the 41 genes having greater than two-fold higher levels of expression in SC-AB grafts compared with SC-SC grafts, 12 genes contained promoter regions matching the annotation for MEF2A (Table 3.1). These were skeletal muscle myosin, heavy polypeptide 4; fast troponin C2; fast-type myosin binding protein C; muscle creatine kinase; X-linked small muscle protein; actinin alpha 3; parvalbumin; myomesin 2; skeletal muscle actin, alpha 1; myoglobin; beta muscle enolase 3; and myosin, light polypeptide 1. These genes were all expressed greater than five-fold higher in SC-AB grafts compared with SC-SC grafts.

The identification of genes encoding muscle proteins in the transplanted adipose tissue raised the question of contamination by skeletal muscle, especially as the transplants were sutured to the rectus abdominus muscle. In both SC-AB and SC-SC grafts, the absence of increased expression of myogenin and MyoD1, key transcription factors involved in the development of skeletal muscle, refutes this (Figure 3.2).

Remarkably, the 12 genes containing MEF2A promoter regions that were upregulated in SC-AB grafts (listed above) were also upregulated in ENDOG-SC adipose tissue in mice that received a subcutaneous transplant into the intra-abdominal space. These genes were not upregulated in either ENDOG-VIS or SHAM-SC depots (Figure 3.3). Interestingly, of the 33 genes displaying greater than ten-fold higher levels of expression in ENDOG-SC grafts compared with SHAM-SC grafts, 7 genes contained MEF2A promoter regions (Table 3.3).

TABLE 3.7.

Gene sets identified by gene set enrichment analysis for transcription factor targets comparing SC-AB and SC-SC grafts. Gene sets showing statistically significant, concordant differences between SC-AB and SC-SC grafts with a normalised enrichment score greater than 2.0 are shown.

Name of gene set	Normalised Enrichment Score	<i>q</i> value	Transcription factor
CTAWWWATA_V\$RSRFC4_Q2	3.00	0	MEF2A
V\$HMEF2_Q6	2.84	0	MEF2A
V\$MEF2_02	2.60	0	MEF2A
V\$RSRFC4_01	2.57	0	MEF2A
V\$RSRFC4_Q2	2.54	0	MEF2A
V\$MEF2_Q6_01	2.46	0	MEF2A
V\$MEF2_01	2.44	0	MEF2A
V\$HNF1_01	2.43	0	HNF1
RGTAMWNATT_V\$HNF1_01	2.27	0	HNF1
V\$MEF2_03	2.24	0	MEF2A
TAAWWATAG_V\$RSRFC4_Q2	2.21	0	MEF2A
YTATTTTNR_V\$MEF2_02	2.16	0	MEF2A
V\$MMEF2_Q6	2.15	0	MEF2A
V\$AP4_Q6_01	2.15	0	TFAP4
CCAWWNAAGG_V\$SRF_Q4	2.10	0	SRF
V\$AMEF2_Q6	2.07	0	MEF2A
V\$TBP_01	2.06	0	TBP
V\$SRF_Q6	2.04	0	SRF
V\$HNF1_C	2.02	0	HNF
V\$HNF1_Q6	2.01	0	HNF
V\$SRF_01	2.01	0	SRF

Myocyte enhancer factor 2A (MEF2A) is a member of the myocyte enhancer factor 2 (MEF2) family of transcription factors that play a key role in skeletal muscle differentiation. Four MEF2 isoforms have been identified - MEF2A, MEF2B, MEF2C and MEF2D. Expression of MEF2A, MEF2B, MEF2C or MEF2D was compared between SC-AB and SC-SC grafts and no significant differences in gene expression were identified ($q>0.25$). Expression of MEF2A and MEF2B was not significantly different between ENDOG-SC, ENDOG-VIS and SHAM-SC grafts ($q>0.1$). However, gene expression of MEF2C and MEF2D was significantly increased in ENDOG-SC compared with SHAM-SC adipose tissue (3 fold and 1.5 fold respectively, $q<0.005$) and ENDOG-SC compared with ENDOG-VIS adipose tissue (3.5 fold and 1.5 fold respectively, $q<0.005$) (Figure 3.4).

Gene expression of MEF2C and MEF2D was selectively upregulated in ENDOG-SC adipose tissue in mice receiving a subcutaneous adipose tissue transplant into the intra-abdominal compartment. As the MEF2 binding site is required for GLUT4 gene expression in both muscle and adipose tissue, GLUT4 gene expression was compared in ENDO-SC and ENDOG-VIS adipose tissue. No significant difference in gene expression was observed ($q>0.2$).

To further explore the potential mechanisms by which SC- AB grafts might affect whole-body metabolism, expression of several key adipokines, specifically leptin, adiponectin, resistin, and retinol-binding protein 4 (Rbp4), was analysed. No significant difference in gene expression for leptin, adiponectin, resistin and RBP4 was observed between the SC-AB and SC-SC adipose tissue grafts ($q>0.1$). Expression of leptin, adiponectin, resistin and RBP4 was decreased in ENDOG-SC adipose tissue compared with both SHAM-SC and ENDOG-VIS adipose tissue ($q<0.04$) (Figure 3.5).

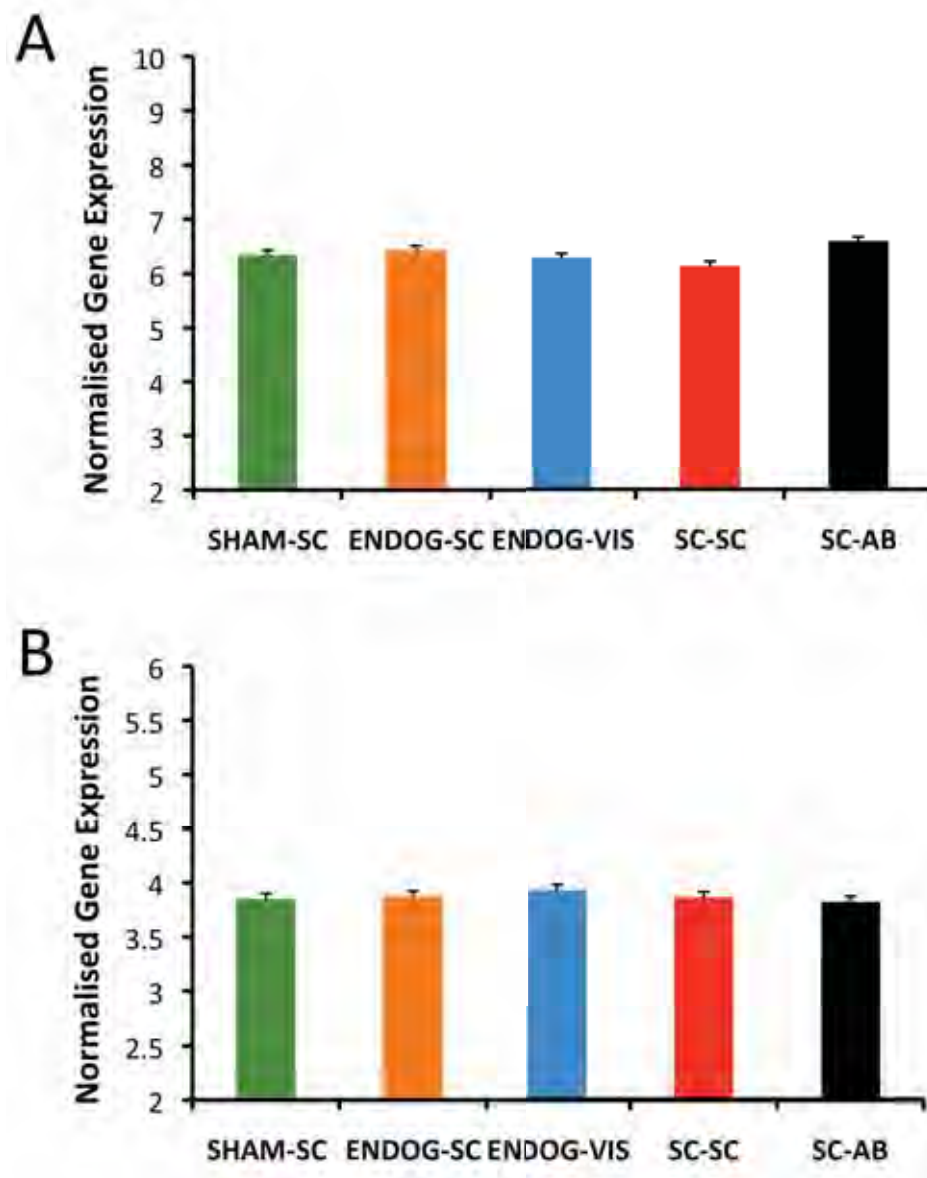


Figure 3.2. Normalised gene expression of myogenin (A) and myogenic differentiation 1 (MyoD1) (B) across adipose tissue depots.

No significant difference in gene expression for myogenin (A) and myogenic differentiation 1 (MyoD1) (B) was observed between the SC-AB, SC-SC, ENDOG-SC, ENDOG-VIS and SHAM-SC adipose tissue depots ($q > 0.1$). Results represent the mean \pm SD (n = 5 per depot).

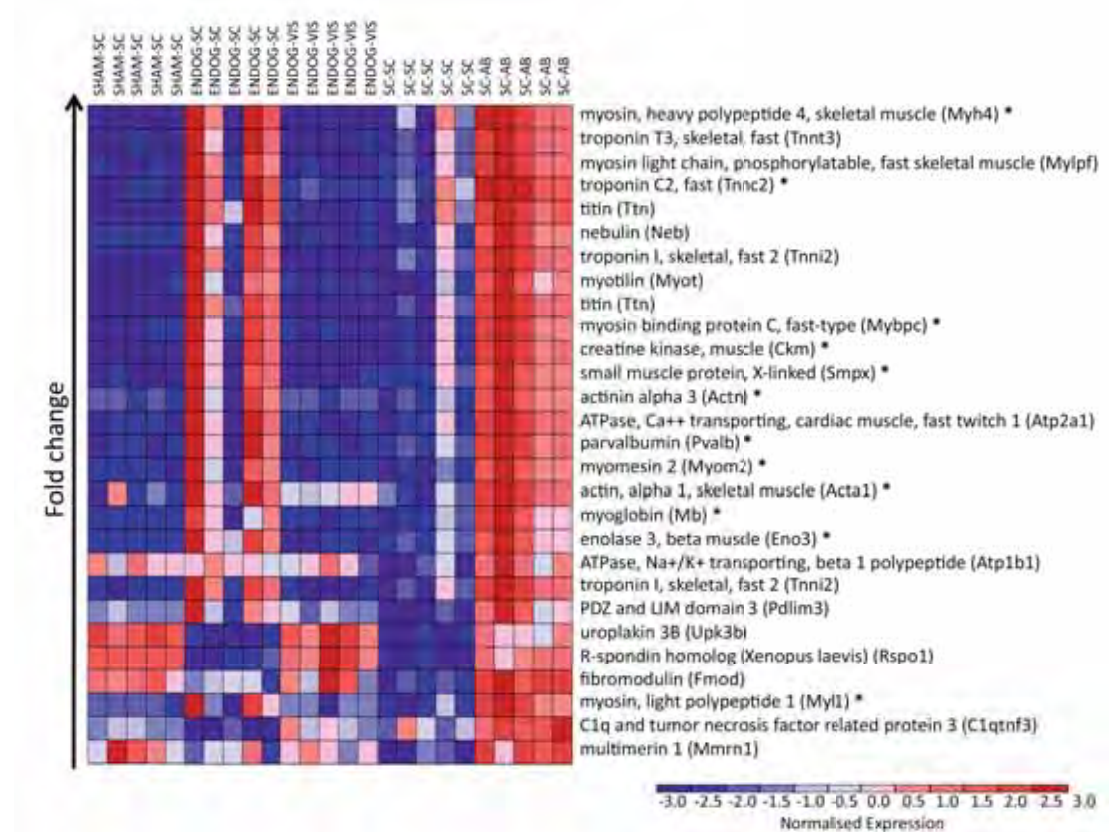


Figure 3.3. Heatmap of normalised gene expression across all adipose tissue depots of genes upregulated more than five fold in SC-AB compared with SC-SC grafts.

Increased expression of genes transcribed by the MEF2A transcription factor (marked *) was identified only in SC-AB and ENDOG-SC adipose tissue depots.

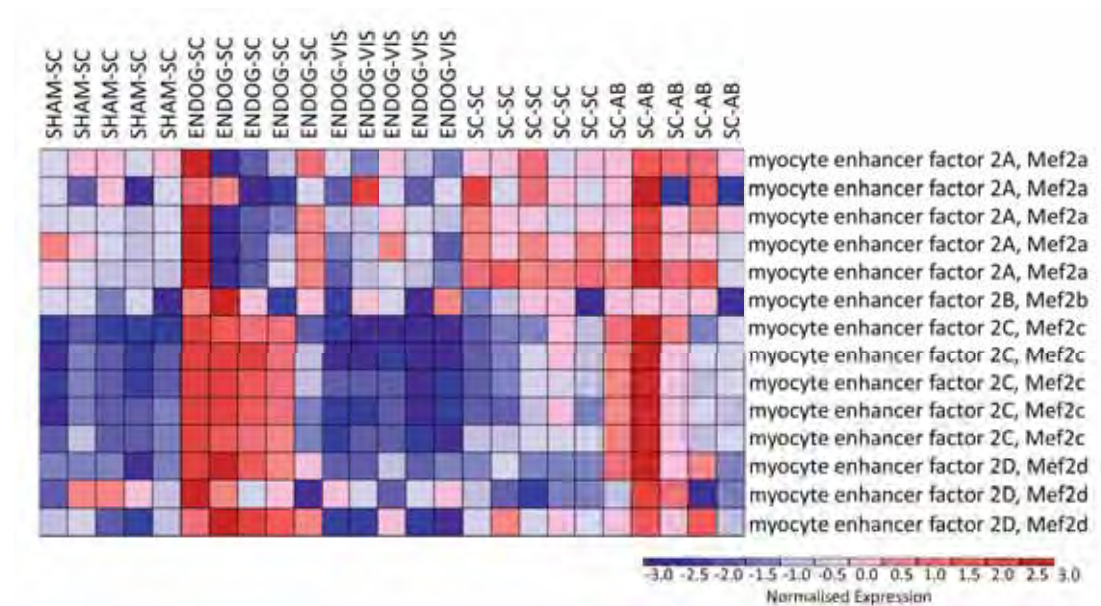


Figure 3.4. Heatmap of normalised gene expression across all adipose tissue depots of MEF2 isoforms.

No significant differences in expression of MEF2A, MEF2B, MEF2C or MEF2D were identified between SC-AB and SC-SC grafts ($q>0.25$). Expression of MEF2A and MEF2B was not significantly different between ENDOG-SC, ENDOG-VIS and SHAM-SC grafts ($q>0.1$). Expression of MEF2C and MEF2D was significantly increased in ENDOG-SC compared with SHAM-SC adipose tissue (3 fold and 1.5 fold respectively, $q<0.005$) and ENDOG-SC compared with ENDOG-VIS adipose tissue (3.5 fold and 1.5 fold respectively, $q<0.005$)

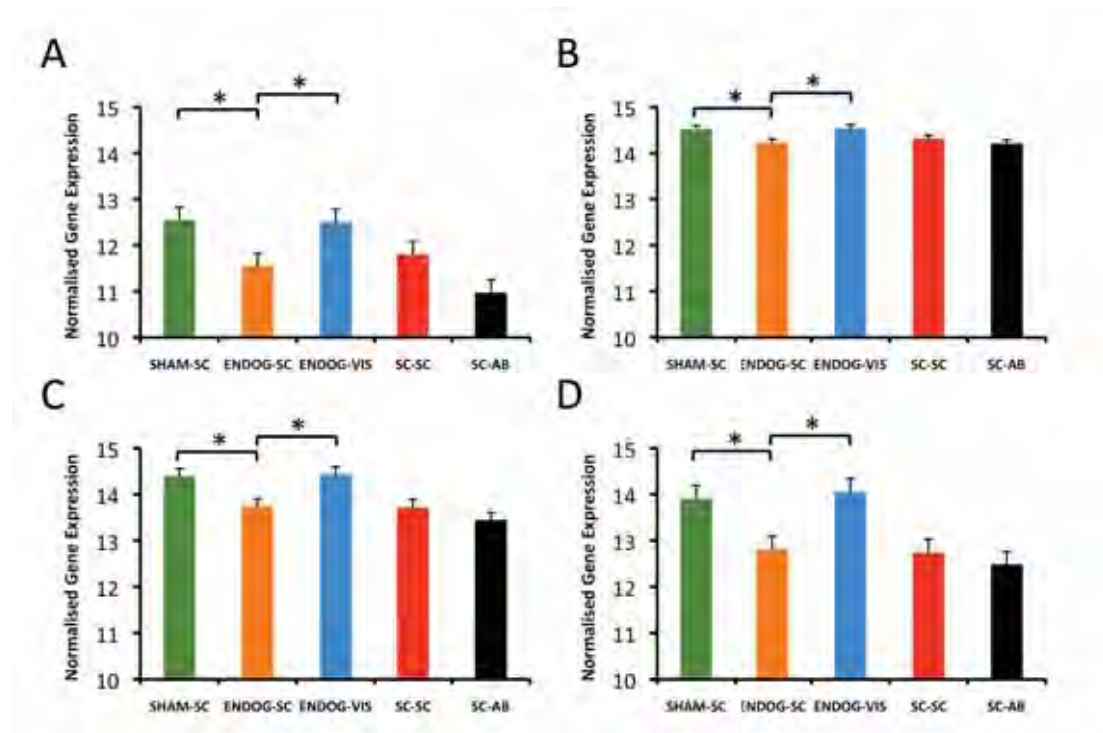


Figure 3.5. Normalised gene expression of leptin (A), adiponectin (B), resistin (C) and RBP4 (D) across adipose tissue depots.

No significant difference in gene expression for leptin **(A)**, adiponectin **(B)**, resistin **(C)** and RBP4 **(D)** was observed between the SC-AB and SC-SC adipose tissue grafts ($q>0.1$). Expression of leptin, adiponectin, resistin and RBP4 was decreased in ENDOG-SC adipose tissue compared with both SHAM-SC and ENDOG-VIS adipose tissue. * denotes statistical significance at $q<0.04$. Results represent the mean \pm SD (n = 5 per depot).

Brown adipose tissue is thermogenic due to an increase in mitochondrial uncoupling protein 1 (UCP-1) levels. UCP-1 is expressed only in brown adipose tissue and uncouples mitochondrial respiration from ATP-production, thus 'wasting' energy in the form of heat (208). Increased expression of UCP-1 in both SC-AB grafts and endogenous adipose tissue beds could explain the metabolic benefit of SC-AB transplantation. No difference in gene expression of uncoupling proteins 2 or 3 was observed in any adipose tissue bed. Gene expression of uncoupling protein 1 was not different between SC-AB and SC-SC grafts. However, there was a small but significant increase in gene expression of uncoupling protein 1 in ENDOG-SC adipose tissue compared with ENDOG-VIS and SHAM-SC adipose tissue (1.2 fold, $q=0.04$ and $q=0.02$, respectively) (Figure 3.6). Brown adipocytes from classic brown adipose tissue depots (inter-scapular and perirenal depots) express myocyte factor 5 (Myf5) (209). There was no difference in gene expression of Myf5 observed in any adipose tissue bed analysed. Therefore, the adipocytes expressing UCP-1 in ENDOG-SC adipose tissue cannot be derived from a Myf-5 positive precursor. Recently a population of brown fat-like adipocytes, having a multilocular morphology and expressing UCP-1, have been identified in white adipose tissue. These have been called adaptive or recruitable brown fat cells, brown in white (brite) cells, or beige cells (210-212). The development of brown fat-like cells in white adipose tissue is dramatically enhanced during adaptation to cold or in response to treatment with β 3-selective adrenergic agonists (213-215). β 3-adrenergic receptors displayed decreased expression in ENDOG-SC compared with SHAM-SC and ENDOG-VIS adipose tissue ($q = 0.02$ and $q = 0.005$, respectively) (Figure 3.7). Catecholamine signalling is transduced by CREB (216). Gene expression of CREB was significantly increased in ENDOG-SC compared with SHAM-SC adipose tissue ($q \leq 0.01$).

Adrenergic stimulation of α 1-adrenoceptors results in activation of glycogen phosphorylase and inactivation of glycogen synthase in rat white adipocytes (217). Gene expression of muscle glycogen phosphorylase was significantly upregulated in SC-AB compared with SC-SC grafts (19 fold, $q=0.05$) and ENDOG-SC compared with SHAM-SC adipose tissue (8.6 fold, $q=0.01$) (Figure 3.8).

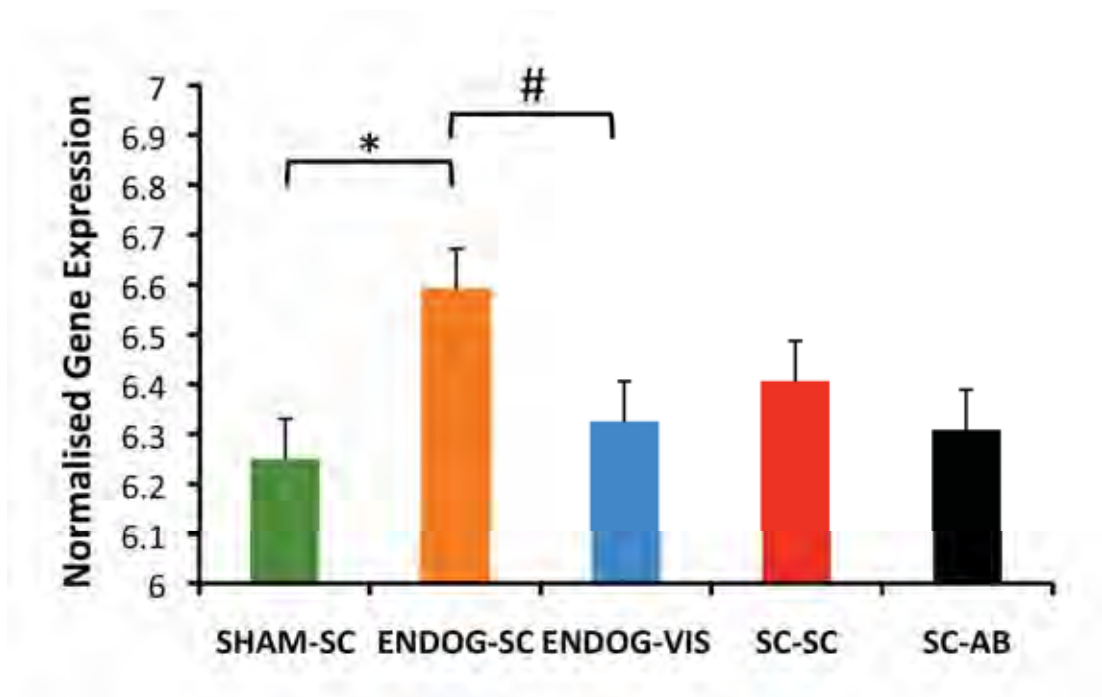


Figure 3.6. Normalised gene expression of UCP-1 across adipose tissue depots.

Expression of UCP-1 was increased in ENDOG-SC adipose tissue compared with both SHAM-SC and ENDOG-VIS adipose tissue. * denotes statistical significance at $q=0.016$. # denotes statistical significance at $q=0.044$. Results represent the mean \pm SD (n = 5 per depot).

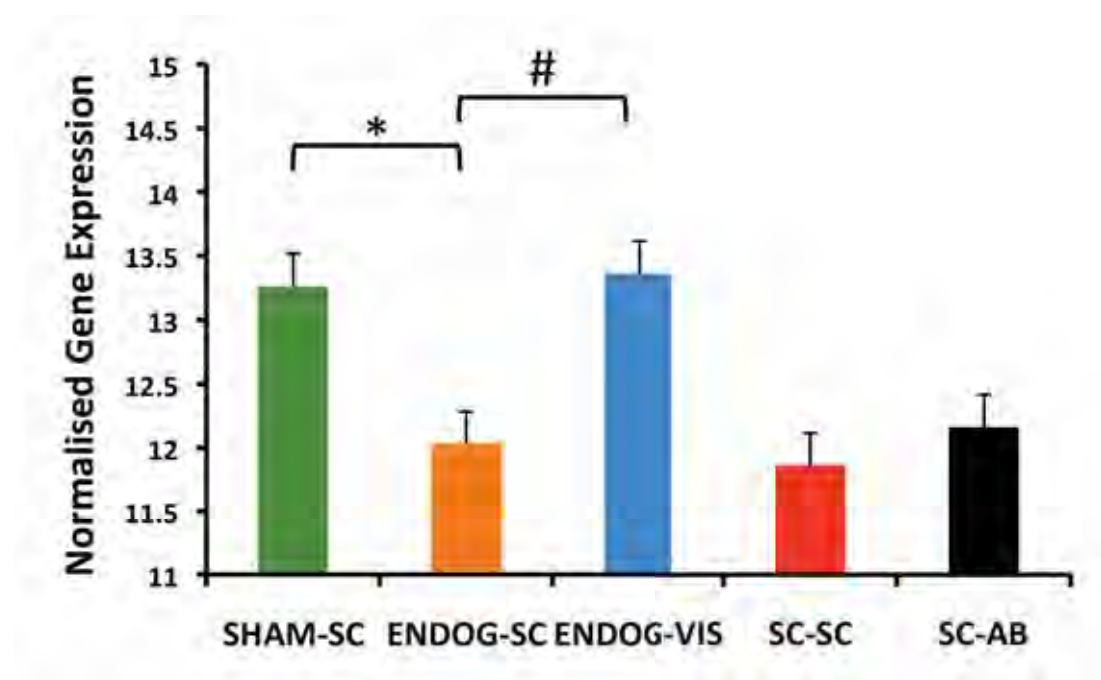


Figure 3.7. Normalised gene expression of β 3-adrenergic receptors across adipose tissue depots.

Expression of β 3-adrenergic receptors was decreased in ENDOG-SC adipose tissue compared with both SHAM-SC and ENDOG-VIS adipose tissue. * denotes statistical significance at $q=0.007$. # denotes statistical significance at $q=0.005$. Results represent the mean \pm SD ($n = 5$ per depot).

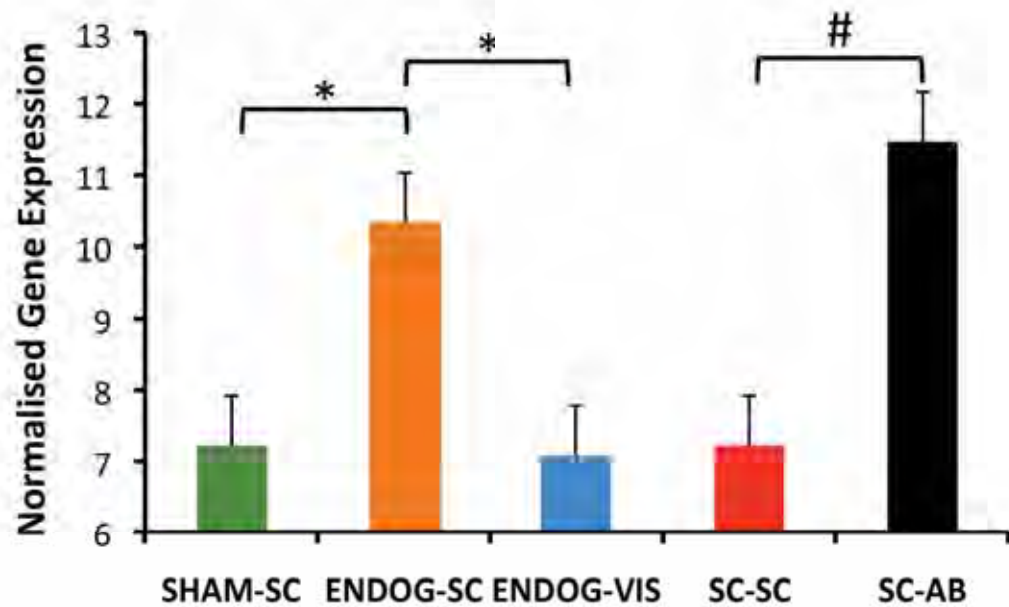


Figure 3.8. Normalised gene expression of glycogen phosphorylase (muscle) across adipose tissue depots.

Expression of glycogen phosphorylase (muscle) was increased in ENDOG-SC adipose tissue compared with both SHAM-SC and ENDOG-VIS adipose tissue and SC-AB compared with SC-SC grafts. * denotes statistical significance at $q=0.01$. # denotes statistical significance at $q=0.05$. Results represent the mean \pm SD ($n = 5$ per depot).

Discussion

Adipose tissue was once thought to be an inert storage depot for excess energy but is now recognized to play a vital role in metabolism. Adipose tissue influences distant metabolic organs through the production of adipokines and other signals produced by the non-adipocyte components of adipose tissue, such as complement components and TNF- α (87). In addition, adipose tissue is innervated by sensory nerves, through which it communicates with the hypothalamus regarding adipose tissue stores, influencing feeding behaviour and adipose tissue metabolism (192). The mechanisms whereby adipose tissue communicates with distant organs remain incompletely understood and it is likely that novel, undiscovered adipokines play an important role. As the beneficial metabolic effects resulting from transplantation of subcutaneous adipose tissue into the intra-abdominal space were not explained by alterations in the levels of known metabolically active adipokines, I proposed that a novel adipokine / adipokines may be responsible.

Using microarray analysis, I compared gene expression between SC-AB and SC-SC grafts. I identified 41 genes that had greater than two-fold higher levels of expression in SC-AB grafts compared with SC-SC grafts. Interestingly, 12 of these genes encoded components of skeletal muscle such as skeletal muscle myosin heavy polypeptide 4, fast troponin C2 and muscle creatine kinase. Given SC-AB transplants were implanted by suturing the donor adipose tissue to the anterior rectus muscle of the anterior abdominal wall, the finding of increased expression of muscle proteins in SC-AB grafts raises the possibility of contamination by adjacent skeletal muscle. Two key findings prove that contamination by skeletal muscle has not occurred. The first is that expression of myogenin and MyoD1 was not increased in SC-AB grafts. Myogenin is essential for the development of functional skeletal muscle (218) and MyoD is expressed only in skeletal muscle or its precursors (219). The second is that a similar upregulation of genes encoding muscle proteins was observed in ENDO-SC adipose tissue in mice receiving a SC-AB transplant but not in SC-SHAM adipose tissue. The finding of a similar upregulation of genes in both SC-

AB grafts and ENDO-SC adipose tissue of a mouse receiving a SC-AB graft suggests that these changes in gene expression are a specific response to the transplantation of subcutaneous adipose tissue into the intra-abdominal compartment and that these changes in gene expression may mediate the beneficial effects on metabolism observed in mice receiving a SC-AB graft. This will be discussed in more detail below.

The finding of increased expression of a cluster of genes encoding muscle proteins in SC-AB adipose tissue grafts led to the hypothesis that these genes may be transcribed by a common transcription factor. Using GSEA, I demonstrated there was an upregulation of genes transcribed by the transcription factor MEF2A in SC-AB grafts. These changes in gene expression were not observed in SC-SC grafts, suggesting that the factor responsible for the induction of these genes may also be responsible for the beneficial metabolic effects resulting from transplantation of subcutaneous adipose tissue into the intra-abdominal compartment. Importantly, a similar upregulation of genes transcribed by the transcription factor MEF2A was also found in the endogenous subcutaneous adipose tissue (ENDOG-SC) of the recipients of SC-AB transplants and not in the subcutaneous adipose tissue of sham-operated mice (SHAM-SC). Gene expression of the isoforms of MEF2 was analysed and increased expression of MEF2C and MEF2D was found in the endogenous subcutaneous adipose tissue of the recipients of SC-AB transplants compared with the subcutaneous adipose tissue of sham-operated mice (SHAM-SC) and the endogenous visceral adipose tissue of the recipients of SC-AB transplants (ENDOG-VIS). This suggests that the same endocrine or neural signal affected both the subcutaneous adipose tissue graft transplanted into the intra-abdominal compartment (SC-AB) and the endogenous subcutaneous adipose tissue in these mice (ENDOG-SC), resulting in increased expression of the transcription factors MEF2C and MEF2D or their downstream targets.

MEF2 proteins belong to the MADS family of transcription factors (named after the first four proteins in which the MADS domain was first identified: minichromosome maintenance 1 (MCM1), which regulates mating-specific genes in yeast; AGAMOUS

and DEFICIENS, which have homeotic function in flower development; and serum-response element (SRE), which regulates serum-inducible and muscle gene expression) (220). Vertebrates have four isoforms of MEF2 - MEF2A, B, C and D, all of which bind to the MEF2 DNA binding site (220). The N-termini of MEF2 factors contain a highly conserved MADS-box and an immediately adjacent motif termed the MEF2 domain, which together mediate dimerization, DNA binding, and co-factor interactions (221, 222). The C-terminal regions of MEF2 proteins, which function as transcriptional activation domains, are divergent among family members (223). MEF2 was first identified as a regulator of muscle gene expression (224). In vertebrates, the four isoforms of MEF2 display highest expression in skeletal muscle, heart and brain, however, MEF2 is also expressed in lymphocytes, neural crest, smooth muscle, endothelium and bone (225). Adipose tissue expresses very low levels of MEF2 (226). The different isoforms of MEF2 display tissue specific distribution. After birth, Mef2A, Mef2B, and Mef2D are expressed ubiquitously (223, 227, 228). MEF-2C expression is restricted to skeletal muscle, spleen, and brain of adult mice and is upregulated during skeletal muscle differentiation (229, 230). In the embryo, MEF2 proteins are involved in the differentiation programs of many cell types including myoblasts (skeletal, cardiac and smooth), chondrocytes and neurons. In adult tissues, MEF2 proteins act in stress-response and remodeling programs; for example, MEF2D is a critical component of the signaling pathways through which adrenergic stimulation drives cardiac hypertrophy (196, 231). MEF2 proteins serve as endpoints for multiple signaling pathways including the mitogen-activated protein (MAP) kinase and calcium signalling pathways. MAP kinase activates MEF2 through phosphorylation of the transcription activation domain. Calcium-dependent signals activate MEF2 by stimulating calcium-dependent kinases that phosphorylate class II HDACs (HDAC 4, 5, 7 and 9), thereby promoting their dissociation from MEF2 and derepressing MEF2 target genes (222).

Of particular interest, the MEF2 binding site is required for GLUT4 gene expression in both muscle and adipose tissue. GLUT4 is the major insulin-responsive glucose transporter and is predominantly expressed in adipose and striated muscle tissues

(232). Cardiac and skeletal muscle expression of GLUT4 is dependent upon binding of a MEF2A-MEF2D heterodimer complex to the MEF2 binding element (233). In addition, GLUT4 enhancer factor (GEF) binds to another regulatory element on the GLUT4 promoter, domain 1. The GLUT4 promoter is regulated through the cooperative function of these two distinct regulatory elements; both are necessary and neither alone is sufficient for optimal transcription of GLUT4 (234). In skeletal muscle, exercise increases the transcription of GLUT4 through an increase in MEF2A nuclear protein while nuclear MEF2D and GEF levels are not changed (235). High-fat feeding reduces the transcription of GLUT4 in adipose tissue as a result of a reduction in the expression of MEF2D whilst expression of MEF2A remains unchanged (236). The precise mechanisms responsible for these tissue-specific changes in MEF2 expression remain to be elucidated with the MEF2 regulators histone deacetylase 5 (HDAC5), PPAR γ coactivator 1 (PGC-1) and p38 MAP kinase proposed to be involved (235). In adipose tissue, AMP-activated protein kinase α has been demonstrated to upregulate both expression of MEF2D and GLUT4 (236), however the precise regulation of MEF2 expression in adipose tissue remains incompletely understood. I observed an increase in gene expression of both MEF2C and MEF2D in ENDOG-SC adipose tissue. MEF2C is not usually expressed in adult adipose tissue and MEF2D expression is usually decreased in high fat feeding. Despite upregulation of MEF2D gene expression in ENDOG-SC adipose tissue, expression levels of GLUT4 were not significantly increased. This implies that the increased glucose uptake observed in ENDOG-SC fat by Tran et al was not mediated by an increase in GLUT4 gene transcription (169).

As the increase in expression of genes controlled by the transcription factor MEF2 was selective to the SC-AB graft and ENDOG-SC adipose tissue, the signal causing upregulation of MEF2 gene expression must be specific to subcutaneous adipose tissue, both endogenous and transplanted. If this signal is humoral, it must act via a signal transduction pathway that is unique to subcutaneous and not visceral adipose tissue. Alternately, the signal may be neural, involving only neural circuits to subcutaneous and not visceral adipose tissue. Adipose tissue is innervated by the

sensory and sympathetic but not parasympathetic nervous systems (66). Five adrenoceptor subtypes are involved in the adrenergic regulation of adipose tissue. β 1-, β 2-, and β 3-adrenergic receptors stimulate adenylyl cyclase activity increasing cAMP production. Conversely, α 2-adrenoceptors inhibit adenylyl cyclase activity decreasing cAMP production. cAMP activates protein kinase A, resulting in phosphorylation of hormone sensitive lipase (HSL), followed by HSL translocation to the lipid droplet and lipolysis. Subcutaneous and visceral adipose tissue depots display regional differences in catecholamine-induced lipolysis. Subcutaneous adipocytes have lower numbers of β 1, β 2 and β 3 adrenoceptors and higher numbers of α 2 adrenoceptors than visceral adipocytes, rendering them less responsive to catecholamine-mediated lipolysis (237). Activation of α 1 adrenoceptors stimulates phospholipase C activity leading to inositol 1,4,5-triphosphate and diacylglycerol formation with a consequent mobilization of intracellular calcium stores and protein kinase C activation. α 1-adrenoceptor-mediated activation of glycogen phosphorylase and inactivation of glycogen synthase has been reported in rat white adipocytes (217).

The sympathetic nervous system has important effects on adipose tissue metabolism. Cold exposure stimulates the activity of the sympathetic nervous system, increasing energy expenditure, improving glucose tolerance, enhancing insulin sensitivity, and stimulating glucose uptake in rat peripheral tissues, including brown adipose tissue, white adipose tissue, the heart, diaphragm, and skeletal muscles (238-240). Chronic cold exposure causes sympathetic nerve fibers to release norepinephrine in fat tissues. Norepinephrine then activates β -adrenergic receptors on brown fat cells to stimulate lipolysis and heat production. SNS activation in brown adipose tissue also results in expansion of brown fat (241). In white fat depots, prolonged exposure to cold causes the emergence of UCP1-expressing brown fat cells (214). Chronic norepinephrine infusion or exposure to β 3-selective adrenergic agonists are able to mimic the metabolic effects of cold exposure in white adipose tissue, increasing glucose uptake (242) and causing

transdifferentiation of white adipocytes to brown adipocytes by inducing the expression of UCP-1 (214).

Remarkably, chronic exposure to β 3-selective adrenergic agonists results in a metabolic phenotype very similar to that of mice receiving a SC-AB graft. Long-term treatment with CL-316,243, a β 3-specific adrenoceptor agonist, in non-obese, chow-fed rats enhances basal and insulin-stimulated glucose uptake by white and brown adipose tissues associated with a decrease in fat pad mass without a decrease in total body weight. Plasma non-esterified fatty acids (NEFA) are not increased (243). Interestingly, long-term treatment with CL-316,243 in obese Zucker-ZDF rats has more pronounced effects with significantly decreased white adipose tissue mass and total body weight, increased glucose uptake in skeletal muscle, brown and white adipose tissues and improved glucose tolerance (244). It is proposed that activation of non-shivering thermogenesis by increased expression of UCP-1 in both brown and white adipose tissue stimulates fatty acid oxidation, decreasing the circulating levels of fatty acids (which would be expected to increase secondary to increased lipolysis), and diminishing triglyceride stores in adipose tissues (244). The intracellular molecular mechanisms through which stimulation of adrenergic receptors modulate glucose transport in adipose tissue are still not clear (245).

In my model of adipose tissue cross-transplantation, I have demonstrated that transplantation of epididymal (intra-abdominal) fat into either the abdominal or subcutaneous space has no observed detrimental effects on metabolism as judged by body weight, adiposity or glucose tolerance. However, the selective transplantation of subcutaneous fat into the intra-abdominal space results in a significant reduction in body fat mass as well as improved glucose tolerance. Using microarray analysis I identified an upregulation of genes controlled by the MEF2 family of transcription factors in the SC-AB adipose tissue grafts. Remarkably, genes controlled by the MEF2 family of transcription factors were also selectively upregulated in the ENDOG-SC adipose tissue of mice receiving a subcutaneous

adipose tissue transplant into the intra-abdominal compartment, with no change in the expression level of these genes identified in the ENDOG-VIS adipose tissue of these mice. Gene expression of the transcription factors MEF2C and MEF2D was increased in ENDOG-SC adipose tissue but not in SC-AB adipose tissue grafts. In ENDOG-SC adipose tissue, therefore, there was a reversal of the downregulation in MEF2D expression that is usually seen in response to high fat feeding as well as the expression of MEF2C, which is not usually expressed in adipose tissue. Furthermore, gene expression of UCP-1 was selectively increased in ENDOG-SC adipose tissue. Upregulation of adrenergic pathways, with increased expression of CREB and muscle glycogen phosphorylase was observed, suggesting that increased adrenergic stimulation of ENDOG-SC adipose tissue is responsible for the increased expression of UCP1 observed. Furthermore, I observed a specific down-regulation of expression of β 3-adrenoceptors in ENDOG-SC adipose tissue. It is well established that a desensitization of the β -adrenergic stimulation of lipolysis occurs in adipocytes after chronic infusion of noradrenaline (246). Initially it was considered that β 3-, unlike β 1- and β 2-adrenoceptors were resistant to desensitization (246), however subsequent evidence suggests that all three receptor subtypes demonstrate a functional desensitization in lipolytic response of white adipocytes to adrenergic stimulation (247). The mechanism remains to be clarified, but it is conceivably due to decreased receptor transcription.

My data suggest that central activation of SNS efferents to subcutaneous adipose tissue mediate the beneficial metabolic effects of transplanting subcutaneous adipose tissue into the intra-abdominal compartment. In this model, the transplantation of subcutaneous adipose tissue into the intra-abdominal compartment activates afferent nerves to the hypothalamus resulting in increased sympathetic nerve stimulation selectively to subcutaneous and not visceral adipose tissue. Chronic adrenergic stimulation of β 3-adrenoceptors accounts for the beneficial effects on metabolism. Increased adrenergic stimulation of endogenous subcutaneous adipose tissue beds results in increased glucose uptake, possibly through activation of MEF2C and MEF2D, increased glycogen catabolism through

increased expression of glycogen phosphorylase and increased mitochondrial thermogenesis, with increased expression of uncoupling protein 1. A novel adipokine may be responsible for the upregulation of afferent neurons. This adipokine may have a unique effect as a result of transplantation of subcutaneous adipose tissue into the intra-abdominal compartment – the process of transplantation allowing this adipokine to act in a paracrine manner on vagal afferent nerves, to which it would never previously have been exposed. Alternately, this adipokine may be acting centrally in the hypothalamus to modulate sympathetic outflow selectively to subcutaneous adipose tissue. It is also possible that a lipid released from subcutaneous adipose tissue is mediating this effect. It has recently been demonstrated that the fatty acid derivatives prostaglandins can induce the expression of UCP-1 in adipose tissue. In response to cold or β_3 -adrenergic agonists white adipocytes in mice increased expression of the enzyme cyclooxygenase-2 (COX-2), which consequently produced prostaglandins, which acted locally, triggering brown fat-specific gene expression in white fat cells (248). The identity of this novel adipokine or lipid intermediate is important as it will provide a potential therapeutic target for obesity-induced insulin resistance and type 2 diabetes.

Chapter 4

Intrinsic depot-specific differences in the secretome of adipose tissue, preadipocytes and adipose tissue derived microvascular endothelial cells

Data from this chapter were published in an equal first author paper “Intrinsic depot-specific differences in the secretome of adipose tissue, preadipocytes and adipose tissue derived microvascular endothelial cells.” Hocking SL, Wu LE, Guilhaus M, Chisholm DJ, James DE. Diabetes 59 (12): 3008 – 16, 2010.

Abstract

Visceral adipose tissue is more closely linked to insulin resistance than subcutaneous adipose tissue. I conducted a quantitative analysis of the secretomes of visceral and subcutaneous whole adipose tissue to identify differences in adipokine secretion that account for the adverse metabolic consequences of visceral adipose tissue. I utilised lectin affinity chromatography followed by comparison of isotope-labelled amino acid incorporation rates (LAC-CILAIR) to quantitate relative differences in the secretomes of visceral and subcutaneous adipose tissue explants. As adipose tissue is comprised of multiple cell types, which may contribute to depot specific differences in secretion, I isolated preadipocytes and microvascular endothelial cells and compared their secretomes to that from whole adipose tissue.

Although there were no discrete depot-specific differences in the composition of the secretomes from whole adipose tissue, preadipocytes or microvascular endothelial cells, visceral adipose tissue exhibited an overall higher level of protein secretion than subcutaneous adipose tissue. More proteins were secreted in two-fold greater abundance from visceral compared with subcutaneous adipose tissue explants (59% vs. 21%), preadipocytes (68% vs. 0%) and microvascular endothelial cells (62% vs. 15%). Furthermore, the protein constitution of the whole adipose tissue secretome was not simply the summation of the secretomes of its cellular constituents. This indicates the importance of cross-talk between the adipocyte and non-adipocyte components of whole adipose tissue, which dictates the physiological functions of adipose tissue. Finally, almost 50% of the adipose tissue secretome was comprised of factors with a role in angiogenesis.

Thus visceral adipose tissue has a higher secretory capacity than subcutaneous adipose tissue and this difference is an intrinsic feature of its cellular components. In view of the number of angiogenic factors in the adipose tissue secretome, I

propose that visceral adipose tissue represents a more readily expandable tissue depot.

Introduction

The epidemiological association between visceral adiposity and insulin resistance and type 2 diabetes mellitus is well established, however the underlying mechanism accounting for this association remains to be fully elucidated. Intrinsic differences in metabolism, the secretion of adipokines and the expression of developmental genes in visceral and subcutaneous adipose tissue together with differences in their anatomical location have provided many hypotheses to explain the link between visceral adiposity and insulin resistance. However, the regional adipose tissue cross-transplantation experiments described in Chapter 2 revealed no detrimental impact on metabolism after the surgical addition of visceral adipose tissue into either the abdominal or subcutaneous compartment. Surprisingly, the surgical addition of subcutaneous adipose tissue selectively into the abdominal compartment had a beneficial impact on metabolism with decreased size of endogenous adipose tissue pads and improved glucose tolerance. These beneficial effects were not observed with transplantation of subcutaneous adipose tissue into the subcutaneous compartment. Therefore, the subcutaneous adipose tissue graft enhanced its beneficial metabolic profile as a result of transplantation into the visceral space. This suggests a crosstalk between the subcutaneous adipose tissue graft and non-adipose cells within the intra-abdominal compartment that is different from the crosstalk between a subcutaneous adipose tissue graft transplanted into the subcutaneous space. The transplantation of epididymal adipose tissue into either the subcutaneous or intra-abdominal compartment had no impact on metabolism suggesting the beneficial effects of subcutaneous adipose tissue are due to its cell-autonomous properties. The mechanism for this cross-talk is not known but may be due to secreted factors from subcutaneous adipocytes or the non-adipose components of subcutaneous adipose tissue acting on nearby tissues – with greater impact after transplantation as these factors are now present in higher concentration or now acting in a paracrine rather than an endocrine manner. The converse may also occur, with secreted factors from intra-abdominal microvascular endothelial cells and/or autonomic neurons impacting on subcutaneous adipocytes

due to their proximity after transplantation. I sought, therefore, to accurately characterise the secretomes of visceral and subcutaneous adipose tissue and in particular, subcutaneous and visceral preadipocytes and microvascular endothelial cells in order to identify depot-specific differences in adipokine expression. The secretome of adipose tissue microvascular endothelial cells has not previously been characterised.

Since the discovery of leptin in 1994 (80), adipose tissue has been increasingly recognised as an endocrine organ, secreting numerous proteins (adipokines) with potent metabolic effects (79). Metabolically beneficial adipokines including leptin and adiponectin are secreted in higher amounts from subcutaneous adipose tissue (81, 84), while pro-inflammatory adipokines such as RBP4, TNF- α , MCP-1, IL-8 and IL-6 are increased in visceral adipose tissue (45, 90, 91, 93, 94). It has been suggested this differential secretion of adipokines may account for the differing metabolic consequences of visceral and subcutaneous adiposity. However, it is unclear if these factors are secreted from adipocytes or other cells resident in adipose tissue such as macrophages. While leptin and adiponectin are secreted by adipocytes, other factors including resistin, visfatin, TNF- α , IL-6 and MCP-1 are principally secreted by macrophages (88). Therefore the adipocyte may not be the principal secretory component of adipose tissue.

I sought to accurately characterise the secretome of adipose tissue and quantitatively compare the secretomes from visceral and subcutaneous adipose tissue explants. Previous studies identified adipocyte secretory factors using 3T3-L1 cell-lines (249, 250) or primary adipocytes (143, 145). These studies have several limitations. Immortalized cell-lines are unable to provide depot-specificity and by isolating adipocytes from non-adipose cells within adipose tissue, cross-talk between these cells is lost. Using whole adipose tissue explants avoids these issues but introduces the presence of non-adipose derived contaminating serum proteins. To circumvent this problem I used comparison of isotope labelled amino acid incorporation rates (CILAIR) (146). Cells or tissues are incubated with isotopically

labelled amino acids, which become incorporated into newly synthesised proteins. This method allows quantitative assessment of differences in protein secretion as a protein with a higher incorporation of isotope is synthesised at a greater rate or in greater abundance (refer to Chapter 1).

The quality of the secretome sample can also be diminished by contamination with cytosolic, non-secretory proteins released from damaged cells. Secreted proteins commonly undergo N-glycosylation, whereas cytosolic proteins do not. I exploited differential N-glycosylation, using lectin affinity chromatography (LAC) to selectively enrich proteins targeted for secretion.

I utilised LAC followed by CILAIR (LAC-CILAIR) to quantitate relative differences in the secretomes of murine visceral and subcutaneous adipose tissue. As adipose tissue is comprised of multiple cell types, which may contribute to depot specific differences in secretion, I isolated preadipocytes and microvascular endothelial cells and compared their secretomes to that from whole adipose tissue. While I did not observe any discrete differences in secretion profile between each depot, visceral adipose tissue exhibited an overall higher level of protein secretion than subcutaneous adipose tissue, for whole adipose tissue, preadipocytes and microvascular endothelial cells. Furthermore, the protein constitution of the whole adipose tissue secretome was not simply the summation of the secretomes of its cellular constituents. Interestingly, a large proportion of the adipose tissue secretome was factors that play a role in angiogenesis. The increased production of these factors from visceral adipose tissue leads to the inescapable speculation that visceral adipose tissue represents a more readily expandable adipose tissue depot than subcutaneous adipose tissue.

Research design and methods

Materials and buffers

All tissue culture reagents were from Gibco unless otherwise stated.

Transfer Medium : Dulbecco's modified eagle medium / Ham's F-12 (DMEM/Ham's F-12) 1:1 containing 1% BSA and supplemented with 100 units/mL penicillin, 0.1 mg/mL streptomycin and 0.25 µg/mL amphotericin B (Antibiotic-Antimycotic, Invitrogen).

SILAC medium : Low glucose Dulbecco's modified eagle medium (DMEM) without leucine, lysine and arginine (Sigma Aldrich) supplemented with 0.105 g/L leucine, 100 units/mL penicillin, 0.1 mg/mL streptomycin, 0.0159 g/L phenol red and 100 nM insulin (DMEM/K-/R-). Glucose was added to a final concentration of 4.5 g/L. 'Heavy' or 'medium' isotopes of arginine (Cambridge laboratories U-¹³C6 U-¹⁵N4 arginine CNLM-539 or U-¹³C6 arginine CLM-2265 0.021 g/L) and lysine (Cambridge laboratories U-¹³C6 U-¹⁵N2 lysine CNLM-291 or 4,4,5,5-D4 lysine CNLM-2640 0.0365 g/L) were added to produce 'heavy' and 'medium' SILAC medium respectively.

Endothelial cell growth medium : Low-glucose Dulbecco's modified eagle medium (DMEM) supplemented with 100 units/mL penicillin, 0.1 mg/mL streptomycin, 20mM HEPES, 1% non-essential amino acids, 50 mM 2-mercaptoethanol, 20% heat-inactivated foetal calf serum, 12 U/mL heparin and 150 µg/mL endothelial cell growth supplement (Sigma).

Endothelial cell SILAC medium : Low glucose Dulbecco's modified eagle medium (DMEM) without leucine, lysine and arginine (Sigma Aldrich) supplemented with 0.105 g/L leucine, 100 units/mL penicillin, 0.1 mg/mL streptomycin, 0.0159 g/L phenol red, 100 nM insulin, 20mM HEPES, 1% non-essential amino acids and 50 mM 2-mercaptoethanol. 'Heavy' or 'medium' isotopes of arginine (Cambridge laboratories U-¹³C6 U-¹⁵N4 arginine CNLM-539 or U-¹³C6 arginine CLM-2265 0.021 g/L) and lysine (Cambridge laboratories U-¹³C6 U-¹⁵N2 lysine CNLM-291 or 4,4,5,5-D4 lysine CNLM-2640 0.0365 g/L) were added to produce 'heavy' and 'medium' SILAC medium respectively.

Preadipocyte growth medium : Dulbecco's modified eagle medium / Ham's F-12 (DMEM/Ham's F-12) 1:1 supplemented with 100 units/mL penicillin, 0.1 mg/mL streptomycin and 10% heat-inactivated foetal calf serum.

Animals

Male C57BL/6J mice were from Animal Resources Centre (Perth, Australia). Animals were kept in a temperature-controlled room ($22\pm 1^{\circ}\text{C}$), 80% relative humidity on a 12-hour light/dark cycle with free access to food and water. Experiments were carried out with approval of Garvan Institute Animal Experimentation Ethics Committee, following guidelines issued by the National Health and Medical Research Council of Australia. For each experiment, 2 – 5 mice were used as tissue donors.

Preparation of Anti-CD31 (Anti-PECAM-1) antibody-coated magnetic beads to isolate endothelial cells

Sheep anti-rat IgG Dynabeads (Invitrogen) were pre-coated with rat anti-mouse monoclonal antibody to CD31 (PECAM-1) (BD Pharmingen) according to the manufacturer's instructions at a concentration of 1 μg antibody per 1×10^7 Dynabeads. Dynabeads were stored in phosphate-buffered saline supplemented with 0.1% BSA at 4°C at 4×10^8 beads/mL.

Adipose tissue explants

Paired visceral (epididymal) and subcutaneous (inguinal) adipose tissue depots were obtained from 6-week old C57BL/6J mice. Adipose tissue pads were immediately transported in warm transfer medium to a tissue culture hood, where they were placed in fresh transfer medium and minced into $\sim 1\text{ mm}^3$ pieces. Minced explants were rinsed in phosphate-buffered saline and centrifuged at 250 g to remove cell debris and red blood cells. Adipose tissue explants (200 μL) were incubated in 1 mL SILAC medium. After 48 h incubation at 37°C in 5% CO_2 , conditioned medium was collected and centrifuged at 2,000 g to pellet cell debris. Lectin affinity chromatography and subsequent mass spectrometry were performed.

Preadipocyte and endothelial cell isolation and culture

Preadipocytes and microvascular endothelial cells were isolated from the same biopsies. Paired visceral and subcutaneous adipose tissue depots were obtained from 6-week old C57BL/6J mice under sterile conditions. Adipose tissue pads were immediately transported in warm transfer medium to a tissue culture hood, where they were placed in fresh transfer medium and minced using scissors into $\sim 1 \text{ mm}^3$ pieces. Medium was removed and replaced with fresh transfer medium containing 1 mg/mL collagenase type I and incubated with gentle shaking at 37°C for one hour. The adipose tissue to digest solution ratio was 4:1. The resulting material was filtered through a $250 \mu\text{m}$ mesh and the adipocytes and free oil separated from the stromovascular components by centrifugation at $250 g$ for 5 minutes at room temperature. The stromovascular pellet was resuspended, washed in phosphate-buffered saline and centrifuged at $250 g$ for 5 minutes at room temperature. This washing step was repeated twice. The stromovascular pellet was resuspended and plated in 2% gelatin-coated 10cm dishes in endothelial cell growth medium. This mixed cell population was cultured for 5-6 days at 37°C in 5% CO_2 . Cells were detached using 0.25% trypsin containing 3.42 mM EDTA and the trypsin subsequently neutralised by addition of Hank's balanced salt solution containing 5% foetal calf serum (HBSS-FCS). The cell solution was centrifuged at $600 g$ for 5 minutes at room temperature. The cell pellet was resuspended in 0.5 mL HBSS-FCS and incubated with $25 \mu\text{L}$ of anti-CD31 (anti-PECAM-1) coated dynabeads for 15 minutes at 4°C under constant rotation. The cell/bead suspension was brought to a total volume of 10 mL with HBSS-FCS and microvascular endothelial cells selected by magnet. Non-selected cells in the wash were transferred to a fresh tube. Wash and selection procedure was repeated 5 times. Selected cells were resuspended in endothelial cell growth medium and transferred to 2% gelatin coated culture dishes. After 3 – 5 days, cells were routinely passaged and plated at equal density in endothelial cell growth medium. Non-selected cells in the wash medium were centrifuged at $600 g$ for 5 minutes at room temperature. The resultant pellet was resuspended in preadipocyte growth medium and plated at equal density in 10 cm culture dishes. Microvascular endothelial cells and preadipocytes were grown until

confluent. At confluence, medium was replaced with endothelial cell SILAC medium and SILAC medium, respectively. After 48 hours, conditioned medium was collected and centrifuged at 2,000 *g* to pellet cell debris. Lectin affinity chromatography and subsequent mass spectrometry was performed.

Lectin affinity chromatography

Conditioned media from paired visceral and subcutaneous depots were mixed in 1:1 ratio and glycoprotein purification performed (153). Briefly, MnCl₂ was added to conditioned media to a final concentration of 1 mM. Samples were incubated overnight at 4°C under constant rotation with 50 µL/mL of 50% slurry of Concanavalin A sepharose beads (GE Healthcare). Beads were washed extensively with Con A binding buffer (0.5 M NaCl, 0.1 M Tris, 1 mM MnCl₂ and 1 mM CaCl₂, pH 7.4). Proteins were eluted with 0.3 M methyl- α -D-mannopyranoside, 0.5 M NaCl, 0.1 M Tris, 10 mM EDTA and 10 mM EGTA, pH 7.4. Eluted proteins were precipitated using chloroform:methanol (251).

Mass spectrometry

Mass spectrometry analysis was kindly performed by Lindsay Wu, The Garvan Institute of Medical Research, Sydney, Australia in collaboration with The Bioanalytical Mass Spectrometry Facility, University of New South Wales, Sydney, Australia. Peptide extraction and mass spectrometry was as previously described (153, 252) using a Waters Ultima tandem mass spectrometer. Mascot distiller software (Matrix Sciences) was used for data analysis. SwissProt database was used for protein identification, taxonomy restricted to *Mus musculus*, MS tolerance set at 0.5 Da and MSMS tolerance set at 0.05 Da. Variable modifications were set to carbamidomethyl, propionamide and oxidation (M). No fixed modifications were used. Trypsin was set as cleavage enzyme after arginine or lysine and a maximum of 2 missed cleavages were permitted. Quantitation method was as follows. Method: constrain search – yes, protein ratio type – weighted, protein score type – standard, report detail – yes, minimum peptides – 1. Protocol: precursor, allow mass time match – yes, allow elution shift – no, all charge states – no. Component “light” was

mode – exclusive, unmodified site – K, position – anywhere, unmodified site – R, position – anywhere. Component “medium” was mode – exclusive, modification – Label: 2(H)4 (K), modification – Label: 13C(6) (R). Component “heavy” was mode – exclusive, modification – Label: 13C(6)15N(2) (K), modification – Label: 13(6)15N(4) (R). For all ratios measured, numerators and denominators were set to 1.0. Integration – trapezium, integration source – survey, precursor range – envelope. Quality: minimum precursor charge – 1, isolated precursor – No, Minimum a(1) – 0.0, peptide threshold type – minimum score. Outlier – auto. A minimum ion score of 60 was chosen as criterion for positive identification. “Heavy (U-¹³C6 U-¹⁵N4 arginine, U-¹³C6 U-¹⁵N2 lysine) to light (naturally occurring lysine and arginine)” (H/L) and “medium (U-¹³C6 arginine, 4,4,5,5-D4 lysine) to light” (M/L) isotope ratios were used to determine relative abundance of proteins from visceral or subcutaneous samples respectively. As visceral and subcutaneous samples are mixed, non-labelled proteins form a “common denominator” that both isotopes are measured against (Figure 4.1). Isotope ratios below 0.05 were discounted as “no label incorporation”. Signal peptides were determined using SignalP 3.0 (141).

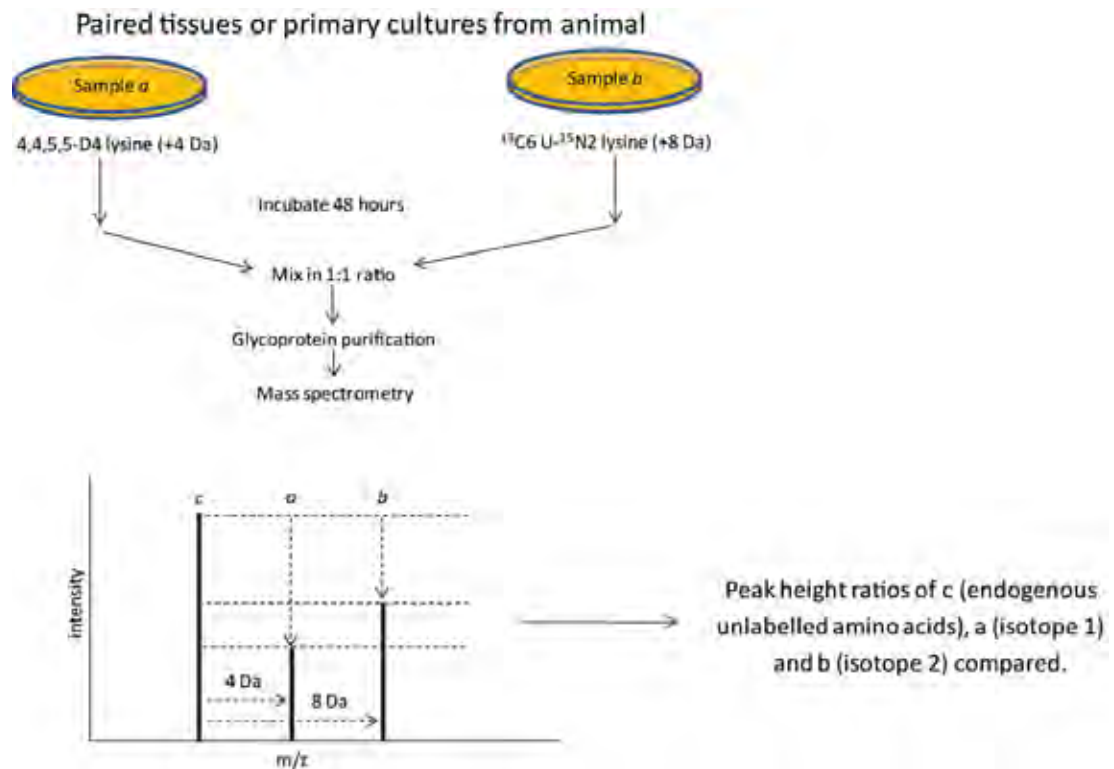


Figure 4.1. LAC-CILAIR workflow for comparing protein synthesis and secretion from two different samples.

Paired cell cultures or tissues are incubated in media containing different isotopes of arginine and lysine, which are subsequently incorporated into newly synthesized and secreted proteins. Paired conditioned media samples are mixed in equal proportions, and proteins are subjected to mass spectrometry. Incorporation of amino acid isotopes results in a shift in molecular weight and mass to charge (m/z) ratio. Peak heights are measured, and their ratios are used to determine relative abundance of proteins from samples a and b.

Results

I hypothesised there would be differences in protein secretion from visceral and subcutaneous adipose tissue. Adipose tissue explants from epididymal (visceral) and inguinal (subcutaneous) depots were incubated for 48 hours in the presence of “heavy” and “medium” isotopes of arginine and lysine, respectively. Medium was collected, mixed in equal ratio and subjected to lectin affinity chromatography. Proteins were precipitated, resolved by SDS-PAGE, trypsin digested and subjected to quantitative mass spectrometry (Table 4.1 and Appendix 1). A total of 145 proteins were identified, of which 86 (60%) were predicted to contain an N-terminal signal peptide using SignalP. Of these, 51 proteins (59%) were present at >2-fold higher abundance in conditioned medium from visceral than subcutaneous adipose tissue, whereas only 18 proteins (21%) were at >2-fold higher abundance in conditioned medium from subcutaneous than visceral adipose tissue. The frequency distribution of the visceral to subcutaneous ratio for detected proteins is shown in Figure 4.2. Proteins without a signal peptide are non-specifically released, newly synthesized cytosolic proteins. The distribution for these background proteins with no signal peptide resembles a normal distribution, whereas the distribution for proteins with a signal peptide is skewed to the right. This indicates that release of true secretory proteins into conditioned medium is increased from visceral relative to subcutaneous adipose tissue. The normal distribution of non-secretory background proteins indicates a similar amount of tissue was present in visceral and subcutaneous adipose tissue samples.

Clustering analysis of detected proteins was performed using the database for annotation, visualisation and integrated discovery (DAVID) (253, 254). Analysis of proteins increased from visceral adipose tissue revealed enrichment of proteins involved in endopeptidase inhibition, including members of the Serpin family, and proteins involved in innate immune system regulation, including members of the complement pathway. Cluster analysis of proteins increased from subcutaneous adipose tissue showed no functional similarities.

TABLE 4.1.
Secreted proteins identified from visceral and subcutaneous adipose tissue explants

Accession	Protein Name	Signal peptide	Functional description	Viscera l/Subcut. ratio
CO3_MOUSE	Complement C3	+	Complement cascade, innate immunity	3.8962
A2M_MOUSE	Alpha-2-macroglobulin	+	Serine protease inhibitor, prevents coagulation & fibrinolysis	1.0462
LAMB1_MOUSE	Laminin subunit beta 1	+	Extracellular matrix	0.0465
LAMC1_MOUSE	Laminin subunit gamma-1	+	Extracellular matrix	5.3939
LAMA2_MOUSE	Laminin subunit alpha-2	+	Extracellular matrix	5.8369
COEA1_MOUSE	Collagen alpha-1 (XIV) chain	+	Extracellular matrix	0.2932
FINC_MOUSE	Fibronectin	+	Extracellular matrix	3.4279
CES3_MOUSE	Carboxylesterase 3	+	Lipase	7.7748
HPT_MOUSE	Haptoglobin	+	Haem binding protein, acute phase reactant	2.5003
CO1A2_MOUSE	Collagen alpha-2 (I) chain	+	Extracellular matrix	1.0944
TRFE_MOUSE	Serotransferrin	+	Iron binding	1.3117
LAMB2_MOUSE	Laminin subunit beta-2	+	Extracellular matrix	0.5017
CFAB_MOUSE	Complement factor B	+	Complement cascade, innate immunity	2.2097
CERU_MOUSE	Ceruloplasmin	+	Copper, iron binding	4.2408
SPA3N_MOUSE	Serine protease inhibitor A3N	+	Trypsin inhibitor	4.1321
SPA3K_MOUSE	Serine protease inhibitor A3K	+	Trypsin inhibitor, also known as contrapsin	3.1605
ESTN_MOUSE	Liver carboxylesterase N	+	Drug detoxification	21.8136
GELS_MOUSE	Gelsolin	+	Depolymerises extracellular actin from necrotic cells	1.0615
CO4B_MOUSE	Complement C4-B	+	Complement cascade, innate immunity	13.7332
NID2_MOUSE	Nidogen-2	+	Extracellular matrix	3.4691
CATB_MOUSE	Cathepsin B	+	Protease activity	6.2497
ANT3_MOUSE	Antithrombin-III	+	Serine protease inhibitor, regulation of blood coagulation	0.1622
PGS2_MOUSE	Decorin	+	Extracellular matrix	4.737

Visceral and subcutaneous adipose tissue explants were incubated in media containing different isotopes of arginine and lysine. Conditioned media were mixed, subjected to lectin affinity chromatography and subjected to quantitative mass spectrometry. Visceral/subcutaneous (H/L / M/L) ratio is shown. The complete dataset is shown in Appendix 1.

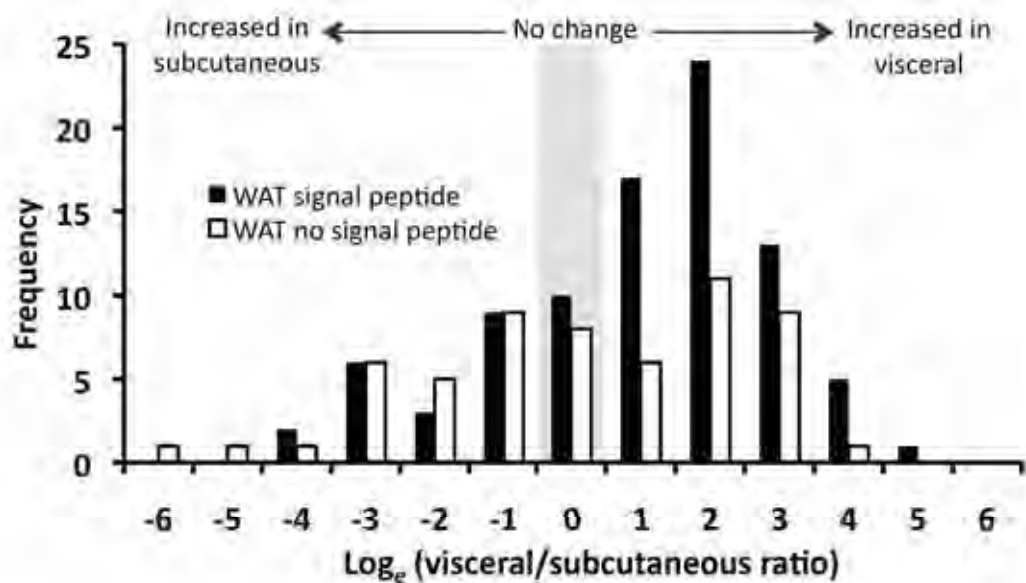


Figure 4.2. Adipose tissue explants secretory proteins are secreted in greater amounts from visceral adipose tissue.

Whole adipose tissue (WAT) explants from visceral and subcutaneous adipose tissue depots were cultured in media containing two different isotopes of arginine and lysine. LAC-CILAIR mass spectrometry was performed, and isotopic ratios calculated. Histogram shows distribution of visceral to subcutaneous ratios for proteins detected. Note use of natural log scale.

Adipose tissue is comprised of adipocytes as well as preadipocytes, microvascular endothelial cells and macrophages, collectively referred to as the stromovascular fraction. Stromovascular cells may make a significant contribution to the secretory capacity of white adipose tissue, perhaps even exceeding that of adipocytes (95). Interplay between cells of the stromovascular fraction and adipocytes may also modulate the secretion profile of adipose tissue. I sought to determine the relative contribution of preadipocytes and microvascular endothelial cells to the whole adipose tissue secretome. In addition, I examined whether depot-specific differences in protein secretion observed from whole adipose tissue explants persisted in cells from the stromovascular fraction.

First I isolated preadipocytes from paired visceral and subcutaneous adipose tissue biopsies. Visceral and subcutaneous preadipocytes were cultured *in vitro* for at least one week before incubation in medium containing isotopic amino acids. Conditioned medium was analysed as before (Table 4.2). Preadipocytes secreted a more limited set of proteins than minced adipose tissue. Of 23 proteins detected, 22 were secretory proteins. Of these, 15 were upregulated >2 fold from visceral compared to subcutaneous preadipocytes. Not one protein was upregulated >2-fold from subcutaneous as compared to visceral preadipocytes. The frequency distribution of the visceral to subcutaneous ratio for detected proteins is shown in Figure 4.3, and is again skewed to the right. This indicates that the release of secretory proteins into conditioned medium is increased from visceral relative to subcutaneous preadipocytes. Cluster analysis of the proteins upregulated from visceral derived preadipocytes showed an enrichment of extracellular matrix proteins.

Next, I examined microvascular endothelial cells isolated from paired visceral and subcutaneous adipose tissue depots. To date the secretome of endothelial cells has not been determined. In addition, it is unknown whether microvascular endothelial cells display depot-specific differences. I isolated microvascular endothelial cells using CD31 magnetic bead separation, and cultured these cells *in vitro*. Conditioned

TABLE 4.2.
Secreted proteins identified from visceral and subcutaneous preadipocytes

Accession	Protein Name	Signal peptide	Functional description	Viscera l/Subcut. ratio
CO1A1_MOUSE	Collagen alpha-1 (I) chain	+	Extracellular matrix	0.5169
CO1A2_MOUSE	Collagen alpha-2 (I) chain	+	Extracellular matrix	4.006
CO3A1_MOUSE	Collagen alpha-1 (III) chain	+	Extracellular matrix	4.702
CO5A2_MOUSE	Collagen alpha-2 (V) chain	+	Extracellular matrix	19.26
FINC_MOUSE	Fibronectin	+	Extracellular matrix	1.579
FBLN2_MOUSE	Fibulin-2	+	Extracellular matrix	5.163
SPRC_MOUSE	SPARC	+	Angiogenesis inhibitor	3.36
PEDF_MOUSE	Pigment epithelium-derived factor	+	Angiogenesis inhibitor, role in insulin resistance	7.085
CO5A1_MOUSE	Collagen alpha-1 (V) chain	+	Extracellular matrix	0.06207
HPT_MOUSE	Haptoglobin	+	Haem binding protein, acute phase reactant	23.01
CATB_MOUSE	Cathepsin B	+	Protease activity	0.8618
IC1_MOUSE	Plasma protease C1 inhibitor	+	Inhibits C1s and C1r protease activity	2.591
PAI1_MOUSE	Plasminogen activator inhibitor 1	+	Serine protease inhibitor, inhibits matrix metalloproteinases, associated with insulin resistance	6.119
CO2A1_MOUSE	Collagen alpha-1 (II) chain	+	Extracellular matrix	3.991
TIMP1_MOUSE	Metalloproteinase inhibitor 1	+	Regulation of extracellular matrix	4.046
CO4A1_MOUSE	Collagen alpha-1 (IV) chain	+	Extracellular matrix	1.003
TITIN_MOUSE	Titin	-	Mechanical contraction	15.4
PGS1_MOUSE	Biglycan	+	Extracellular matrix	4.14
CATL1_MOUSE	Cathepsin L1	+	Cysteine protease	17.19
EGFR_MOUSE	Epidermal growth factor receptor	+	Regulation of growth and proliferation	4.062
COBA2_MOUSE	Collagen alpha-2 (XI) chain	+	Extracellular matrix	1.566
FSTL1_MOUSE	Follistatin-related protein 1	+	Growth factor binding	8.844
ATS7_MOUSE	A disintegrin and metalloproteinase with thrombospondin motifs 7	+	Regulation of extracellular matrix	0.3296

Visceral and subcutaneous preadipocytes were incubated in media containing different isotopes of arginine and lysine. Conditioned media were mixed, subjected to lectin affinity chromatography and subjected to quantitative mass spectrometry. Visceral/subcutaneous (H/L / M/L) ratio is shown.

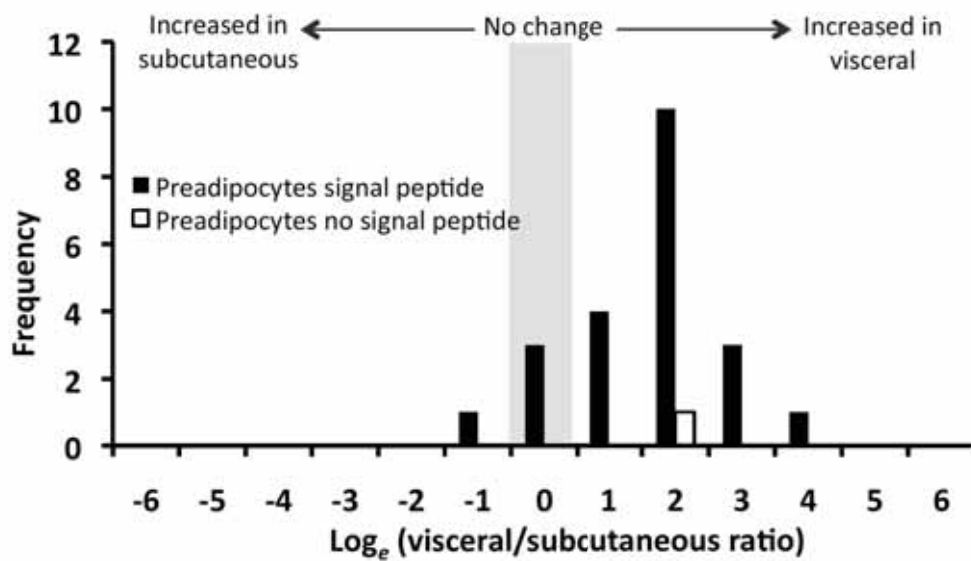


Figure 4.3. Preadipocyte secretory proteins are secreted in greater amounts from visceral adipose tissue.

Preadipocytes from visceral and subcutaneous adipose tissue depots were cultured in media containing two different isotopes of arginine and lysine. LAC-CILAIR mass spectrometry was performed, and isotopic ratios calculated. Histogram shows distribution of visceral to subcutaneous ratios for proteins detected. Note use of natural log scale.

media from cells incubated in isotopic amino acids were collected and analysed as before (Table 4.3 and Appendix 2). Of 66 detected proteins, 34 (52%) displayed an N-terminal signal peptide. Of these, 21 (62%) were increased >2 fold from visceral microvascular endothelial cells, and only 5 were increased >2 fold from subcutaneous microvascular endothelial cells. The frequency distribution of the visceral to subcutaneous ratio for detected proteins is shown in Figure 4.4. Once again, these data are skewed towards increased protein secretion from visceral microvascular endothelial cells. This is consistent with the enhanced secretory capacity of visceral adipose tissue I have observed in both whole adipose tissue and isolated preadipocytes. The proteins identified include a number that are known to be secreted from endothelial cells, including thrombospondin-1 and thrombospondin-2, and extracellular matrix proteins such as fibronectin and collagens. Additionally, several proteins not shown to be secreted from adipose tissue microvascular endothelial cells were identified. These include the most abundantly detected protein, adipocyte enhancer binding protein 1 (AEBP1). This protein influences inflammation in macrophages via a direct interaction with PXR and PPAR γ sites. Multiple members of the complement pathway were also identified. Cluster analysis showed proteins more abundantly secreted from visceral microvascular endothelial cells were involved in extracellular matrix formation, including collagen and fibronectins, and endopeptidase inhibition, including members of the Serpin family. There were no defined clusters for the five secretory proteins more abundantly secreted from subcutaneous microvascular endothelial cells.

When the secretomes of whole adipose tissue explants, preadipocytes and microvascular endothelial cells were compared, eight common secreted proteins were identified (Figure 4.5). Seven secreted proteins were shared between the whole adipose tissue and microvascular endothelial cell secretomes and four between the whole adipose tissue and preadipocyte secretomes. These proteins included those involved in extracellular matrix formation, such as collagen and fibronectin and other known adipocyte proteins such as osteonectin. Interestingly

TABLE 4.3.
Secreted proteins identified from visceral and subcutaneous microvascular endothelial cells

Accession	Protein Name	Signal peptide	Functional description	Viscera l/Subcut. ratio
TENA_MOUSE	Tenascin	+	Extracellular matrix	0.1746
AEBP1_MOUSE	Adipocyte enhancer-binding protein 1	+	Transcriptional repressor	14.6159
COL1A2_MOUSE	Collagen alpha-2(I) chain	+	Extracellular matrix	0.1228
TSP1_MOUSE	Thrombospondin-1	+	Angiogenesis inhibitor	1.4505
IC1_MOUSE	Plasma protease C1 inhibitor	+	Inhibits C1s and C1r protease activity	4.7622
EMIL1_MOUSE	EMILIN-1	+	Extracellular matrix	0.0258
PGS1_MOUSE	Biglycan	+	Extracellular matrix	7.9442
CO1A1_MOUSE	Collagen alpha-1(I) chain	+	Extracellular matrix	2.9346
PGBM_MOUSE	Basement membrane-specific heparan sulfate proteoglycan core protein	+	Extracellular matrix	0.7816
PGS2_MOUSE	Decorin	+	Extracellular matrix	3.5699
CO3A1_MOUSE	Collagen alpha-1(III) chain	+	Extracellular matrix	3.9785
PAI1_MOUSE	Plasminogen activator inhibitor 1	+	Serine protease inhibitor, inhibits matrix metalloproteinases, associated with insulin resistance	2.0433
TITIN_MOUSE	Titin	-	Mechanical contraction	0.3374
1433Z_MOUSE	14-3-3 protein zeta/delta	-	Phosphoprotein binding, modulation of enzymatic activity	0.4732
A2M_MOUSE	Alpha-2-macroglobulin	+	Serine protease inhibitor, prevents coagulation and fibrinolysis	9.6076
LIPL_MOUSE	Lipoprotein lipase	+	Lipoprotein associated lipid hydrolysis	1.695
ACTBL_MOUSE	Beta-actin-like protein 2	-	Cytoskeleton	0.1492
APOE_MOUSE	Apolipoprotein E	+	Lipid transport	3.1261
ITIH3_MOUSE	Inter-alpha-trypsin inhibitor heavy chain H3	+	Serine protease inhibitor	0.2654
H2B1C_MOUSE	Histone H2B type 1-C/E/G	-	DNA binding	1.7378

Visceral and subcutaneous microvascular endothelial cells were incubated in media containing different isotopes of arginine and lysine. Conditioned media were mixed, subjected to lectin affinity chromatography and subjected to quantitative mass spectrometry. Visceral/subcutaneous (H/L / M/L) ratio is shown. The complete dataset is shown in Appendix 2.

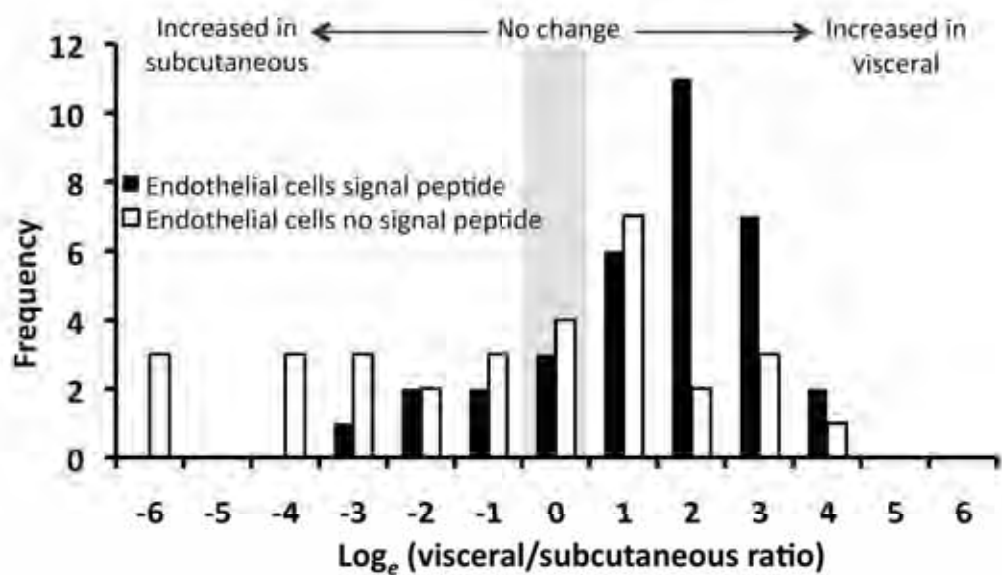


Figure 4.4. Endothelial cell secretory proteins are secreted in greater amounts from visceral adipose tissue.

Microvascular endothelial cells from visceral and subcutaneous adipose tissue depots were cultured in media containing two different isotopes of arginine and lysine. LAC-CILAIR mass spectrometry was performed, and isotopic ratios calculated. Histogram shows distribution of visceral to subcutaneous ratios for proteins detected. Note use of natural log scale.

these data suggest that the majority of proteins comprising the whole adipose tissue secretome are secreted either by adipocytes themselves or by other cells in the stromovascular fraction, such as macrophages and neurons. To interrogate this further I compared the secretome of whole adipose tissue explants to the secretomes of differentiated 3T3-L1 adipocytes (153) and isolated rat adipocytes (143). Of the 86 proteins identified in the whole adipose tissue secretome, 26 were shared with the 3T3-L1 adipocyte secretome and 21 were shared with the isolated rat adipocyte secretome (Figure 4.6). These data confirm that adipocytes alone are not the principal source of secreted proteins. It is possible that other cells types in the stromovascular fraction such as macrophages and neurons are the source of secreted proteins. To interrogate this further I compared the secretome of whole adipose tissue explants to the secretome of human macrophages and only 3 common proteins were identified, which were gelsolin (an actin-depolymerising factor), vimentin (a type III intermediate filament protein) and cathepsin D (a lysosomal aspartyl protease functioning in intracellular protein breakdown) (255).

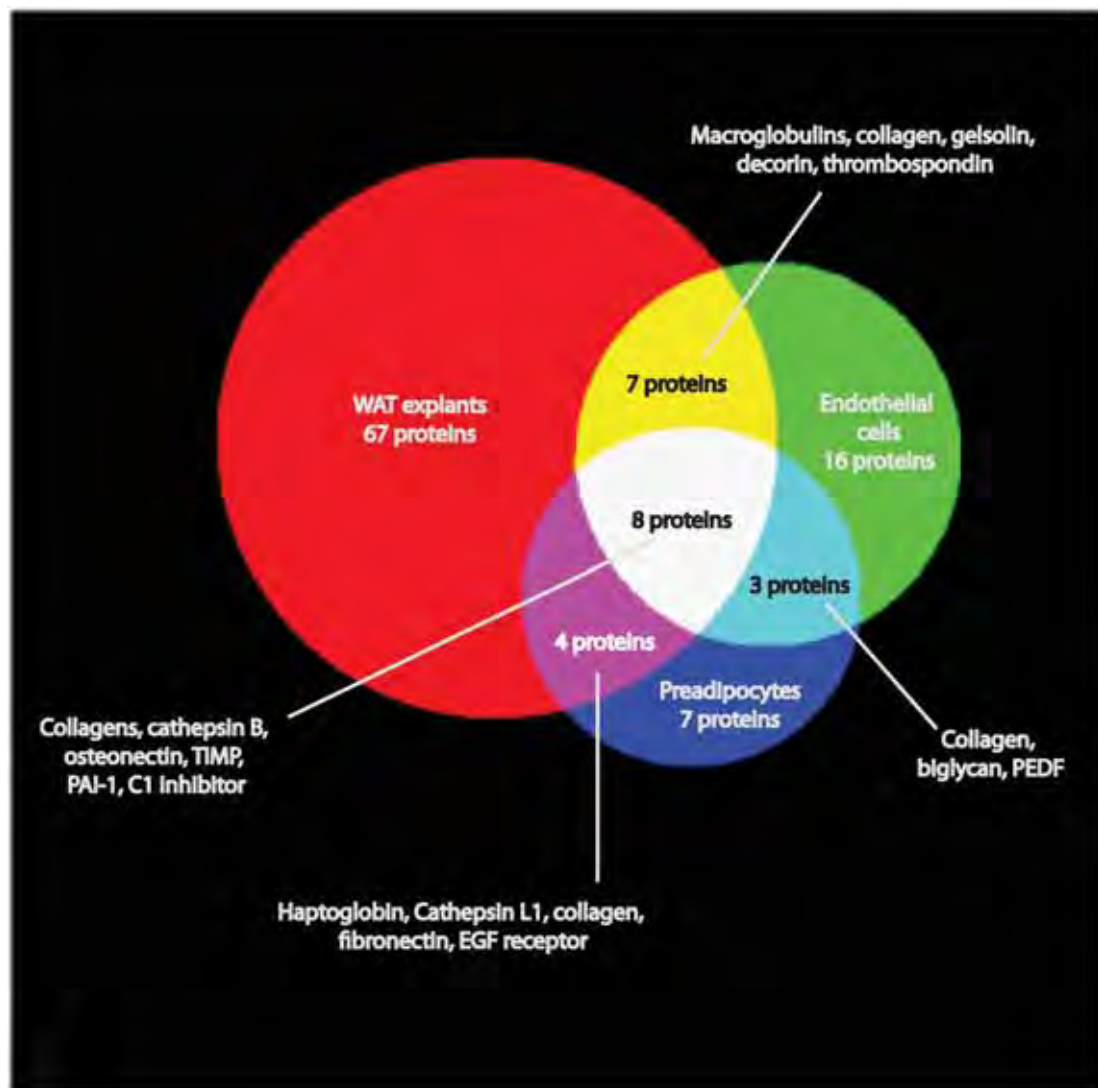


Figure 4.5. Venn diagram showing protein secretion from white adipose tissue explants, preadipocytes and microvascular endothelial cells.

A total of 116 secretory proteins were detected from white adipose tissue explants, preadipocytes and microvascular endothelial cells. PEDF – pigment epithelial derived factor, PAI-1 – plasminogen activator inhibitor 1, TIMP – tissue inhibitor of metalloproteinase 1. Diagram composed using 3-Venn applet (256).

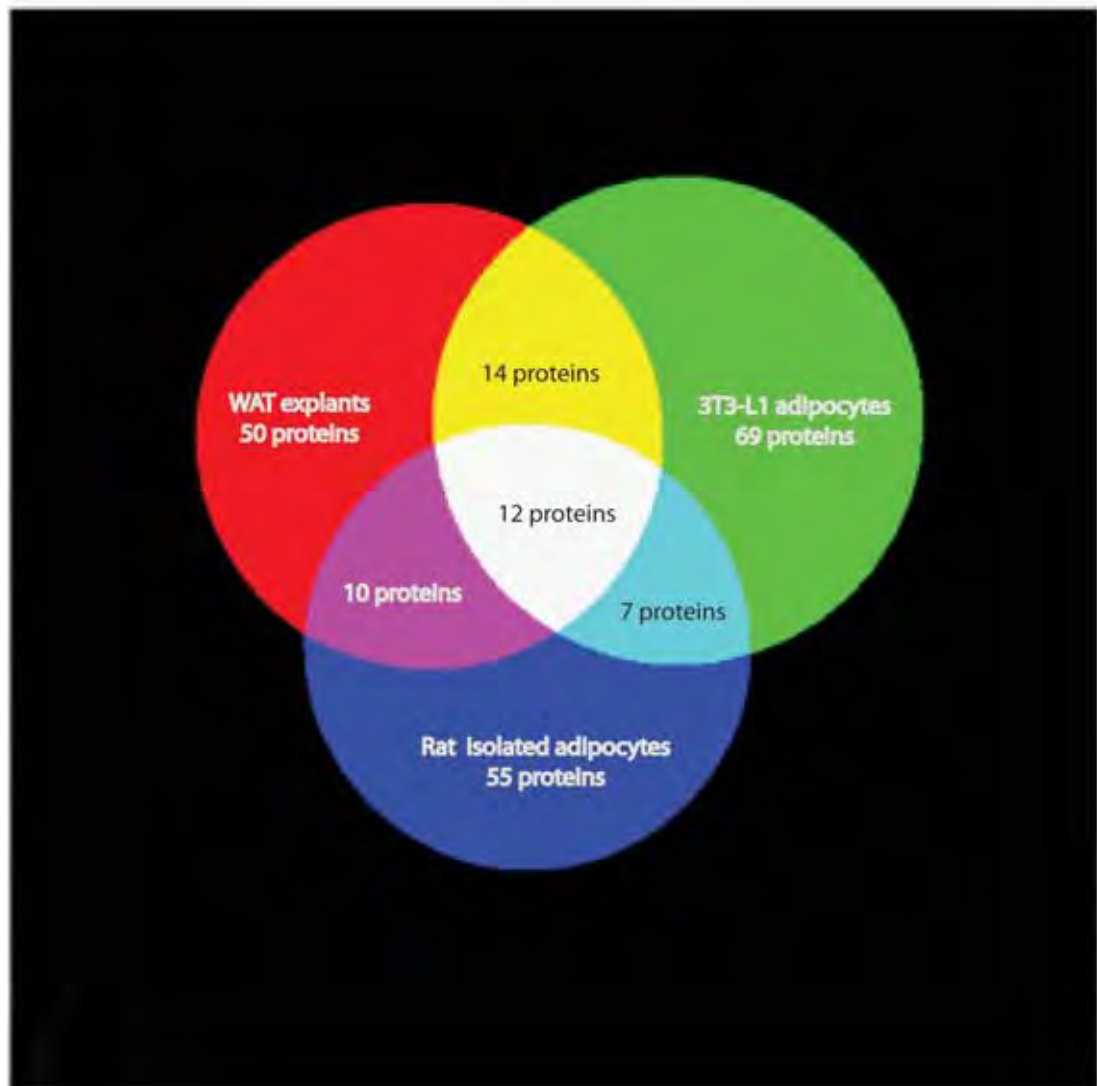


Figure 4.6. Venn diagram showing protein secretion from whole adipose tissue (WAT) explants, 3T3-L1 adipocytes and isolated rat adipocytes (from Chen et al 2005) (143).

The 12 proteins detected in all three samples were adiponectin, adipsin, angiotensinogen (Serpina8), cathepsin B, cathepsin D, collagen α -1 (IV), collagen α -2 (IV), complement C1s, haptoglobin, laminin subunit β -2, osteonectin, and thrombospondin-1. Diagram composed using 3-Venn applet (256).

Discussion

In this study I have made 3 important observations. First, the overall secretory capacity of visceral adipose tissue is considerably higher than subcutaneous adipose tissue. Second, this enhanced secretory capacity of visceral adipose tissue extends to cells of the stromovascular fraction – preadipocytes and microvascular endothelial cells. Third, adipose tissue as a whole secretes more proteins than its individual component parts, suggesting the adipocyte is not the principal secretory component of adipose tissue. The secretome of adipose tissue is likely due to the complex interplay between its component cell types.

To interrogate the adipose tissue secretome, I combined two techniques, comparison of isotope labelled amino acid incorporation rates (CILAIR) (146) and lectin affinity chromatography (LAC) (153). Using this streamlined method excluded contaminating proteins from entrapped serum and intracellular contents from damaged cells. Metabolic labelling identifies proteins that are newly synthesized during the culture period. Proteins already in the secretory pathway will remain unlabelled, as will contaminants from serum and cell debris (144). Lectin affinity chromatography selectively enriches for proteins targeted for secretion, thus overcoming contamination from dead or damaged cells. Abundant serum proteins, such as albumin, that are non-glycosylated are removed. This obviates the need for multiple washing steps to dilute these contaminating serum proteins, decreasing sample processing time and the negative impact of prolonged tissue handling. Despite these measures, unlabelled proteins will remain in the medium. As conditioned media from visceral and subcutaneous samples are mixed, non-labelled (“light”) proteins form a “common denominator” that both isotopes are measured against. This eliminates any potential confounding from unlabelled contaminants differentially distributed between the two depots. The technique of LAC-CILAIR is a useful and valid tool for interrogation of the adipose tissue secretome, indicated by the detection of well-known adipokines including adiponectin, adipisin and PAI-1.

First, I compared rates of protein secretion from visceral and subcutaneous adipose tissue explants. Visceral adipose tissue explants secreted quantitatively more proteins than subcutaneous adipose tissue explants. Of proteins secreted in >2 fold abundance, 59% were from visceral adipose tissue explants compared with 21% from subcutaneous adipose tissue explants. This upregulation of protein secretion from visceral adipose tissue was consistent across cells of the stromovascular fraction with 68% of proteins secreted in >2-fold abundance from visceral adipose tissue preadipocytes compared with 0% from subcutaneous adipose tissue preadipocytes and 62% of proteins secreted in >2-fold abundance from visceral adipose tissue microvascular endothelial cells compared with 15% from subcutaneous adipose tissue microvascular endothelial cells (Table 4.4).

Preadipocytes and microvascular endothelial cells were cultured *in-vitro* for at least one week prior to application of labelled media, so were no longer subject to paracrine influences from their depot of origin. This suggests increased protein secretion is an intrinsic characteristic of components of visceral adipose tissue. The detection of a small number of proteins secreted in 2-fold greater abundance from subcutaneous depots provides evidence that our technique does not selectively detect enhanced protein secretion from the visceral depot.

Cluster analysis of proteins secreted in greater abundance from visceral adipose tissue revealed members of the acute phase response and innate immune system. These data raise two interesting hypotheses. The first, visceral adipose tissue is more pro-angiogenic than subcutaneous adipose tissue, as many proteins involved in the acute phase response, for example haptoglobin (257), and innate immune system (258) are also involved in angiogenesis. The capacity for angiogenesis is a crucial requirement for adipose tissue expansion and cells of the adipose tissue stromovascular fraction are able to differentiate into adipocytes and endothelial cells and vice versa (40). Anti-angiogenic agents have been proposed as novel therapeutic options in obesity as they induce weight loss in obese mouse models without adverse effect (43). In support of this hypothesis, cluster analysis of the 14

TABLE 4.4.

Summary of numbers of proteins detected, and relative abundance between visceral and subcutaneous adipose tissue samples.

	WAT explants	Endothelial cells	Preadipocytes
incorporated label	145	66	23
signal peptide	86	34	22
signal peptide, visceral / subcutaneous ratio > 2	51	21	15
signal peptide, subcutaneous / visceral ratio > 2	18	5	0
no signal peptide, visceral / subcutaneous ratio > 2	23	10	1
no signal peptide, subcutaneous / visceral ratio > 2	22	14	0
% proteins identified with signal peptide	59%	52%	96%
% total ion score from signal peptide containing proteins	88%	76%	99%

proteins secreted more abundantly from visceral preadipocytes revealed proteins involved in extracellular matrix production. This, together with our finding that visceral adipose tissue secretes pro-angiogenic factors, suggests that visceral preadipocytes are better adapted for rapid adipose tissue expansion than subcutaneous preadipocytes.

The second hypothesis, visceral adipose tissue secretes more pro-inflammatory cytokines than subcutaneous adipose tissue. This is consistent with recent data that visceral adipose tissue, particularly in obesity, develops chronic low-grade inflammation with macrophage infiltration. This is associated with insulin resistance. Proteins involved in macrophage recruitment were secreted in greater abundance from visceral microvascular endothelial cells. This suggests that adipose tissue microvascular endothelial cells play a pivotal role in enticing circulating macrophages into adipose tissue. However, adipose tissue utilised for this study was derived from young, lean animals. In this setting, the upregulation of these cytokines is more likely targeted for angiogenesis and adipose tissue proliferation rather than a pro-inflammatory milieu. Furthermore, recruitment of macrophages into adipose tissue is not always associated with inflammation as macrophages in adipose tissue from lean mice express IL-10, which protects adipocytes from insulin resistance (259).

This study represents the first survey of the endothelial cell secretome. In comparing microvascular endothelial cells from visceral and subcutaneous adipose tissue, significant quantitative differences in protein secretion were demonstrated. Among the endothelial secretome were thrombospondins 1, 2 and 3, known to be secreted by endothelial cells, as well as a number of proteins not previously documented as endothelial secreted factors. Surprisingly, many were known adipocyte secretory proteins, including growth arrest specific 6 (GAS6), plasminogen activator inhibitor-1 (PAI-1), periostin, pentraxin-related protein 3 (PTX3) and SPARC. Of particular interest was identification of adipocyte enhancer binding protein 1 (AEBP1), a secreted protein proposed to act as a transcriptional

repression factor through binding of the enhancer sequence of the aP2/FABP4 gene in adipocytes, as well as PPAR γ and LXR sites in macrophages (260, 261).

Preadipocytes deficient in AEBP1 are hyperproliferative, with enhanced adipogenesis (262). AEBP1 can be detected in whole adipose tissue samples, but not when adipocytes are purified from adipose tissue (263). Given our discovery of AEBP1 secretion from endothelial cells, I consider it likely that the source of AEBP1 in adipose tissue is endothelial cells. In this study, I found that microvascular endothelial cells from visceral adipose tissue secreted far more AEBP1 than microvascular endothelial cells from subcutaneous adipose tissue. This observation could be important for explaining the deleterious effects of visceral adipose tissue.

In this study, I interrogated the secretome of whole adipose tissue and subsequently cells of the stromovascular fraction, preadipocytes and microvascular endothelial cells, to determine which component of adipose tissue was principally responsible for adipokine secretion. A total of 115 proteins were identified from these three samples, of which 67 were unique to adipose tissue explants, 16 unique to microvascular endothelial cells, and 7 unique to preadipocytes. Eight proteins were identified in all samples, including members of the collagen family, osteonectin, metalloproteinase inhibitor 1, C1 esterase inhibitor, plasminogen activator inhibitor-1 and cathepsin B. These data suggest adipocytes themselves or other cells in the stromovascular fraction not interrogated in this study, including macrophages and neurons, are the key secretory cells within adipose tissue. When the secretome of whole adipose tissue was compared with the secretomes of both differentiated 3T3-L1 adipocytes and primary rat adipocytes, only 26 (29%) and 20 (22%) common proteins respectively were identified. These data infer that adipocytes alone are not the principal source of secreted proteins in adipose tissue. As the adipose tissue came from lean animals, the expected number of macrophages should be low and in fact only 3 secreted proteins common to the secretomes of whole adipose tissue and human macrophages were found. This leads to the important conclusion that the secretome of whole adipose tissue is not

simply the sum of each of its component parts but is the result of a paracrine interaction between the multiple cell types within adipose tissue.

Chapter 5

General Discussion

Current knowledge of the relationship between subcutaneous and visceral adiposity and metabolic disease.

Obesity has become a global, epidemic health problem. Obesity increases the risk of numerous diseases, including type 2 diabetes, cardiovascular disease, dyslipidemia, and cancer (3). However, not all obese patients have the same risk of developing the metabolic sequelae of obesity. Individuals with peripheral obesity, are at little or no risk of the metabolic complications of obesity, whereas individuals with central obesity, are prone to these complications (6-8). Increased intra-abdominal fat depots are associated with insulin resistance, increased risk of type 2 diabetes, dyslipidemia, accelerated atherosclerosis, and mortality (74, 264, 265). By contrast, an increased amount of subcutaneous fat, especially in the gluteofemoral regions is associated with improved insulin sensitivity and a lower risk of developing type 2 diabetes, dyslipidemia, and atherosclerosis (10, 266). Proposed mechanisms for these metabolic differences between central and peripheral obesity include lability of lipolysis in visceral adipose tissue, differential adipokine production from visceral adipose tissue and excessive production of inflammatory molecules from immune cells within adipose tissue, whose numbers increase more in visceral adipose tissue than other adipose tissue depots in obesity. Due to the location of visceral adipose tissue, there is direct drainage of free fatty acids, adipokines and inflammatory molecules to the liver via the portal vein where they can exert adverse effects on metabolism in liver and other tissues (267). However, the relatively small contribution of visceral fat to the total circulating load of fatty acids and inflammatory molecules makes it difficult to rationalise these proposed mechanisms. Human studies have shown that although portal free fatty acid flux from visceral adipose tissue does increase in obesity, it only constitutes approximately 20% of total portal free fatty acid flux, with the remainder derived from the systemic circulation (76)

An alternate hypothesis is that subcutaneous adiposity is protective against metabolic disease in obesity. Assessment of insulin sensitivity in humans with

visceral obesity has shown lower levels of insulin resistance in individuals that also have subcutaneous obesity (10, 266). In fact the subcutaneous fat depot may play a 'buffering' role for fatty acids, preventing the exposure of other insulin-sensitive tissues to their detrimental effects (268). This hypothesis is consistent with the effects of thiazolidinedione treatment, which improves insulin sensitivity despite increasing total body fat mass by primarily increasing the subcutaneous fat depot (16). In contrast, in HIV-related lipodystrophy there is a loss of subcutaneous fat, but a relative increase in visceral fat. This redistribution of adipose tissue results in insulin resistance and hyperlipidemia (269). This suggests that subcutaneous adipose tissue crucially stores surplus energy in a metabolically 'safe' form (270). However the importance of adipokine production by subcutaneous adipocytes, particularly leptin and adiponectin, which are reduced in lipodystrophy, cannot be discounted. Leptin therapy in lipodystrophy results in considerable metabolic improvement, without increasing subcutaneous fat depots (59, 61). Further evidence for the beneficial metabolic effects of subcutaneous adiposity is provided from studies in *ob/ob* mice. *Ob/ob* mice lack leptin and exhibit obesity, hyperphagia, and a diabetes-like syndrome of hyperglycemia, glucose intolerance and elevated plasma insulin. When obese *ob/ob* mice are engineered to overexpress adiponectin in adipose tissue, there is a massive increase in subcutaneous adiposity, and this is associated with improved insulin sensitivity and decreased glucose and insulin levels (271). These mice represent a novel model of morbid obesity, in which expansion of adipose tissue is associated with improved metabolism, suggesting that if adipose tissue can expand to accommodate surplus calories, insulin resistance can be ameliorated. This may account for an anomaly observed in human studies, in which a subset of patients is consistently identified who have extremely high body mass index but appear protected from metabolic disease, the so-called 'metabolically healthy obese' (272).

These observations of the positive metabolic aspects of subcutaneous adiposity and the adverse consequences of its deficiency in both experimental animals and humans has led to a hypothesis of the desirability of subcutaneous adipose tissue

‘expandability’ to accommodate excess lipid supply, avoiding its spillover into ‘ectopic’ sites, most particularly the liver, skeletal muscle and pancreas (273). The underlying assumption is that human adipose tissue has a finite capacity to expand, through a combination of adipocyte hyperplasia (although this is limited in adults) and hypertrophy, which varies on an individual-to-individual basis and which may be genetically determined. The determinants of this ‘set point’ remain unclear (270).

Opposing the adipose tissue expandability hypothesis is evidence from studies of angiogenesis inhibition in adipose tissue. As adipose tissue expansion by either adipocyte hyperplasia or hypertrophy is dependent on neovascularisation, one might expect that strategies designed to block adipose tissue angiogenesis would phenocopy lipodystrophic models, with reduction in adipose tissue beds resulting in insulin resistance and ectopic lipid deposition in liver and muscle. Remarkably, in direct contrast to lipodystrophy models, reduction of adipose tissue by elimination of adipose vasculature improves insulin sensitivity, even when the animal is challenged with high fat feeding. This paradoxical improvement in insulin sensitivity despite reduced adipose tissue mass is mediated by reduced food intake (62-64) and suggests that regression of adipose tissue vasculature by endothelial apoptosis confers a paracrine interaction between microvasculature and nerve cells, functioning to limit food intake via the central nervous system. Of particular interest, the reduction in caloric intake is not explained by changes in secretion of known adipokines, such as leptin, or expression of hypothalamic genes that regulate food intake. Consequently, these data point to the existence of a novel component of the regulation of energy balance that reflects the status of white adipose tissue vasculature (64).

The concept of cross-talk between adipose tissue and distant organs is not novel and several previous studies have demonstrated that cross-talk exists between adipose tissue and distant organs (reviewed in Minokoshi, Kahn, Kahn 2003 (173)). Traditionally, the focus of the communication between adipose tissue and distant organs has centered on factors secreted from this tissue, including leptin and

adiponectin and other 'adipokines' (274). However, cross-talk between adipose tissue and distant organs can also occur through non-adipokine mediated pathways, with bidirectional communication between the brain and adipose tissue occurring via the sympathetic nervous system (SNS) and sensory innervation of this tissue. Sensory nerves convey information about body fat stores to the brain (192) and interact with the SNS innervation of adipose tissue to maintain adiposity (193). It is proposed that leptin, through leptin receptors present on afferent nerves (275), activates sensory nerves, conveying information about lipid stores to the brain. As an example, local intra-adipose tissue microinjection of leptin into epididymal adipose tissue elicits increases in sympathetic nerve activity in the contralateral epididymal adipose tissue pad (276). This suggests the presence of a reflex arc composed of afferent sensory nerves from adipose tissue and efferent sympathetic nerves from the hypothalamus (192), which functions to regulate adipose tissue stores. Importantly, SNS drive to adipose tissue is not homogeneous. For example, central melanocortin receptor agonism caused by a single 3rd ventricular melanotan II (MTII) injection increases sympathetic outflow to subcutaneous but not intra-abdominal adipose tissue beds (194). This implies there are depot-specific neural circuits between hypothalamic centers that control appetite and white adipose tissue depots, which may provide another mechanism whereby visceral and subcutaneous adipose tissue have differential effects on metabolic disease.

Given the complexity of the differences between subcutaneous and visceral adipose tissue, both intrinsic (expression of adipokines and response to lipolytic stimuli) and extrinsic (neuronal innervation, sites of vascular drainage and the effects of hormones and growth factors acting in a paracrine fashion) I addressed the question of whether the adverse metabolic effects associated with visceral adiposity versus subcutaneous adiposity are due to anatomic location or to cell-autonomous differences between these adipose depots using an adipose tissue cross-transplantation strategy.

The technique of adipose tissue transplantation.

The development of a technique that enabled the transplantation of metabolically meaningful amounts of adipose tissue was a major advance in the field of obesity research. In order to understand how adipose tissue influences whole body physiology a tool is required that is able to study adipocyte metabolism and investigate the metabolic and endocrine communication between adipose tissue and the rest of the body. The targets for investigation include adipocyte metabolism, secreted factors or adipokines, depot-specific characteristics of adipocytes, given the growing evidence that subcutaneous and visceral fat are metabolically distinct, and the influence of vascularisation and innervation on adipocyte metabolism. Although cell culture systems are extremely useful in the study of adipocytes in vitro, they cannot be used to assess the impact of adipocyte manipulations on whole body metabolism. Cell culture systems are also unable to replicate depot-specific environments, which are dependent on interactions between adipocytes and local non-adipose cells. Adipose tissue transplantation has become a powerful tool for studying adipose tissue physiology as it allows investigation of the communication, both metabolic and endocrine, between adipose tissue and the rest of the body. Transplanting adipose tissue from genetically modified and knock-out animals into wild-type donors, allows the assessment of the impact of mutant adipose tissue on whole body metabolism.

I extended the technique of adipose tissue transplantation to permit depot-specificity for both the donor graft and for the recipient engraftment site. Prior to my study and that of Konrad et al (168), adipose tissue grafts had been transplanted only into the subcutaneous compartment (119-122, 216, 277, 278). By developing the technique of intra-abdominal adipose tissue transplantation, I was able to selectively increase adipose tissue into either the subcutaneous (utilising the Gavrilova et al's method (119)) or intra-abdominal compartment. Depot-specific increases in adipose tissue mass are not possible with physiological weight gain. Furthermore, a cross-transplantation approach could be utilised, enabling the assessment of the intrinsic differences between subcutaneous and visceral adipose

tissue.

Intra-abdominal transplantation of subcutaneous adipose tissue reduces obesity and improves glucose tolerance in fat-fed mice

Using a regional adipose tissue cross-transplantation technique, I demonstrated that mice receiving subcutaneous transplants into the intra-abdominal compartment displayed significantly reduced fat mass, in both transplanted and endogenous adipose tissue beds and improved glucose tolerance. These metabolic benefits were not observed in mice transplanted with subcutaneous adipose tissue into the subcutaneous space nor with intra-abdominal adipose tissue into either compartment. These findings suggest a unique beneficial metabolic effect of transplanting subcutaneous adipose tissue into the intra-abdominal compartment, which is mediated by a substance, produced as a result of transplanting subcutaneous fat into the abdominal compartment, that can act systemically to reduce adiposity and improve glucose metabolism. A possible mechanism behind the selective metabolic advantage of transplanting subcutaneous adipose tissue into the abdominal compartment is suggested by my finding that subcutaneous transplants underwent a significant reduction in size when transposed into the abdominal space. This implies that a failure of subcutaneous adipose tissue expansion within the intra-abdominal compartment, results in a signal that reduces endogenous body fat stores. This finding is analogous to the reduction in adipose tissue mass and paradoxical improvement in insulin sensitivity observed following treatment with angiogenesis inhibitors (43, 63).

My data suggests that cross-talk occurs between transplanted subcutaneous adipose tissue and endogenous adipose tissue beds. Adipokines known to be responsible for mediating metabolic effects, including adiponectin and leptin, do not appear to play a role in this model (169). It is likely, therefore, that a novel adipokine is playing a crucial role in mediating the beneficial metabolic effects in this model. To address this hypothesis, I utilised gene expression analysis to compare gene expression in subcutaneous adipose tissue grafts transplanted into

the intra-abdominal compartment with subcutaneous adipose tissue grafts transplanted into the subcutaneous compartment. I identified selective upregulation of genes controlled by the transcription factor MEF2 in subcutaneous adipose tissue grafts transplanted into the intra-abdominal compartment. Similarly, I identified selective upregulation of genes controlled by the transcription factor MEF2 in the endogenous subcutaneous adipose tissue of mice that received a subcutaneous adipose tissue graft into the intra-abdominal compartment relative to the endogenous subcutaneous adipose tissue of sham-operated animals. In adult tissues, expression of MEF2 is increased in response to stress, including adrenergic stimulation (196). A pattern of changes in gene expression consistent with chronic adrenergic stimulation of adipose tissue was observed selectively in the endogenous subcutaneous adipose tissue of mice that received a subcutaneous adipose tissue graft transplanted into the intra-abdominal compartment, including increased expression of uncoupling protein 1 and glycogen phosphorylase. This suggests that a humoral or neural signal that selectively upregulates adrenergic stimulation of subcutaneous adipose tissue may mediate the metabolic benefit observed after transplantation of subcutaneous adipose tissue into the intra-abdominal compartment.

I propose that transplantation of subcutaneous adipose tissue into the intra-abdominal compartment allows a novel adipokine (or other intermediate) to activate vagal afferent nerves to the hypothalamus. The act of transplantation allows this adipokine to act in a paracrine manner on vagal afferent nerves, to which it would never previously have been exposed. Activation of vagal afferents to the hypothalamus results in increased sympathetic outflow selectively to subcutaneous and not visceral adipose tissue. Chronic adrenergic stimulation of subcutaneous adipose tissue accounts for the beneficial effects on metabolism. Increased adrenergic stimulation of endogenous subcutaneous adipose tissue beds results in increased glucose uptake (mediated by both α and β -adrenoceptors), possibly through activation of MEF2C and MEF2D, increased glycogen degradation through increased expression of glycogen phosphorylase (mediated by α 2-

adrenoceptors) and increased mitochondrial thermogenesis, with increased expression of uncoupling protein 1 (mediated by β 3-adrenoceptors). An alternate hypothesis is that transplantation of subcutaneous adipose tissue into the intra-abdominal compartment releases a humoral factor that acts on central receptors in the hypothalamus to modulate sympathetic outflow selectively to subcutaneous adipose tissue.

Future directions

1. Confirmation of microarray findings by real-time PCR and immunohistochemistry.

The key findings from Chapter 2 were the upregulation of genes controlled by the transcription factor MEF2 in both subcutaneous adipose tissue transplanted into the intra-abdominal compartment (SC-AB) grafts and endogenous inguinal adipose tissue in mice receiving a SC-AB graft (ENDOG-SC). The expression of genes controlled by the transcription factor MEF2 will be analysed by real-time PCR in subcutaneous adipose tissue transplanted into the intra-abdominal compartment (SC-AB), subcutaneous adipose tissue transplanted into the subcutaneous compartment (SC-SC), endogenous subcutaneous (inguinal) adipose tissue from a SC-AB transplant recipient (ENDOG-SC), endogenous visceral (epididymal) adipose tissue from a SC-AB transplant recipient (ENDOG-VIS) and subcutaneous (inguinal) adipose tissue from a sham-operated animal (SHAM-SC). The expression levels of the following genes will be determined - troponin C2, fast; myosin binding protein C, fast-type; myosin, heavy polypeptide 4, skeletal muscle; parvalbumin; actin, alpha 1, skeletal muscle; creatine kinase, muscle; myomesin 2; myosin, light polypeptide 1; actinin alpha 3; small muscle protein, X-linked; tropomyosin 2, beta; solute carrier family 2 (facilitated glucose transporter), member 4 (GLUT4) and enolase 3, beta muscle. In addition the expression of myocyte enhancer factor 2A, myocyte enhancer factor 2C and myocyte enhancer factor 2D will be determined. Immunohistochemistry will be performed to determine which cell types within the adipose tissue bed express these genes of interest. The expression of UCP-1 and glycogen phosphorylase will also be determined by real-time PCR.

Immunohistochemistry will be performed to determine which cell type is expressing these genes. I hypothesise that real-time PCR analysis will confirm the findings from the microarray analysis; that immunohistochemistry staining for UCP-1 will localise to newly formed brown adipocytes (also called beige adipocytes) within the adipose tissue depots; and that immunohistochemistry staining for glycogen phosphorylase will localise to white adipocytes.

2. Establish a time course of re-innervation of subcutaneous to intra-abdominal grafts

A key component of my proposed model is the re-innervation of subcutaneous to intra-abdominal (SC-AB) grafts by both afferent and efferent nerves. Time-course measurements by Tran et al (169) indicated that the beneficial effects of SC-AB transplantation took at least eight weeks to develop. If re-innervation of the SC-AB graft is necessary for the beneficial metabolic effects of SC-AB transplantation, evidence of re-innervation should occur at the same time as the beneficial effects on metabolism. The time-course of re-innervation of adipose grafts will be determined in mice receiving a subcutaneous adipose tissue transplant into the subcutaneous and intra-abdominal space (SC-SC and SC-AB, respectively) and mice receiving an intra-abdominal adipose tissue transplant into the subcutaneous and intra-abdominal space (AB-SC and AB-AB, respectively). Appearance of re-innervation will be correlated with changes in fat mass and improvements in glucose tolerance, relative to sham-operated mice. Mice will be sacrificed 4,8,10 and 13 weeks after transplantation. Endogenous and transplanted adipose tissue depots will be harvested and immunohistochemistry for PGP 9.5 (a marker of peripheral nerves), tyrosine hydroxylase (TH, a marker of noradrenaline turnover), and substance P (SP) and calcitonin gene-related peptide (CGRP, both markers of sensory nerves) will be performed on paraffin-embedded sections of adipose tissue. I expect that re-innervation of fat grafts will be detectable at 8 weeks after transplantation. I predict that the fat grafts will be re-innervated by both sensory (afferent) and efferent (sympathetic noradrenergic) fibers and anticipate that the improved glucose tolerance and reductions in transplanted and endogenous fat

mass will only be observed in SC-AB transplant recipients after re-innervation of the graft.

3. Determine whether afferent signalling from and efferent signalling to SC-AB transplants is necessary for the beneficial effects on metabolism

To determine whether afferent signalling from SC-AB transplants is necessary for the beneficial effects on metabolism, SC-AB grafts will undergo sensory denervation with capsaicin at 8 weeks post-transplantation. Immunohistochemistry, as described above, will be performed to ensure the effectiveness of the sensory denervation. I expect that sensory denervation by local microinjection of capsaicin will prevent the improved glucose tolerance and reduction of fat mass observed in SC-AB mice.

To determine whether efferent sympathetic outflow to SC-AB transplants is necessary for the beneficial effects on metabolism, SC-AB grafts will be chemically sympathectomised from 8 weeks post-transplantation. Chemical sympathectomy will be performed by daily subcutaneous injections of guanethidine monosulfate (40 mg/kg/day) for two weeks. The effectiveness of sympathectomy will be assessed by measuring TH immunoreactivity and noradrenaline content in endogenous and transplanted adipose tissue pads. I expect that chemical sympathectomy will not only prevent the innervation-induced increases in TH immunoreactivity and noradrenaline content in SC-AB grafts, but will also prevent the changes in fat mass and improved glucose tolerance seen in the endogenous adipose tissue in SC-AB transplant recipients.

Another method to determine whether efferent sympathetic outflow to SC-AB transplants is necessary for the beneficial effects on metabolism is to treat the mice with propranolol, a non-selective β -receptor antagonist. I expect treatment with β -receptor antagonists will prevent the changes in fat mass and improved glucose tolerance seen in SC-AB transplant recipients. To determine whether the beneficial metabolic effects that result from SC-AB transplantation are mediated by β 3-

adrenoceptors, mice will be treated with the selective β 3-antagonist L-748337. I expect treatment with a specific β 3-receptor antagonist will prevent the changes in fat mass seen in SC-AB transplant recipients, however improved glucose tolerance may persist as this may be mediated by α 1-adrenergic receptors (279).

4. Determine whether leptin released from SC-AB grafts is acting on afferent sensory nerves to trigger hypothalamic sympathetic outflow to endogenous subcutaneous adipose tissue beds.

It is well-established that subcutaneous adipose tissue secretes more leptin than visceral adipose tissue, both from studies of leptin secretion from whole adipose tissue explants and cultured adipocytes (280). As the differences in leptin secretion persist in isolated adipocytes maintained in cell culture, this implies that increased secretion of leptin is an intrinsic property of subcutaneous adipocytes. Increased leptin secretion is also evident from subcutaneous preadipocytes and persists even when subcutaneous adipocytes are differentiated *in vitro* from precursor cells (155). Therefore enhanced leptin secretion from subcutaneous adipose tissue is likely to be maintained even when engrafted into the intra-abdominal compartment. As mentioned above, it is proposed that leptin, through leptin receptors present on afferent nerves (275), activates sensory nerves, conveying information about lipid stores to the brain. Furthermore, in rats, leptin can elicit local activation of bilateral sympathetic outflow by injecting it directly into epididymal adipose tissue (276). Therefore in my model, increased leptin secretion from subcutaneous adipose tissue transplanted into the intra-abdominal compartment may be acting in a paracrine manner on regional afferent sensory nerves, thereby conveying information to the hypothalamus about increased adipose tissue stores. As a consequence, there is increased sympathetic outflow to endogenous subcutaneous adipose tissue.

To determine whether leptin is required for the beneficial effects of SC-AB transplantation, additional transplants will be performed using leptin-deficient *ob/ob* mice as donors. Previous studies of adipose tissue transplants from *ob/ob*

donors have observed that grafts from 8-week old mice are generally unsuccessful due to inflammation and necrosis, although grafts from 2-week old donors are generally viable (121). This may be due to the massive adipocyte hypertrophy that occurs in *ob/ob* mice with aging. I expect that transplantation of leptin-deficient adipose tissue may lessen the decrease in fat mass and improvement in glucose tolerance observed in mice receiving a SC-AB graft, however it is possible that no difference in the metabolic benefit of SC-AB transplantation will be observed. If no difference is observed this will confirm that leptin does not play a direct role in this model. It would remain possible that SC-AB transplanted adipose tissue produces a factor that improves sensitivity to leptin. This is suggested by Tran et al.'s finding that fat mass decreased and glucose tolerance improved in SC-AB grafts recipients despite falling leptin levels (169).

5. Determine whether upregulation of genes controlled by the transcription factor MEF2 occurs in other insulin-sensitive tissue, including muscle and liver.

mRNA will be extracted from liver, white and red muscle, interscapular brown adipose tissue and mid-brain to determine if upregulation of genes controlled by the transcription factor MEF2 occurs in other insulin sensitive tissues in mice receiving SC-AB grafts. Interestingly, Tran et al observed increased glucose uptake into liver but not muscle during hyperinsulinemic-euglycemic clamp (169). MEF2 regulates transcription of GLUT4, the major glucose transporter in skeletal muscle. As glucose uptake into skeletal muscle is not increased, I expect that upregulation of genes controlled by the transcription factor MEF2 will not be observed in skeletal muscle. Upregulation of genes controlled by the transcription factor MEF2 is likely to be found in liver, brain and interscapular brown adipose tissue.

6. Determine whether the failure of SC-AB grafts to expand is due to defective angiogenesis.

Administration of anti-angiogenic agents to mice from different obesity models results in dose-dependent weight reduction and adipose tissue loss (43, 63). Similarly, targeting of a pro-apoptotic peptide to the adipose tissue vasculature

causes a reduction in fat mass (62). Extraordinarily, the reason for reduced fat mass in these animals appears to be linked to reduced appetite, as these animals consume approximately 30% less energy during high fat feeding (64). This has given rise to the concept that there is an intricate link between adipose blood supply and food intake. Targeted apoptosis of adipose tissue vasculature with a proapoptotic peptide leads to a significant reduction in food intake, independently of leptin, neuropeptide Y and Agouti-related protein levels (64). These data support the presence of direct neural communication between the centers in the brain, which control appetite and hunger, and the adipose tissue vasculature. This may represent another adipose tissue – brain – adipose tissue neural circuit that functions independently of leptin. Autonomic nerves and microvasculature in adipose tissue are intimately related (65, 66) and it is conceivable that regression of adipose tissue vasculature by endothelial apoptosis confers a paracrine interaction between microvasculature and nerve cells, functioning to limit food intake via the central nervous system. Alternately, this may be mediated by a secreted factor from the adipose tissue vasculature. In the context of shrinking adipose tissue depots, a reduction in food intake protects the animal from ectopic storage of lipid in muscle and liver, with its resultant detrimental metabolic consequences, which would otherwise be the inevitable consequence of unbridled caloric intake.

Failure of SC-AB grafts to increase in size may be due to a defect in the formation of a new blood supply to the engrafted adipose tissue depot. To investigate this further, additional transplants will be performed using wild-type donors into C57BL/6 mice carrying GFP as a transgene on the b-actin promoter (Actb). This model will allow the interaction between the donor adipose tissue (non-fluorescent) and endogenous blood vessels and nerves (fluorescent) to be visualised using fluorescent microscopy. Using the new technique of two-photon microscopy it will be possible to image living tissue, due to the superior depth of penetration of this technique above traditional confocal microscopy. This will minimise the alteration in tissue architecture that occurs as a result of fixation, which is particularly problematic in adipose tissue due to its high lipid content. Furthermore

it will be possible to identify whether the adipose tissue graft is infiltrated by inflammatory cells from the host and whether adipocyte precursors derived from the host (either from circulating stem cells or infiltrating endothelial cells) differentiate into adipocytes, either white or beige, within the adipose tissue graft. The innervation and vascular supply to the grafts can also be assessed and whether there is differential neural and vascular supply to white versus brown adipocytes within the graft will be determined.

Final conclusions.

Obesity and type 2 diabetes is a global pandemic with 220 million people world wide having diabetes. Diabetes is associated with significant morbidity, including cardiovascular disease, foot ulceration and eventual limb amputation, retinopathy leading to blindness and chronic renal impairment progressing to dialysis. Diabetes is also a life threatening condition. Recent WHO calculations indicate that worldwide almost 3 million deaths per year are attributable to diabetes (281). In North America about 90% of people with type 2 diabetes are obese (body mass index $>30 \text{ kg/m}^2$), overweight (body mass index 25-29.9), or have a medical history of being so (282). Although lifestyle measures involving dietary modifications and increased exercise can reduce the progression from impaired glucose tolerance or 'pre-diabetes' to type 2 diabetes, in practical terms this is rarely successful (283). The problem of obesity, insulin resistance and type 2 diabetes is compounded by the fact that most current treatments for diabetes cause weight gain (insulin, sulfonylureas, meglitinides and thiazolidinediones) or are weight neutral (metformin, alpha glucosidase inhibitors and dipeptidyl peptidase IV inhibitors). Glucagon-like peptide 1 receptor agonists are the only currently available diabetes treatments subsidized by the pharmaceutical benefits scheme in Australia that cause weight loss (284). The identification of future treatments for co-existent obesity and type 2 diabetes that improve glucose tolerance whilst decreasing fat mass and preserving lean body mass is urgently needed.

This study revealed that transplantation of subcutaneous adipose tissue into the intra-abdominal compartment prevented high-fat diet-induced obesity and glucose intolerance in mice. The proposed mechanism mediating this beneficial effect on metabolism is increased sympathetic nerve stimulation to endogenous subcutaneous adipose tissue that results from activation of afferent nerves to the hypothalamus after transplantation of subcutaneous adipose tissue into the intra-abdominal compartment. Chronic adrenergic stimulation of β 3-adrenoceptors would account for the beneficial effects on metabolism. Increased adrenergic stimulation of endogenous subcutaneous adipose tissue beds would result in increased glucose uptake, possibly through activation of MEF2C and MEF2D, increased glycogen breakdown through increased expression of glycogen phosphorylase and increased mitochondrial thermogenesis, with increased expression of uncoupling protein 1. A novel adipokine is proposed to be responsible for the activation of afferent neurons. This adipokine is postulated to have a unique effect as a result of transplantation of subcutaneous adipose tissue into the intra-abdominal compartment – the process of transplantation allowing this adipokine to act in a paracrine manner on vagal afferent nerves, to which it would never previously have been exposed. Alternately, this adipokine may be acting centrally in the hypothalamus to modulate sympathetic outflow selectively to subcutaneous adipose tissue. These findings highlight important new interactions between adipocyte-derived hormones and the central and peripheral nervous system. The identification of the subcutaneous adipose tissue derived factor that is able to upregulate the expression of UCP-1 in endogenous subcutaneous white adipose tissue beds through increased sympathetic outflow to adipose tissue is important as this intermediate has the potential to become an important therapy in obesity and type 2 diabetes. Previous attempts to utilise non-selective β 3-adrenergic agonists as a treatment for obesity in humans failed due to unwanted β 1 and β 2 mediated side-effects including tachycardia and tremors. With the cloning of the human β 3-adrenoceptor it should be possible to develop a highly selective, full agonist but to date such a compound remains elusive (285). The identification of a factor that is able to stimulate β 3-adrenergic receptors selectively in adipose tissue through

endogenous neural circuits has the potential to become an important therapy in diabetes and obesity.

References

1. 2000 Obesity: preventing and managing the global epidemic. Report of a WHO consultation. World Health Organ Tech Rep Ser 894:i-xii, 1-253
2. **Dunstan D, Zimmet P, Welborn T, Sicree R, Armstrong T, Atkins R, Cameron A, Shaw J, Chadban S** 2001 Diabetes & associated disorders in Australia - 2000 : the accelerating epidemic / The Australian Diabetes, Obesity and Lifestyle Study (AusDiab). Melbourne :: International Diabetes Institute
3. **Willett WC, Dietz WH, Colditz GA** 1999 Guidelines for healthy weight. N Engl J Med 341:427-434
4. **Chan JM, Rimm EB, Colditz GA, Stampfer MJ, Willett WC** 1994 Obesity, fat distribution, and weight gain as risk factors for clinical diabetes in men. Diabetes Care 17:961-969
5. **Colditz GA, Willett WC, Rotnitzky A, Manson JE** 1995 Weight gain as a risk factor for clinical diabetes mellitus in women. Ann Intern Med 122:481-486
6. **Vague J** 1956 The degree of masculine differentiation of obesities: a factor determining predisposition to diabetes, atherosclerosis, gout, and uric calculous disease. Am J Clin Nutr 4:20-34
7. **Bjorntorp P** 1990 Abdominal obesity and risk. Clin Exp Hypertens A 12:783-794
8. **Kissebah AH, Vydellingum N, Murray R, Evans DJ, Hartz AJ, Kalkhoff RK, Adams PW** 1982 Relation of body fat distribution to metabolic complications of obesity. J Clin Endocrinol Metab 54:254-260
9. **Carey DG, Jenkins AB, Campbell LV, Freund J, Chisholm DJ** 1996 Abdominal fat and insulin resistance in normal and overweight women: Direct measurements reveal a strong relationship in subjects at both low and high risk of NIDDM. Diabetes 45:633-638
10. **Snijder MB, Dekker JM, Visser M, Bouter LM, Stehouwer CD, Kostense PJ, Yudkin JS, Heine RJ, Nijpels G, Seidell JC** 2003 Associations of hip and thigh circumferences independent of waist circumference with the incidence of type 2 diabetes: the Hoorn Study. Am J Clin Nutr 77:1192-1197
11. **Raji A, Seely EW, Arky RA, Simonson DC** 2001 Body Fat Distribution and Insulin Resistance in Healthy Asian Indians and Caucasians. J Clin Endocrinol Metab 86:5366-5371
12. **Gan SK, Kriketos AD, Ellis BA, Thompson CH, Kraegen EW, Chisholm DJ** 2003 Changes in aerobic capacity and visceral fat but not myocyte lipid levels predict increased insulin action after exercise in overweight and obese men. Diabetes Care 26:1706-1713
13. **Tiikkainen M, Bergholm R, Rissanen A, Aro A, Salminen I, Tamminen M, Teramo K, Yki-Jarvinen H** 2004 Effects of equal weight loss with orlistat and placebo on body fat and serum fatty acid composition and insulin resistance in obese women. Am J Clin Nutr 79:22-30
14. **Kirk E, Reeds DN, Finck BN, Mayurranjan SM, Patterson BW, Klein S** 2009 Dietary fat and carbohydrates differentially alter insulin sensitivity during caloric restriction. Gastroenterology 136:1552-1560

15. **Ross R, Dagnone D, Jones PJ, Smith H, Paddags A, Hudson R, Janssen I** 2000 Reduction in obesity and related comorbid conditions after diet-induced weight loss or exercise-induced weight loss in men. A randomized, controlled trial. *Ann Intern Med* 133:92-103
16. **Mori Y, Murakawa Y, Okada K, Horikoshi H, Yokoyama J, Tajima N, Ikeda Y** 1999 Effect of troglitazone on body fat distribution in type 2 diabetic patients. *Diabetes Care* 22:908-912
17. **Klein S, Fontana L, Young VL, Coggan AR, Kilo C, Patterson BW, Mohammed BS** 2004 Absence of an effect of liposuction on insulin action and risk factors for coronary heart disease. *N Engl J Med* 350:2549-2557
18. **Thorne A, Lonnqvist F, Aelman J, Hellers G, Arner P** 2002 A pilot study of long-term effects of a novel obesity treatment: omentectomy in connection with adjustable gastric banding. *Int J Obes Relat Metab Disord* 26:193-199
19. **Csendes A, Maluenda F, Burgos AM** 2009 A prospective randomized study comparing patients with morbid obesity submitted to laparotomic gastric bypass with or without omentectomy. *Obes Surg* 19:490-494
20. **Herrera MF, Pantoja JP, Velazquez-Fernandez D, Cabiedes J, Aguilar-Salinas C, Garcia-Garcia E, Rivas A, Villeda C, Hernandez-Ramirez DF, Davila A, Zarain A** 2010 Potential additional effect of omentectomy on metabolic syndrome, acute-phase reactants, and inflammatory mediators in grade III obese patients undergoing laparoscopic Roux-en-Y gastric bypass: a randomized trial. *Diabetes Care* 33:1413-1418
21. **Fabbrini E, Tamboli RA, Magkos F, Marks-Shulman PA, Eckhauser AW, Richards WO, Klein S, Abumrad NN** 2010 Surgical removal of omental fat does not improve insulin sensitivity and cardiovascular risk factors in obese adults. *Gastroenterology* 139:448-455
22. **Cook KS, Min HY, Johnson D, Chaplinsky RJ, Flier JS, Hunt CR, Spiegelman BM** 1987 Adipsin: a circulating serine protease homolog secreted by adipose tissue and sciatic nerve. *Science* 237:402-405
23. **Cannon B, Nedergaard J** 2004 Brown adipose tissue: function and physiological significance. *Physiol Rev* 84:277-359
24. **van Marken Lichtenbelt WD, Vanhommerig JW, Smulders NM, Drossaerts JM, Kemerink GJ, Bouvy ND, Schrauwen P, Teule GJ** 2009 Cold-activated brown adipose tissue in healthy men. *N Engl J Med* 360:1500-1508
25. **Nedergaard J, Bengtsson T, Cannon B** 2007 Unexpected evidence for active brown adipose tissue in adult humans. *Am J Physiol Endocrinol Metab* 293:E444-452
26. **Cypess AM, Lehman S, Williams G, Tal I, Rodman D, Goldfine AB, Kuo FC, Palmer EL, Tseng YH, Doria A, Kolodny GM, Kahn CR** 2009 Identification and importance of brown adipose tissue in adult humans. *N Engl J Med* 360:1509-1517
27. **Virtanen KA, Lidell ME, Orava J, Heglind M, Westergren R, Niemi T, Taittonen M, Laine J, Savisto NJ, Enerback S, Nuutila P** 2009 Functional brown adipose tissue in healthy adults. *N Engl J Med* 360:1518-1525
28. **Saito M, Okamatsu-Ogura Y, Matsushita M, Watanabe K, Yoneshiro T, Nio-Kobayashi J, Iwanaga T, Miyagawa M, Kameya T, Nakada K, Kawai Y,**

- Tsujisaki M** 2009 High incidence of metabolically active brown adipose tissue in healthy adult humans: effects of cold exposure and adiposity. *Diabetes* 58:1526-1531
29. **Zingaretti MC, Crosta F, Vitali A, Guerrieri M, Frontini A, Cannon B, Nedergaard J, Cinti S** 2009 The presence of UCP1 demonstrates that metabolically active adipose tissue in the neck of adult humans truly represents brown adipose tissue. *FASEB J* 23:3113-3120
 30. **Prins JB, O'Rahilly S** 1997 Regulation of adipose cell number in man. *Clin Sci (Lond)* 92:3-11
 31. **Spalding KL, Arner E, Westermark PO, Bernard S, Buchholz BA, Bergmann O, Blomqvist L, Hoffstedt J, Naslund E, Britton T, Concha H, Hassan M, Ryden M, Frisen J, Arner P** 2008 Dynamics of fat cell turnover in humans. *Nature* 453:783-787
 32. **Klyde BJ, Hirsch J** 1979 Increased cellular proliferation in adipose tissue of adult rats fed a high-fat diet. *J Lipid Res* 20:705-715
 33. **Marques BG, Hausman DB, Martin RJ** 1998 Association of fat cell size and paracrine growth factors in development of hyperplastic obesity. *Am J Physiol* 275:R1898-1908
 34. **Tang W, Zeve D, Suh JM, Bosnakovski D, Kyba M, Hammer RE, Tallquist MD, Graff JM** 2008 White fat progenitor cells reside in the adipose vasculature. *Science* 322:583-586
 35. **Rodeheffer MS, Birsoy K, Friedman JM** 2008 Identification of white adipocyte progenitor cells in vivo. *Cell* 135:240-249
 36. **Voros G, Maquoi E, Demeulemeester D, Clerx N, Collen D, Lijnen HR** 2005 Modulation of angiogenesis during adipose tissue development in murine models of obesity. *Endocrinology* 146:4545-4554
 37. **Silha JV, Krsek M, Sucharda P, Murphy LJ** 2005 Angiogenic factors are elevated in overweight and obese individuals. *Int J Obes (Lond)* 29:1308-1314
 38. **Miyazawa-Hoshimoto S, Takahashi K, Bujo H, Hashimoto N, Yagui K, Saito Y** 2005 Roles of degree of fat deposition and its localization on VEGF expression in adipocytes. *Am J Physiol Endocrinol Metab* 288:E1128-1136
 39. **Crandall DL, Hausman GJ, Kral JG** 1997 A review of the microcirculation of adipose tissue: anatomic, metabolic, and angiogenic perspectives. *Microcirculation* 4:211-232
 40. **Wosnitza M, Hemmrich K, Groger A, Graber S, Pallua N** 2007 Plasticity of human adipose stem cells to perform adipogenic and endothelial differentiation. *Differentiation* 75:12-23
 41. **Rehman J, Traktuev D, Li J, Merfeld-Clauss S, Temm-Grove CJ, Bovenkerk JE, Pell CL, Johnstone BH, Considine RV, March KL** 2004 Secretion of angiogenic and antiapoptotic factors by human adipose stromal cells. *Circulation* 109:1292-1298
 42. **Hutley LJ, Herington AC, Shurety W, Cheung C, Vesey DA, Cameron DP, Prins JB** 2001 Human adipose tissue endothelial cells promote preadipocyte proliferation. *Am J Physiol Endocrinol Metab* 281:E1037-1044

43. **Rupnick MA, Panigrahy D, Zhang CY, Dallabrida SM, Lowell BB, Langer R, Folkman MJ** 2002 Adipose tissue mass can be regulated through the vasculature. *Proc Natl Acad Sci U S A* 99:10730-10735
44. **Khan T, Muise ES, Iyengar P, Wang ZV, Chandalia M, Abate N, Zhang BB, Bonaldo P, Chua S, Scherer PE** 2009 Metabolic dysregulation and adipose tissue fibrosis: role of collagen VI. *Mol Cell Biol* 29:1575-1591
45. **Weisberg SP, McCann D, Desai M, Rosenbaum M, Leibel RL, Ferrante AW, Jr.** 2003 Obesity is associated with macrophage accumulation in adipose tissue. *J Clin Invest* 112:1796-1808
46. **Ross R, Masuda J, Raines EW, Gown AM, Katsuda S, Sasahara M, Malden LT, Masuko H, Sato H** 1990 Localization of PDGF-B protein in macrophages in all phases of atherogenesis. *Science* 248:1009-1012
47. **McLaren J, Prentice A, Charnock-Jones DS, Millican SA, Muller KH, Sharkey AM, Smith SK** 1996 Vascular endothelial growth factor is produced by peritoneal fluid macrophages in endometriosis and is regulated by ovarian steroids. *J Clin Invest* 98:482-489
48. **Chung ES, Chauhan SK, Jin Y, Nakao S, Hafezi-Moghadam A, van Rooijen N, Zhang Q, Chen L, Dana R** 2009 Contribution of macrophages to angiogenesis induced by vascular endothelial growth factor receptor-3-specific ligands. *Am J Pathol* 175:1984-1992
49. **Pang C, Gao Z, Yin J, Zhang J, Jia W, Ye J** 2008 Macrophage infiltration into adipose tissue may promote angiogenesis for adipose tissue remodeling in obesity. *Am J Physiol Endocrinol Metab* 295:E313-322
50. **Leibovich SJ, Poverini PJ, Shepard HM, Wiseman DM, Shively V, Nuseir N** 1987 Macrophage-induced angiogenesis is mediated by tumour necrosis factor-alpha. *Nature* 329:630-632
51. **Niu J, Azfer A, Zhelyabovska O, Fatma S, Kolattukudy PE** 2008 Monocyte chemotactic protein (MCP)-1 promotes angiogenesis via a novel transcription factor, MCP-1-induced protein (MCPIP). *J Biol Chem* 283:14542-14551
52. **Chesney J, Metz C, Bacher M, Peng T, Meinhardt A, Bucala R** 1999 An essential role for macrophage migration inhibitory factor (MIF) in angiogenesis and the growth of a murine lymphoma. *Mol Med* 5:181-191
53. **Fan Y, Ye J, Shen F, Zhu Y, Yeghiazarians Y, Zhu W, Chen Y, Lawton MT, Young WL, Yang GY** 2008 Interleukin-6 stimulates circulating blood-derived endothelial progenitor cell angiogenesis in vitro. *J Cereb Blood Flow Metab* 28:90-98
54. **Garg A** 2004 Acquired and inherited lipodystrophies. *N Engl J Med* 350:1220-1234
55. **Barroso I, Gurnell M, Crowley VEF, Agostini M, Schwabe JW, Soos MA, Maslen GL, Williams TDM, Lewis H, Schafer AJ, Chatterjee VKK, O'Rahilly S** 1999 Dominant negative mutations in human PPAR[gamma] associated with severe insulin resistance, diabetes mellitus and hypertension. *Nature* 402:880-883
56. **Savage DB, Tan GD, Acerini CL, Jebb SA, Agostini M, Gurnell M, Williams RL, Umpleby AM, Thomas EL, Bell JD, Dixon AK, Dunne F, Boiani R, Cinti S,**

- Vidal-Puig A, Karpe F, Chatterjee VKV, O'Rahilly S** 2003 Human metabolic syndrome resulting from dominant-negative mutations in the nuclear receptor peroxisome proliferator-activated receptor- α . *Diabetes* 52:910-917
57. **Agostini M, Schoenmakers E, Mitchell C, Szatmari I, Savage D, Smith A, Rajanayagam O, Semple R, Luan Ja, Bath L, Zalin A, Labib M, Kumar S, Simpson H, Blom D, Marais D, Schwabe J, Barroso I, Trembath R, Wareham N, Nagy L, Gurnell M, O'Rahilly S, Chatterjee K** 2006 Non-DNA binding, dominant-negative, human PPAR[γ] mutations cause lipodystrophic insulin resistance. *Cell Metabolism* 4:303-311
 58. **Petersen KF, Oral EA, Dufour S, Befroy D, Ariyan C, Yu C, Cline GW, DePaoli AM, Taylor SI, Gorden P, Shulman GI** 2002 Leptin reverses insulin resistance and hepatic steatosis in patients with severe lipodystrophy. *J Clin Invest* 109:1345-1350
 59. **Oral EA, Simha V, Ruiz E, Andewelt A, Premkumar A, Snell P, Wagner AJ, DePaoli AM, Reitman ML, Taylor SI, Gorden P, Garg A** 2002 Leptin-replacement therapy for lipodystrophy. *N Engl J Med* 346:570-578
 60. **Simha V, Szczepaniak LS, Wagner AJ, DePaoli AM, Garg A** 2003 Effect of leptin replacement on intrahepatic and intramyocellular lipid content in patients with generalized lipodystrophy. *Diabetes Care* 26:30-35
 61. **Chong AY, Lupsa BC, Cochran EK, Gorden P** 2010 Efficacy of leptin therapy in the different forms of human lipodystrophy. *Diabetologia* 53:27-35
 62. **Kolonin MG, Saha PK, Chan L, Pasqualini R, Arap W** 2004 Reversal of obesity by targeted ablation of adipose tissue. *Nat Med* 10:625-632
 63. **Brakenhielm E, Cao R, Gao B, Angelin B, Cannon B, Parini P, Cao Y** 2004 Angiogenesis inhibitor, TNP-470, prevents diet-induced and genetic obesity in mice. *Circ Res* 94:1579-1588
 64. **Kim DH, Woods SC, Seeley RJ** 2010 Peptide designed to elicit apoptosis in adipose tissue endothelium reduces food intake and body weight. *Diabetes* 59:907-915
 65. **Slavin BG, Ballard KW** 1978 Morphological studies on the adrenergic innervation of white adipose tissue. *Anat Rec* 191:377-389
 66. **Bartness TJ, Bamshad M** 1998 Innervation of mammalian white adipose tissue: implications for the regulation of total body fat. *Am J Physiol* 275:R1399-1411
 67. **Unger RH** 2003 Minireview: weapons of lean body mass destruction: the role of ectopic lipids in the metabolic syndrome. *Endocrinology* 144:5159-5165
 68. **Yamauchi T, Kamon J, Waki H, Terauchi Y, Kubota N, Hara K, Mori Y, Ide T, Murakami K, Tsuboyama-Kasaoka N, Ezaki O, Akanuma Y, Gavrilova O, Vinson C, Reitman ML, Kagechika H, Shudo K, Yoda M, Nakano Y, Tobe K, Nagai R, Kimura S, Tomita M, Froguel P, Kadowaki T** 2001 The fat-derived hormone adiponectin reverses insulin resistance associated with both lipodystrophy and obesity. *Nat Med* 7:941-946

69. **Muoio DM, Dohm GL, Fiedorek FT, Jr., Tapscott EB, Coleman RA** 1997 Leptin directly alters lipid partitioning in skeletal muscle. *Diabetes* 46:1360-1363
70. **Perseghin G, Scifo P, De Cobelli F, Pagliato E, Battezzati A, Arcelloni C, Vanzulli A, Testolin G, Pozza G, Del Maschio A, Luzzi L** 1999 Intramyocellular triglyceride content is a determinant of in vivo insulin resistance in humans: a ¹H-¹³C nuclear magnetic resonance spectroscopy assessment in offspring of type 2 diabetic parents. *Diabetes* 48:1600-1606
71. **Krssak M, Falk Petersen K, Dresner A, DiPietro L, Vogel SM, Rothman DL, Roden M, Shulman GI** 1999 Intramyocellular lipid concentrations are correlated with insulin sensitivity in humans: a ¹H NMR spectroscopy study. *Diabetologia* 42:113-116
72. **Ryysy L, Hakkinen AM, Goto T, Vehkavaara S, Westerbacka J, Halavaara J, Yki-Jarvinen H** 2000 Hepatic fat content and insulin action on free fatty acids and glucose metabolism rather than insulin absorption are associated with insulin requirements during insulin therapy in type 2 diabetic patients. *Diabetes* 49:749-758
73. **Goodpaster BH, He J, Watkins S, Kelley DE** 2001 Skeletal muscle lipid content and insulin resistance: evidence for a paradox in endurance-trained athletes. *J Clin Endocrinol Metab* 86:5755-5761
74. **Bjorntorp P** 1990 "Portal" adipose tissue as a generator of risk factors for cardiovascular disease and diabetes. *Arteriosclerosis* 10:493-496
75. **Engfeldt P, Arner P** 1988 Lipolysis in human adipocytes, effects of cell size, age and of regional differences. *Horm Metab Res Suppl* 19:26-29
76. **Nielsen S, Guo Z, Johnson CM, Hensrud DD, Jensen MD** 2004 Splanchnic lipolysis in human obesity. *J Clin Invest* 113:1582-1588
77. **Gabriely I, Ma XH, Yang XM, Atzmon G, Rajala MW, Berg AH, Scherer P, Rossetti L, Barzilai N** 2002 Removal of visceral fat prevents insulin resistance and glucose intolerance of aging: an adipokine-mediated process? *Diabetes* 51:2951-2958
78. **Barzilai N, She L, Liu BQ, Vuguin P, Cohen P, Wang J, Rossetti L** 1999 Surgical removal of visceral fat reverses hepatic insulin resistance. *Diabetes* 48:94-98
79. **Galic S, Oakhill JS, Steinberg GR** 2010 Adipose tissue as an endocrine organ. *Mol Cell Endocrinol* 316:129-139
80. **Zhang Y, Proenca R, Maffei M, Barone M, Leopold L, Friedman JM** 1994 Positional cloning of the mouse obese gene and its human homologue. *Nature* 372:425-432
81. **Van Harmelen V, Reynisdottir S, Eriksson P, Thorne A, Hoffstedt J, Lonnqvist F, Arner P** 1998 Leptin secretion from subcutaneous and visceral adipose tissue in women. *Diabetes* 47:913-917
82. **Heymsfield SB, Greenberg AS, Fujioka K, Dixon RM, Kushner R, Hunt T, Lubina JA, Patane J, Self B, Hunt P, McCamish M** 1999 Recombinant leptin for weight loss in obese and lean adults: a randomized, controlled, dose-escalation trial. *JAMA* 282:1568-1575

83. **Chandran M, Phillips SA, Ciaraldi T, Henry RR** 2003 Adiponectin: more than just another fat cell hormone? *Diabetes Care* 26:2442-2450
84. **Lihn AS, Bruun JM, He G, Pedersen SB, Jensen PF, Richelsen B** 2004 Lower expression of adiponectin mRNA in visceral adipose tissue in lean and obese subjects. *Mol Cell Endocrinol* 219:9-15
85. **Motoshima H, Wu X, Sinha MK, Hardy VE, Rosato EL, Barbot DJ, Rosato FE, Goldstein BJ** 2002 Differential regulation of adiponectin secretion from cultured human omental and subcutaneous adipocytes: effects of insulin and rosiglitazone. *J Clin Endocrinol Metab* 87:5662-5667
86. **Perrini S, Laviola L, Cignarelli A, Melchiorre M, De Stefano F, Caccioppoli C, Natalicchio A, Orlando MR, Garruti G, De Fazio M, Catalano G, Memeo V, Giorgino R, Giorgino F** 2008 Fat depot-related differences in gene expression, adiponectin secretion, and insulin action and signalling in human adipocytes differentiated in vitro from precursor stromal cells. *Diabetologia* 51:155-164
87. **Kershaw EE, Flier JS** 2004 Adipose tissue as an endocrine organ. *J Clin Endocrinol Metab* 89:2548-2556
88. **Curat CA, Wegner V, Sengenès C, Miranville A, Tonus C, Busse R, Bouloumié A** 2006 Macrophages in human visceral adipose tissue: increased accumulation in obesity and a source of resistin and visfatin. *Diabetologia* 49:744-747
89. **Yang Q, Graham TE, Mody N, Preitner F, Peroni OD, Zabolotny JM, Kotani K, Quadro L, Kahn BB** 2005 Serum retinol binding protein 4 contributes to insulin resistance in obesity and type 2 diabetes. *Nature* 436:356-362
90. **Kloting N, Graham TE, Berndt J, Kralisch S, Kovacs P, Wason CJ, Fasshauer M, Schon MR, Stumvoll M, Bluher M, Kahn BB** 2007 Serum retinol-binding protein is more highly expressed in visceral than in subcutaneous adipose tissue and is a marker of intra-abdominal fat mass. *Cell Metab* 6:79-87
91. **Hotamisligil GS, Shargill NS, Spiegelman BM** 1993 Adipose expression of tumor necrosis factor- α : direct role in obesity-linked insulin resistance. *Science* 259:87-91
92. **Harman-Boehm I, Bluher M, Redel H, Sion-Vardy N, Ovadia S, Avinoach E, Shai I, Kloting N, Stumvoll M, Bashan N, Rudich A** 2007 Macrophage infiltration into omental versus subcutaneous fat across different populations: effect of regional adiposity and the comorbidities of obesity. *J Clin Endocrinol Metab* 92:2240-2247
93. **Bruun JM, Lihn AS, Madan AK, Pedersen SB, Schiott KM, Fain JN, Richelsen B** 2004 Higher production of IL-8 in visceral vs. subcutaneous adipose tissue. Implication of nonadipose cells in adipose tissue. *Am J Physiol Endocrinol Metab* 286:E8-13
94. **Bruun JM, Lihn AS, Pedersen SB, Richelsen B** 2005 Monocyte chemoattractant protein-1 release is higher in visceral than subcutaneous human adipose tissue (AT): implication of macrophages resident in the AT. *J Clin Endocrinol Metab* 90:2282-2289
95. **Fain JN, Madan AK, Hiler ML, Cheema P, Bahouth SW** 2004 Comparison of the release of adipokines by adipose tissue, adipose tissue matrix, and

- adipocytes from visceral and subcutaneous abdominal adipose tissues of obese humans. *Endocrinology* 145:2273-2282
96. **Xu H, Barnes GT, Yang Q, Tan G, Yang D, Chou CJ, Sole J, Nichols A, Ross JS, Tartaglia LA, Chen H** 2003 Chronic inflammation in fat plays a crucial role in the development of obesity-related insulin resistance. *J Clin Invest* 112:1821-1830
 97. **Shoelson SE, Herrero L, Naaz A** 2007 Obesity, inflammation, and insulin resistance. *Gastroenterology* 132:2169-2180
 98. **Skurk T, Alberti-Huber C, Herder C, Hauner H** 2007 Relationship between adipocyte size and adipokine expression and secretion. *J Clin Endocrinol Metab* 92:1023-1033
 99. **Trayhurn P, Wang B, Wood IS** 2008 Hypoxia in adipose tissue: a basis for the dysregulation of tissue function in obesity? *Br J Nutr* 100:227-235
 100. **Cinti S, Mitchell G, Barbatelli G, Murano I, Ceresi E, Faloia E, Wang S, Fortier M, Greenberg AS, Obin MS** 2005 Adipocyte death defines macrophage localization and function in adipose tissue of obese mice and humans. *J Lipid Res* 46:2347-2355
 101. **Spencer M, Yao-Borengasser A, Unal R, Rasouli N, Gurley CM, Zhu B, Peterson CA, Kern PA** 2010 Adipose tissue macrophages in insulin resistant subjects are associated with collagen VI, fibrosis and demonstrate alternative activation. *Am J Physiol Endocrinol Metab*
 102. **Wajchenberg BL, Giannella-Neto D, da Silva ME, Santos RF** 2002 Depot-specific hormonal characteristics of subcutaneous and visceral adipose tissue and their relation to the metabolic syndrome. *Horm Metab Res* 34:616-621
 103. **Rebuffe-Scrive M, Bronnegard M, Nilsson A, Eldh J, Gustafsson JA, Bjorntorp P** 1990 Steroid hormone receptors in human adipose tissues. *J Clin Endocrinol Metab* 71:1215-1219
 104. **Fried SK, Russell CD, Grauso NL, Brolin RE** 1993 Lipoprotein lipase regulation by insulin and glucocorticoid in subcutaneous and omental adipose tissues of obese women and men. *J Clin Invest* 92:2191-2198
 105. **DiGirolamo M, Fine JB, Tagra K, Rossmanith R** 1998 Qualitative regional differences in adipose tissue growth and cellularity in male Wistar rats fed ad libitum. *Am J Physiol* 274:R1460-1467
 106. **Kovsan J, Osnis A, Maissel A, Mazor L, Tarnovscki T, Hollander L, Ovadia S, Meier B, Klein J, Bashan N, Rudich A** 2009 Depot-specific adipocyte cell lines reveal differential drug-induced responses of white adipocytes--relevance for partial lipodystrophy. *Am J Physiol Endocrinol Metab* 296:E315-322
 107. **Gesta S, Bluher M, Yamamoto Y, Norris AW, Berndt J, Kralisch S, Boucher J, Lewis C, Kahn CR** 2006 Evidence for a role of developmental genes in the origin of obesity and body fat distribution. *Proc Natl Acad Sci U S A* 103:6676-6681
 108. **Billings E, Jr., May JW, Jr.** 1989 Historical review and present status of free fat graft autotransplantation in plastic and reconstructive surgery. *Plast Reconstr Surg* 83:368-381

109. **Bucky LP, Percec I** 2008 The science of autologous fat grafting: views on current and future approaches to neoadipogenesis. *Aesthet Surg J* 28:313-321; quiz 322-314
110. **Hausberger FX** 1955 Quantitative studies on the development of autotransplants of immature adipose tissue of rats. *Anat Rec* 122:507-515
111. **Iyama K, Ohzono K, Usuku G** 1979 Electron microscopical studies on the genesis of white adipocytes: differentiation of immature pericytes into adipocytes in transplanted preadipose tissue. *Virchows Arch B Cell Pathol Incl Mol Pathol* 31:143-155
112. **Ashwell M, Meade CJ, Medawar P, Sowter C** 1977 Adipose tissue: contributions of nature and nurture to the obesity of an obese mutant mouse (ob/ob). *Proc R Soc Lond B Biol Sci* 195:343-353
113. **Enser M, Ashwell M** 1983 Fatty acid composition of triglycerides from adipose tissue transplanted between obese and lean mice. *Lipids* 18:776-780
114. **Ashwell M** 1992 Why do people get fat: is adipose tissue guilty? *Proc Nutr Soc* 51:353-365
115. **Mauer MM, Harris RB, Bartness TJ** 2001 The regulation of total body fat: lessons learned from lipectomy studies. *Neurosci Biobehav Rev* 25:15-28
116. **Rooks C, Bennet T, Bartness TJ, Harris RB** 2004 Compensation for an increase in body fat caused by donor transplants into mice. *Am J Physiol Regul Integr Comp Physiol* 286:R1149-1155
117. **Lacy EL, Bartness TJ** 2004 Autologous fat transplants influence compensatory white adipose tissue mass increases after lipectomy. *Am J Physiol Regul Integr Comp Physiol* 286:R61-70
118. **Lacy EL, Bartness TJ** 2005 Effects of white adipose tissue grafts on total body fat and cellularity are dependent on graft type and location. *Am J Physiol Regul Integr Comp Physiol* 289:R380-R388
119. **Gavrilova O, Marcus-Samuels B, Graham D, Kim JK, Shulman GI, Castle AL, Vinson C, Eckhaus M, Reitman ML** 2000 Surgical implantation of adipose tissue reverses diabetes in lipoatrophic mice. *J Clin Invest* 105:271-278
120. **Kim JK, Gavrilova O, Chen Y, Reitman ML, Shulman GI** 2000 Mechanism of insulin resistance in A-ZIP/F-1 fatless mice. *J Biol Chem* 275:8456-8460
121. **Colombo C, Cutson JJ, Yamauchi T, Vinson C, Kadowaki T, Gavrilova O, Reitman ML** 2002 Transplantation of adipose tissue lacking leptin is unable to reverse the metabolic abnormalities associated with lipoatrophy. *Diabetes* 51:2727-2733
122. **Chen HC, Jensen DR, Myers HM, Eckel RH, Farese RV, Jr.** 2003 Obesity resistance and enhanced glucose metabolism in mice transplanted with white adipose tissue lacking acyl CoA:diacylglycerol acyltransferase 1. *J Clin Invest* 111:1715-1722
123. **Ong SE, Mann M** 2005 Mass spectrometry-based proteomics turns quantitative. *Nat Chem Biol* 1:252-262
124. **Aebersold R, Mann M** 2003 Mass spectrometry-based proteomics. *Nature* 422:198-207

125. **de Leenheer AP, Thienpont LM** 1992 Applications of isotope dilution-mass spectrometry in clinical chemistry, pharmacokinetics, and toxicology. *Mass Spectrometry Reviews* 11:249-307
126. **Miyagi M, Rao KC** 2007 Proteolytic 18O-labeling strategies for quantitative proteomics. *Mass Spectrom Rev* 26:121-136
127. **Ross PL, Huang YN, Marchese JN, Williamson B, Parker K, Hattan S, Khainovski N, Pillai S, Dey S, Daniels S, Purkayastha S, Juhasz P, Martin S, Bartlet-Jones M, He F, Jacobson A, Pappin DJ** 2004 Multiplexed protein quantitation in *Saccharomyces cerevisiae* using amine-reactive isobaric tagging reagents. *Mol Cell Proteomics* 3:1154-1169
128. **Gygi SP, Rist B, Gerber SA, Turecek F, Gelb MH, Aebersold R** 1999 Quantitative analysis of complex protein mixtures using isotope-coded affinity tags. *Nat Biotechnol* 17:994-999
129. **DeSouza L, Diehl G, Rodrigues MJ, Guo J, Romaschin AD, Colgan TJ, Siu KW** 2005 Search for cancer markers from endometrial tissues using differentially labeled tags iTRAQ and cICAT with multidimensional liquid chromatography and tandem mass spectrometry. *J Proteome Res* 4:377-386
130. **Ong SE, Blagoev B, Kratchmarova I, Kristensen DB, Steen H, Pandey A, Mann M** 2002 Stable isotope labeling by amino acids in cell culture, SILAC, as a simple and accurate approach to expression proteomics. *Mol Cell Proteomics* 1:376-386
131. **Mann M** 2006 Functional and quantitative proteomics using SILAC. *Nat Rev Mol Cell Biol* 7:952-958
132. **Blobel G, Dobberstein B** 1975 Transfer of proteins across membranes. I. Presence of proteolytically processed and unprocessed nascent immunoglobulin light chains on membrane-bound ribosomes of murine myeloma. *J Cell Biol* 67:835-851
133. **Blobel G, Dobberstein B** 1975 Transfer of proteins across membranes. II. Reconstitution of functional rough microsomes from heterologous components. *J Cell Biol* 67:852-862
134. **Walter P, Gilmore R, Blobel G** 1984 Protein translocation across the endoplasmic reticulum. *Cell* 38:5-8
135. **von Heijne G** 1990 The signal peptide. *J Membr Biol* 115:195-201
136. **Nickel W** 2003 The mystery of nonclassical protein secretion. A current view on cargo proteins and potential export routes. *Eur J Biochem* 270:2109-2119
137. **Tashiro K, Tada H, Heilker R, Shirozu M, Nakano T, Honjo T** 1993 Signal sequence trap: a cloning strategy for secreted proteins and type I membrane proteins. *Science* 261:600-603
138. **Tsuruga H, Kumagai H, Kojima T, Kitamura T** 2000 Identification of novel membrane and secreted proteins upregulated during adipocyte differentiation. *Biochem Biophys Res Commun* 272:293-297
139. **Bozaoglu K, Bolton K, McMillan J, Zimmet P, Jowett J, Collier G, Walder K, Segal D** 2007 Chemerin is a novel adipokine associated with obesity and metabolic syndrome. *Endocrinology* 148:4687-4694
140. **Ohgaki S, Iida K, Yokoo T, Watanabe K, Kihara R, Suzuki H, Shimano H, Toyoshima H, Yamada N** 2007 Identification of ISG12b as a putative

- interferon-inducible adipocytokine which is highly expressed in white adipose tissue. *J Atheroscler Thromb* 14:179-184
141. **Bendtsen JD, Nielsen H, von Heijne G, Brunak S** 2004 Improved prediction of signal peptides: SignalP 3.0. *J Mol Biol* 340:783-795
 142. **Bendtsen JD, Jensen LJ, Blom N, Von Heijne G, Brunak S** 2004 Feature-based prediction of non-classical and leaderless protein secretion. *Protein Eng Des Sel* 17:349-356
 143. **Chen X, Cushman SW, Pannell LK, Hess S** 2005 Quantitative proteomic analysis of the secretory proteins from rat adipose cells using a 2D liquid chromatography-MS/MS approach. *J Proteome Res* 4:570-577
 144. **Alvarez-Llamas G, Szalowska E, de Vries MP, Weening D, Landman K, Hoek A, Wolffenbuttel BH, Roelofsen H, Vonk RJ** 2007 Characterization of the human visceral adipose tissue secretome. *Mol Cell Proteomics* 6:589-600
 145. **Zvonic S, Lefevre M, Kilroy G, Floyd ZE, DeLany JP, Kheterpal I, Gravois A, Dow R, White A, Wu X, Gimble JM** 2007 Secretome of primary cultures of human adipose-derived stem cells: modulation of serpins by adipogenesis. *Mol Cell Proteomics* 6:18-28
 146. **Roelofsen H, Dijkstra M, Weening D, de Vries MP, Hoek A, Vonk RJ** 2009 Comparison of isotope-labeled amino acid incorporation rates (CILAIR) provides a quantitative method to study tissue secretomes. *Mol Cell Proteomics* 8:316-324
 147. **Scheele G, Dobberstein B, Blobel G** 1978 Transfer of proteins across membranes, Biosynthesis in vitro of pretrypsinogen and trypsinogen by cell fractions of canine pancreas. *Eur J Biochem* 82:593-599
 148. **Helenius A, Aebi M** 2004 Roles of N-linked glycans in the endoplasmic reticulum. *Annu Rev Biochem* 73:1019-1049
 149. **Lis H, Sharon N** 1993 Protein glycosylation. Structural and functional aspects. *Eur J Biochem* 218:1-27
 150. **Shental-Bechor D, Levy Y** 2008 Effect of glycosylation on protein folding: a close look at thermodynamic stabilization. *Proc Natl Acad Sci U S A* 105:8256-8261
 151. **Freeze HH** 2001 Lectin affinity chromatography. *Curr Protoc Protein Sci* Chapter 9:Unit 9 1
 152. **Jung K, Cho W, Regnier FE** 2009 Glycoproteomics of plasma based on narrow selectivity lectin affinity chromatography. *J Proteome Res* 8:643-650
 153. **Crowe S, Wu LE, Economou C, Turpin SM, Matzaris M, Hoehn KL, Hevener AL, James DE, Duh EJ, Watt MJ** 2009 Pigment epithelium-derived factor contributes to insulin resistance in obesity. *Cell Metab* 10:40-47
 154. **Lafontan M, Berlan M** 2003 Do regional differences in adipocyte biology provide new pathophysiological insights? *Trends Pharmacol Sci* 24:276-283
 155. **van Harmelen V, Dicker A, Ryden M, Hauner H, Lonnqvist F, Naslund E, Arner P** 2002 Increased lipolysis and decreased leptin production by human omental as compared with subcutaneous preadipocytes. *Diabetes* 51:2029-2036
 156. **Coleman DL** 1973 Effects of parabiosis of obese with diabetes and normal mice. *Diabetologia* 9:294-298

157. **Coleman DL** 1978 Obese and diabetes: two mutant genes causing diabetes-obesity syndromes in mice. *Diabetologia* 14:141-148
158. **Chen H, Charlat O, Tartaglia LA, Woolf EA, Weng X, Ellis SJ, Lakey ND, Culpepper J, Moore KJ, Breitbart RE, Duyk GM, Tepper RI, Morgenstern JP** 1996 Evidence that the diabetes gene encodes the leptin receptor: identification of a mutation in the leptin receptor gene in db/db mice. *Cell* 84:491-495
159. **Moussa NM, Claycombe KJ** 1999 The yellow mouse obesity syndrome and mechanisms of agouti-induced obesity. *Obes Res* 7:506-514
160. **Surwit RS, Kuhn CM, Cochrane C, McCubbin JA, Feinglos MN** 1988 Diet-induced type II diabetes in C57BL/6J mice. *Diabetes* 37:1163-1167
161. **Winzell MS, Ahren B** 2004 The high-fat diet-fed mouse: a model for studying mechanisms and treatment of impaired glucose tolerance and type 2 diabetes. *Diabetes* 53 Suppl 3:S215-219
162. **West DB, Boozer CN, Moody DL, Atkinson RL** 1992 Dietary obesity in nine inbred mouse strains. *Am J Physiol* 262:R1025-1032
163. **Surwit RS, Feinglos MN, Rodin J, Sutherland A, Petro AE, Opara EC, Kuhn CM, Rebuffe-Scrive M** 1995 Differential effects of fat and sucrose on the development of obesity and diabetes in C57BL/6J and A/J mice. *Metabolism* 44:645-651
164. **Yaltirik M, Dedeoglu K, Bilgic B, Koray M, Ersev H, Issever H, Dulger O, Soley S** 2003 Comparison of four different suture materials in soft tissues of rats. *Oral Dis* 9:284-286
165. **Matthews DR, Hosker JP, Rudenski AS, Naylor BA, Treacher DF, Turner RC** 1985 Homeostasis model assessment: insulin resistance and beta-cell function from fasting plasma glucose and insulin concentrations in man. *Diabetologia* 28:412-419
166. **Lee S, Muniyappa R, Yan X, Chen H, Yue LQ, Hong E-G, Kim JK, Quon MJ** 2008 Comparison between surrogate indexes of insulin sensitivity and resistance and hyperinsulinemic euglycemic clamp estimates in mice. *American Journal of Physiology - Endocrinology And Metabolism* 294:E261-E270
167. **Mather K** 2009 Surrogate measures of insulin resistance: of rats, mice, and men. *American Journal of Physiology - Endocrinology And Metabolism* 296:E398-E399
168. **Konrad D, Rudich A, Schoenle EJ** 2007 Improved glucose tolerance in mice receiving intraperitoneal transplantation of normal fat tissue. *Diabetologia* 50:833-839
169. **Tran TT, Yamamoto Y, Gesta S, Kahn CR** 2008 Beneficial effects of subcutaneous fat transplantation on metabolism. *Cell Metab* 7:410-420
170. **Andrikopoulos S, Blair AR, Deluca N, Fam BC, Proietto J** 2008 Evaluating the glucose tolerance test in mice. *Am J Physiol Endocrinol Metab* 295:E1323-1332
171. **Hutley L, Shurety W, Newell F, McGeary R, Pelton N, Grant J, Herington A, Cameron D, Whitehead J, Prins J** 2004 Fibroblast growth factor 1: a key regulator of human adipogenesis. *Diabetes* 53:3097-3106

172. **Kreier F, Fliers E, Voshol PJ, Van Eden CG, Havekes LM, Kalsbeek A, Van Heijningen CL, Sluiter AA, Mettenleiter TC, Romijn JA, Sauerwein HP, Buijs RM** 2002 Selective parasympathetic innervation of subcutaneous and intra-abdominal fat--functional implications. *J Clin Invest* 110:1243-1250
173. **Minokoshi Y, Kahn CR, Kahn BB** 2003 Tissue-specific ablation of the GLUT4 glucose transporter or the insulin receptor challenges assumptions about insulin action and glucose homeostasis. *J Biol Chem* 278:33609-33612
174. **Abel ED, Peroni O, Kim JK, Kim YB, Boss O, Hadro E, Minnemann T, Shulman GI, Kahn BB** 2001 Adipose-selective targeting of the GLUT4 gene impairs insulin action in muscle and liver. *Nature* 409:729-733
175. **Kahn BB, Flier JS** 2000 Obesity and insulin resistance. *J Clin Invest* 106:473-481
176. **Graham TE, Yang Q, Bluher M, Hammarstedt A, Ciaraldi TP, Henry RR, Wason CJ, Oberbach A, Jansson PA, Smith U, Kahn BB** 2006 Retinol-binding protein 4 and insulin resistance in lean, obese, and diabetic subjects. *N Engl J Med* 354:2552-2563
177. **Cho YM, Youn BS, Lee H, Lee N, Min SS, Kwak SH, Lee HK, Park KS** 2006 Plasma retinol-binding protein-4 concentrations are elevated in human subjects with impaired glucose tolerance and type 2 diabetes. *Diabetes Care* 29:2457-2461
178. **Kloting N, Fasshauer M, Dietrich A, Kovacs P, Schon MR, Kern M, Stumvoll M, Bluher M** 2010 Insulin-sensitive obesity. *Am J Physiol Endocrinol Metab* 299:E506-515
179. **Yao-Borengasser A, Varma V, Bodles AM, Rasouli N, Phanavanh B, Lee MJ, Starks T, Kern LM, Spencer HJ, 3rd, Rashidi AA, McGehee RE, Jr., Fried SK, Kern PA** 2007 Retinol binding protein 4 expression in humans: relationship to insulin resistance, inflammation, and response to pioglitazone. *J Clin Endocrinol Metab* 92:2590-2597
180. **Ulgen F, Herder C, Kuhn MC, Willenberg HS, Schott M, Scherbaum WA, Schinner S** 2010 Association of serum levels of retinol-binding protein 4 with male sex but not with insulin resistance in obese patients. *Arch Physiol Biochem* 116:57-62
181. **Promintzer M, Krebs M, Todoric J, Luger A, Bischof MG, Nowotny P, Wagner O, Esterbauer H, Anderwald C** 2007 Insulin resistance is unrelated to circulating retinol binding protein and protein C inhibitor. *J Clin Endocrinol Metab* 92:4306-4312
182. **von Eynatten M, Lepper PM, Liu D, Lang K, Baumann M, Nawroth PP, Bierhaus A, Dugi KA, Heemann U, Allolio B, Humpert PM** 2007 Retinol-binding protein 4 is associated with components of the metabolic syndrome, but not with insulin resistance, in men with type 2 diabetes or coronary artery disease. *Diabetologia* 50:1930-1937
183. **Ribel-Madsen R, Friedrichsen M, Vaag A, Poulsen P** 2009 Retinol-binding protein 4 in twins: regulatory mechanisms and impact of circulating and tissue expression levels on insulin secretion and action. *Diabetes* 58:54-60
184. **Chavez AO, Coletta DK, Kamath S, Cromack DT, Monroy A, Folli F, DeFronzo RA, Tripathy D** 2009 Retinol-binding protein 4 is associated with impaired

- glucose tolerance but not with whole body or hepatic insulin resistance in Mexican Americans. *Am J Physiol Endocrinol Metab* 296:E758-764
185. **Zisman A, Peroni OD, Abel ED, Michael MD, Mauvais-Jarvis F, Lowell BB, Wojtaszewski JF, Hirshman MF, Virkamaki A, Goodyear LJ, Kahn CR, Kahn BB** 2000 Targeted disruption of the glucose transporter 4 selectively in muscle causes insulin resistance and glucose intolerance. *Nat Med* 6:924-928
 186. **Kim JK, Zisman A, Fillmore JJ, Peroni OD, Kotani K, Perret P, Zong H, Dong J, Kahn CR, Kahn BB, Shulman GI** 2001 Glucose toxicity and the development of diabetes in mice with muscle-specific inactivation of GLUT4. *J Clin Invest* 108:153-160
 187. **Bruning JC, Michael MD, Winnay JN, Hayashi T, Hersch D, Accili D, Goodyear LJ, Kahn CR** 1998 A Muscle-Specific Insulin Receptor Knockout Exhibits Features of the Metabolic Syndrome of NIDDM without Altering Glucose Tolerance. *Molecular cell* 2:559-569
 188. **Fishman RB, Dark J** 1987 Sensory innervation of white adipose tissue. *Am J Physiol* 253:R942-944
 189. **Giordano A, Morroni M, Santone G, Marchesi GF, Cinti S** 1996 Tyrosine hydroxylase, neuropeptide Y, substance P, calcitonin gene-related peptide and vasoactive intestinal peptide in nerves of rat periovarian adipose tissue: an immunohistochemical and ultrastructural investigation. *J Neurocytol* 25:125-136
 190. **Shi H, Bartness TJ** 2005 White adipose tissue sensory nerve denervation mimics lipectomy-induced compensatory increases in adiposity. *Am J Physiol Regul Integr Comp Physiol* 289:R514-R520
 191. **Shi H, Song CK, Giordano A, Cinti S, Bartness TJ** 2005 Sensory or sympathetic white adipose tissue denervation differentially affects depot growth and cellularity. *Am J Physiol Regul Integr Comp Physiol* 288:R1028-1037
 192. **Bartness TJ, Shrestha YB, Vaughan CH, Schwartz GJ, Song CK** 2010 Sensory and sympathetic nervous system control of white adipose tissue lipolysis. *Mol Cell Endocrinol* 318:34-43
 193. **Song CK, Schwartz GJ, Bartness TJ** 2009 Anterograde transneuronal viral tract tracing reveals central sensory circuits from white adipose tissue. *Am J Physiol Regul Integr Comp Physiol* 296:R501-511
 194. **Brito MN, Brito NA, Baro DJ, Song CK, Bartness TJ** 2007 Differential activation of the sympathetic innervation of adipose tissues by melanocortin receptor stimulation. *Endocrinology* 148:5339-5347
 195. **Wang ZW, Zhou YT, Lee Y, Higa M, Kalra SP, Unger RH** 1999 Hyperleptinemia depletes fat from denervated fat tissue. *Biochem Biophys Res Commun* 260:653-657
 196. **Kim Y, Phan D, van Rooij E, Wang DZ, McAnally J, Qi X, Richardson JA, Hill JA, Bassel-Duby R, Olson EN** 2008 The MEF2D transcription factor mediates stress-dependent cardiac remodeling in mice. *J Clin Invest* 118:124-132
 197. **Reich M, Liefeld T, Gould J, Lerner J, Tamayo P, Mesirov JP** 2006 GenePattern 2.0. *Nat Genet* 38:500-501

198. **Irizarry RA, Bolstad BM, Collin F, Cope LM, Hobbs B, Speed TP** 2003 Summaries of Affymetrix GeneChip probe level data. *Nucleic Acids Res* 31:e15
199. **Gautier L, Cope L, Bolstad BM, Irizarry RA** 2004 affy--analysis of Affymetrix GeneChip data at the probe level. *Bioinformatics* 20:307-315
200. **Ihaka R, Gentleman R** 1996 R: A Language for Data Analysis and Graphics. *Journal of Computational and Graphical Statistics* 5:299 - 314
201. **Gentleman RC, Carey VJ, Bates DM, Bolstad B, Dettling M, Dudoit S, Ellis B, Gautier L, Ge Y, Gentry J, Hornik K, Hothorn T, Huber W, Iacus S, Irizarry R, Leisch F, Li C, Maechler M, Rossini AJ, Sawitzki G, Smith C, Smyth G, Tierney L, Yang JY, Zhang J** 2004 Bioconductor: open software development for computational biology and bioinformatics. *Genome Biol* 5:R80
202. **Smyth GK** 2004 Linear models and empirical bayes methods for assessing differential expression in microarray experiments. *Stat Appl Genet Mol Biol* 3:Article3
203. **Storey JD, Tibshirani R** 2003 Statistical significance for genomewide studies. *Proc Natl Acad Sci U S A* 100:9440-9445
204. **Subramanian A, Tamayo P, Mootha VK, Mukherjee S, Ebert BL, Gillette MA, Paulovich A, Pomeroy SL, Golub TR, Lander ES, Mesirov JP** 2005 Gene set enrichment analysis: a knowledge-based approach for interpreting genome-wide expression profiles. *Proc Natl Acad Sci U S A* 102:15545-15550
205. **Mootha VK, Lindgren CM, Eriksson KF, Subramanian A, Sihag S, Lehar J, Puigserver P, Carlsson E, Ridderstrale M, Laurila E, Houstis N, Daly MJ, Patterson N, Mesirov JP, Golub TR, Tamayo P, Spiegelman B, Lander ES, Hirschhorn JN, Altshuler D, Groop LC** 2003 PGC-1alpha-responsive genes involved in oxidative phosphorylation are coordinately downregulated in human diabetes. *Nat Genet* 34:267-273
206. **Patti ME, Butte AJ, Crunkhorn S, Cusi K, Berria R, Kashyap S, Miyazaki Y, Kohane I, Costello M, Saccone R, Landaker EJ, Goldfine AB, Mun E, DeFronzo R, Finlayson J, Kahn CR, Mandarino LJ** 2003 Coordinated reduction of genes of oxidative metabolism in humans with insulin resistance and diabetes: Potential role of PGC1 and NRF1. *Proc Natl Acad Sci U S A* 100:8466-8471
207. **Petersen KF, Dufour S, Befroy D, Garcia R, Shulman GI** 2004 Impaired mitochondrial activity in the insulin-resistant offspring of patients with type 2 diabetes. *N Engl J Med* 350:664-671
208. **Nagase I, Yoshida T, Kumamoto K, Umekawa T, Sakane N, Nikami H, Kawada T, Saito M** 1996 Expression of uncoupling protein in skeletal muscle and white fat of obese mice treated with thermogenic beta 3-adrenergic agonist. *J Clin Invest* 97:2898-2904
209. **Seale P, Bjork B, Yang W, Kajimura S, Chin S, Kuang S, Scime A, Devarakonda S, Conroe HM, Erdjument-Bromage H, Tempst P, Rudnicki MA, Beier DR, Spiegelman BM** 2008 PRDM16 controls a brown fat/skeletal muscle switch. *Nature* 454:961-967
210. **Enerback S** 2009 The origins of brown adipose tissue. *N Engl J Med* 360:2021-2023

211. **Ishibashi J, Seale P** 2010 Medicine. Beige can be slimming. *Science* 328:1113-1114
212. **Petrovic N, Walden TB, Shabalina IG, Timmons JA, Cannon B, Nedergaard J** 2010 Chronic peroxisome proliferator-activated receptor gamma (PPARgamma) activation of epididymally derived white adipocyte cultures reveals a population of thermogenically competent, UCP1-containing adipocytes molecularly distinct from classic brown adipocytes. *J Biol Chem* 285:7153-7164
213. **Cousin B, Cinti S, Morroni M, Raimbault S, Ricquier D, Penicaud L, Casteilla L** 1992 Occurrence of brown adipocytes in rat white adipose tissue: molecular and morphological characterization. *J Cell Sci* 103 (Pt 4):931-942
214. **Ghorbani M, Himms-Hagen J** 1997 Appearance of brown adipocytes in white adipose tissue during CL 316,243-induced reversal of obesity and diabetes in Zucker fa/fa rats. *Int J Obes Relat Metab Disord* 21:465-475
215. **Himms-Hagen J, Melnyk A, Zingaretti MC, Ceresi E, Barbatelli G, Cinti S** 2000 Multilocular fat cells in WAT of CL-316243-treated rats derive directly from white adipocytes. *Am J Physiol Cell Physiol* 279:C670-681
216. **Park BH, Wang MY, Lee Y, Yu X, Ravazzola M, Orci L, Unger RH** 2006 Combined leptin actions on adipose tissue and hypothalamus are required to deplete adipocyte fat in lean rats: implications for obesity treatment. *J Biol Chem* 281:40283-40291
217. **Lafontan M, Berlan M** 1993 Fat cell adrenergic receptors and the control of white and brown fat cell function. *J Lipid Res* 34:1057-1091
218. **Hasty P, Bradley A, Morris JH, Edmondson DG, Venuti JM, Olson EN, Klein WH** 1993 Muscle deficiency and neonatal death in mice with a targeted mutation in the myogenin gene. *Nature* 364:501-506
219. **Weintraub H, Davis R, Tapscott S, Thayer M, Krause M, Benezra R, Blackwell TK, Turner D, Rupp R, Hollenberg S, et al.** 1991 The myoD gene family: nodal point during specification of the muscle cell lineage. *Science* 251:761-766
220. **Shore P, Sharrocks AD** 1995 The MADS-box family of transcription factors. *Eur J Biochem* 229:1-13
221. **Black BL, Olson EN** 1998 Transcriptional control of muscle development by myocyte enhancer factor-2 (MEF2) proteins. *Annu Rev Cell Dev Biol* 14:167-196
222. **McKinsey TA, Zhang CL, Olson EN** 2002 MEF2: a calcium-dependent regulator of cell division, differentiation and death. *Trends Biochem Sci* 27:40-47
223. **Martin JF, Miano JM, Hustad CM, Copeland NG, Jenkins NA, Olson EN** 1994 A Mef2 gene that generates a muscle-specific isoform via alternative mRNA splicing. *Mol Cell Biol* 14:1647-1656
224. **Gossett LA, Kelvin DJ, Sternberg EA, Olson EN** 1989 A new myocyte-specific enhancer-binding factor that recognizes a conserved element associated with multiple muscle-specific genes. *Mol Cell Biol* 9:5022-5033

225. **Edmondson DG, Lyons GE, Martin JF, Olson EN** 1994 Mef2 gene expression marks the cardiac and skeletal muscle lineages during mouse embryogenesis. *Development* 120:1251-1263
226. **Mora S, Yang C, Ryder JW, Boeglin D, Pessin JE** 2001 The MEF2A and MEF2D isoforms are differentially regulated in muscle and adipose tissue during states of insulin deficiency. *Endocrinology* 142:1999-2004
227. **Breitbart RE, Liang CS, Smoot LB, Laheru DA, Mahdavi V, Nadal-Ginard B** 1993 A fourth human MEF2 transcription factor, hMEF2D, is an early marker of the myogenic lineage. *Development* 118:1095-1106
228. **Yu YT, Breitbart RE, Smoot LB, Lee Y, Mahdavi V, Nadal-Ginard B** 1992 Human myocyte-specific enhancer factor 2 comprises a group of tissue-restricted MADS box transcription factors. *Genes Dev* 6:1783-1798
229. **Martin JF, Schwarz JJ, Olson EN** 1993 Myocyte enhancer factor (MEF) 2C: a tissue-restricted member of the MEF-2 family of transcription factors. *Proc Natl Acad Sci U S A* 90:5282-5286
230. **McDermott JC, Cardoso MC, Yu YT, Andres V, Leifer D, Krainc D, Lipton SA, Nadal-Ginard B** 1993 hMEF2C gene encodes skeletal muscle- and brain-specific transcription factors. *Mol Cell Biol* 13:2564-2577
231. **Potthoff MJ, Olson EN** 2007 MEF2: a central regulator of diverse developmental programs. *Development* 134:4131-4140
232. **Martin S, Slot JW, James DE** 1999 GLUT4 trafficking in insulin-sensitive cells. A morphological review. *Cell Biochem Biophys* 30:89-113
233. **Mora S, Pessin JE** 2000 The MEF2A isoform is required for striated muscle-specific expression of the insulin-responsive GLUT4 glucose transporter. *J Biol Chem* 275:16323-16328
234. **Knight JB, Eyster CA, Griesel BA, Olson AL** 2003 Regulation of the human GLUT4 gene promoter: interaction between a transcriptional activator and myocyte enhancer factor 2A. *Proc Natl Acad Sci U S A* 100:14725-14730
235. **McGee SL, Sparling D, Olson AL, Hargreaves M** 2006 Exercise increases MEF2- and GEF DNA-binding activity in human skeletal muscle. *FASEB J* 20:348-349
236. **Feng L, Gao L, Guan Q, Hou X, Wan Q, Wang X, Zhao J** 2008 Long-term moderate ethanol consumption restores insulin sensitivity in high-fat-fed rats by increasing SLC2A4 (GLUT4) in the adipose tissue by AMP-activated protein kinase activation. *J Endocrinol* 199:95-104
237. **Tavernier G, Galitzky J, Valet P, Remaury A, Bouloumie A, Lafontan M, Langin D** 1995 Molecular mechanisms underlying regional variations of catecholamine-induced lipolysis in rat adipocytes. *Am J Physiol* 268:E1135-1142
238. **Vallerand AL, Perusse F, Bukowiecki LJ** 1990 Stimulatory effects of cold exposure and cold acclimation on glucose uptake in rat peripheral tissues. *Am J Physiol* 259:R1043-1049
239. **Vallerand AL, Perusse F, Bukowiecki LJ** 1987 Cold exposure potentiates the effect of insulin on in vivo glucose uptake. *Am J Physiol* 253:E179-186
240. **Vallerand AL, Lupien J, Bukowiecki LJ** 1986 Cold exposure reverses the diabetogenic effects of high-fat feeding. *Diabetes* 35:329-334

241. **Klingenspor M** 2003 Cold-induced recruitment of brown adipose tissue thermogenesis. *Exp Physiol* 88:141-148
242. **Liu X, Perusse F, Bukowiecki LJ** 1994 Chronic norepinephrine infusion stimulates glucose uptake in white and brown adipose tissues. *Am J Physiol* 266:R914-920
243. **de Souza CJ, Hirshman MF, Horton ES** 1997 CL-316,243, a beta3-specific adrenoceptor agonist, enhances insulin-stimulated glucose disposal in nonobese rats. *Diabetes* 46:1257-1263
244. **Liu X, Perusse F, Bukowiecki LJ** 1998 Mechanisms of the antidiabetic effects of the beta 3-adrenergic agonist CL-316243 in obese Zucker-ZDF rats. *Am J Physiol* 274:R1212-1219
245. **Nonogaki K** 2000 New insights into sympathetic regulation of glucose and fat metabolism. *Diabetologia* 43:533-549
246. **Carpene C, Galitzky J, Collon P, Esclapez F, Dauzats M, Lafontan M** 1993 Desensitization of beta-1 and beta-2, but not beta-3, adrenoceptor-mediated lipolytic responses of adipocytes after long-term norepinephrine infusion. *J Pharmacol Exp Ther* 265:237-247
247. **Atgie C, Faintrenie G, Carpene C, Bukowiecki LJ, Geloën A** 1998 Effects of chronic treatment with noradrenaline or a specific beta3-adrenergic agonist, CL 316 243, on energy expenditure and epididymal adipocyte lipolytic activity in rat. *Comp Biochem Physiol A Mol Integr Physiol* 119:629-636
248. **Vegiopoulos A, Muller-Decker K, Strzoda D, Schmitt I, Chichelnitskiy E, Ostertag A, Berriel Diaz M, Rozman J, Hrabe de Angelis M, Nusing RM, Meyer CW, Wahli W, Klingenspor M, Herzig S** 2010 Cyclooxygenase-2 controls energy homeostasis in mice by de novo recruitment of brown adipocytes. *Science* 328:1158-1161
249. **Kratchmarova I, Kalume DE, Blagoev B, Scherer PE, Podtelejnikov AV, Molina H, Bickel PE, Andersen JS, Fernandez MM, Bunkenborg J, Roepstorff P, Kristiansen K, Lodish HF, Mann M, Pandey A** 2002 A proteomic approach for identification of secreted proteins during the differentiation of 3T3-L1 preadipocytes to adipocytes. *Mol Cell Proteomics* 1:213-222
250. **Wang P, Mariman E, Keijer J, Bouwman F, Noben JP, Robben J, Renes J** 2004 Profiling of the secreted proteins during 3T3-L1 adipocyte differentiation leads to the identification of novel adipokines. *Cell Mol Life Sci* 61:2405-2417
251. **Wessel D, Flugge UI** 1984 A method for the quantitative recovery of protein in dilute solution in the presence of detergents and lipids. *Anal Biochem* 138:141-143
252. **Larance M, Ramm G, Stockli J, van Dam EM, Winata S, Wasinger V, Simpson F, Graham M, Junutula JR, Guilhaus M, James DE** 2005 Characterization of the role of the Rab GTPase-activating protein AS160 in insulin-regulated GLUT4 trafficking. *J Biol Chem* 280:37803-37813
253. **Dennis G, Jr., Sherman BT, Hosack DA, Yang J, Gao W, Lane HC, Lempicki RA** 2003 DAVID: Database for Annotation, Visualization, and Integrated Discovery. *Genome Biol* 4:P3

254. **Huang da W, Sherman BT, Lempicki RA** 2009 Systematic and integrative analysis of large gene lists using DAVID bioinformatics resources. *Nat Protoc* 4:44-57
255. **Dupont A, Tokarski C, Dekeyser O, Guihot AL, Amouyel P, Rolando C, Pinet F** 2004 Two-dimensional maps and databases of the human macrophage proteome and secretome. *Proteomics* 4:1761-1778
256. **Chow S, Rodgers P** 2005 Extended Abstract: Constructing Area-Proportional Venn and Euler Diagrams with Three Circles. In: *Euler Diagrams Workshop*. Paris
257. **Cid MC, Grant DS, Hoffman GS, Auerbach R, Fauci AS, Kleinman HK** 1993 Identification of haptoglobin as an angiogenic factor in sera from patients with systemic vasculitis. *J Clin Invest* 91:977-985
258. **Rohrer B, Long Q, Coughlin B, Wilson RB, Huang Y, Qiao F, Tang PH, Kunchithapautham K, Gilkeson GS, Tomlinson S** 2009 A targeted inhibitor of the alternative complement pathway reduces angiogenesis in a mouse model of age-related macular degeneration. *Invest Ophthalmol Vis Sci* 50:3056-3064
259. **Lumeng CN, Bodzin JL, Saltiel AR** 2007 Obesity induces a phenotypic switch in adipose tissue macrophage polarization. *J Clin Invest* 117:175-184
260. **He GP, Muise A, Li AW, Ro HS** 1995 A eukaryotic transcriptional repressor with carboxypeptidase activity. *Nature* 378:92-96
261. **Majdalawieh A, Zhang L, Fuki IV, Rader DJ, Ro HS** 2006 Adipocyte enhancer-binding protein 1 is a potential novel atherogenic factor involved in macrophage cholesterol homeostasis and inflammation. *Proc Natl Acad Sci U S A* 103:2346-2351
262. **Ro HS, Zhang L, Majdalawieh A, Kim SW, Wu X, Lyons PJ, Webber C, Ma H, Reidy SP, Boudreau A, Miller JR, Mitchell P, McLeod RS** 2007 Adipocyte enhancer-binding protein 1 modulates adiposity and energy homeostasis. *Obesity (Silver Spring)* 15:288-302
263. **Ro HS, Kim SW, Wu D, Webber C, Nicholson TE** 2001 Gene structure and expression of the mouse adipocyte enhancer-binding protein. *Gene* 280:123-133
264. **Carey VJ, Walters EE, Colditz GA, Solomon CG, Willett WC, Rosner BA, Speizer FE, Manson JE** 1997 Body fat distribution and risk of non-insulin-dependent diabetes mellitus in women. The Nurses' Health Study. *Am J Epidemiol* 145:614-619
265. **Wang Y, Rimm EB, Stampfer MJ, Willett WC, Hu FB** 2005 Comparison of abdominal adiposity and overall obesity in predicting risk of type 2 diabetes among men. *Am J Clin Nutr* 81:555-563
266. **Tanko LB, Bagger YZ, Alexandersen P, Larsen PJ, Christiansen C** 2003 Peripheral adiposity exhibits an independent dominant antiatherogenic effect in elderly women. *Circulation* 107:1626-1631
267. **Kabir M, Catalano KJ, Ananthnarayan S, Kim SP, Van Citters GW, Dea MK, Bergman RN** 2005 Molecular evidence supporting the portal theory: a causative link between visceral adiposity and hepatic insulin resistance. *Am J Physiol Endocrinol Metab* 288:E454-461

268. **Manolopoulos KN, Karpe F, Frayn KN** 2010 Gluteofemoral body fat as a determinant of metabolic health. *Int J Obes (Lond)* 34:949-959
269. **Carr A, Samaras K, Burton S, Law M, Freund J, Chisholm DJ, Cooper DA** 1998 A syndrome of peripheral lipodystrophy, hyperlipidaemia and insulin resistance in patients receiving HIV protease inhibitors. *AIDS* 12:F51-58
270. **Huang-Doran I, Sleight A, Rochford JJ, O'Rahilly S, Savage DB** 2010 Lipodystrophy: metabolic insights from a rare disorder. *J Endocrinol* 207:245-255
271. **Kim JY, van de Wall E, Laplante M, Azzara A, Trujillo ME, Hofmann SM, Schraw T, Durand JL, Li H, Li G, Jelicks LA, Mehler MF, Hui DY, Deshaies Y, Shulman GI, Schwartz GJ, Scherer PE** 2007 Obesity-associated improvements in metabolic profile through expansion of adipose tissue. *J Clin Invest* 117:2621-2637
272. **Bluher M** 2010 The distinction of metabolically 'healthy' from 'unhealthy' obese individuals. *Curr Opin Lipidol* 21:38-43
273. **Virtue S, Vidal-Puig A** 2010 Adipose tissue expandability, lipotoxicity and the Metabolic Syndrome -- An allostatic perspective. *Biochimica et Biophysica Acta (BBA) - Molecular and Cell Biology of Lipids* 1801:338-349
274. **Trayhurn P, Bing C** 2006 Appetite and energy balance signals from adipocytes. *Philos Trans R Soc Lond B Biol Sci* 361:1237-1249
275. **Burdyga G, Lal S, Spiller D, Jiang W, Thompson D, Attwood S, Saeed S, Grundy D, Varro A, Dimaline R, Dockray GJ** 2003 Localization of orexin-1 receptors to vagal afferent neurons in the rat and humans. *Gastroenterology* 124:129-139
276. **Niijima A** 1999 Reflex effects from leptin sensors in the white adipose tissue of the epididymis to the efferent activity of the sympathetic and vagus nerve in the rat. *Neurosci Lett* 262:125-128
277. **Klebanov S, Astle CM, Desimone O, Ablamunits V, Harrison DE** 2005 Adipose tissue transplantation protects ob/ob mice from obesity, normalizes insulin sensitivity and restores fertility. *J Endocrinol* 186:203-211
278. **Sennello JA, Fayad R, Pini M, Gove ME, Fantuzzi G** 2006 Transplantation of wild-type white adipose tissue normalizes metabolic, immune and inflammatory alterations in leptin-deficient ob/ob mice. *Cytokine* 36:261-266
279. **Flechtner-Mors M, Jenkinson CP, Alt A, Biesalski HK, Adler G, Ditschuneit HH** 2004 Sympathetic regulation of glucose uptake by the alpha1-adrenoceptor in human obesity. *Obes Res* 12:612-620
280. **Russell CD, Petersen RN, Rao SP, Ricci MR, Prasad A, Zhang Y, Brolin RE, Fried SK** 1998 Leptin expression in adipose tissue from obese humans: depot-specific regulation by insulin and dexamethasone. *Am J Physiol* 275:E507-515
281. **Roglic G, Unwin N, Bennett PH, Mathers C, Tuomilehto J, Nag S, Connolly V, King H** 2005 The burden of mortality attributable to diabetes: realistic estimates for the year 2000. *Diabetes Care* 28:2130-2135
282. **Gregg EW, Cheng YJ, Narayan KM, Thompson TJ, Williamson DF** 2007 The relative contributions of different levels of overweight and obesity to the

increased prevalence of diabetes in the United States: 1976-2004. *Prev Med* 45:348-352

283. **Gillies CL, Abrams KR, Lambert PC, Cooper NJ, Sutton AJ, Hsu RT, Khunti K** 2007 Pharmacological and lifestyle interventions to prevent or delay type 2 diabetes in people with impaired glucose tolerance: systematic review and meta-analysis. *BMJ* 334:299
284. **Bailey CJ** 2011 The challenge of managing coexistent type 2 diabetes and obesity. *BMJ* 342:d1996
285. **Weyer C, Gautier JF, Danforth E, Jr.** 1999 Development of beta 3-adrenoceptor agonists for the treatment of obesity and diabetes--an update. *Diabetes Metab* 25:11-21

Appendix 1

Secreted proteins identified from visceral and subcutaneous whole adipose tissue explants.

Accession	Protein Name	Signal peptide	Functional description	Viscera I/Subcut. ratio
CO3_MOUSE	Complement C3	+	Complement cascade, innate immunity	3.8962
A2M_MOUSE	Alpha-2-macroglobulin	+	Serine protease inhibitor, prevents coagulation & fibrinolysis	1.0462
LAMB1_MOUSE	Laminin subunit beta 1	+	Extracellular matrix	0.0465
LAMC1_MOUSE	Laminin subunit gamma-1	+	Extracellular matrix	5.3939
LAMA2_MOUSE	Laminin subunit alpha-2	+	Extracellular matrix	5.8369
COEA1_MOUSE	Collagen alpha-1(XIV) chain	+	Extracellular matrix	0.2932
FINC_MOUSE	Fibronectin	+	Extracellular matrix	3.4279
CES3_MOUSE	Carboxylesterase 3	+	Lipase	7.7748
HPT_MOUSE	Haptoglobin	+	Haem binding protein, acute phase reactant	2.5003
CO1A2_MOUSE	Collagen alpha-2(I) chain	+	Extracellular matrix	1.0944
TRFE_MOUSE	Serotransferrin	+	Iron binding	1.3117
LAMB2_MOUSE	Laminin subunit beta-2	+	Extracellular matrix	0.5017
CFAB_MOUSE	Complement factor B	+	Complement cascade, innate immunity	2.2097
CERU_MOUSE	Ceruloplasmin	+	Copper, iron binding	4.2408
SPA3N_MOUSE	Serine protease inhibitor A3N	+	Trypsin inhibitor	4.1321
SPA3K_MOUSE	Serine protease inhibitor A3K	+	Trypsin inhibitor, also known as contrapsin	3.1605
ESTN_MOUSE	Liver carboxylesterase N	+	Drug detoxification	21.8136
GELS_MOUSE	Gelsolin	+	Depolymerises extracellular actin from necrotic cells	1.0615
CO4B_MOUSE	Complement C4-B	+	Complement cascade, innate immunity	13.7332
NID2_MOUSE	Nidogen-2	+	Extracellular matrix	3.4691
CATB_MOUSE	Cathepsin B	+	Protease activity	6.2497
ANT3_MOUSE	Antithrombin-III	+	Serine protease inhibitor, regulation of blood coagulation	0.1622
PGS2_MOUSE	Decorin	+	Extracellular matrix	4.737
CO3A1_MOUSE	Collagen alpha-1 (III) chain	+	Extracellular matrix	2.4722
MRC1_MOUSE	Macrophage mannose receptor 1	+	Innate immunity	0.2451
BCAM_MOUSE	Basal cell adhesion molecule	+	Cell adhesion	0.1956
CFAH_MOUSE	Complement factor H	+	Innate immunity	2.8502
MUG2_MOUSE	Murinoglobulin-2	+	Negative acute phase reactant	2.2843
FIBG_MOUSE	Fibrinogen gamma chain	+	Coagulation	0.034
ACE_MOUSE	Angiotensin-converting enzyme	+	Blood pressure regulation	4.8181
PTX3_MOUSE	Pentraxin-related protein PTX3	+	Innate immunity	18.8319
IC1_MOUSE	Plasma protease C1 inhibitor	+	Innate immunity	8.8505
SPA3M_MOUSE	Serine protease inhibitor A3M	+	Serine protease inhibitor	1.9963
SPA3C_MOUSE	Serine protease inhibitor A3C	+	Serine protease inhibitor	4.9315
NGAL_MOUSE	Neutrophil gelatinase-associated lipocalin	+	Innate immunity	3.4368
CFAD_MOUSE	Complement factor D	+	Innate immunity	1.0363
TSP1_MOUSE	Thrombospondin-1	+	Angiogenesis inhibitor	11.1698
SODE_MOUSE	Extracellular superoxide dismutase	+	Antioxidant	32.3922
EST1_MOUSE	Liver carboxylesterase 1	+	Lipid and drug metabolism	29.1106
VIME_MOUSE	Vimentin	+	Cytoskeletal component	0.1172
SPA3G_MOUSE	Serine protease inhibitor A3G	+	Serine protease inhibitor	4.1362
HA11_MOUSE	H-2 class I histocompatibility antigen, D-B alpha chain	+	Innate immunity	2.7651

NAR3_MOUSE	Ecto-ADP-ribosyltransferase 3	+	Regulation of t-cell function	2.2346
ACTB_MOUSE	Actin, cytoplasmic 1	-	Cytoskeleton	0.0113
ENPP2_MOUSE	Ectonucleotide pyrophosphatase/phosphodiesterase family member 2	+	Angiogenesis	4.1023
CATD_MOUSE	Cathepsin D	+	Aspartic protease	15.1463
DAG1_MOUSE	Dystroglycan	+	Structural integrity in muscle tissues	0.4972
APOH_MOUSE	Beta-2-glycoprotein 1	+	Coagulation	0.0429
LDHA_MOUSE	L-Lactate dehydrogenase A chain	-	Glycolysis	3.738
1433E_MOUSE	14-3-3 protein epsilon	-	Regulatory molecule	0.1222
PRDX1_MOUSE	Periredoxin-1	+	Antioxidant	0.0192
HA18_MOUSE	H-2 class I histocompatibility antigen, Q8 alpha chain	+	Innate immunity	11.9042
HA17_MOUSE	H-C class I histocompatibility antigen, Q7 alpha chain	+	Innate immunity	10.7956
PRDX3_MOUSE	Thioredoxin-dependent peroxide reductase, mitochondrial	-	Antioxidant	12.5873
SPRC_MOUSE	SPARC	+	Angiogenesis inhibitor	1.3967
CS1B_MOUSE	Complement C1s-B subcomponent	+	Innate immunity	3.4848
TIMP1_MOUSE	Metalloproteinase inhibitor 1	+	Regulation of extracellular matrix	4.7096
CO4A2_MOUSE	Collagen alpha-2 (IV) chain	+	Extracellular matrix	0.8723
PGCP_MOUSE	Plasma glutamate carboxypeptidase	+	Hydrolysis of circulating peptides	0.4097
EGFR_MOUSE	Epidermal growth factor receptor	+	Cell growth, proliferation and differentiation	0.394
CSF1_MOUSE	Macrophage colony-stimulating factor 1	+	Innate immunity	2.2038
ECM1_MOUSE	Extracellular matrix protein 1	+	Extracellular matrix	0.1997
ADIPO_MOUSE	Adiponectin	+	Fat metabolism and insulin sensitivity	0.0218
ACTH_MOUSE	Actin, gamma-enteric smooth muscle	-	Cytoskeleton	0.0008
SPA3F_MOUSE	Serine protease inhibitor A3F	+	Serine protease inhibitor	3.596
MAOX_MOUSE	NADP-dependent malic enzyme	-	Malate metabolic processing	1.3692
KV2A7_MOUSE	Ig kappa chain V-II region 26-10	-	Immunity	39.7792
CADH5_MOUSE	Cadherin-5	+	Cell adhesion	0.719
HA10_MOUSE	H-2 class I histocompatibility antigen, Q10 alpha chain	+	Innate immunity	17.1972
BPA1_MOUSE	Bullous pemphigoid antigen 1, isoforms 1/2/3/4	-	Cell adhesion	9.2942
ANGT_MOUSE	Angiotensinogen	+	Blood pressure regulation	50.0499
ITIH2_MOUSE	Inter-alpha-trypsin inhibitor heavy chain H2	+	Regulate the localization, synthesis and degradation of hyaluronan	0.0169
CATL1_MOUSE	Cathepsin L1	+	Lysosomal function	15.3019
MACF1_MOUSE	Microtubule-actin cross-linking factor 1	-	Cytoskeleton	1.0881
CO2_MOUSE	Complement C2	+	Innate immunity	8.581
AMRP_MOUSE	Alpha-2-macroglobulin receptor-associated protein	+	Interacts with LRP1/alpha-2-macroglobulin receptor	0.7802
PXDC2_MOUSE	Plexin domain-containing protein 2	+	Angiogenesis	3.1057
SAP_MOUSE	Sulfated glycoprotein 1	+	Epithelial cell differentiation	34.6713
CD14_MOUSE	Monocyte differentiation antigen CD14	+	Innate immunity	54.9729
CAH3_MOUSE	Carbonic anhydrase 3	-	Reversible hydration of carbon dioxide	0.0235
CYB5_MOUSE	Cytochrome b5	-	Sterol biosynthesis	0.145
PLXC1_MOUSE	Plexin-C1	+	Cell adhesion	0.2068
A2MP_MOUSE	Alpha-2-macroglobulin-P	+	Serine protease inhibitor, prevents coagulation and fibrinolysis	0.3333
POSTN_MOUSE	Periostin	+	Bone and tooth formation	0.018

DYH3_MOUSE	Dynein heavy chain 3, axonemal	-	Cell motility	1.1125
PLOD1_MOUSE	Procollagen-lysine, 2-oxoglutarate 5-dioxygenase 1	+	Extracellular matrix	2.3807
CO1A1_MOUSE	Collagen alpha-1(I) chain	+	Extracellular matrix	13.8932
ACTBL_MOUSE	Beta-actin-like protein 2	-	Cytoskeleton	0.003
HERC2_MOUSE	Probable E3 ubiquitin-protein ligase HERC2	-	DNA repair	0.7363
MSH3_MOUSE	DNA mismatch repair protein Msh3	-	Component of DNA mismatch repair system	2.8729
ASPM_MOUSE	Abnormal spindle-like microcephaly-associated protein homolog	-	Coordination of mitotic processes	2.0761
ASAP2_MOUSE	Arf-GAP with SH3 domain, ANK repeat and PH domain-containing protein 2	-	Vesicle formation and phagocytosis	0.7028
SPTB1_MOUSE	Spectrin beta chain, erythrocyte	-	Cytoskeleton	0.3966
GVIN1_MOUSE	Interferon-induced very large GTPase 1	-	Innate immunity	11.8529
NAL9C_MOUSE	NACHT, LRR and PYD domains-containing protein 9C	-	Inflammation	0.0441
DPEP1_MOUSE	Dipeptidase 1	+	Hydrolyzes a wide range of dipeptides	0.0357
CHD9_MOUSE	Chromodomain-helicase-DNA-binding protein 9	-	Transcriptional coactivator for PPARA	4.4816
CAD13_MOUSE	Cadherin-13	+	Cell adhesion	6.5059
GAS7_MOUSE	Growth arrest specific 7	-	Maturation and morphological differentiation of cerebellar neurons	0.2346
CYC_MOUSE	Cytochrome c, somatic	-	Electron carrier protein	0.1362
S22A3_MOUSE	Solute carrier family 22 member 3	-	Organic cation transporter 3	0.0241
ANR53_MOUSE	Ankyrin repeat domain-containing protein 53	-	Cell-extracellular matrix interaction	10.0498
TTF2_MOUSE	Transcription termination factor 2	-	Transcription	0.1806
PAI1_MOUSE	Plasminogen activator inhibitor 1	+	Serine protease inhibitor, inhibits matrix metalloproteinases, associated with insulin resistance	9.7866
MMRN2_MOUSE	Multimerin-2	+	Extracellular matrix	4.6797
SACS_MOUSE	Sacsin	-	Regulator of the Hsp70 chaperone machinery	0.6014
MGAP_MOUSE	MAX gene-associated protein	-	Transcription factor	8.7736
EVPL_MOUSE	Envoplakin	-	Component of the cornified envelope of keratinocytes	3.2461
UBR4_MOUSE	E3 ubiquitin-protein ligase UBR4	-	Cytoskeletal organisation	0.3207
NCOR1_MOUSE	Nuclear receptor corepressor 1	-	Transcriptional repression	0.6675
ILRL1_MOUSE	Interleukin-1 receptor-like 1	+	Immunity	0.4894
NAR5_MOUSE	Ecto-ADP-ribosyltransferase 5	+	Regulation of t-cell function	0.0518
GANAB_MOUSE	Neutral alpha-glucosidase AB	+	Glycan metabolism	0.217
CC136_MOUSE	Coiled-coil domain-containing protein 136	-	Membrane protein	0.169
TRPM7_MOUSE	Transient receptor potential cation channel subfamily M member 7	-	Divalent cation channel	0.0408
STRUMP_MOUSE	Strumpelin	-	Cytoskeleton	16.8345
PARD3_MOUSE	Partitioning defective homolog	-	Cell adhesion	0.1408
CD158_MOUSE	Coiled-coil domain-containing	-	Membrane protein	3.106

	protein 158			
ACLY_MOUSE	ATP-citrate synthase	-	De novo lipid synthesis	0.021
ACTN4_MOUSE	Alpha-actinin-4	-	Cytoskeleton	1.9221
RPAP1_MOUSE	RNA polymerase II-associated protein 1	-	Transcription	3.4288
LRP2_MOUSE	Low-density lipoprotein receptor-related protein 2	+	HDL endocytosis	1.3135
CAH2_MOUSE	Carbonic anhydrase 2	-	Reversible hydration of carbon dioxide	2.2056
NAL9B_MOUSE	NACHT, LRR and PYD domains-containing protein 9B	-	Inflammation	0.7537
VINC_MOUSE	Vinculin	-	Cell adhesion	4.645
EIF3A_MOUSE	Eukaryotic translation initiation factor 3 subunit A	-	Protein synthesis	4.3212
MA7D2_MOUSE	MAP7 domain-containing protein 2	-	No functional information	6.7425
BRCA2_MOUSE	Breast cancer type 2 susceptibility protein homolog	-	DNA repair	3.8641
TBCK_MOUSE	TBC domain-containing protein kinase-like protein	-	No functional information	16.6585
MDHM_MOUSE	Malate dehydrogenase, mitochondrial	-	Carbohydrate metabolism	12.6742
MYO5A_MOUSE	Myosin-Va	-	Melanosome transport	0.0777
CO6A1_MOUSE	Collagen alpha-1 (VI) chain	+	Extracellular matrix	1.9258
LAMP1_MOUSE	Lysosome-associated membrane glycoprotein 1	+	Presents carbohydrate ligands to selectins	2.5343
ZSWM5_MOUSE	Zinc finger SWIM domain-containing protein 5	-	No functional information	0.1203
UBP36_MOUSE	Ubiquitin carboxyl-terminal hydrolase 36	-	May be required for maintaining multiple types of adult stem cells	0.6201
MGT5A_MOUSE	N-acetylglucosaminyl-transferase V	-	Biosynthesis of glycoprotein oligosaccharides	3.4498
WDR64_MOUSE	WD repeat-containing domain protein 64	-	No functional information	7.6007
KIF27_MOUSE	Kinesin-like protein KIF27	-	Plays an essential role in motile ciliogenesis	0.1688
IFIT2_MOUSE	Interferon-induced protein with tetratricopeptide repeats 2	-	Innate immunity	0.0997
MINT_MOUSE	Mxs2-interacting protein	-	Regulation of transcription	0.6154
SEM7A_MOUSE	Semaphorin-7A	+	Innate immunity	3.2088
ATRX_MOUSE	Transcriptional regulator ATRX	-	Regulation of transcription	0.0796
MA7D1_MOUSE	MAP7 domain-containing protein 1	-	No functional information	0.2126
F91A1		-	No functional information	0.044
GLU2B_MOUSE	Glucosidase 2 subunit beta	+	Glycan metabolism	0.2904

Appendix 2

Secreted proteins identified from visceral and subcutaneous microvascular endothelial cells.

Accession	Protein Name	Signal peptide	Functional description	Viscera I/Subcut. ratio
TENA_MOUSE	Tenascin	+	Extracellular matrix	0.1746
AEBP1_MOUSE	Adipocyte enhancer-binding protein 1	+	Transcriptional repressor	14.6159
COL1A2_MOUSE	Collagen alpha-2(I) chain	+	Extracellular matrix	0.1228
TSP1_MOUSE	Thrombospondin-1	+	Angiogenesis inhibitor	1.4505
IC1_MOUSE	Plasma protease C1 inhibitor	+	Inhibits C1s and C1r protease activity	4.7622
EMIL1_MOUSE	EMILIN-1	+	Extracellular matrix	0.0258
PGS1_MOUSE	Biglycan	+	Extracellular matrix	7.9442
CO1A1_MOUSE	Collagen alpha-1(I) chain	+	Extracellular matrix	2.9346
PGBM_MOUSE	Basement membrane-specific heparan sulfate proteoglycan core protein	+	Extracellular matrix	0.7816
PGS2_MOUSE	Decorin	+	Extracellular matrix	3.5699
CO3A1_MOUSE	Collagen alpha-1(III) chain	+	Extracellular matrix	3.9785
PAI1_MOUSE	Plasminogen activator inhibitor 1	+	Serine protease inhibitor, inhibits matrix metalloproteinases, associated with insulin resistance	2.0433
TITIN_MOUSE	Titin	-	Mechanical contraction	0.3374
1433Z_MOUSE	14-3-3 protein zeta/delta	-	Phosphoprotein binding, modulation of enzymatic activity	0.4732
A2M_MOUSE	Alpha-2-macroglobulin	+	Serine protease inhibitor, prevents coagulation and fibrinolysis	9.6076
LIPL_MOUSE	Lipoprotein lipase	+	Lipoprotein associated lipid hydrolysis	1.695
ACTBL_MOUSE	Beta-actin-like protein 2	-	Cytoskeleton	0.1492
APOE_MOUSE	Apolipoprotein E	+	Lipid transport	3.1261
ITIH3_MOUSE	Inter-alpha-trypsin inhibitor heavy chain H3	+	Serine protease inhibitor	0.2654
H2B1C_MOUSE	Histone H2B type 1-C/E/G	-	DNA binding	1.7378
KPYM_MOUSE	Pyruvate kinase isozymes M1/M2	-	Glycolysis	2.2684
CATB_MOUSE	Cathepsin B	+	Protease activity	3.402
HBA_MOUSE	Hemoglobin subunit alpha	-	Oxygen-transport metalloprotein	0.0004
GELS_MOUSE	Gelsolin	+	Depolymerises extracellular actin from necrotic cells	0.1961
PEDF_MOUSE	Pigment epithelium-derived factor	+	Angiogenesis inhibitor, role in insulin resistance	0.3728
CPXM1_MOUSE	Probable carboxypeptidase X1	+	Cell-cell interactions	15.2617
LDHA_MOUSE	L-lactate dehydrogenase A chain	-	Pyruvate metabolism	1.9669
MUG1_MOUSE	Murinoglobulin-1	+	Negative acute phase reactant	11.0995
TRFE_MOUSE	Serotransferrin	+	Iron binding	6.4169
BPA1_MOUSE	Bullous pemphigoid antigen 1, isoforms 1/2/3/4	-	Cell-cell interactions/adhesion	0.0477
SODE_MOUSE	Extracellular superoxide dismutase [Cu-Zn]	-	Anti-oxidant	0
MYH9_MOUSE	Myosin-9	-	Muscle protein	2.094
FBLN4_MOUSE	EGF-containing fibulin-like extracellular matrix protein 2	+	Extracellular matrix	1.1211
SPRC_MOUSE	SPARC	+	Angiogenesis inhibitor	2.8342
TSP2_MOUSE	Thrombospondin-2	+	Angiogenesis inhibitor	3.499
TIMP1_MOUSE	Metalloproteinase inhibitor 1	+	Regulation of extracellular matrix	10.8362

ENOA_MOUSE	Alpha-enolase	-	Glycolysis	0.009
PPGB_MOUSE	Lysosomal protective protein	+	Lysosome function	28.7965
LRP1_MOUSE	Pro low density lipoprotein receptor-related protein 1	+	Endocytosis and phagocytosis	1.617
CTRO_MOUSE	Citron Rho-interacting kinase	-	Protein kinase	0.046
CO4A2_MOUSE	Collagen alpha-2 (IV) chain	+	Extracellular matrix	4.5144
K1C20_MOUSE	Keratin, type I cytoskeletal 20	-	Fibrous structural protein	0.0021
ZZZ3_MOUSE	ZZ-type zinc finger-containing protein 3	-	Transcription regulation	7.9886
THIO_MOUSE	Thioredoxin	-	Antioxidant	19.3581
NIN_MOUSE	Ninein	-	Centrosomal function	0.345
ATRX_MOUSE	Transcriptional regulator ATRX	-	Transcription regulation	0.9238
NRAP_MOUSE	Nebulin-related-anchoring protein	-	Cell-extracellular matrix interaction	3.0468
VIME_MOUSE	Vimentin	-	Cytoskeletal component	23.2241
ANK2_MOUSE	Ankyrin-2	-	Cell-extracellular matrix interaction	1.3459
TF3C1_MOUSE	General transcription factor 3 C1	-	Transcription regulator	2.1781
ALDOA_MOUSE	Fructose-bisphosphate aldolase A	-	Glycolysis	0.5166
ATM_MOUSE	Serine-protein kinase ATM	-	DNA damage sensor	0.0823
C1RA_MOUSE	Complement C1r-A subcomponent	+	Complement cascade, innate immunity	0.0766
UBE2N_MOUSE	Ubiquitin-conjugating enzyme E2 N	-	Protein modification	0.024
PYRG2_MOUSE	CTP synthase 2	-	Synthesis of cytosine nucleotides	0.0073
ARPC4_MOUSE	Actin-related protein 2/3 complex subunit 4	-	Extracellular matrix	9.0303
RBP2_MOUSE	E3 SUMO-protein ligase RanBP2	-	Protein modification	0.0003
DPOE1_mouse	DNA polymerase epsilon catalytic subunit A	-	DNA repair	0.0125
MMP3_MOUSE	Stromelysin-1	+	Extracellular matrix	3.8353
CO2A1	Collagen alph-1 (II) chain	+	Extracellular matrix	21.0985
XIRP2_MOUSE	Xin actin-binding repeat-containing protein 2	-	Cytoskeletal protein	5.6558
NFX1_MOUSE	Transcriptional repressor NF-X1	-	Regulation of inflammatory response	0.0813
MUG2_MOUSE	Murinoglobulin-2	+	Acute phase reactant	10.3309
KNG1_MOUSE	Kininogen-1	+	Coagulation	0.7265
UNC80_MOUSE	Protein unc-80 homolog	-	Component of sodium channel	2.1276
ABCA5_MOUSE	ATP-binding cassette sub-family A member 5	-	Processing of autolysosomes	0.0164